Effects of Merkel Cell Polyomavirus T Antigen Expression on Cell Transformation of Merkel Cells

Noor Suhana Binti Adzahar

Submitted in accordance with the requirements for the degree of

Doctor of Philosophy

University of Leeds
Faculty of Biological Sciences
School of Molecular and Cellular Biology

April, 2016

The candidate confirms that the work submitted is her own and that appropriate credit has been given where reference has been made to the work of others.

Acknowledgements

In the name of Allah the Most Gracious and the Most Merciful.
All praise is due to Allah, the Lord of the Worlds. There is no power and no strength except with Allah permission and help.

First and foremost, I would like to express my gratitude and thanks to my supervisor Professor Adrian Whitehouse for his constant guidance, patience and for the many hours that he has aided me throughout my PhD research and thesis write up. Thanks to all the members of Whitehouse and Hewitt groups, past and present, for making the lab such enjoyable place to work and for throwing useful suggestions and help either in the formal group meeting or discussions in the lab.

Acknowledgements also go to Dr Andrew MacDonald, Professor Eric Blair and their groups, who have provided assistance and reagents as well as useful suggestions during my study over the past three years. An additional thanks to the funding bodies, Ministry of Higher Education, Government of Malaysia for funding my work and full scholarship during the past three and half years. Not to forget, thanks also goes to my direct employer Universiti Malaysia Pahang for the opportunity given to me study abroad and for sponsored additional family allowances for my two children as dependent to be here with me throughout my PhD.

Massive thanks to my dad, my in law parents, my dear family and friends for their continual support and always believing me. A very special thank you to my husband Muhammad Adam Lee who always listen, encourage and being there for me when I needed it the most. For my children, Farra Diana Lee and Aaron Hafiz Lee, thank you for their love, putting their trust and also for their understanding on our busy schedules. Last but not the least, I dedicated this thesis to my beloved mum, Hamidah Binti Sulaiman (*June 1953 – October 2010*).

Abstract

Merkel cell carcinoma (MCC) is a rare but highly metastatic skin cancer that affects immunosuppressed individuals. The MCC tumour arises from mechanoreceptor merkel cells in the basal layer of the epidermis and is able to spread through the dermal lymphatic system. Merkel cell polyomavirus (MCPyV) has been detected in the majority of MCC tumour samples. Truncation mutations of the large tumour antigen (LT) are observed in the integrated genome rendering the virus replication defective. These replication-disabling mutations are only present in MCPyV isolates found in cancers and absent from viruses derived from non-tumour tissues. As such aberrant expression of truncated LT (tLT) and small T (ST) antigens is thought to be implicated in MCC development. Elucidating the cellular pathways affected by the MCPyV T antigens involved in oncogenesis and tumour progression is essential to understand the effects of these oncoproteins in cellular transformation and tumourigenesis. A quantitative proteomic approach has been used to identify cellular proteins and pathways that are differentially expressed upon expression of MCPyV tLT. Bioinformatic analysis of the stable isotope labelling by amino acid in cell culture (SILAC) datasets highlight several pathways that are dysregulated upon tLT expression. These pathways include cell cycle regulation, cell death and survival, and cell-cell connections. Further analysis confirmed the effects of MCPyV tLT on these pathways showing alterations within the cell cycle, specifically disrupting the G1 checkpoint to enhance entry to the S-phase, which may prolonged the S phase to allow viral DNA replication. In addition, results suggest that MCPyV tLT expression may also delay the apoptosis-inducing properties of various compounds but was not capable to fully inhibit the apoptotic cascade. In contrast, although proteomic analysis highlighted a number of cell-cell connections related pathways to be differentially altered upon tLT expression, follow up experiments were not able to confirm these results.

Table of Contents

List of Tables

List of Figures

Abbreviations

α	alpha
β	beta
κ	kappa
γ	gamma
%	percentage
°c	degrees celsius
µg	microgram
µL	microlitre
µm	micrometer
µM	micromolar
µg/mL	microgram per mililiter
57kT	57 kDa T antigen
4E-BP1	eukaryotic translation initiation factor 4E-binding protein 1
ATM	ataxia telangiectasia mutated
aa	amino acid
ADP	adenosine diphosphate
AIDS	acquired immune deficiency syndrome
AJ	adherens junctions
ALTO	alternative T antigen open reading frame
Amp	ampicillin
AP-1	activator protein 1
APC	anaphase promoting complex
APC/C	anaphase promoting complex/cyclosome
ATP	adenosine triphosphate
ATR	ataxia–telangiectasia and Rad3 related
BAD	Bcl-2-associated death promoter
BAK	Bcl-2 homologous antagonist/killer
BAX	Bcl-2-like protein 4
BCL-2	B-cell lymphoma 2
BCL-xl	B-cell lymphoma-extra large
BCR	breakpoint cluster region protein
BGH	bovine growth hormone
BKPyV	BK virus
bp	base pair
BRAF	serine/threonine-protein kinase B-Raf
Brd4	chromatin-associated bromodomain containing protein 4
BSA	bovine serum albumin
C-terminus	carboxy-terminus
CaCl2	calcium cloride
Cdc	cell division cycle
Cdh	Cadherin
CDK	cyclin dependent kinase

CDK4	cell division kinase-4
CDKs	cyclin dependent kinases
cDNA	complementary DNA
ChPyV	chimpanzee polyomavirus
CK20	cytokeratin 20
cm	centimetre
CO_2	carbon dioxide
CR	complement receptor
CREB	cAMP response element-binding protein
cul	cullin
DAPI	4',6-Diamidino-2-Phenylindole
DAVID	The Database for Annotation, Visualization and Integrated Discovery
DDR	DNA damage response
dH_2O	destilled water
DMEM	Dulbecco's modified Eagle's medium
DMSO	dimethyl sulphoxide
DNA	deoxyribonucleic acid
Dnase	deoxyribonuclease
dNTP	deoxyribonucleoside (5'-) triphosphate
dox	doxycycline hyclate
ds	double stranded
DTT	dithiothreitol
E. coli	*Escherichia coli*
E2F	E2 factor
EB-1	end binding protein - 1
EBV	Epstein-Barr virus
ECL	enhanced chemiluminescence
ECM	extra cellular matrix
EDTA	ethylenediaminetetraacetic acid disodium salt
EGFP	enhanced green fluorescent protein
eIF4E	eukaryotic translation initiation factor 4E
EMT	epithelial to mesenchymal trasition
ERK	extracellular signal-regulated kinases
EtBr	ethidium bromide
FACS	fluorescence-activated cell sorting
FCS	foetal calf serum
FFPE	formalin-fixed, paraffin-embedded
FRT	FLP recombination target
GAG	glycosaminoglycan
GAPDH	glyceraldehyde 3-phosphate dehydrogenase
GFP	green fluorescent protein
GOI	gene of interest
GST	Glutathione S-transferase
H_2O	water
HBV	Hepatitis B virus
HCl	hydrochloric acid

HCMV	human cytomegalovirus
HCV	hepatitis C virus
HEK	human embryonic kidney
His	histidine
HPV	human papilloma virus
HPyV	human polyomavirus
Hr	hour
HRP	horseradish peroxidase
HRR	homologous recombination-direct DNA repair
Hrs	hours
hTERT	human telomerase reverse transcriptase
HTLV	human T-cell leukaemia virus
IF	immunofluorescence
IFN	interferon
IkB	Inhibitor of kappa B
INPP1	Inositol polyphosphate phosphatase 1
IP	immunoprecipitation
IPA	Ingenuity Pathway Analysis
IPTG	Isopropyl-β-D-thio-galactoside
IR	isoleucine arginine
IRS 1	insulin receptor substrate 1
JCV	JC virus
Kan	kanamycin
kb	kilobase
kbp	kilobase pair
KCl	potassium chloride
kDa	kilodalton
KEGG	Kyoto Encyclopedia of Genes and Genomes
Kif14	kinesin-like protein 14
KIPyV	Karolinska Institute polyomavirus
KOAc	potassium acetate
KOH	potassium hydroxide
KRAS	Kirsten Rat Sarcoma Viral Oncogene Homolog
KS	Kaposi's sarcoma
KSHV	Kaposi's sarcoma-associated herpesvirus
LANA-1	latency-associated nuclear antigen
LB	Luria broth
LBD	LT-binding domain
LC-MS/MS	Liquid chromatography–mass spectrometry/mass spectrometry
LT	large T antigen
M	molar
MAPK	Mitogen-activated protein kinases
MCC	Merkel cell carcinoma
MCPyV	Merkel cell polyomavirus
Mdm2	mouse double minute 2 homolog
mg	miligram
$MgCl_2$	magnesium chloride

$MgSO_4$	magnesium sulphate
min	minute
miRNA	micro RNA
miRNA	microRNA
mL	mililitre
mM	milimolar
$MnCl_2$	Manganese(II) chloride
MOPS	3-(N-morpholino)propanesulfphonic acid
MPyV	murine polyomavirus
MPyV	murine polyomavirus
mRNA	messenger RNA
MS	mass spectrometry
MT	middle T antigen
mTOR	mammalian target of rapamycin
MUR	Merkel cell polyomavirus unique region
MWPyV	Malawi polyomavirus
MXPyV	MX polyomavirus
N-terminus	amino terminus
NaCl	sodium chloride
NaOH	sodium hydrochloride
NCCR	non coding control region
NF-kB	nuclear factor kB
ng	nanogram
NLS	nuclear localisation signal
NP-40	tergitol-type NP-40
OBD	origin binding domain
ORF	Open reading frame
PAGE	polyacrylamide gel electrophoresis
PARP	Poly (ADP-ribose) polymerase
PBS	Phosphate-buffered saline
PCR	polymerase chain reaction
PI	Propidium Iodide
PI3-K	Phosphatidylinositol-4,5-bisphosphate 3-kinase
Pim-2	Pim-2 proto-oncogene, serine/threonine kinase
PML	promyelocytic leukemia
PML	progressive multifocal leukoencephalotheraphy
PP2A	protein phosphatase 2A
PP4C	protein phosphatase 4 catalytic subunit
PPL	periplakin
PS	pentanucleotide sequences
PTEN	phosphatase and tensin homolog
Rb	retinoblastoma protein
RbCl	rubidium chloride
RFC	cellular replication factor C
RI	ribonuclease inhibitor
RIPA	radioimmunoprecipitation assay buffer
RNA	ribonucleic acid

RNAi	RNA interference
RNase	ribonuclease
rpm	revolutions per minute
RPMI	Roswell Park Memorial Institute medium
RSV	Rous sarcoma virus
RT	reverse transciptase
SCC	squamous cell carcinoma
SDS	sodium dodecyl sulphate
SILAC	Stable isotope labeling by amino acids in cell culture
Skp2	S-Phase Kinase-Associated Protein 2
SLNB	Sentinel lymph node biopsy
SOC	Super Optimal broth with Catabolite repression
Sp-1	specificity protein 1
ST	small T antigen
STLPyV	St Louis polyomavirus
SV40	Simian vacuolating virus 40
TAME	Tosyl-L-Arginine Methyl Ester
TBE	TBE tris-borate-EDTA buffer
TEMED	N-N-N'-N'-tetramethylethylenediamine
TJ	tight junctions
tLT	truncated large T
Tris	Tris (hydroxymethyl)-aminoethane
tRNA	transfer ribonucleic acid
TSPyV	trichodysdysplasia spinulosa-associated polyomavirus
U	unit
Ub	ubiquitin
UV	ultraviolet
V	volt
v/v	volume per volume
VEGF	vascular endothelial growth factor
Vn	vitronectin
VP	viral protein
w/v	weight per volume
WCL	whole cell lysate
WHIM	warts, hypogammaglobulinemia, infection and myelokathexis
WTLT	full length large T
WUPyV	Washington University polyomavirus
ZO	zona occludens

Bases

A	adenine
T	thymine
C	cytosine
G	guanine

Amino acids

Glycine	Gly	G
Alanine	Ala	A
Valine	Val	V
Leucine	Leu	L
Isoleucine	Ile	I
Serine	Ser	S
Threonine	Thr	T
Cysteine	Cys	C
Methionine	Met	M
Tyrosine	Tyr	Y
Proline	Pro	P
Aspartate	Asp	D
Glutamate	Glu	E
Asparagine	Asn	N
Glutamine	Gln	Q
Lysine	Lys	K
Arginine	Arg	R
Histidine	His	H
Phenylalanine	Phe	F
Tryptophan	Trp	W

Chapter 1

INTRODUCTION

1.0. Introduction

1.1. Cancer

Cancer is a group of diseases that exhibit the common feature of abnormal uncontrolled growth, with potential to invade and spread to other parts of the body. The hallmarks of cancer comprise six biological capabilities acquired during the development of the tumour. These features include proliferative signalling, evading growth suppressors, resisting cell death, enabling replicative immortality, inducing angiogenesis, and activating invasion and metastasis (Hanahan and Weinberg, 2000, 2011).

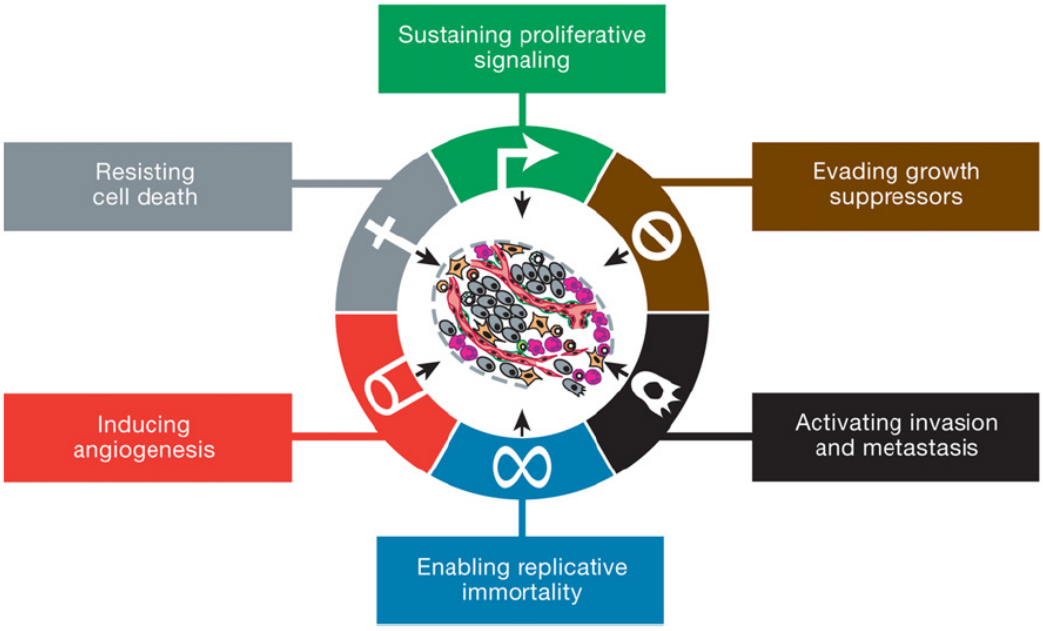

Figure 1.1: The hallmarks of cancer.

The hallmarks of cancer includes six biological capabilities acquired through the development of tumour. Illustration adapted from (Hanahan and Weinberg, 2011).

A fundamental trait of cancer cells is their ability to sustain progressive proliferation. This feature does not usually occur in healthy cells and tissues where they are able to control the production and release of the appropriate growth-promoting signals essential in cell growth and regulating cell division. Thus, the homeostasis of cell numbers are

maintained according to the cell's needs and functions. Cancer cells on the other hand deregulate these checkpoint signals and emit signals which drive progression through the cell cycle, inducing cell proliferation, increasing the cell numbers and enhancing cell survival, as well as up regulating energy metabolism. Cancer cells are also capable of inducing angiogenesis locally and becoming resistant to apoptosis as well as tissue invasion resulting in metastasis. These hallmarks of cancers are present in variable degrees in different diseases, among different cases of the same cancer and even in a given malignant tumour after time (Hanahan and Weinberg, 2000). Transformed cells have already acquired some of these hallmarks when they develop into a malignant tumour, and further mutations strengthen these oncogenic properties during tumour progression. Furthermore, new features may also be acquired, enabling the malignant tumour to become more heterogeneous and aggressive. These cancer determining features and pathways can also be required for efficient viral replication (Elgui de Oliveira, 2007). As such, infection by oncogenic viruses offers a prone-to-transformation scenario, in which the development of a malignant tumour is likely to happen.

1.2. Viruses and Cancer

There are many causes of cancers and infectious agents, such as viruses, are considered to be an important factor in the development of various human tumours. The estimated total number of cancers attributable to infection is approximately 1.9 million cases per year, or 17.8% of the global cancer burden (Parkin, 2006). In the developed world, cancer accounts for 20% of all deaths and is the highest cause of death after cardiovascular disease. Viral infection is thought to play a significant role in cancer formation and maintenance. The first tumour virus, Rous sarcoma virus (RSV) which causes tumours in chickens, was discovered in 1911 by Peyton Rous (Javier and Butel, 2008). Following this discovery, several other mammalian tumour viruses were identified including murine polyomavirus (MPyV) and simian vacuolating virus 40 (SV40) (Moore and

Chang, 2010b; Stewart et al., 1958; Sweet and Hilleman, 1960). The known human tumour viruses, including Epstein-Barr virus (EBV), hepatitis B virus (HBV), human papilloma virus (HPV), human T-lymphotrophic virus (HTLV-1), hepatitis C virus (HCV), Kaposi's sarcoma-associated herpesvirus (KSHV) and Merkel cell polyomavirus (MCPyV). Through intensive research it has been shown that most cancer associated viruses express specific oncoproteins which facilitate cell growth, proliferation and transformation of the host cell (Table 1.1).

Virus	**Family/Genome**	**Examples of Oncoproteins**	**Associated cancers**
Epstein-Barr Virus (EBV) - 1964	Herpesviridae - dsDNA	LMP1	Burkitt's lymphoma, nasopharyngeal carcinoma, most lymphoproliferative disorders
Hepatitis B Virus (HBV) - 1965	Hepadnaviridae - ssDNA and dsDNA	HBx	Some hepatocellular carcinomas
Human T-lymphotrophic virus-1 (HTLV-1) - 1980	Retroviridae - ssRNA	Tax	Adult T cell lymphoma
Human papillomaviruses (HPV) 16 and 17 - 1983 and 1984	Papillomaviridae - dsDNA	E5, E6, E7	Cervical cancer and most penile cancers
Hepatitis C Virus (HCV) - 1989	Hepaciviridae - (+)ssRNA	NS5A	Some hepatocellular carcinomas and lymphomas
Kaposi's scarcoma associated herpesvirus (KSHV) - 1994	Herpesviridae - dsDNA	LANA, vflip, vBcl-2 and others	Kaposi's sarcoma, primary effusion lymphoma and some multicentric Castleman's disease
Merkel Cell Polyomavirus (MCPyV) - 2008	Polyomaviridae - dsDNA	T antigens - LT and ST	80-95% Merkel cell carcinoma cases

Table 1.1: Human tumour viruses and their oncoproteins.

List of the known human tumour viruses, date of discovery, virus family, genome structure and the viral-associated cancer. Adapted from (Moore and Chang, 2010b).

Studying tumour viruses has also revealed fundamental molecular events that trigger the development of all human cancers, regardless of etiology. Both RNA and DNA tumour virus research has contributed distinct insights into the disease process by revealing central roles for cellular oncogene

activation and tumour suppressor gene inactivation, respectively. Most known cellular oncogenes have been identified through studies of human tumour viruses. In addition, viruses have been important in the identification of the p53 tumour suppressor protein and many functions of the retinoblastoma (Rb) tumour suppressor gene.

1.3. Polyomaviruses

Polyomaviruses are non-enveloped, double stranded DNA viruses with icosahedral capsids. Their DNA genomes are approximately 5 kbp in length. The *Polyomaviridae* family mostly infect birds, mammals and humans (Van Ghelue et al., 2012). However, each respective polyomavirus only infects specific species, thus they have a limited host range (Imperiale, 2001). The polyomaviruses are classified as the only genus in the *polyomaviridae* family. The name polyomavirus is derived from words *poly-*, which means 'many' and *–oma*, which means 'tumours'. The first polyomavirus identified was murine polyomavirus (MPyV), followed by simian vacuolating virus 40 (SV40), two years later in 1960. These two viruses have been widely used as model systems for understanding polyomavirus DNA structure, replication and transcription (White and Khalili, 2004). Moreover, they have been valuable tools for studying virus-induced transformation mechanisms (Siebrasse et al., 2012a). This has led to fundamental insights into carcinogenesis, due to SV40 having the ability to transform human cells *in vitro* and induce tumours in rodents *in vivo* (Moens et al., 2007).

Human polyomaviruses were first discovered and isolated about 30 years ago. Starting with the isolation of BK virus (BKPyV) from urine of a renal transplant patient (Gardner et al., 1971) and JCPyV from the brain of a patient with progressive multifocal leukoencephalotheraphy (PML) (Padgett et al., 1971). JCPyV is a common infection during childhood and early adolescence with seroprevalence of 70 to 90% in adult population (Padgett

and Walker, 1973; Shackelton et al., 2006). However, it is now established as the causative agent in PML, as PML mainly occurs in patients with compromised immune systems, such as acquired immune deficiency syndrome (AIDS) and transplant patients. Under these conditions, virus reactivation can occur resulting in lytic replication in oligodendrocytes leading to focus formation and demyelinated areas (Safak and Khalili, 2003). JCPyV has also been shown to induce transformation of human and rodent cells *in vitro* and in animal models (Nozawa et al., 1987). Both JCPyV and BKPyV share approximately 75% sequence identity and have similar infection routes (Chesters et al., 1983). Like JCPyV, BKPyV reactivation can occur under immune suppression leading to a lytic replication cycle (Egli et al., 2009).

In 2007 two additional human polyomaviruses were identified by deep sequencing of DNAse-treated respiratory fluids from patients with respiratory tract infections. They were named after the institutions in which they were isolated; namely Karolinska Institute polyomavirus (KIPyV) (Allander et al., 2007) and Washington University polyomavirus (WUPyV) (Gaynor et al., 2007). Since then, other polyomaviruses have been discovered through a variety of techniques. Most of the methods used involved virus enrichment from samples, treatment with DNase to eliminate unencapsidated DNA, followed by protease treatment to disrupt the virions, followed by deep-sequencing. In 2008, Merkel cell polyomavirus (MCPyV) was discovered using digital transcriptome subtraction prepared from a Merkel cell carcinoma (MCC) specimen. Here, human sequences were subtracted to identify novel viral sequences. In the same year, trichodysplasia spinulosa-associated polyomavirus (TSPyV) was isolated and discovered from trichodysplasia spinulosa lesions from inner root sheath cells of hair follicles using the rolling circle amplification method (van der Meijden et al., 2010). Again, lytic reactivation of TSPyV in immune-compromised individuals results in this rare skin disease. Human polyomavirus 6 (HPyV6) and human polyomavirus 7 (HPyV7), have also been identified using the same method from human skin, using degenerate primers corresponding to other human polyomavirus sequences. However,

individuals harbouring HPyV6 or HPyV7 showed no clinical symptoms (Schowalter et al., 2010). Another novel human polyomavirus 9 (HPyV9) was isolated from kidney transplant patients (Scuda et al., 2011) and Malawi polyomavirus (MWPyV) was isolated from healthy stool samples and named after the source of the original virus isolate (Siebrasse et al., 2012a). HPyV10 was discovered from a patient presenting with warts, hypogammaglobulinemia, infection and myelokathexis (WHIM) syndrome (Buck et al., 2012). Notably, within the last 4 years, MX polyomavirus (MXPyV) was also isolated from acute diarrheal samples of children (Yu et al., 2012), human polyomavirus 12 (HPyV12) from resected liver samples (Korup et al., 2013) and St Louis polyomavirus (STLPyV) was isolated from stool specimens obtained from both the Gambia and the United States (Lim et al., 2013).

To date, over 21 full genome sequences of polyomaviruses have been deposited in Genbank. Through phylogenetic analysis of the human polyomaviruses protein sequences'; JCPyV, BKPyV, KIPyV and WUPyV appear to be closely related to SV40. In contrast, MCPyV appears to be more closely related to the archetypal murine polyomavirus (MPyV). Therefore, due to the explosion in new polyomaviruses being identified, the role of the human polyomaviruses in disease is now a focus of intense research.

1.3.1. Genome organization of polyomaviruses

The polyomavirus genome is small, circular and double stranded; between 5.0 and 5.3 kbp in length (JCPyV-5130 bp; BKPyV-5153 bp; KIPyV-5040 bp, WUPyV-5229 bp; MCPyV-5387 bp). It is contained within a non enveloped, 40-45 nm icosahedral capsid. Generally, the genome can be divided into three functional regions; the early region encoding regulatory proteins involved in viral DNA replication and gene expression; the late region that encodes the capsid proteins; and origin of replication and transcription control elements (Figure 1.2).

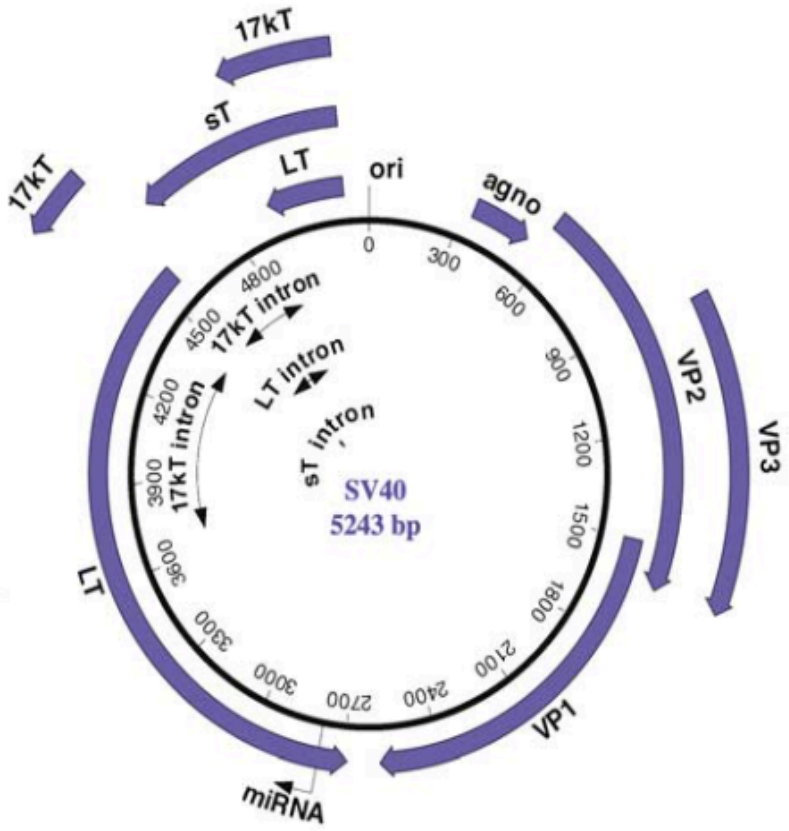

Figure 1.2: Schematic presentation of genome organization of SV40.

SV40 genomic DNA is composed of three elements: the early and late coding units and the regulatory region. The early unit encodes large T antigen (LT), small t antigen (sT), 17K T antigen (17KT). The late unit encodes the three structural proteins (VP1, VP2, and VP3) and the agnoprotein (agno) and a pre-microRNA (miRNA). The regulatory region (ori) contains sequences for the early and late promoter and the origin of replication. Image taken from (Ahuja et al., 2005).

Transcription of the early and late coding regions produce primary transcripts, which undergo differential splicing producing multiple mRNAs encoding a variety of distinct proteins. The early region encodes the T antigens, namely the large T antigen (LT), the small T antigen (ST) and the middle T antigen (MT). The late region, transcribed in the other direction encodes three structural proteins required for viral capsid formation: VP1, VP2 and VP3. The additional protein, VP4, also termed as agnoprotein was observed in SV40, BKPyV and JCPyV which may function as a viroporin (Raghava et al., 2011; Suzuki et al., 2010).

1.3.2. Virus life cycle

The life cycle of polyomaviruses has been well characterised, primarily using SV40 as a model to provide a better understanding of processes involved in polyomavirus infection and replication. Figure 1.3 highlights a schematic overview of the life cycle of polyomavirus.

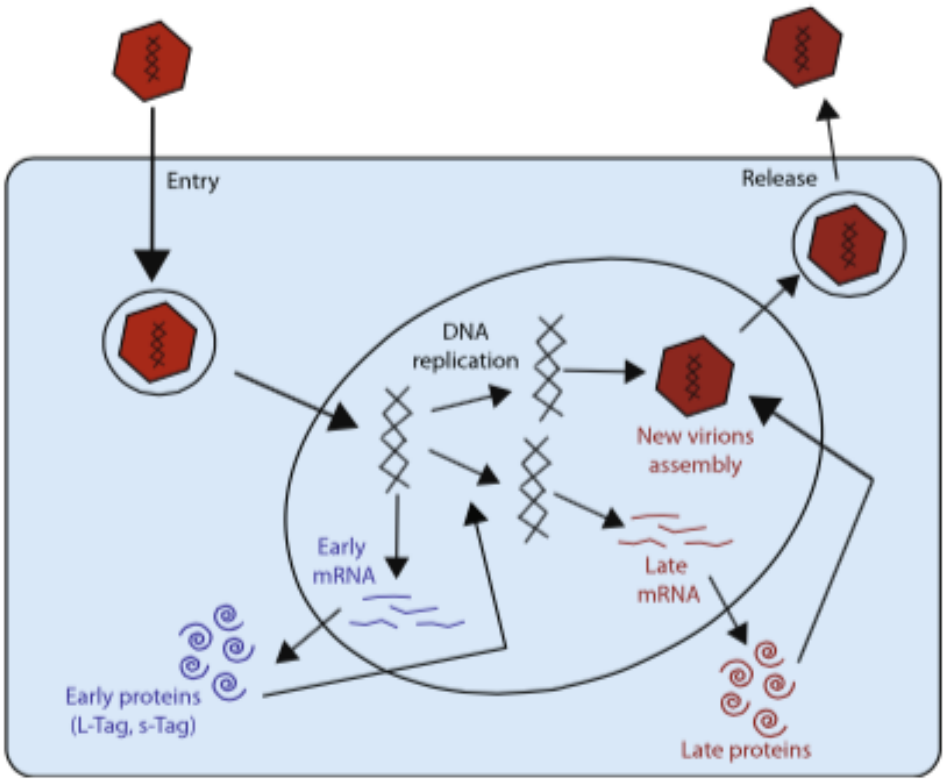

Figure 1.3: The life cycle of the polyomavirus.

Life cycle of the polyomaviruses. After entry, viral particles (red) pass through the cytoplasm to reach the nucleus, where the main processes of viral replication take place. The first step consists of expression of the early genes (blue), especially the large tumour antigen (LT) which is necessary for replication of the viral genome. The following step permits the production of structural proteins (late stage, red) prior to the assembly of new virions and their release into the extracellular medium (adapted from Fields, 4th edition).

The virus enters the cell by attaching to specific cell receptors, mainly sialic acids on cell surface. For example, JCPyV binds to host cells via α2-6-linked sialic acids on cell membrane glycoproteins and glycolipids (Komagome et al., 2002); while initial attachement of SV40 is through the cell receptor ganglioside GM1 (Campanero-Rhodes et al., 2007; Neu et al., 2008) and both BKPyV and MPyV bind to sialylated glycans (Low et al.,

2006; Tsai et al., 2003). The viral capsid enters the cell by endocytosis and is transported to the nucleus, where the DNA is uncoated and viral transcription begins. It starts with the expression of the early transcription unit, producing a series of alternative mRNA transcripts, which encode the tumour antigens of the virus, the large and small tumour antigens (LT and ST). The ST antigen comprises a 17 kDa protein (~180 residues), localised to the nucleus and cytoplasm (Moens et al., 2007). ST is expressed from the same transcriptional start site as LT but the ST transcription reads through the splice site to encode the rest of the ST protein. Both LT and ST share the same N-terminal region, which consists of a complement receptor type 1 (CR1) and heat shock protein-binding domains, however, only ST contains a protein phosphatase 2A (PP2A) family interaction domain. Upon expression and translation of the late viral capsid proteins, virus assembly occurs in the nucleus. The packaged virus particles are then released by cell lysis or by cell membrane fusion exocytosis (Ahuja et al., 2005).

1.3.3. Integration of the polyomaviruses

Integration of the viral genome into host chromosomal DNA has been demonstrated for many polyomaviruses, including MPyV, SV40, JCPyV and BKPyV (Chenciner et al., 1980; Hirai et al., 1971; Mandl and Frisque, 1986). The pattern of integration of SV40 occurs at random sites in host chromosomes, although some integration sites were more predominant in selected clones (Hara and Kaji, 1987). This has been confirmed recently in MCPyV, where integration was observed to be random but localised in certain sites within the host genome (Feng et al., 2008; Martel-Jantin et al., 2012). Martel-Jantin et al., discovered this viral junction was located within the second exon of the LT antigen, after the pRB binding domain. This suggests that integration may result in MCPyV LT tumour truncations removing the helicase binding domains, inhibiting viral replication, facilitating host cell transformation (Houben et al., 2010a; Martel-Jantin et al., 2012; Shuda et al., 2008).

1.3.4. The oncogenic potential of polyomavirus T antigens.

All polyomaviruses encode both LT and ST antigens, which are important regulatory oncoproteins required for viral replication. However, due to the small genome size, polyomaviruses rely strongly on host cellular replication machinery to replicate their genomes. For example, they have to reprogram the host cell cycle to induce progression into S-phase, in order to create an optimal environment for virus replication (Moens et al., 2007). This is thought to be an important mechanism in polyomavirus-induced cellular transformation as early gene expression in non-permissive cells results in aberrant cell cycle stimulation and interference with host cell signalling pathways (Ahuja et al., 2005). Importantly, research using SV40 suggests that both SV40 T antigens are required for transformation of human fibroblasts; ST alone is incapable of transforming cells but enhances LT-induced cell transformation (Noda et al., 1987). Therefore, it is believed that the SV40 LT antigen is the major oncoprotein involved in the neoplastic process of polyomaviruses, while ST enhances SV40 LT-mediated transformation and oncogenic progression.

1.3.4.1. Large T antigen

The large T (LT) antigen is a multifunctional nuclear phosphoprotein, approximately 700 amino acids residues in length. LT contains the conserved J domain within its N-terminus and a unique C-terminal region (Figure 1.4). The J domain comprises a protein binding domain for Hsc70 and a conserved Cr1 domain. Within its unique region the LT protein contains multiple distinct protein binding domains, such as the LxCxE motif, which are required for pRb binding (DeCaprio et al., 1988). LT also contains a DNA binding domain within the mid-region of the protein and a C-terminal bipartite region, which facilitates an interaction between LT and the tumour suppressor protein p53, which promotes viral DNA replication (Kierstead and Tevethia, 1993; Peden et al., 1989).

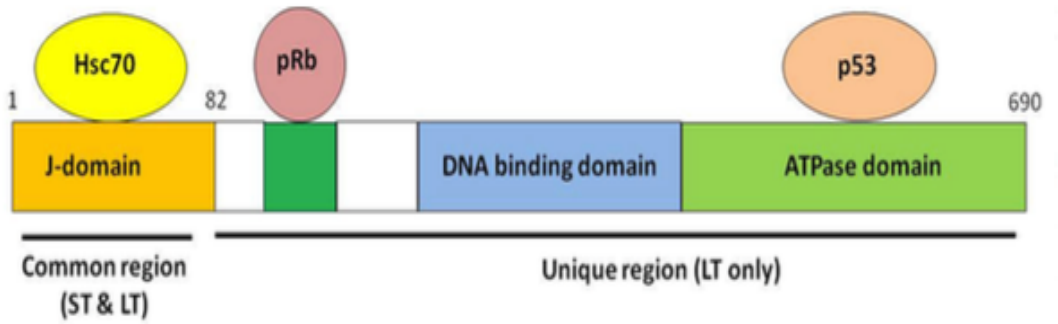

Figure 1.4: Schematic diagram of polyomavirus large T antigen.

The J domain is a common region found in both LT and ST antigens. J domain contains a binding region to Hsc70, while the unique region posses only in LT contains a binding domain for pRb, a DNA binding domain and an ATPase domain which interacts with p53. Image taken from (Khalili et al., 2008b).

1.3.4.1.1. Role of LT in the virus life cycle

The LT antigen promotes cell cycle dysregulation by driving the host cell into S-phase, aided by LT helicase and ATPase activity, which promotes DNA unwinding, along with additional specific domains required for binding cellular replication proteins (Moens et al., 2007). In SV40, LT acts as an essential factor in early viral DNA replication and binds to the viral origin of replication, through its DNA binding domain (Stahl et al., 1986). Binding promotes DNA helix unwinding and transcription complex formation (Dean et al., 1987). Here, LT stimulates viral DNA replication by the recruitment of cellular proteins required for transcription complex formation at the viral promoter region. Both the J domain and the ATPase domain of SV40 LT are necessary for direct binding of LT to the catalytic subunit of DNA polymerase-α (Dornreiter et al., 1990). Moreover, the DNA helicase activity of SV40 LT is required for efficient viral DNA replication, through this activity SV40 LT also interacts with components of the holoenzyme, namely nucleolin and topoisomerase 1, required for DNA unwinding (Seinsoth et al., 2003).

1.3.4.1.2. Role of LT in host cell transformation

Several studies have shown that expression of SV40 LT alone is sufficient to induce transformation of rat fibroblast cells and is thought to be a result of binding to the tumour suppressor proteins, p53 and Rb (Ahuja et al., 2005; Saenz-Robles et al., 2001; Sullivan and Pipas, 2002). However, mutations in other regions of LT which do not disrupt these interactions also inhibit LT-induced transformation, suggesting other LT functions may contribute to tumourigenesis. Taking this observation into consideration, it suggests that both BKPyV and SV40 LT can induce mutagenic effects in the host DNA by affecting DNA repair and response pathways (Sachsenmeier and Pipas, 2001).

1.3.4.1.2.1. Binding tumour suppressor proteins

LT-mediated transformation is primarily due to its interactions with the cellular tumour suppressor proteins, pRb and p53 (Moens et al., 2007; Saenz-Robles et al., 2001). Here LT is believed to exert its functions by inhibiting these tumour suppressor proteins so that cells are able to enter the S phase, enhancing viral genome replication. Importantly, LT binding mutants defective for pRb binding are incapable of inducing cellular transformation (Bollag et al., 2000; Chen and Paucha, 1990; DeCaprio et al., 1988; Harris et al., 1998). An active pRb functions as a tumour suppressor protein by preventing excessive cell growth and inhibits cell cycle progression until the cell is ready to divide. Active pRb proteins bind to E2F factors and repress E2F-dependent gene expression, such as C-myc and C-fos which are required for S-phase entry (Rowland and Bernards, 2006). Figure 1.5 illustrates the interactions of polyomavirus LT antigen targeting the tumour suppressor proteins, p53 and pRb.

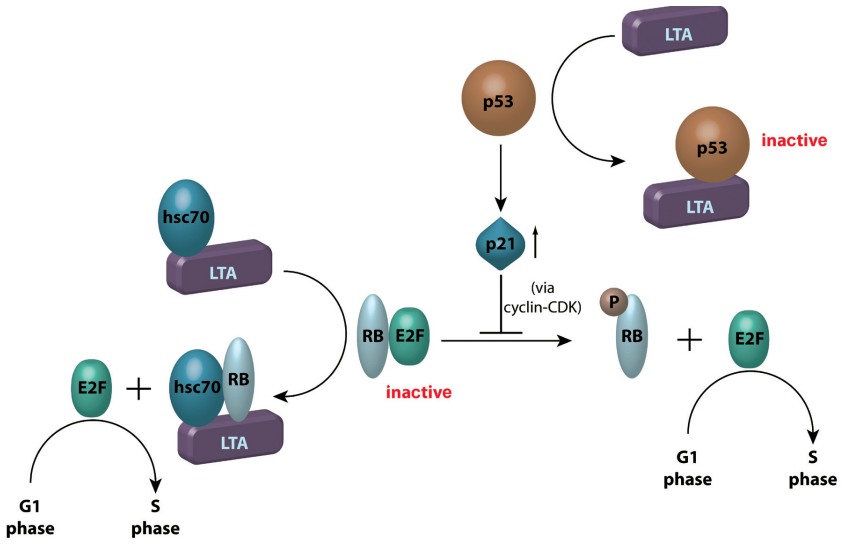

Figure 1.5: The effects of polyomavirus LT antigen on regulatory pathways, targeting the regulatory pathway implicating in the inactivation of pRb-E2F and p53.

LT antigen may effect the functions through its binding to p53 and pRb. This binding inactivates the function of p53 and subsequently blocked the expression of p21, which is cyclin-dependent kinase inhibitor causing the cell cycle checkpoints dysfunction. Active Rb proteins binds to E2F to inhibits cell cycle progression. The interactions of RB to LT antigen (LTA) release E2F from the RB-E2F complex, causing the progression of cell cycle from G1 phase to S phase. The release of E2F also can also through the phosprorylation of RB. Image taken from (Becker et al., 2009).

In addition, LT also affects expression levels of the pRb protein and its other related family members, such as p107 and p130. This is supported by studies demonstrating that expression of SV40 LT lowers the expression levels of p130 in mouse embryonic fibroblasts while the BKPyV LT protein has been shown to reduce the levels of expression of all three pRb family members (Harris et al., 1996). The tumour suppressor protein, p53 functions as a regulator of the cell cycle as well as directing apoptosis and DNA damage repair. Aberrant p53 regulation is the most common feature of many human cancers. Polyomavirus regulation of p53 is required as inhibition of pRb activity by LT binding results in the transcription of E2F responsive genes resulting in the activation of $p14^{ARF}$, whose downstream effect results in activation of p53 and transcription of p53-regulated genes (Quelle et al., 1995). This would result in cell growth arrest and apoptosis. However, LT binding renders p53 transcriptionally inactive, as p53 can no longer access and bind to p53-responsive promoters (Jiang et al., 1993; Segawa et al., 1993). Expression of LT alone is sufficient to downregulate

the expression of p53 responsive genes, allowing virus replication to proceed in permissive cells but in non-permissive cells this can lead to host cell transformation (Mietz et al., 1992; White and Khalili, 2004).

1.3.4.1.2.2. Binding Cullin 7

SV40 LT is also able to interact with cullin 7 (cul7), a core protein in the E3 ubiquitin ligase protein degradation complex (Dias et al., 2002). This interaction prevents cell growth in low serum conditions and exhibits deficiencies in anchorage dependent growth (Ali et al., 2004). This demonstrates the importance of this interaction in relation to tumourigenesis, however the mechanism involved is yet to be understood.

1.3.4.1.2.3. IRS 1

Polyomavirus LT expression can result in inhibition of the homologous recombination-direct DNA repair (HRR) response (Trojanek et al., 2006). Both JCPyV and SV40 LT antigens have been shown to induce translocation of insulin receptor substrate 1 (IRS 1) to the nucleus, resulting in an interaction between IRS1 and Rad51, a DNA repair component (Lassak et al., 2002; Prisco et al., 2002). Moreover, the expression of a dominant negative IRS 1 mutant inhibits anchorage independent growth of JCPyV LT transformed cells (Lassak et al., 2002). This suggests that there may be multiple mechanisms which mediate anchorage independent growth of transformed cells.

1.3.4.1.2.4. Binding β-catenin

β-catenin is a subunit of the cadherin protein complex and functions as an intracellular signal transducer in the Wnt signalling pathway. β-catenin is able to form complexes with transcription factors and activate transcription

of specific target genes, such as C-myc and cyclin D1 (Enam et al., 2002; Gan et al., 2001). Activation of the Wnt signalling pathway has been associated with tumour formation and progression in various cancer types (Mandl and Frisque, 1986; Reya and Clevers, 2005). Moreover, mutations and overexpression of β-catenin are also observed in many cancers (Morin, 1999). Several studies have shown that LT can directly bind to β-catenin, thereby increasing its stability and enhancing activation of its target genes. As such, this is an additional contributing mechanism involved in LT-inducing tumour formation (Enam et al., 2002; Gan et al., 2001).

1.3.4.2 Small T antigen

The Small T (ST) antigen coding region is approximately 500 base pairs in length, encoding a 17 kDa protein. ST localises to the nucleus and cytoplasm and is highly conserved across the polyomavirus family (Moens et al., 2007). The common region, termed the J domain, is present in the N-terminal of the protein, and contains a conserved DnaJ (HPDDKGG) binding domain for the cellular heat shock protein, Hsc70, which acts as a chaperone protein to prevent protein aggregation during viral infection, replication and cellular stress (Figure 1.6). The carboxy-terminal of ST contains a conserved motif (CxxP/CxC) at 97-103 residues which is required for binding protein phosphatase 2A (PP2A), which is the major serine/threonine phosphatase in mammalian cells (Janssens and Goris, 2001; Rodriguez-Viciana et al., 2006).

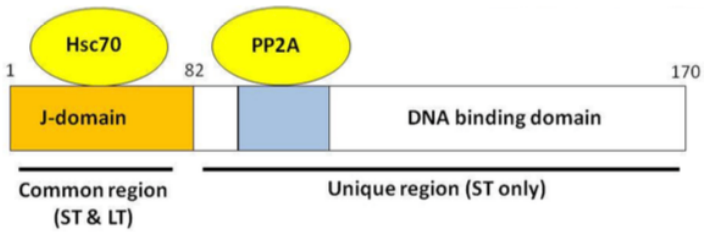

Figure 1.6: Schematic representation of polyomavirus small T antigens and the binding domains within the protein.

The J domain is a common region found in both LT and ST. J domain possess the binding site for Hsc70. The C-terminal ST protein contains a DNA binding domain and a PP2A binding domain. Image taken from (Khalili et al., 2008b).

1.3.4.2.1. ST interacts with PP2A

Several lines of evidence indicate that the functional region of the polyomavirus ST antigens lie within the unique region and specifically within the interacting domain of phosphatase 2A (PP2A) (Janssens and Goris, 2001). PP2A is the major serine/threonine phosphatase in mammalian cells and regulates many biological processes; including development, differentiation and growth control. The enzyme exists as a heterotrimeric complex composed of the core enzyme consisting of the C subunit and a regulatory A subunit, and variable isoform B subunits (Usui et al., 1988). The variability of numerous B subunits allows distinct substrate specificity (Janssens and Goris, 2001). Due to these multiple substrates, PP2A is an essential regulator of multiple downstream signalling pathways affecting signal transduction, apoptosis, cell cycle regulation and proteolysis pathways (Mumby, 2007).SV40 ST targets PP2A function by replacing its B subunit, which can inactivate its activity; leading to increased cell proliferation and anchorage independent growth of cells (Khalili et al., 2008a). Figure 1.7 illustrates the interaction of ST with PP2A and the resulting effect on inhibition of the PP2A complex.

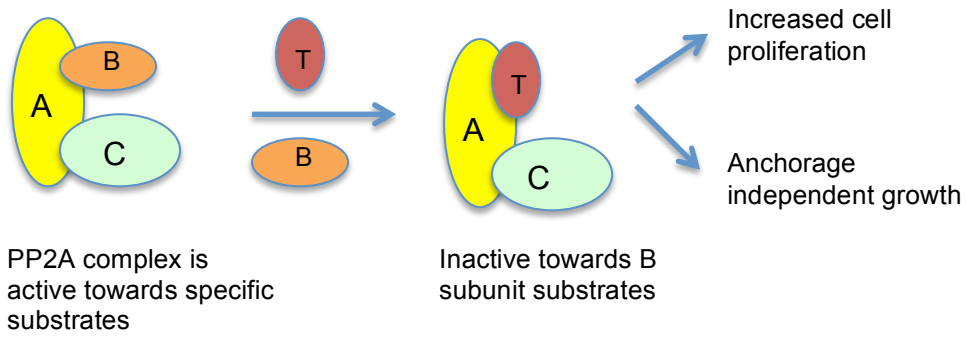

Figure 1.7: Polyomavirus ST protein interaction with PP2A.

PP2A complex comprises three subunit; A, B and C. Subunit B and T antigen competitively compete the binding site. ST binds to the PP2A complex and replaces the B subunit of the PP2A complex resulting in inactivation of the PP2A enzyme towards its respective substrate. This interaction results in cell proliferation and anchorage independent growth of the cells. Image taken from (Khalili et al., 2008a).

There are two isoforms of the PP2A A subunit; the alpha (α) and beta (β). SV40 ST has been shown to only interact with the Aα but not Aβ subunit

(Zhou et al., 2003). Here the SV40 ST-PP2A binding site overlaps and blocks the B subunit binding site (Ruediger et al., 1994). ST can therefore act as a competitive inhibitor and compete with the B subunits for A subunit binding. Multiple experiments have shown that SV40 ST inhibits PP2A activity both *in vitro* and *in vivo* by preventing the binding of multiple different substrates to PP2A (Hahn et al., 2002; Yang et al., 1991; Yu et al., 2001). Moreover, ST may also function as transfer factor, changing the specificity of PP2A targeting in cells; for example modulating the transcriptional activity of cellular genes, including the androgen receptor (Yang et al., 2005), which may also contribute to cellular transformation.

1.3.4.2.2. Role of ST in the viral life cycle

Expression of SV40 ST increases viral early promoter activity and also promotes the ability of LT to induce expression from the late promoter (Bikel and Loeken, 1992). Microarray studies on SV40 ST-expressing human embryonic kidney cells, have shown that ST promotes the expression of cellular survival genes involved in cell motility, cancer growth, metastasis and cell survival (Moreno et al., 2004a). However in some cases, when LT is present in high levels, the requirement for ST is reduced (Bikel et al., 1987).

The major role of ST involves the interaction with PP2A, as mentioned previously. This interaction is thought to contribute to virus replication indirectly by disrupting the cell cycle and driving cells into S-phase, thus allowing recruitment of the host cell machinery required for viral replication (Sontag et al., 1993). ST has also been shown to affect cell cycle progression by decreasing cellular levels of p27/kip1 (Khalili et al., 2008b). The mechanism by which ST mediates this decrease is not fully understood, although it is possible that the ST-PP2A interaction could result in a reduction of cyclin E/CDK2 dephosphorylation, which in turn would regulate p27/kip1 levels and stimulate cell cycle progression. ST expression also upregulates other cell cycle progression factors, including cyclin D1 and B and thymidine kinase (Moreno et al., 2004b).

1.3.4.2.3. Role of ST in cell transformation

A number of studies have shown that deletions within the common region between LT and ST, the J domain, inhibits T antigen-mediated transformation (Khalili et al., 2008b). It is thought that, through the J domain, T antigens play an important role in promoting S-phase entry, as well as promoting virus replication in permissive cells and transformation in non-permissive cells. Specifically, the SV40 ST has been shown to be essential for cell cycle progression, anchorage independent growth and transformation (Hahn et al., 2002). The ST-PP2A interaction can affect the expression of transcription factors, such as C-myc. C-myc is activated by phosphorylation and this promotes binding to more than 15% of human gene promoters and enhancer sequences (Martinato et al., 2008). The ST-PP2A interaction inhibits dephosphorylation of C-myc, thus promoting C-myc stabilisation (Tiemann et al., 1995). In turn, this can directly induce cell transformation by altering cell proliferation, growth and apoptotic signalling (Yeh et al., 2004). In addition, ST also activates other cellular transcription factors; such as activator protein 1 (AP-1), specificity protein 1 (Sp1), cAMP response element-binding protein (CREB) and nuclear factor κB (NF-kB). These transcription factors are also important in regulating cell proliferation and cell growth (Conkright and Montminy, 2005; Moens et al., 2007; Ozanne et al., 2007; Piva et al., 2006). Furthermore, SV40 ST has also been shown to induce aberrant activation of the phosphatidylinositol 3-kinase (PI3K) pathway, resulting in phosphorylation of cellular targets, such as Akt (Yuan and Cantley, 2008). Akt is a serine/threonine kinase important in cell survival, metabolism and angiogenesis. The inhibition of Akt activity can repress ST-mediated transformation (Rodriguez-Viciana et al., 2006). Inhibition of Akt dephosphorylation may also increase telomerase phosphorylation and activity (Kang et al., 1999). It is also thought that ST may possess anti-apoptosis capabilities and antagonize the LT-induced cellular apoptosis response, which enhances transformation of rat embryo fibroblasts. This is supported by mutational analysis of LT, in which mutants defective in the pRB-binding domain fail to induce an apoptotic response.

However, a mutant in the p53-binding domain remains functional in inducing apoptosis (Kolzau et al., 1999).

1.3.4.3. Middle T antigen

The middle T (MT) antigen is an alternative spliced product of rodent polyomavirus early transcripts. They usually comprise 421 amino acids, encoding a 55 kDa protein (Ito et al., 1977). MT is the major transforming protein of rodent polyomaviruses. Expression of MT is sufficient for transformation and is also essential for tumourigenesis (Fluck and Schaffhausen, 2009). MT possesses similar structural domains to ST and is composed of all but the final 4 C-terminal amino acids of ST, thus sharing the J domain and PP2A binding domains (Figure 1.8). The remaining 230 amino acids of the C-terminal portion of MT are unique and contain multiple phosphorylation sites. Phosphorylation of this region is crucial for the ability of MT to recruit or activate specific cellular components (Ito et al., 1977). Moreover, the six amino acids at the C-terminus of the hydrophobic domain are essential for cellular transformation, as removal of this region completely abolished transformation (Zhou et al., 2011).

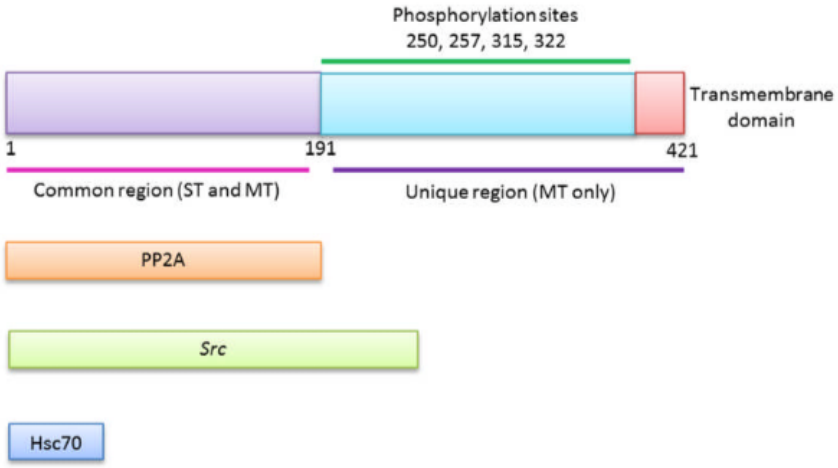

Figure 1.8: Schematic representation of the polyomavirus MT antigen.

MT contains a common region with ST, including the J domain, PP2A binding, Src binding and Hsc70 binding domains. The unique region has multiple phosphorylation sites and a transmembrane binding domain. Adapted from Fluck and Schaffhausen, 2009)

1.4. Merkel cell carcinoma

Merkel cell carcinoma (MCC) is a rare but highly aggressive neuroendocrine skin carcinoma. The tumour is associated with Merkel cells, which are oval cells of epidermal lineage from Merkel cell-neurite receptor complexes (Morrison et al., 2009). These receptor complexes are located in touch-sensitive areas of the skin, such as hair follicles and epithelial structures known as “touch domes” and are a major component of the somatosensory system that mediate light-touch responses (Maricich et al., 2009). MCC is able to spread through the dermal lymphatic system and exhibits a high mortality rate, approximately 28% of patients die within 2 years of diagnosis (Poulsen, 2004b; Tadmor et al., 2011b). MCC is always associated with immunosuppression. Moreover, there is slight male predominance but the main risk factors associated with MCC are being a fair-skinned individual, being 65 years or older and there is also a strong association with sun exposure. The five-year relative survival rate is 75%, 59% and 25% for localised, regional and distant MCC, respectively (Agelli and Clegg, 2003). Thus, the early identification and targeted treatment of this cancer is significantly important. Primary treatment of MCC involves surgical excision of the tumour. Removal can also be combined with ionising radiation therapy for patients who undergo removal of larger tumours as an adjuvant to reduce the risk of recurrence (Gupta et al., 2006). Distant metastasis is commonly treated with chemotherapy as surgery for metastatic MCC has limited success and is mostly palliative in nature (Bichakjian et al., 2007).

1.4.1. Epidemiology of MCC

In the general population, incidence of MCC was higher in males, whites, and in people older than 65 years (Agelli and Clegg, 2003). MCC incidence in United States is 0.6 per 100,000 persons annually, however the number is increasing (Afanasiev et al., 2013). The rising incidence also seen in Australia (8%) and Netherlands (3.5%) within 2001 to 2007 (Agelli et al.,

2010; Reichgelt and Visser, 2011). This rising incidence is believed due to the awareness and improved diagnostic techniques. The median age is around 70 years at time of diagnosis, while very low statistic of cases for patients 49 years below, approximately 4% and rare in children with only scattered case reports (Albores-Saavedra et al., 2010). Immunodefiency also one of the risk factors in incidence of MCC. Approximately 13-fold greater diagnosis in patients with AIDS and 10-fold greater for patients with solid organ transplant (Becker, 2010). Patients with a history of photochemotheraphy treatment showed an incidence of MCC 100 times greater than in the general population (Lunder and Stern, 1998),suggesting that the immunosuppressant and UV exposure are additional risk factors of MCC besides age.

1.4.2. Diagnosis of MCC and histopathology

MCC was first described as a flesh-coloured or blueish-red glassy painless nodule (less than 2 cm in diameter) or a mass (more than 2 cm in diameter) anywhere on the body including the forearm, lip, face, leg, buttocks, head and neck (Toker, 1972). Histopathologically, there were irregular aggregates of pyknotic cells with little cytoplasm (Tope and Sangueza, 1994). MCC tumours are visualised as a lesion of nested small round cells with scanty cytoplasm, a round nucleus, dispersed granular chromatin and not clearly visible nucleoli, amongst infiltrating cells and vascular invasion (Wong and Wang, 2010). The diagnosis of the MCC includes clinical nodal evaluation and sentinel lymph node biopsy (SLNB). SLNB is highly recommended in diagnosis of MCC for both stage I and stage II with significant accurate result (Paulson et al., 2013). Currently, treatment of primary MCC includes surgical excision with complete removal of the tumour, and followed by radiotheraphy to minimise the reoccurance (Gupta et al., 2006). Patients with distant metastasis are mostly treated utilising chemotherapy (Bichakjian et al., 2007). Depending on the stages of the MCC infection, the effectiveness of treatment varies among the patients' immune system and response to the therapy.

1.4.3. Merkel cell polyomaviruses (MCPyV)

In 2008, a novel human polyomavirus was discovered and isolated from MCC tumours. Here digital transcriptome subtraction was employed, where mRNA was extracted from a primary MCC tumour followed by cDNA library preparation and next-generation sequencing. The subsequent sequence data was analysed, all known human sequences removed and remaining sequences then compared against pathogen databases. In contrast with other human polyomaviruses, MCPyV is the first human polyomavirus that has been conclusively shown to be associated with a human malignancy. In approximately 80%-97% of MCC tumours, the MCPyV genome is integrated into the host chromosome in a clonal pattern, which suggests that MCPyV integration precedes clonal expansion of the tumour cells (Feng et al., 2008). Following these findings several others have reported similar statistics for clonal integration of the virus genome into the cellular genome of MCC tumours (Laude et al., 2010, Martel-Jantin et al., 2012 and Sastre-Garau et al., 2009) and MCC cell lines (Fischer et al., 2010). In addition, MCC tumour metastases were also found to be MCPyV positive and possess the same integration patterns as the original tumour (Laude et al., 2010).

Serological data from patient blood detecting MCPyV structural proteins, VP1 and VP2 suggests that the majority of the general population is seropositive, with 80% of the adult population positive, while 50% of children under the age of 15 are positive (Kean et al., 2009). As such MCPyV is probably a common skin commensal. Interestingly, in addition to MCC samples, MCPyV DNA has been isolated from Kaposi's sarcoma (Katano et al., 2009), small cell lung carcinoma (Andres et al., 2009) and various melanoma skin cancers (Kassem et al., 2009). Although, whether MCPyV is a contributing factor to these cancers is controversial and yet to be fully demonstrated. However, there is a more significance correlation between MCPyV and squamous cell carcinoma (SCC) recently highlighted, with the presence of MCPyV in 40% of cutaneous SSC cases (Reisinger et

al., 2010). Similar findings to MCC have been demonstrated with mutated non-replicating genomes identified contained truncated versions of LT. However, further characterisation of the role of MCPyV in SSC is now required.

1.4.2.1. Epidemiology of MCPyV

MCPyV is thought to be acquired in early childhood, causing a widespread and asymptomatic infection in immunocompetent individuals. MCPyV is typically detected in most of the MCCs and as a result is suspected as one of the causative roles in carcinogenesis of the MCC. Recent molecular and serological data showed that MCPyV infection is most common in the upper and lower respiratory tract samples, and also found in tonsils, nasal swabs and nasopharyngeal aspirates in adults (Kantola et al., 2009). Seroprevalence of MCPyV in the general population is approximately 61 to 96.2%, with seroprevalence in adults over age 80 higher than 90% (Nicol et al., 2013; Zhang et al., 2014). On the other hand, the seroprevalence among children aged 1 to 4 years is approximately 40%, which is increased to 87% in children aged 15 to 19 years (Nicol et al., 2013).

1.4.2.2. MCPyV genome

Similar to other polyomaviruses, the MCPyV genome comprises 5387 base pairs, organised into three distinct regions; the non-coding control region (NCCR) containing the viral promoters and bi-directional origin of replication, and the early and late protein coding regions. Figure 1.9 illustrates the genomic organisation of MCPyV. Genomic sequence analysis shows that MCPyV is closely related to other polyomaviruses. Specifically, phylogenetic studies comparing data from all polyomavirus structural genes and LT sequences, demonstrated that surprisingly MCPyV is most closely related to MPyV and Chimpanzee polyomavirus (ChPyV), compared to SV40 (Siebrasse et al., 2012b).

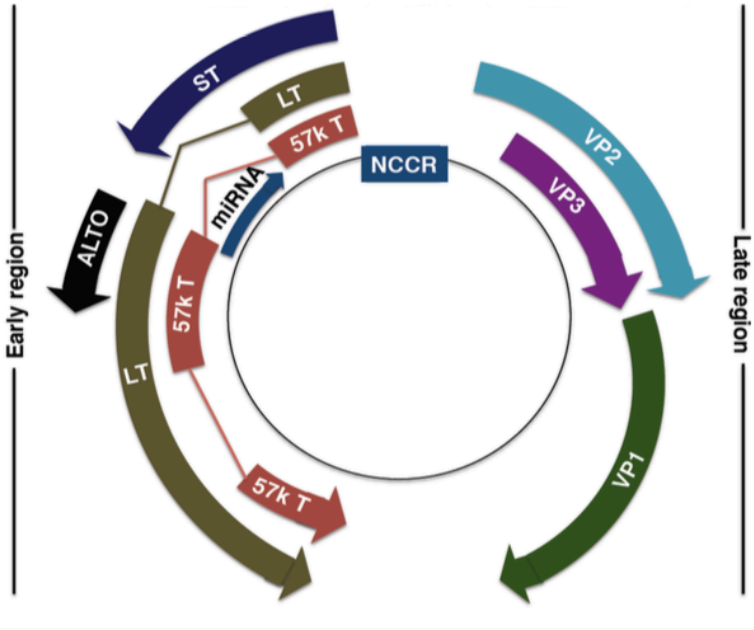

Figure 1.9: Genome organisation of MCPyV.

Schematic representation of genome organization of MCPyV divided into three distinct regions. Non-coding region (NCCR) comprises origin of replication and bi-directional promoters. Early gene region: Large T antigen (LT), small T antigen (ST), 57kT antigen (57kT), alternative T antigen open reading frame (ALTO), and microRNA (miRNA). Late gene region: capsid proteins (VP1-3). Image taken from Stakaityte et al., (2014).

1.4.2.2.1. MCPyV Origin of Replication

The MCPyV non-coding control region (NCCR) contains the origin of replication, which is approximately 71 base pairs in length. The origin of replication contains an AT-rich region, an early enhancer domain and a binding site for the LT antigen. The binding site is composed of ten repeating guanine-rich pentanucleotide sequences (PS), in which eight of them correspond to the general polyomavirus consensus of 5′-GAGGG-3′. However the other two PS are different to ones to those found in other polyomaviruses. In MCPyV these unique remaining PS are 5′-GGGGC-3′ and 5′-GAGCC-3′. Mutational analysis has shown that only four of the eight of these PS are essential for origin replication activity. However single point

mutations within this region can reduce LT assembly on the origin, resulting in elimination of viral replication (Kwun et al., 2009). Kwun and colleagues also demonstrated that tumour-derived LT containing truncating mutations in either the origin-binding domain or the helicase domain also prevent LT-origin assembly.

1.4.2.2.2. MCPyV T antigens

The genes encoding the early antigens of MCPyV, also known as T antigens are approximately 3 kbp and the resulting transcrips are differentially spliced to produce mRNAs encoding the large T antigen (LT), the small T antigen (ST) and the 57 kDa T antigen (57kT) (Feng et al., 2008). All the T antigens share the same short amino-terminal sequence, which consists of the conserved CR1 epitope, which is functionally similar to the cell transforming region of adenoviruses and DnaJ domain that is essential for binding to the cellular heat shock protein Hsc70 (Feng et al., 2008). Alternative splicing produces a distinct carboxy-terminus, which determines the variability in the functions of the T antigen spliced products. Figure 1.10 illustrates the schematic presentation of each different spliced product of MCPyV T antigens and their protein binding sites.

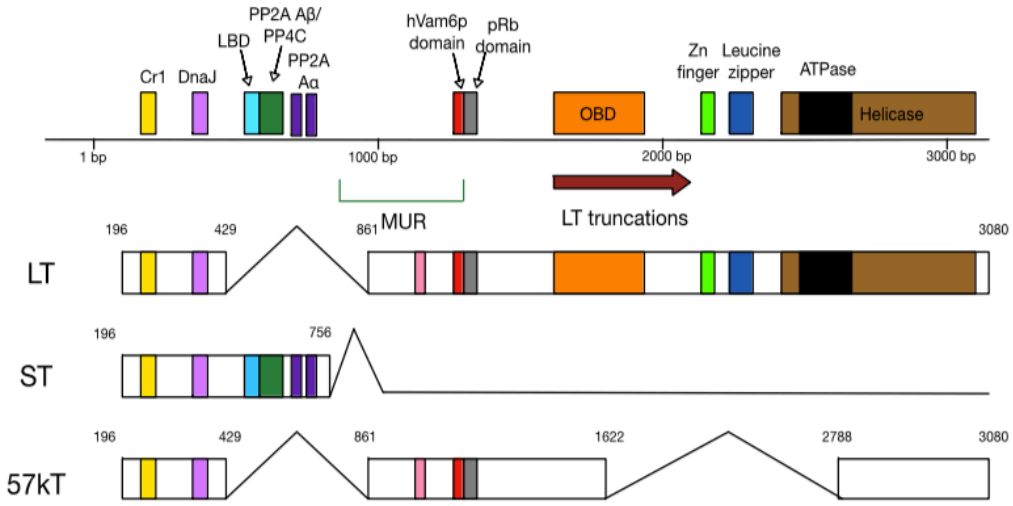

Figure 1.10: Mapping of the multiply-spliced MCPyV T antigens.

The T antigens of MCPyV are LT, ST and 57kT. All three encode CR1 (yellow, LXXLL) and DnaJ (lilac, HPDKGG) domains. ST contains two PP2A Aα binding sites (R7 and L142), a PP2A Aβ/PP4C binding site (amino acids 97–111) and an large T-stabilisation domain (LSD, amino acids 91–95). LT shares the pRb binding domain with 57kT; in addition, it has unique origin binding (OBD), zinc finger, leucine zipper, ATPase and helicase domains. The MCPyV-unique region (MUR) of LT contains the hVam6p binding site. Image taken from Stakaityte et al., (2014).

1.4.2.2.2.1. MCPyV Large T antigen (LT)

The MCPyV LT protein comprises approximately 816 amino acids and its mRNA composed of two exons. Similar to the other polyomaviruses, the MCPyV LT gene contains major functional domains, such as a highly conserved pRb binding domain (LxCxE), an origin binding domain (OBD) and a nuclear localisation signal (NLS) (Shuda et al., 2008). The NLS functions in nuclear localisation of LT when expressed in mammalian cells (Liu et al., 2011b). Interestingly, although MCPyV LT possesses similar binding domains to SV40 LT, they only share approximately 30% sequence identity (Topalis et al., 2013), indicating novel functional regions may be present within the MCPyV LT. For example, MCPyV LT possess an unique region (MUR), approximately 200 amino acid sequence (Liu et al., 2011b) and also encodes a virus miRNA important in regulating early gene expression (Seo et al., 2009).

1.4.2.2.2.2. MCPyV Small T antigen (ST)

The MCPyV ST encodes a protein comprising 186 amino acids. The ST has a major role in viral replication as well as cellular transformation. It shares the common J domain, but the unique carboxy-terminal region is produced by transcriptional read-through of the exon splice site used by both the 57kT and LT transcripts. This unique region contains the protein phosphatase 2A (PP2A) Aα subunit binding site, which is important for virus replication and virus-induced transformation in other polyomaviruses (Pallas et al., 1990). Recently, a PP2A Aβ and/or protein phosphatase 4C (PP4C) binding site has also been discovered located near its carboxy terminus, which may have a role in protecting MCPyV from the cellular immune response (Griffiths et al., 2013). Following this discovery, another MCPyV ST domain was identified, the LT-binding domain (LBD). LBD functions to stabilise LT and aids in the replication of the MCPyV genome (Kwun et al., 2013).

1.4.2.2.2.3. MCPyV 57 kiloDalton T Antigen (57kT)

The MCPyV 57kT is a 432 amino acids. It shares the common J domain region with LT and ST, and possess similar protein binding domains such as Hsc70, CR1 epitope, MUR and pRb domains. Little information exists about the role of 57kT. However 57kT has been shown to have a high degree of homology with SV40 17kT, suggesting that it could function independently and in cooperation with the T antigens in promoting host cell proliferation *in vivo* (Comerford et al., 2012; Zerrahn et al., 1993).

1.4.2.2.3. Alternative T antigen open reading frame

Recently an overprinted gene within the T antigen locus was discovered, namely the alternative T antigen open reading frame (ALTO). ALTO contains the 200 amino acid MUR region of LT, in the +1 frame relative to

the second exon of LT gene and expressed during viral genome replication. Through the phylogenetic tree analysis, ALTO is believed to be evolutionarily related to the middle T antigen of murine polyomavirus (Carter et al., 2013). The start codon of ALTO overlaps with the YGS/T motif of LT and is located near the pRb binding domain (Carter et al., 2013).

1.4.2.2.4. MCPyV Late Proteins

The late MCPyV region, by differential splicing and internal translation, produces three capsid proteins: VP1, VP2, and VP3. The major capsid protein VP1 is the major component of the virus capsid consisting of 72 pentamers with a 5:2 ratio of the minor protein VP2. Both VP1 and VP2 have been shown to self-assemble into virus-like particles *in vitro* (Touze et al., 2010). VP3 is a product of internal translation of VP2, surprisingly however, it does not form part of the native MCPyV capsid (Schowalter and Buck, 2013). The virus capsid is unenveloped and is about 40-55 nm in size, comparable to other polyomaviruses, despite the absence of VP3.

The crystal structure of VP1 was determined as a symmetrical, ring-shaped homopentamer with the five monomers arranged around a central five-fold axis. Each VP1 monomer is composed of two antiparallel β sheets, which form a β-sandwich with jelly-roll topology. Variable loops create unique interaction surfaces on the outer surface of the pentamer (Neu et al., 2012). VP1 has a nuclear-localisation signal (NLS) at its amino-terminus, and shows a diffuse nuclear pattern. VP2 on the other hand seems to lack a NLS and is localized in the cytoplasm. However, co-expression of VP1 redistributes VP2 to nuclear compartment (Schowalter and Buck, 2013). VP2 seems to be dispensable for most entry steps in some cell lines, as it does not affect trafficking, viral DNA packaging, or binding to cellular receptors (Neu et al., 2012; Schowalter and Buck, 2013).

1.4.2.2.5. MCPyV MicroRNA

In addition to the structural proteins, the late region also encodes a 22-nucleotide-long microRNA (miRNA), MCPyV-miR-M1-5p. The miRNA is transcribed from the antisense strand of the LT coding region (Seo et al., 2009). Recent analysis suggests that the MCPyV-miR-M1-5p might regulate the expression of the early genes, reducing the levels of early gene transcripts. This is due to its complementarity with a section of the LT transcript. It may also have a role to play in cellular transformation, as its expression is preserved in at least half of MCPyV-positive MCC tumours (Lee et al., 2011).

1.4.2.3. The Lifecycle of MCPyV

MCPyV virus particles are chronically shed from human skin, indicating that the natural host cell may reside in the epidermis (Schowalter et al., 2010). At present, only a limited number of human-derived primary keratinocytes and transformed melanocytes have been shown to be susceptible to MCPyV infection. However, it is possible to propagate the virus in human embryonic kidney cell-derived cultures (HEK-293), where LT and ST are over-expressed *in trans*, also known as 293-4T cells (Schowalter et al., 2011). This system is now used to to study the life cycle of MCPyV.

1.4.2.3.1. MCPyV Attachment and Entry

Unlike most polyomaviruses which utilize gangliosides or sialic acid-containing glycolipids, the initial stages of host cell attachment for MCPyV appear to involve glycosaminoglycans, in particular heparan sulphate and chondroitin sulphate. MCPyV is also able to bind gangliosides, specifically Gt1b, which carries three different sialic acids, and is probably required for post-attachment entry (Schowalter et al., 2011). Figure 1.11 illustrates the current model of MCPyV entry, a two-step attachment-and-entry process involving two separate types of host cell plasma membrane factors. The

utilisation of glycosaminoglycans by MCPyV for cellular attachment is similar to the entry tactics of papillomaviruses, which are exclusively tropic for keratinocytes, a type of epithelial cell. This is a possible example of convergent evolution, and further suggests the epidermis as the natural host reservior for MCPyV.

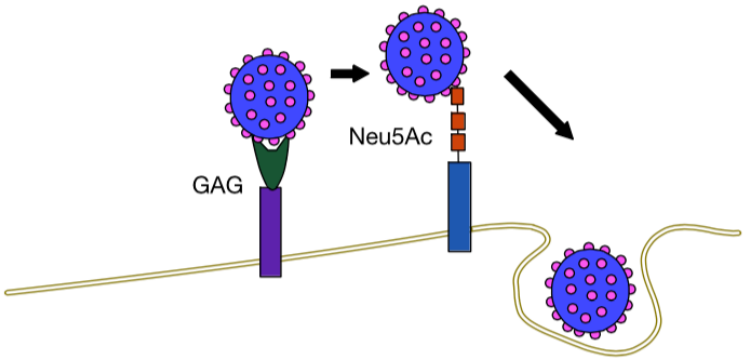

Figure 1.11: Two-step attachment and entry receptors of MCPyV.

Initial attachment involved the MCPyV binds to glycosaminoglycan (GAG), such as heparan sulfate. The second step involved binding to Neu5Ac-ganglioside to facilitate viral entry. Image taken from Stakaityte et al., (2014).

1.4.2.3.2. MCPyV Replication

MCPyV is able to complete its replication cycle in the host cell nucleus and form virions, without inducing tumourigenesis in permissive cells. As a small double-stranded DNA virus, it relies on multiple host factors to successfully transcribe its genome and replicate. The T antigens are vital for this purpose and are expressed immediately upon entry into the nucleus of the host cell. Similar to other polyomaviruses, these gene products induce the host cell to enter S-phase, altering the cellular environment to be preferable for virus replication. Once sufficient levels of the T antigens are present, it is thought that the MCPyV-encoded miRNA inhibits further early gene transcription in a negative feedback loop, thus shifting the focus to genome replication and the expression of the late region encoding the capsid proteins (Seo et al., 2009).

Similar to other polyomaviruses, expression of LT is thought to initiate viral genome replication. In SV40, LT oligomerises to form hexameric molecules, which then bind to the origin of replication (Wessel et al., 1992). The LT helicase domain is then responsible for unwinding genomic DNA allowing replication to proceed in a bidirectional manner. The origin of replication core region of MCPyV is composed of a poly(T) rich tract and eight GAGGC-like motifs, which are required for initiation of replication (Harrison et al., 2011). In addition, MCPyV LT also possess several unique features that affect virus replication. For example, LT interacts with several novel cellular host proteins such as hVam6p, Brd4 and DDR factors, which are believed to play important roles in MCPyV LT-mediated DNA replication (Liu et al., 2011b; Tsang et al., 2014; Wang et al., 2012).

LT is necessary for the replication of MCPyV DNA, however it does not facilitate the process efficiently on its own. ST is also needed to enhance replication, with knockdown of ST leading to inhibition of replication (Kwun et al., 2013). ST is thought to specifically play a role in genome replication by promoting the hyper-phosphorylation of the translation regulator eIF4E binding protein (4E-BP1) (Shuda et al., 2011b), resulting in an increase in the production of cellular proteins and host factors necessary for viral replication. In addition, ST also prevents the turnover of LT by targeting the cellular SCF ubiquitin E3 ligase, Fbw7. Fbw7 acts as the recognition component that targets LT for proteasomal degradation (Welcker and Clurman, 2008). Fbw7 is important as a tumour suppressor protein and is deregulated in several human cancers (Maser et al., 2007; Wood et al., 2007), with loss of Fbw7 resulting in tumourigenesis and genetic instability (Mao et al., 2004; Rajagopalan et al., 2004).

1.4.2.3.3. MCPyV Assembly and Egress

Little is presently known about MCPyV assembly and egress from the host cell (Neumann et al., 2011). There is a suggestion that LT-mediated sequestration of hVam6p to the nucleus during virus replication might contribute in viral uncoating or to egress via lysosomal processing (Liu et

al., 2011b). MCPyV does not encode an agnoprotein, which is known to play an essential role in virus particle assembly and maturation in other polyomaviruses, such as SV40, JCPyV and BKPyV (Khalili et al., 2005). Moreover, MCPyV does not encode an equivalent of SV40 VP4, which has been shown to trigger lytic virion release (Daniels et al., 2007). Thus, alternative pathways must be involved in MCPyV assembly and egress, however, these are yet to be elucidated. However, there is the possibility that the natural process of keratinocyte desquamation in the skin might serve as mechanism of MCPyV virion release.

1.4.2.4. MCPyV and Tumourigenesis

The role of MCPyV as the causative factor in the development of MCC is closely related to integration of the viral genome and to defective viral replication in the tumour cells, resulting in aberrant expression of the ST and truncated LT antigens, which eventually leads to cellular proliferation (Moore and Chang, 2010b).

Upon MCPyV integration, the viral genome retains full-length LT, which is capable of initiating host DNA replication. This unlicensed replication will result in replication fork collision and DNA breakage, which will eventually lead to cytopathic cell death (Shuda et al., 2008). Thus a second mutation is needed to eliminate LT-initiated DNA replication for the cell to survive once MCPyV has integrated, and only a cell with both mutations is likely to develop into a tumour. The requirement for two separate events prior to tumourigenesis may help to explain why MCC is so rare (Moore and Chang, 2010b). It is also possible, however, that LT may first become truncated, with MCPyV going through rolling circle replication prior to integration (DeCaprio and Garcea, 2013). Expression of truncated LT leads to defective DNA repair and cell cycle arrest upon exposure to ultraviolet (UV) radiation (Demetriou et al., 2012), and this increase in genomic instability may promote integration of the viral genome. Besides the mutations within LT antigen, several groups have also reported mutations

in the origin of replication and the VP1 gene in MCC-derived MCPyV genomic sequences that prevent efficient replication and progeny virion production, respectively (Feng et al., 2011; Kassem et al., 2008; Kwun et al., 2009; Neumann et al., 2011).

The exact functions and transforming activities of the MCPyV truncated large T antigen are unknown. However, the truncated version of the LT antigen was shown to be more effective in promoting growth of human and mouse fibroblasts compared to full length LT and the 57kT protein (Cheng et al., 2013). The reason why truncating mutations occur in MCPyV is unknown, as this has not been found in other polyomaviruses. The enhanced tumourigenicity of truncated forms of the LT antigen found in MCC might be due to removal of C-terminal residues that have been shown to possess growth inhibitory effects in several cell types (Liu et al., 2013). Interestingly, the truncated version of LT expressed in different tumours varies in size, depending on the site of their deletions (Kassem et al., 2008). However, all result in the inhibition of viral replication that may result in cell lysis and death. As such, there is a strong pressure in tumour cells to inhibit viral replication (Moore and Chang, 2010a). However, the integrated replication defective virus in MCC cells retains motifs that potentially contribute to uncontrolled cell growth and cell survival (Moore and Chang, 2010b). This results in a defective integrated virus, which expresses viral ST and the truncated version of the LT protein. Figure 1.12 illustrates the mutation events that occurring in the viral genome and truncation of LT in MCPyV.

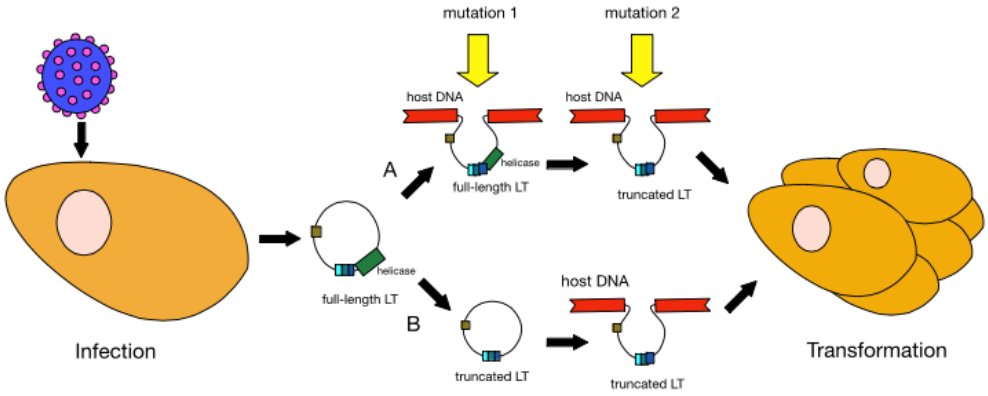

Figure 1.12: Mechanism by which MCPyV may induce MCC tumourigenesis, involving two mutation events.

In mechanism A, the first mutation involves viral genome integration into the host chromosomes; which leads to autonomous viral origin DNA replication and wild type of T antigen is expressed in the cells. The replicated DNA strands may collide with cellular replication forks causing DNA fragmentation. When the second mutation occurs resulting in viral LT antigen losing its helicase binding region, this eliminates the ability for the virus to replicate. In mechanism B, the truncation of LT is thought to occur before integration. Either way, these changes in the virus lead to cellular transformation and tumour proliferation. Image taken from Stakaityte et al. (2014).

1.4.2.5. Differences in MCPyV T antigen function

Considering the extensive research performed characterising the functions of the SV40 T antigens, it was presumed that the MCPyV LT antigen would be the major oncogene and major contributing factor to the development of MCC, as overexpression of SV40 LT is sufficient to transform mouse fibroblasts. In contrast, MCPyV ST was found expressed in most MCC samples, approximately up to 97% occurrence in MCC cases. Moreover, ST expression, even at low levels, is essential for tumourigenesis, as knockdown of MCPyV ST alone showed total inhibition of the growth of MCPyV-positive MCC cells (Shuda et al., 2011a). LT DNA is present at an average of 5.2 copies per tumour cell and LT protein expression has also been detected in the nuclei of these cells (Shuda et al., 2009). Surprisingly, the expression levels of LT protein in MCCs range from barely detectable to extremely high levels. This raises a question of whether MCC tumours with low or undetectable levels of MCPyV LT protein expression have additional specific mutations in either oncogenes or tumour suppressor

genes that might also contribute to cell transformation and tumour formation.

1.4.2.5.1. Role of MCPyV LT

LT is highly expressed in 75% of MCPyV-positive MCC tumour samples (Shuda et al., 2009). However, expression of full length or truncated LT is insufficient to initiate cellular transformation (Shuda et al., 2011b). As such, MCPyV LT is believed to be important in enhancing proliferation and survival of MCC tumours (Houben et al., 2010a), but not in inducing transformation. This might be due to the inability of full length and truncated LT to interact with p53, diminishing the transforming activity of MCPyV LT (Cheng et al., 2013). However, the truncated LT has been shown to be more efficient at inducing cellular proliferation compared to the full length construct, which has growth inhibitory effects contained with the last 100 amino acids residues of the C-terminus (Cheng et al., 2013). MCPyV LT has been shown to be involved in viral replication and manipulation of host pathways through multiple cellular protein-protein interactions.

1.4.2.5.1.1. Interaction of MCPyV LT with tumour suppressor proteins

The transforming ability of LT in polyomaviruses is dependent upon manipulation of the key tumour suppressor proteins, p53 and Rb. The cell cycle checkpoint protein p53 is activated by cellular stress and blocks genome replication under conditions that could perpetuate DNA damage-induced errors (Vousden and Lane, 2007). This is achieved by p53 promoting the expression of genes that induce DNA repair, cell-cycle arrest and apoptosis. Binding of SV40 LT to p53 inhibits this transcriptional activity and therefore permits inappropriate cellular proliferation (Lane and Crawford, 1979). The Rb protein functions to control entry into S-phase of the cell cycle. In resting cells pRb is bound to E2F, however upon activation of cyclin-dependent kinases pRb is phosphorylated which disrupts this complex. This permits E2F to activate the transcription of genes required

for cell cycle progression. The conserved LXCXE motif within LT mediates binding to Rb and inhibits the interaction with E2F (Figure 1.13). This bypasses the S-phase checkpoint and leads to uncontrolled cell proliferation.

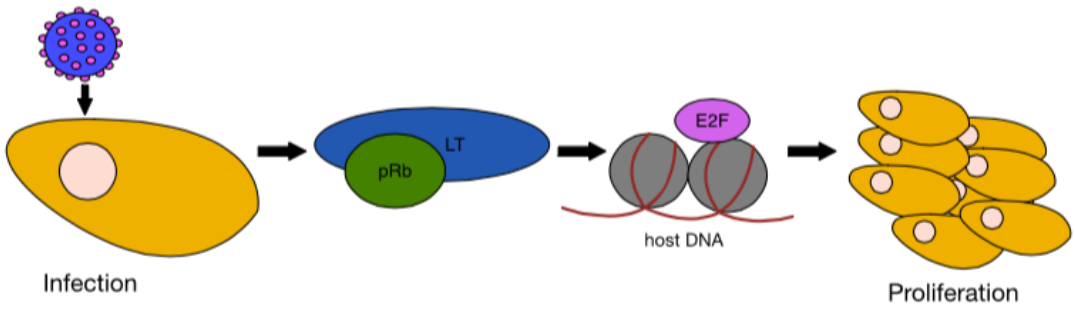

Figure 1.13: Effects of LT expression on cell proliferation.

During infection of MCPyV, expression of LT antigen binds to the tumour suppressor protein, pRb and deactivates it. The released of the E2F factors resulting the transcription of cell cycle progression-associated gene and entering the S-phase to allow unlicensed viral replication and leads to cell proliferation. Image taken from Stakaityte et al. (2014).

In contrast to other polyomaviruses, MCPyV LT is truncated in tumour cells. The majority of reported LT mutations involve truncation of the entire C-terminal domain, suggesting an additional selective pressure upon transforming cells for removal of this region of LT. Truncated LT has also been shown to be more efficient at inducing cellular proliferation than full length LT (Cheng et al., 2013). Following this, recent studies have demonstrated that MCPyV infection activates the cellular DNA damage response in a manner dependent upon the LT carboxy-terminus (Li et al., 2013). Activation of DNA damage kinases was found to promote cell cycle arrest in a p53-dependent manner. Comparable to this, SV40 infection also activates the ATM DNA damage pathway (Shi et al., 2005). However, cellular proliferation is not restricted as the SV40 LT inhibits downstream activities of p53. Therefore MCPyV LT truncations are likely to be selected to avoid activation of the DNA damage response (DDR) in the absence of p53 inactivation.

1.4.2.5.1.2. Interaction of MCPyV LT with hVam6p

Sequence comparison of polyomavirus LT have highlighted that some of the binding sites or domains within MCPyV LT appear to be distinct from other polyomaviruses. A recent review highlights that the MCPyV T antigens might utilise novel cellular targets proteins allowing MCPyV T antigens to perform distinct functions from other polymaviruses. These observations are supported by tandem affinity pull-down assays which have demonstrated that MCPyV LT uniquely interacts with the cytoplasmic vacuolar sorting protein, hVam6p (Liu et al., 2011a). Mutation studies showed that MCPyV LT binds to hVam6p via its unique region, MUR (Liu et al., 2011b). hVam6p is relocalised from the cytoplasm to the nucleus upon expression of MCPyV LT, disrupting its lysosome clustering. This interaction and relocalisation of hVam6p is not observed upon expression of SV40 LT. hVam6p is believed to function as an antiviral host factor. Overexpression analysis of hVam6p showed its ability to significantly reduce the number of MCPyV virions by approximately 90% (Feng et al., 2011). In addition, mutation studies abrogating the LT-hVam6p binding domain significantly increased infectious virion production between 4-6 fold (Feng et al., 2011; Liu et al., 2011b). However the mechanism involved is yet to be determined. This suggests a possible role of hVam6p as a MCPyV anti-viral cellular response factor.

1.4.2.5.1.3. Interaction of MCPyV with Brd4

MCPyV LT-mediated viral replication is associated with the interaction of MCPyV LT and the chromatin-associated bromodomain containing protein 4 (Brd4). Brd4 acts by recruiting cellular replication factors required for viral replication. For example, the LT-Brd4 interaction facilitates recruitment of the cellular replication factor C (RFC) to MCPyV replication complexes (Wang et al., 2012). RFC then loads PCNA clamp and DNA polymerase δ, both of which are required for elongation of MCPyV DNA (Feng et al., 2011). Viral DNA replication can be inhibited by expression of a dominant negative Brd4 inhibitor (Wang et al., 2012), highlighting the important role

of the LT-Brd4 interaction in facilitating successful viral DNA replication.

1.4.2.5.1.4. Interaction of MCPyV LT with survivin

MCPyV LT also targets survivin, a member of the inhibitor of apoptosis protein family that is upregulated in a number of lymphomas and metastatic melanoma (Ambrosini et al., 1997). Survivin functions as an inhibitor of apoptosis by prolonging cell viability, and later contributes to cellular transformation by facilitating the insurgence of mutations and promoting cellular resistance to chemotherapy. Knockdown of MCPyV T antigens in MCPyV positive MCC cells shows that survivin mRNA and protein levels fall, resulting in MCC cell death (Arora et al., 2012a). Interestingly, survivin gene transcription is enhanced as well as other S-phase proteins, including E2F1 and cyclin E, in LT-expressing cells (Arora et al., 2012a). As survivin protein expression is critical to the survival of MCPyV-positive cells, the small molecule survivin inhibitor, called YM155, potently and selectively shown to initiates irreversible and programmed MCPyV-positive MCC cell death (Arora et al., 2012b). Besides MCPyV, both SV40 and JCPyV infections exhibit upregulation of survivin expression (Ambrosini et al., 1997; Jiang et al., 2004; Pina-Oviedo et al., 2007; Raj et al., 2008). As such, identifying cellular pathways, such as those involving survivin, could lead to the rapid identification of additional drug candidates for treating virus-induced cancers.

1.4.2.5.1.5. Interaction of MCPyV LT with DNA damage response (DDR) factors

DNA damage response (DDR) factors are thought to play a role in MCPyV LT-mediated DNA replication (Tsang et al., 2014). The DNA damage response pathways, namely ATM and ATR, are redistributed in the nucleus upon expression of LT, specifically they are localised to replication foci where they co-localise with LT, to support efficient viral DNA replication (Tsang et al., 2014). Besides MCPyV, HPV infection has also been shown

to induce DDR activation and recruitment of these factors at their viral replication sites (Gillespie et al., 2012), suggesting similar host factors may be involved in MCPyV replication and the virus life cycle.

1.4.2.5.2. Role of MCPyV Small T (ST) antigen

MCPyV ST is expressed in most MCC samples, in approximately 97% of all MCC cases. It has also been suggested that low level ST protein expression is sufficient for tumourigenesis, as siRNA-mediated depletion of MCPyV ST showed total growth inhibition of MCPyV-positive MCC cells (Shuda et al., 2011a). Moreover, expression of ST is also sufficient to induce rodent fibroblast transformation, loss of contact inhibition, anchorage-dependent and serum independent growth. In contrast, these phenotypic changes are not observed in the cells expressing full length or truncated forms of LT (Shuda et al., 2011b).

1.4.2.5.2.1. Interaction with protein phosphatase

MCPyV ST contains a binding domain for PP2A, as well as another cellular phosphatase, PP4C (Griffiths et al., 2013). However unlike other polyomaviruses, the transforming effect of MCPyV ST may not involve its binding and interaction with PP2A (Shuda et al., 2011a). Although MCPyV ST does bind to the PP2A structural Aα subunit and the catalytic subunit, no effect on host cell or virus replication has been identified upon deletion of this domain. Specifically, mutants with disrupted MCPyV ST-PP2A Aα interaction could still induce both cell transformation and anchorage-dependent colony formation (Shuda et al., 2011b). In contrast, in SV40, binding of PP2A resulted in altered binding to substrates and specificity of the PP2A holoenzymes (Pallas et al., 1990; Sontag et al., 1993). As such, this ST-PP2A Aα interaction is critical for SV40 induced transformation and cell proliferation. In contrast, the mode of action of MCPyV ST oncogenicity may utilise other mechanisms, specifically through its interactions to PP2A Aβ and/or PP4C.

1.4.2.5.2.2. ST dysregulated cap-dependent translation

MCPyV ST is also believed to function downstream of the mTOR signalling pathway (Figure 1.14), by reducing the turnover of phosphorylated 4E-BP1 and leading to enhanced eIF4E activity and increased protein production and cell proliferation (Shuda et al., 2011b). MCPyV ST phosphorylates and inactivates the translational inhibitor 4E-BP1, a key regulator for translation of initiation factor eIF4E (Shuda et al., 2011b). This finding is distinct from SV40, which promotes the Akt pathway by inhibition of PP2A Aα activity resulting in dephosphorylation of Akt (Rodriguez-Viciana et al., 2006; Zhao et al., 2003).

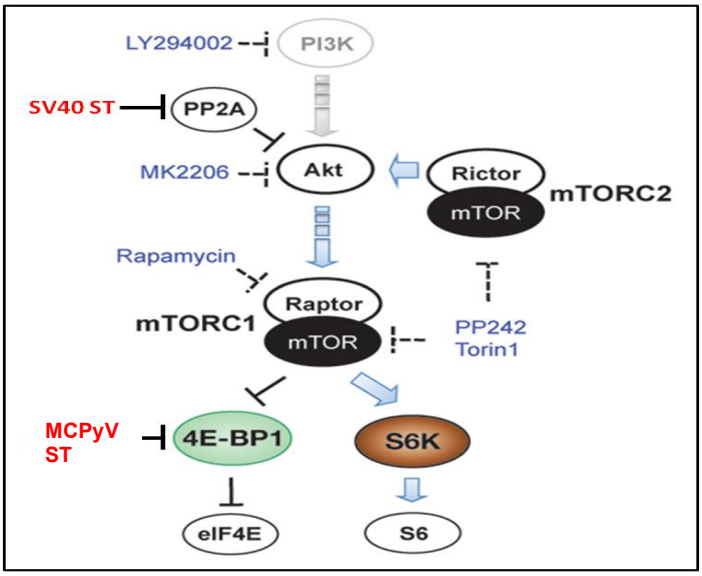

Figure 1.14: The different target proteins of MCPyV ST and SV40 ST in mTOR signaling pathway.

Akt-mTOR pathway involve activities of Akt, mTORC1 (raptor complex), mTORC2 (Rictor complex), and S6K kinases. MCPyV ST targets the 4E-BP1, which prevents 4E-BP1 from sequestering the eIF4E cap-dependent translational factor; compared to SV40 ST, which inhibits PP2A leading to Akt phosphorylation. Several kinase inhibitors such as LY294002, MK2206, rapamycin and PP242 Torin 1 with their respective targets also shown in the figure. Adapted from Shuda et al., (2011).

1.4.2.5.2.3. ST prevents proteasomal degradation of LT

A novel LT-binding domain (LBD) has also been identified within the MCPyV ST protein, which is thought to play a role in preventing LT

proteolysis (Kwun et al., 2013). Interestingly, a mutation within the LBD region ablates the ability of MCPyV ST to induce transformation (Kwun et al., 2013). This mutant does not effect ST's ability to bind to PP2A, confirming that ST induced transformation is independent of its interaction with PP2A. Interestingly however, MCPyV ST targets the cellular ubiquitin ligase SCF^{Fwb7} resulting in the stabilization of cell cycle regulators, such as c-Myc and cyclin E (Kwun et al., 2013).

1.4.2.5.2.4. ST involvement in host innate immune response

MCPyV ST has been shown to inhibit NF-κB mediated transcription via an interaction with NEMO. This renders NF-κB incapable of translocating to the nucleus and activating transcription (Griffiths et al., 2013). This interaction is dependent on ST binding to the cellular phosphatase PP2A Aβ and/or PP4C, which promote dephosphorylation of the IKK complex. This ST-mediated disruption of the NF-κB pathway may help to downregulate the host innate immune response and enhance persistence of the MCPyV infection. Besides MCPyV, other viruses have also been shown to be capable of preventing NF-κB mediated signaling (Le Negrate, 2012). HPV E7 and HCV core protein inhibit IKB degradation preventing NF-κB translocating to the nucleus, while cytomegalovirus (CMV) disrupts NF-κB activation through a direct interaction with NEMO (Fliss et al., 2012; Joo et al., 2005; Randall et al., 2012; Spitkovsky et al., 2002).

1.4.2.5.2.5. ST promotes cell motility and migration

Knight et al (2015) demonstrated that MCPyV ST promotes the destabilisation of the host cell microtubule network through an interaction with the cellular microtubule degrading protein, stathmin. This destabilisation of microtubules enhances cell motility of ST-expressing cells and may have implications for the highly metastatic nature of MCC (Knight et al., 2015). Moreover, regulation of this process involves binding of ST

with the cellular catalytic subunit of PP4C, which enhances the dephosphorylation and activation of stathmin.

1.5. Regulation pathways in cancer

Quantitative proteomic analysis performed using cells expressing MCPyV T antigens, several cancer-related pathways were found to be differentially affected. The elucidation of possible functions of MCPyV ST and truncated LT will be discussed regarding the basis of these pathways, in particular focussing on their possible roles in dysregulating the cell cycle, apoptosis, cell junctions and cell motility.

1.5.1. Cell cycle regulations

Regulation of the cell cycle involves numerous mechanisms, including the regulation of cyclin-dependent kinases (CDK) by cyclins, CDK inhibitors, phosphorylation of cellular proteins, cell checkpoint controls and DNA damage effects (Vermeulen et al., 2003). The alteration of this important cellular event can lead to aberrant cell proliferation and development of cancer. Cell division involves two consecutive processes, DNA replication and segregation of replicated chromosomes into two separate cells. Replication of DNA happens during the interphase stage, termed the S-phase. The S phase is preceded by G_1, here the cells prepare for DNA synthesis, following S phase is G_2, a gap where cells prepare for mitosis (M). Thus, G_1, S, G_2 and M phases are the subdivisions of the standard cell cycle (Figure 1.15). Of note is that cells in G_1 can also enter a resting state, G_0 before commitment to DNA replication.

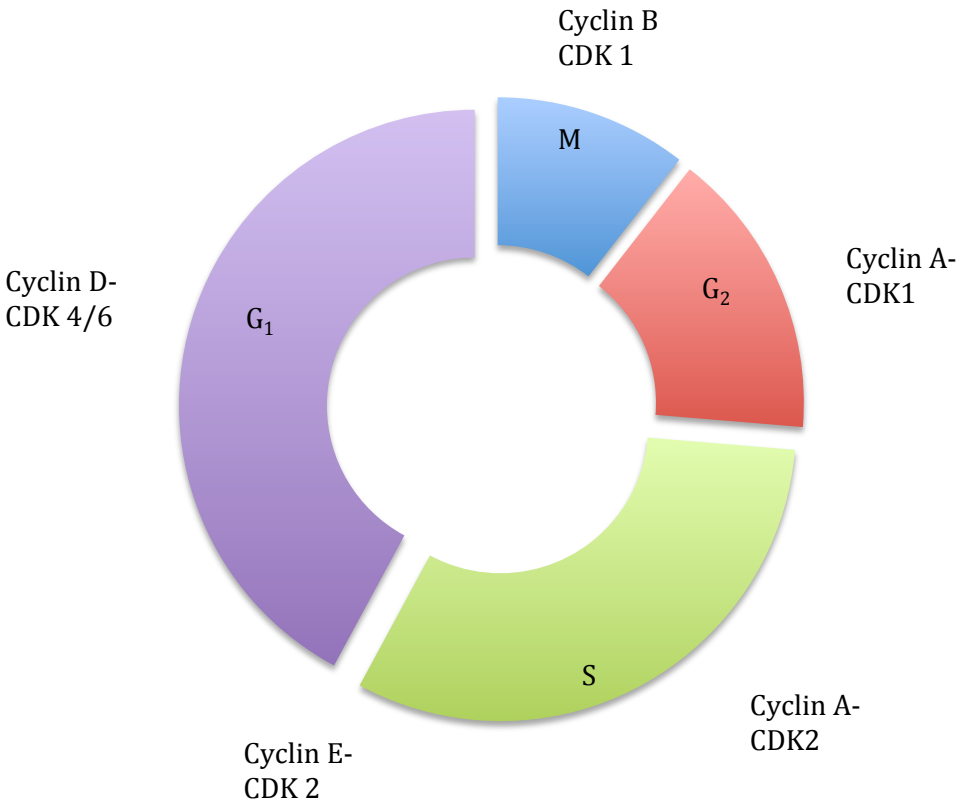

Figure 1.15: Stages in the cell cycle with the regulatory CDKs and cyclins.

The stages of the cell cycle consist of a DNA synthesis (S) phase and mitotic (M) phase, separated with gap (G_1 and G_2). The control of each cell cycle stage is regulated by the complexes of CDKs and cyclins at specific points in the cell cycle. The kinase subunits (CDKs) are expressed along with their activating proteins (cyclins), which the levels falls and increase; regulates the progression of each phases. The association and phosphorylation of the kinase and their cyclins essential in each phases. Adapted from (Suryadinata et al., 2010).

Successful progress through the cell cycle requires the coordination of various macromolecular complexes to regulate synthesis, assembly and movements; here chromosomes must be replicated, condensed, segregated and decondensed (Hartwell and Kastan, 1994). Coordination of these processes are achieved by a series of changes (phase transitions) in the CDKs. In mammalian cells, a succession of kinase subunits (CDK4, CDK2 and CDC2) are expressed along with a succession of cyclins (D, E, A and B), as cells progress from G_1 to mitosis (Sherr, 1993). CDK protein levels remain relatively stable during the cell cycle, but their activating proteins, cyclins, rise and fall in level during the cell cycle (Evans et al., 1983; Pines and Hunter, 1991). Different cyclins are required at different

phases, such as association of cyclin A with CDK2 is required for passage into S-phase, while association with CDK1 is required for entry into mitosis (M) phase (Vermeulen et al., 2003).

1.5.1.1. Restriction points and checkpoints

The restriction point is a point of no return in G_1, in which the cell is committed to cell cycle progression and division. There are various checkpoints ensuring the orderly sequence of cell cycle events (Hartwell and Weinert, 1989). At the G_1-S checkpoint, the control is dependent on p53 levels, whereby the cellular level of p53 is normally low. However, DNA damage can lead to rapid induction of p53 activity (Levine, 1997). This causes a checkpoint arrest, preventing cell cycle progression to allow DNA repair. If DNA damage occurs during G_2, cells are able to initiate a cell cycle arrest in the presence or absence of p53 (Vermeulen et al., 2003). A second checkpoint involves CDK1, in which mitosis can be prevented by maintaining high levels of CDK1 in its inhibited form. This could be achieved by inhibitory phosphorylation or by sequestration of components of the CDK1-cyclin B complex (Vermeulen et al., 2003).

1.5.1.2. Cell cycle and cancer

Genetic alteration of regulators of the cell division can result in uncontrolled cell proliferation. Therefore dysregulation of the cell cycle is associated with cancer. Mutated genes observed in cancer include genes that encode CDKs, cyclins, CDK-activating enzymes, CK1, CDK substrates and checkpoint proteins (McDonald and El-Deiry, 2000; Sherr, 1996).

1.5.1.3. DNA viruses effect cell cycle regulation

A number of DNA viruses use different strategies to regulate the cell cycle checkpoint and modulate cellular proliferation pathways. They target critical regulators in the cell cycle to provide beneficial conditions to achieve

efficient viral replication (Swanton and Jones, 2001). Many viruses induce quiescent cells to enter the cell cycle to increase pools of deoxynucleotides, and some small DNA viruses promote entry into the S-phase to activate the host cell replication machinery. Alternatively, some larger viruses can arrest cells in specific stages of the cell cycle to limit the competition with the host for replication resources. Arrest at a specific cell cycle stage may inhibit early cell death in infected cells and evade immune defences or assist virus assembly (Bagga and Bouchard, 2014). Cell cycle arrest may also be implicated in helping delay the initiation of the apoptotic cascade in infected cells (He et al., 2010). Arrest at the G2/M checkpoint may also assist the virus to avoid host immune defences by preventing production of new cells (Zeng et al., 2010). As such, the alteration of the cell cycle associated with viral infection contributes to cell transformation, tumour progression and maintenance.

1.5.1.4. Anaphase Promoting Complex (APC)

The anaphase promoting complex (APC), is an E3 ubiquitin ligase required for the ubiquitination and subsequent proteasomal degradation of multiple cell cycle regulatory and effector proteins. Without the APC, cells cannot separate sister chromatids during anaphase, exit mitosis, or properly enter S phase (Thornton et al., 2006). Several viruses have been reported to target the APC due to its important role in the cell cycle. For example, in human cytomegalovirus (HCMV) virus infection, a novel viral regulator protein pUL21, has been shown to induce degradation of specific APC subunits (Fehr et al., 2012). Besides HCMV, a number of viruses that encode APC regulators are known to cause cancer, these viruses include HTLV-1, HPV and HBV (DeCaprio, 2009; Hwang et al., 1998; King et al., 1995; Robert et al., 2002). This also suggests that virus-mediated regulation of APC may be central in the development of cancer. Due to its importance in cell cycle control, the APC is also a potential candidate as an anticancer drug target (Zeng et al., 2010). However, APC targets more than 30 proteins for ubiquitination and degradation, thus inhibition of this

complex would stabilize its substrates, which may be important for virus replication (Peters, 2006).

1.5.2. Cell death and cell survival

Cells can respond to stress in various ways ranging from the activation of survival pathways to the initiation of cell death to eliminate damaged cells. This initial response is to defend against and recover from the stress stimulus. Apoptosis is a programmed mechanism that allows the cell to commit suicide. As such, apoptosis is important for cell survival in multicellular organisms as it is a mechanism to remove damaged or infected cells that may interfere with the normal functioning of the organism. Cells undergoing apoptosis show morphological changes such as shrinkage, blebbing of the plasma membrane, chromatin condensation and DNA fragmentation (Kerr et al., 1972). Typical apoptotic features include: activation of a number of apoptotic protease (caspase) enzymes, PARP cleavage and alterations in expression levels of p53 or Bcl-2 family members. Alteration in the apoptosis process can contribute to tumourigenesis and tumour progression (Fulda, 2010). Many viruses have developed the ability to control host survival and death to ensure efficient propagation while inactivating or avoiding the host immune response during infection (McLean et al., 2008).

1.5.2.1. Viruses disruption of host apoptotic pathways

Prevention of apoptosis during herpes infection, specifically persistent oncogenic viruses such as Epstein-Barr Virus (EBV), is via upregulation of the host cell anti-apoptotic proteins Bcl-2, A20 and Bfl-1 by the multifunctional viral protein LMP-1 (D'Souza et al., 2000; Fries et al., 1996; Henderson et al., 1991). In addition, EBV encodes a homologue of Bcl-2, designated BHRF-1 (Henderson et al., 1993). Other human herpesvirus, such as Kaposi's sarcoma associated herpesvirus (KSHV), also encode

homologues of Bcl-2 and as a result have been shown to block apoptosis efficiently in mammalian cells (Cheng et al., 1997; Sarid et al., 1997).

In addition, viral gene products are also able to modulate a number of regulatory networks that direct cells towards apoptosis. For instance, p53 is negatively regulated by the oncoprotein mouse double minute 2 homolog (Mdm2) and targeted for ubiquitin-mediated proteolysis (Piette et al., 1997). DNA tumour viruses like adenovirus, SV40 and HPV drive infected cells to deregulate growth regulatory pathways via releasing transcription factors, E2F family from pRB complex. This release of E2F activates genes necessary for cell cycle progression, however on the downside the mechanism also activates p53 by the upregulation of $p14^{ARF}$ expression (Bates et al., 1998). As such, these viruses need mechanisms to counteract the upregulation of p53. The SV40 LT antigen sequesters p53 and prevents binding to its recognition element in cellular DNA (Yanai and Obinata, 1994). In contrast, the HPV E6 protein promotes the degradation of p53 by forming a complex with E6-AP, a ubiquitin protein ligase (Scheffner et al., 1990). In addition, KSHV latency-associated nuclear antigen (LANA-1) has been shown to target both pRB/E2F and to interact with p53 (Radkov et al., 2000).

1.5.3. Cell-cell connections

Cells connect to each other through intercellular adhesion. Adhesion occurs through specific cell adhesion molecules, depending on the type of interaction. Cell–cell adhesion is ensured by junction complexes that contains tight junctions (TJ) and adherens junctions (AJ) (Farquhar and Palade, 1963). Cell junctions function to maintain the integrity of epithelial tissues and also regulate signalling between cells. Importantly, dysregulation of cell junctions can lead to oncogenic transformation and metastasis (Talbot et al., 2012).

1.5.3.1. Cell junctions

The tight junction is a multifunctional complex essential for a functional cell adhesive barrier involved in paracellular permeability regulation and establishing cell polarity (Soini, 2012). The junction complex comprises of transmembrane proteins occludin and claudin, in association with junctional adhesion molecules, JAMs (Figure 1.16). The zonula occludens (ZO) proteins are involved in linking these transmembrane proteins with the actin cytoskeleton and also function in the regulation of these signalling complexes (Hartsock and Nelson, 2008). Claudin 1 and claudin-11 have been reported to have roles in cell proliferation, while ZO-1,2,3 have been shown to be implicated in regulatory suppression of cell proliferation and oncogenesis (Aijaz et al., 2006; Matter et al., 2005). ZO-1 has a specific role in reducing cell proliferation, depending on the cellular density via reducing the nuclear accumulation of cell division kinase-4 (CDK4) (Paris et al., 2008).

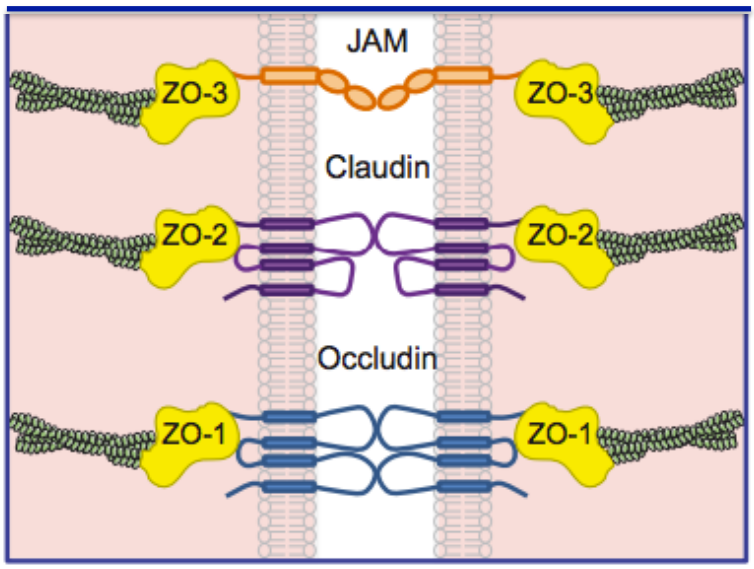

Figure 1.16: Components of the tight junction in polarized epithelial cells.

Tight junction with transmembrane proteins (top to bottom): junctional adhesion molecule (JAM), claudin and occludin. All these proteins are associated with the zonula occludens proteins ZO-1, ZO-2 and ZO-3 through their cytosolic tails, while ZO proteins link the transmembrane proteins to the actin cytoskeleton. Image adapted from Mateo et al., (2015).

Downregulation of tight junction proteins and their associated adhesion factors has been strongly implicated in the transformation and invasion of tumours. Dysregulation of the transmembrane protein occludin has been shown to increase progression and metastatic potential in several cancers (Kurrey et al., 2005; Orban et al., 2008; Tobioka et al., 2004). Specifically, altered levels of occludin and ZO-1 protein expression have been shown when comparing primary and metastatic cells, which suggest that downregulation of the tight junction proteins occur during the metastatic cascade indicating the importance of these proteins in cancer metastasis (Orban et al., 2008).

On other hand, adheren junctions are sites of lateral cell-cell adhesion and have a specific role as anchoring junctions for establishing an intercellular adhesive structure between the cytoskeleton and plasma membrane (Kundu et al., 2008). There are three primary protein families which form adherens junctions, namely cadherins, armadillo proteins and plakins (Dusek and Attardi, 2011). Downregulation of these cell adhesion complexes are essential for separation of cells for metastasis. As such, carcinoma cells have shown significant loss of intracellular adhesive properties (Cavallaro and Christofori, 2004). Here, reduction in expression levels of the invasion suppressor protein E-cadherin coupled with an increased expression of N-cadherin correlates with invasiveness and migration of cancer cells (Beavon, 2000). DNA tumour viruses have also been shown to be involved in promoting loss of cell adhesion. For instance, HPV E6 interacts with E6AP, a ubiquitin protein ligase which promotes degradation of epithelial cell tight junctions (Talis et al., 1998). Moreover, the SV40 ST antigen also promotes redistribution and downregulation of proteins involved in tight junction complexes, such as E-cadherin, ZO-1, claudin 1 and occludin through an interaction with PP2A (Nunbhakdi-Craig et al., 2003). MCPyV infection also leads to the relocalisation of E-cadherin inducing the redistribution of cell membrane adhesion complexes to the nucleus in MCC tumours (Han et al., 2000), although the mechanism involved in this process is yet to be elucidated.

1.6. Thesis Aims

Several studies have demonstrated the importance of the MCPyV T antigens in viral replication and host cell transformation. Both ST and LT expression is detected in most MCC samples indicating significant roles of these T antigens in MCC tumorigenesis. Upon commencing this study, the Whitehouse laboratory had identified a group of proteins that were differentially expressed upon MCPyV ST expression through SILAC-based proteomic analysis. Aligned with this analysis, work in this thesis describes further experiments to determine the effects of both ST and truncated MCPyV LT expression on the cellular proteome. The aims for this thesis are:

1. To screen selected cellular proteins that are differentially expressed in SILAC dataset upon expression of MCPyV ST protein. Quantitative proteomic analysis of this dataset identified several interesting differentially expressed cellular target proteins that were associated with enhancing motility, invasion and migration in various cancers, such as vitronectin (Vn), kinesin-like protein 14 (Kif14) and periplakin (PPL). As such these ST-cellular protein interactions had potential for ST-induced cancer development and might be related to MCPyV functioning.
2. To develop a stable cell line with the ability to inducibly express the MCPyV truncated LT antigen. The production of the MCPyV tLT stable cell lines would allow the screening of cellular differential expression of protein levels using a SILAC quantitative proteomic based assay. Several bioinformatic tools were then utilised to identify significant pathways and protein complexes affected by MCPyV tLT antigen.
3. To evaluate several cellular proteins and pathways that are potentially affected upon expression of MCPyV tLT. In Chapter 5, assays on cell cycle, apoptosis and cell survival pathways as well as cell-cell connections is used to evaluate the effects of MCPyV truncated LT expression.

Chapter 2

Materials and Methods

2.0. Materials and methods

2.1. Materials

2.1.1. Cell lines and mammalian cell culture reagents

Human embryonic kidney (HEK) 293 FlipIn cells were used for preparation of inducible MCPyV truncated LT stable cell lines and transfection; HEK 293T cells were used for pull-down and immunoprecipitation assays; while MCC13 cells were used for immunofluorescence analysis. Stable inducible referred as i293-ST, iEGFP and iEGFP-ST were previously generated in the Whitehouse laboratory were used to study the level of expression of selected cellular proteins upon induction of ST. All the tissue culture media and culture supplements were purchased from either Life Technologies™, Lonza™, Sigma-Aldrich™ or Dundee Cell Products (for SILAC media only). Selection antibiotics were provided by either InVivoGen™ or Life Technologies™ and Lipofectamine™ 2000 was sourced from Life Technologies™.

2.1.2. Chemicals

All chemicals and solvents (analytical grade) were provided by Sigma-Aldrich®, Melford Laboratories Ltd. and Life Technologies™, unless stated otherwise. Solutions were sterilised using 0.22 µm filters (Millipore), or by autoclaving (121°C, 30 minutes, 15 psi). All water used, unless mentioned otherwise, was deionised water obtained from an ELGA PURELAB ultra machine (ELGA).

2.1.3. Enzymes

Restriction enzymes were obtained from New England BioLabs, and other enzymes and their suppliers are listed in Table 2.1.

Enzyme	**Supplier**
Platinum® *Pfx* DNA polymerase	Life Technologies™
Taq DNA polymerase	
Superscript® II reverse transcriptase	
Proteinase K	
RNase out	
T4 DNA ligase	New England BioLabs Inc.
DNA-free™ DNase I treatment kit	Ambion®
DNase I Amplification Grade	Sigma-Aldrich®
2x SensiMix™ SYBR No-ROX kit	Bioline

Table 2.1: List of enzymes used and the supplier.

2.1.4. Antibodies

Antibodies were used in Western blot analysis, immunofluorescent and immunoprecipitation assays to study the expression of proteins, the subcellular localization of transfected proteins and the protein-protein interactions of T antigen with target cellular proteins. Primary antibodies were obtained from a variety of suppliers, detailed in Table 2.2. Horseradish peroxidase (HRP) conjugated anti-mouse and anti-rabbit secondary antibodies were supplied by Dako™ and used for western blotting at 1:5000 concentration . Alexa-fluor conjugated anti-mouse and

anti-rabbit antibodies used for immunofluorescence microscopy were from Life Technologies™. The 2T2 antibody (kindly provided by Dr Christopher Buck, National Cancer Institute, Bethesda, MD), which recognises the J-domain leader peptides present in both MCPyV ST and MCPyV LT was used at 1:5 dilution for immunoblot analysis.

Antibody	**Origin**	**Working dilution**		**Supplier**
		WB	**IF**	
Anti-FLAG (F7425)	Rabbit	1:2500	-	Sigma
Anti-GST (G1160)	Mouse	1:3000	-	
Anti-GAPDH (ab8245)	Mouse	1:5000	-	
Anti-Vitronectin (ab13413)	Mouse	1:1000	1:200	Abcam
Anti-Kif14 (ab3746)	Rabbit	1:1000	1:100	
Anti-Periplakin (ab196256)	Rabbit	1:500	1:200	
Anti-GFP (632592)	Mouse	1:5000	-	Living Colors
Anti-Myc (M4439)	Mouse	1:5000	1:250	Sigma
Anti-Lamin B (NA12)	Mouse	1:5000	-	Calbiochem
Anti-ZO-1 (ab59720)	Rabbit	1:1000	1:200	Abcam
Anti-2T2	Mouse	1:5	-	Dr C Buck
Anti-CDK2 (ab32147)	Rabbit	1:1000	-	Abcam
Anti-CDK1 (246IP)	Mouse	1:1000	-	Abcam
Anti-cyclin A (H-432) Sc-751, Lot #G0811	Rabbit	1:500	-	Santa Cruz
Anti-cyclin B1 (H-433) Sc-752,Lot # H0112	Rabbit	1:500	-	Santa Cruz
Anti-Cyclin E (M-20) Sc-481, Lot # G0212	Rabbit	1:500	-	Santa Cruz
Anti-Cyclin D1 (M-20) Sc-718, Lot #A1911	Rabbit	1:500	-	Santa Cruz
Anti-phospho p53	Rabbit	1:1000	-	Cell Signaling

(Ser15) #9284S				technology
Anti-p53 (DO-1) Sc-126	Mouse	1:2000	-	Santa Cruz
Anti-caspase 3 (#9662)	Rabbit	1:1000	-	Cell signalling technology
Anti-Bad (#92925)	Rabbit	1:1000	1:100	Cell signalling technology
Anti-phospho Bad (Ser112) #5284P	Rabbit	1:1000	1:100	Cell signalling technology
Anti-β-catenin (ab3572)	Rabbit	1:1000	1:200	Abcam
Anti-cleaved PARP (#D214)	Rabbit	1:1000	-	Cell signalling technology
Anti-myc (C3956)	Rabbit	-	1:200	Sigma

Table 2.2: List of primary antibodies and working dilutions used for various applications and their suppliers.

2.1.5. Plasmid constructs

Plasmid constructs used in this thesis are listed in Table 2.3.

Plasmid	**Parent vector**	**Source/contributor**
pEGFP	pEGFPcl	Clontech
pEGFP-ST	pEGFPcl	Whitehouse Laboratory
pEGFP-tLT	pEGFPcl	Whitehouse Laboratory
pGST	pGEX-4T	Amersham
pGST-Vn	pGEX-4T	Whitehouse Laboratory
pGST-ST	pGEX-4T	Whitehouse Laboratory
i293-ST	pcDNA5/frt/To/His	Whitehouse Laboratory
i293-tLT	pcDNA5/frt/To/His	This work
pSV40 LT	pBabe puro (ori)	Prof Blair (University of Leeds)

pMCPyV WTLT	pCDNA4HisMax	Prof Blair (University of Leeds)
pESG wtp53	pESG-IBAwt	Prof Blair (University of Leeds)
Kif14 protein vector (human) (PV053856)	pPM-C-His	NBS Biologicals Ltd

Table 2.3: List of recombinant plasmid, parent vector and their source or contributors.

2.1.6. Oligonucleotides

Oligonucleotide primers for DNA sequencing and polymerase chain reaction (PCR) were supplied by Sigma-Aldrich®. A full list of primers used are shown in Table 2.4. Oligo$(dT)_{12-8}$ was supplied by Sigma, in order to perform reverse transcription.

Primer name	**Application**	**Sequence (5′-3′)**
pCDNA5 FRT-TOLT forward	PCR, cloning	GGGGGTACCACCATGGATTTAG TCCTAAATAGGAAAG (Kpn1)
pCDNA5 FRT-TOLT Reverse	PCR, cloning	CGAGCGGCCGCTCACTTATCGTCGTC ATCCTTGTAATCATGATCGAATGGAGG AGGGGT (Not1)
Bad For	qRT-PCR	GTTCCAGATCCCAGAGTTTG
Bad Rev	qRT-PCR	CCTCCATGATGGCTGCTG
PPL For	qRT-PCR	TGAATTCTCGGAAATCAACATGGCAGC
PPL Rev	qRT-PCR	AGTCGACCTTCTGCCCAGATACCAAGA
Kif For	qRT-PCR	AGCAGTTCTGAAAGGGAGCA
Kif Rev	qRT-PCR	ATCACTGGCCAAGTTGCGAA
Vn For	qRT-PCR	CCTTCACCGACCTCAAGAAC
Vn Rev	qRT-PCR	GAAGCCGTCAGAGATATTTCG

ZO1 For	qRT-PCR	CGGTCCTCTGAGCCTGTAAG
ZO1 Rev	qRT-PCR	GGATCTACATGCGACGACAA
GAPDH For	qRT-PCR	GTGGTCGTTGAGGGCAATG
GAPDH Rev	qRT-PCR	TGTCAGTGGTGGACCTGAC

Table 2.4: Oligonucleotide sequences and their application.

2.2. Methods

2.2.1. Molecular Cloning

2.2.1.1. Construction of recombinant MCPyV truncated LT construct

Truncated LT gene was amplified from genomic cDNA using the pCDNA5 FRT-TOLT forward and reverse primers. The primer sequences are listed in Table 2.4. DNA was PCR amplified (Section 2.2.1.1.) and separated by agarose gel electrophoresis (Section 2.2.1.3.). Appropriate size DNA bands were cut and gel purified using QIAquick® Gel Extraction Kit (Qiagen). according to the manufacturer's standard protocol. The PCR product was excised with specific restriction enzymes and ligated into the appropriate linearised double stranded DNA vector via a cloning vector, such as pCR Blunt (Invitrogen$^{TM)}$. The ligation mixtures were transformed in chemically competent bacteria (Section 2.2.1.7.) and selected by appropriate antibiotic. Successful inserts were verified by restriction digestion analysis (Section 2.2.1.5) and PCR amplification (Section 2.2.1.2.). All constructs were purified (Section 2.2.1.9.) and sequenced to validate the identity of the inserted fragments (Section 2.2.1.10.).

2.2.1.2. Polymerase chain reaction (PCR)

PCR amplification was performed in thin-walled 0.2 ml PCR tubes (Axygen), using a TC-412 thermal cycler (Techne^{TM}). Reactions were carried out using Platinum® *Pfx* or *Taq* DNA polymerase. Pfx DNA polymerase was used for gene amplification during cloning due to the need for a proofreading enzyme, while Taq DNA polymerase was used for screening of positive transformants. Reactions were performed in a total volume of 50 µl, containing the following components: 1-10 ng template DNA, 0.2 mM of each primer, 1× polymerase amplification buffer, 1.5 mM $MgSO_4$/$MgCl_2$, 1 µl DNA polymerase, 200 µM dNTPs. The conditions for PCR amplification were set up at 95 °C for 5 minutes, followed by 35 cycles of 95°C for 1 minute, 60°C for 1 minute and 72°C for 2 minutes. A final extension at 72°C for 10 minutes. PCR products were then analysed by agarose gel electrophoresis (Section 2.2.1.3).

2.2.1.3. Agarose gel electrophoresis

Double stranded DNA fragments were separated by agarose gel electrophoresis, using 1% agarose gels. Agarose was dissolved in TBE buffer [90 mM Tris-base, 2 mM EDTA, 80 mM boric acid] to which 0.5 µg/mL ethidium bromide was added. A 10 x solution of gel loading buffer [0.25% (w/v) Orange G dye, 30% (v/v) glycerol] was mixed with DNA samples, resulting in 1x final concentration. A DNA ladder, 100 bp or 1 kb (Invitrogen^{TM}) was run alongside the samples. Electrophoresis was performed with TBE buffer in HE 99× Max horizontal electrophoresis tanks (Hoefer) at 100 V for 1 hour. DNA was visualised under ultra-violet light and corresponding images were taken using the GeneGenius bio-imaging system (Syngene).

2.2.1.4. Purification of DNA

DNA bands of the expected size of the PCR product were excised from the agarose gels and purified using the QIAquick gel extraction kit (Qiagen), according to the manufacturer's instructions. The weight of the DNA gel slice was recorded and the slice was dissolved in 3 gel volume of buffer QG followed by incubation at 50°C for 10 minutes. Upon melting of the agarose slices, one volume of isopropanol was added to the sample and mixed. This mixture was then applied to a QIAquick column and centrifuged for 1 minute at 13,000 × g at room temperature. The column was washed using 750 µL wash buffer and centrifuged for 1 minute at 13,000 × g, room temperature. DNA was eluted into a sterile eppendorf tube by applying 30 µL elution buffer followed by centrifugation for 1 minute at 13,000 × g at room temperature. Purified DNA was stored at -20°C until further use.

2.2.1.5. Restriction enzyme digestion

Restriction enzyme digestion was performed according to the manufacturer's protocol with compatible buffers if double digestion was required. Reactions were carried out in a total volume of 10-20 µL with 1U of restriction enzyme used per 1 µg of DNA to be digested. Reactions were incubated for 2 hours at 37°C followed by incubation at 65°C for a minimum of 20 minutes to inactivate the reactions. Resulting fragments were analysed by agarose electrophoresis (section 2.2.1.3.) and gel purified (section 2.2.1.4.).

2.2.1.6. DNA ligation

Ligations were performed using T4 DNA ligase buffer, 1 U of T4 DNA ligase (Invitrogen^{TM}), added to approximately 10-100 ng of linearised vector and insert DNA with 1:3 molar ratio of vector to insert, in a total volume of 10 µl. Reagents were mixed gently and incubated at 16°C for 1 hour.

2.2.1.7. Preparation of chemically competent DH5α

All cloning was carried out using *Escherichia coli* (*E.coli*) strain DH5α. Chemically competent *E.coli* was prepared using a rubidium chloride-based method. Liquid cultures were grown in autoclaved Luria broth (LB) [1% (w/v) tryptone, 0.5% (w/v) NaCl, 0.5% (w/v) yeast extract, pH 7.5] and incubated at 37°C with shaking. DH5α cells were streaked on LB agar plates (1% NaCl, 1% Tryptone, 0.5% Yeast Extract and 1.5% Agar) followed by incubation at 37°C. One colony was used to inoculate 2 mL of LB media and incubated for 5 hours at 37°C with shaking. Following this, 0.5 mL of the culture was used to inoculate 50 mL of LB media and the cells were grown at 37°C with shaking until an OD_{600} of 0.3-0.6 was reached. The cells were subsequently pelleted by centrifugation at 5,000 × g for 5 minutes at 4°C. The pellet was resuspended in 40 mL ice-cold filter-sterilised TFB1 buffer [30 mM KOAc, 10 mM $CaCl_2$, 50 mM $MnCl_2$,100 mM RbCl, 15% (v/v) glycerol, adjusted to pH 5.8 with acetic acid] and incubated for 5 minutes at 4°C. The cells were centrifuged at 5,000 × g for 5 minutes at 4°C followed by gentle resuspension of cells in 2 mL ice-cold filter-sterilised TFB2 buffer [10 mM MOPS, 75 mM $CaCl_2$, 10 mM RbCl, 15% (v/v) glycerol, adjusted to pH 6.4 with KOH]. This was followed by incubation at 4°C for 20 minutes and subsequently cells were aliquoted and quickly frozen on dry ice, followed by storage at -80°C.

2.2.1.8. Bacterial transformation

Plasmids were transformed into 50 µL *E. coli* DH5α competent cells (originally from Invitrogen) for cloning purposes or *E. coli* BL21 (originally from Novogen) for bacterial expression studies. Competent cells were thawed on ice. Approximately 10 ng of plasmid DNA was added and mixed by gentle pipetting. Cells were incubated for 30 min on ice and placed in a 42°C water bath for 50 sec. The heat-shocked cells were then incubated on ice for 2 min. After incubation, 0.25 mL of SOC medium [2% tryptone, 0.5% yeast extract, 10 mM NaCl, 2.5 mM KCl, 10 mM $MgCl_2$, 10 mM $MgSO_4$,

and 20 mM glucose] was added to the cells and these were incubated at 37°C for 1 hour. Finally, 100 µL of transformed cells were plated onto LB plates supplemented with the appropriate antibiotic and plates were incubated overnight at 37°C.

2.2.1.9. Plasmid extraction

Small scale purification of plasmid DNA was carried out to using QIAprep Spin Miniprep Kit (Qiagen)., while large scale preparation of plasmid DNA were performed using a Maxiprep kit (Qiagen) according to the supplier's protocol. The 5 mL (small scale) and 500 mL (large scale) of overnight bacterial culture was harvested by centrifugation at 4000 × g for 10 min. The pelleted bacterial cells were resuspended with 10 mL resuspension buffer (50 mM Tris-HCl, pH 8.0 and 10 mM EDTA) supplemented with RNase A (100 µg/mL). The homogenous bacterial cell suspension was lysed with 10 mL lysis buffer [0.2 M NaOH and 1% (w/v) SDS] and incubated for 5 min at room temperature. The lysed cells were precipitated with 10 mL precipitation buffer [3.1 M potassium acetate, pH 5.5] and centrifuged at 13,000 × g for 10 min at room temperature. The supernatant was then transferred onto an equilibrated anion-exchange resin column and allowed to drain by gravity flow. The column was washed with 60 mL wash buffer [0.1 M sodium acetate, pH 5.0, 825 mM NaCl] and bound plasmid DNA was eluted with 15 mL elution buffer [100 mM Tris-HCl, pH 8.5, 1.25 M NaCl]. The eluted plasmid DNA was precipitated with 10.5 mL isopropanol at room temperature and centrifuged at 13,000 × g for 30 min at 4°C. The precipitated plasmid was washed with 10 mL 70% (v/v) ethanol and centrifuged at 13,000 × g for 15 min at 4°C. The DNA pellet was air-dried and resuspended in 100 µL DNase free water.

2.2.1.10. DNA sequencing

Putative positive plasmids were extracted and DNA concentration was quantified by NanoDrop prior to be sent for DNA sequencing. Plasmid DNA was sent to GATC at a concentration of 30 ng/µL in 50 µL total

volume. DNA sequencing was performed by GATC Biotech to confirm the correct cloned sequences. Primers used for sequencing were T7 and BGH reverse primer. All sequences were aligned and blast against public GenBank databases.

2.2.2. Mammalian Cell Culture

2.2.2.1. Cell lines

Human embryonic kidney HEK 293 FlpIn™ (Life Technologies) were kindly supplied by Stuart Wilson (University of Sheffield, UK) were used as the parental cell line for generation of the i293-tLT (this work) as well as stable inducible cell lines generated by members of Whitehouse laboratory, i293-ST, iEGFP and iEGFP-ST. In addition, the human non-small cell lung carcinoma cell line, H1299 were provided by Professor Eric Blair (University of Leeds, UK) and a Merkel cell carcinoma cell line that was MCPyV negative, MCC13 was obtained from the European Collection of Authenticated Cell Cultures (ECACC).

2.2.2.2. Cell lines maintenance

HEK 293 FlpIn™, i293-ST, i293-tLT, i293-T, iEGFP, iEGFP-ST cell lines were maintained in Dulbecco's modified Eagle's medium (DMEM, Invitrogen™), supplemented with 10% (v/v) foetal bovine serum (FBS) and 5 U/mL penicillin and streptomycin. HEK 293 FlipIn™ cells were maintained in DMEM containing 100 µg/mL zeocin (Invitrogen™), while i293-ST, i293-tLT, iEGFP and iEGFP-ST cells were maintained in DMEM containing 100 µg/mL Hygromycin B (Invitrogen™). All cell lines were passaged every 3 to 4 days. Confluent cell layers were removed from 75 cm^2 tissue culture vessel surfaces by kinetic force. The cells were split 1:20 into flasks with 10% DMEM containing appropriate antibiotics. The H1299 cells were maintained in 10% DMEM and passaged every 3-4 days, whereby the confluent cell layer was removed by trypsinisation and the cells were

subsequently split 1:20 into new flask containing 10% DMEM. The MCC13 cells were maintained in Roswell Park Memorial Institute (RPMI) media, supplemented with 5 U/ml penicillin and streptomycin and 15% FBS. The MCC13 cells were passaged in the same manner as H1299 cells but using 15% RPMI. For long term storage of cell lines, cells were aliquoted into 1.8 mL Cryotubes (NUNC^{TM}) at 1 × 10^6 cells/mL. Cells were resuspended in freezing media [90% (v/v) FCS, 10% (v/v) DMSO], cryotubes were then stored at -80°C for 24 hours in an isopropanol containing freezing container (Nalgene) and then transferred to liquid nitrogen for long term storage. All cell lines were incubated in an InCu saFe Copper-Enriched Stainless Steel CO_2 incubator (Panasonic), with 5% CO_2 concentration.

2.2.2.3. Maintaining cells in SILAC media

Media used to label i293-tLT cells prior to SILAC based quantitative proteomic analysis was purchased from Dundee Cell Products and supplemented with 10% dialysed foetal calf serum (Dundee Cell Products). i293-tLT cells were passaged 8 times in both R_0K_0 DMEM (containing ^{12}C L-Arginine and ^{12}C L- Lysine), and R_6K_4 DMEM (containing ^{13}C L-Arginine and ^{13}C L-Lysine), herein referred to as ‘’light DMEM’’ and ‘’heavy DMEM’’, respectively to ensure full incorporation of the labelled amino acids. Upon each passage, both light DMEM media and heavy DMEM media was supplemented with Hygromycin B (Life Technologies^{TM}). For SILAC analysis, a set of i293-tLTcells was grown in light DMEM and maintained uninduced while another set of cells was grown in heavy DMEM and induced with doxycyline for 48 hours prior harvested for protein fractionation.

2.2.2.4. Preparation of inducible tLT stable cell lines

To generate a cell line with inducible MCPyV tLT expression, 293 FlipIn cells were co-transfected with tLT-FLAG (in pCDNA5/FRT) and pPGK/Flip/ObpA plasmid constructs at a 1:9 ratio. The cell line was

selected and maintained under Hygromycin B selection at 100 µg/ml and referred to as i293-tLT. The cell line was derived from a single clone, and propagated until confluency, before the induction and expression of the desired protein of interest was tested.

2.2.2.5. Mammalian cell culture based protocols

2.2.2.5.1. Transfection of mammalian cells

A standard transfection protocol was followed for all assays unless stated otherwise. Approximately 5 × 10^5 were seeded into a well (35 mm diameter) of a 6-well plate the day before transfection, to allow cells to grow to 70% confluency upon transfection. All transfections were performed using Lipofectamine™ 2000, according to the manufacturers protocol. Per reaction (1 well of a 6-well plate), 3 µL Lipofectamine™ 2000 was diluted in 100 µL media (either DMEM or RPMI depending on the cell line) and mixed with 1 µg total plasmid DNA, which was also diluted in 100 µL media. This mixture was incubated for 10 minutes at room temperature, during this time the media on the seeded cells was replaced with either 2 mL DMEM or RPMI (for 6-8 hour transfections). If overnight transfection needed, DMEM or RPMI containing 2.5% FBS were used, herein referred to as “2.5% DMEM’’ or “2.5% RPMI’’. Following incubation the transfection mixture was then added to the cells in a drop-wise manner and cells were incubated at 37°C for either 6 hours or 16 hours, depending upon the experiment. Following this time the transfection media was replaced with the corresponding media for that cell line (either 10% DMEM, 10% RPMI, 15% RPMI, respectively) and allowed to express the respective recombinant proteins for 24, 48 or 72 hours depending upon experiment.

2.2.2.5.2. Induction of i293-ST and i293-tLT cells

Approximately 1x10^5 of i293-ST or i293-tLT cells were seeded into each well of a 6-well plate. Once cells were adhered to the tissue culture dish, 4

µL doxycycline hyclate (Life Technologies^{TM}) was added to 2 mL complete DMEM, at a final concentration of 2 µg/mL. Cells were harvested after incubation at 37°C for 24 and 48 hours' time points. SILAC analysis of i293-tLT required cell growth on a large scale, resulting in 5 x 175 cm^3 tissue culture vessels (Sigma-Aldrich^{TM}). Concurrent with this, approximately 1 x 10^7 cells per flask were induced with 2 µg/mL doxycycline hyclate in a volume of 30 mL R_6K_4 DMEM, while control cells, grown in 30 mL R_0K_0 DMEM, were left uninduced.

2.2.3. Protein Analysis

2.2.3.1. Preparation of mammalian cell lysates

For experiments that required analysis of cellular proteins, mammalian cells were removed from the tissue culture plates by pipetting with 1 mL PBS. Adherent cells such as MCC13 and H1299 were removed from the surface of the culture plate by scraping in the presence of 1 mL PBS. The cells suspension was then centrifuged at 500 × g at room temperature. The cell pellet was resuspended and lysed in 100 µL RIPA lysis buffer [150 nM Tris-HCl, 50 mM Tris base ultrapure, 1% NP40, pH 7.6, with 1 x protease inhibitor EDTA (Roche)], which was pre-chilled to 4°C. This was incubated on ice for 30 minutes, with mixing every 10 minutes, followed by centrifugation of the cell lysates in a pre-chilled centrifuge at 4°C, 13,200 × g for 10 minutes. The supernatant was then transferred to a clean Eppendorf and stored at -20°C until further use. The harvested proteins were quantified by Bradford assay to ensure equal loading prior to analysis by immuno blotting.

2.2.3.2. Bradford assay

A standard curve of a serial dilution series (0.1-1.0 mg/mL) BSA dissolved in RIPA lysis buffer [150 nM Tris-HCl, 50 mM Tris base ultrapure, 1% NP40, pH 7.6, with 1 x protease inhibitor EDTA (Roche)] was generated.

The concentration of each protein sample was determined from its absorbance by interpolation. Generally, 5 µL of standards or samples were pipetted into wells, followed by adding of 250 µL 1 × dye reagent (BioRad) to each well. The samples were mixed thoroughly using a microplate mixer, followed by incubation at room temperature for 15 minutes before the absorbance at 595 nm was measured by using microplate reader.

2.2.3.3. SDS-PAGE

Cell lysates were mixed with protein solubilising buffer [50 mM Tris-HCl (pH 6.8), 2% (w/v) SDS, 20% (v/v) glycerol, 50 µg/mL bromophenol blue, 10 mM DTT] and boiled at 95 °C for 10 minutes. Appropriate percentages of acrylamide gel were prepared according to the size of tested proteins. The reagents and the volumes added are listed in Table 2.5. All SDS-PAGE was performed using a Mini-PROTEAN 3 cell (Bio-Rad), set up according to the manufacturer's instructions. Gels were run in Tris-glycine running buffer [25 mM Tris, 192 mM glycine, 0.1% (w/v) SDS] at 180 V for 1 hour. The BenchMark pre-stained protein standards were run alongside samples to indicate their molecular weight.

Reagents	**6%**	**10%**	**12%**
Acrylamide/bis-acrylamide	2.0 mL	1.7 mL	2.0 mL
1 M Tris-HCl (pH 8.8)	1.3 mL	1.3 mL	1.3 mL
10% (w/v) SDS	50 µL	50 µL	50 µL
dH_2O	2.6 mL	1.9 mL	1.6 mL
10% (w/v) ammonium persulfate	50 µL	50 µL	50 µL
TEMED	8 µL	4 µL	4 µL

Table 2.5: Reagents and the volumes required to prepare SDS-PAGE resolving gels of an indicated percentage acrylamide.

2.2.3.4. Immunoblotting

Proteins separated by SDS-PAGE were transferred to Hybond C membranes (Amersham Biosciences), using the Bio-Rad Mini Trans-Blot Electrophoretic Transfer Cell (BioRad), as stated in the manufacturer's instructions. The gel and membrane were sandwiched between four pieces of Whatman 3 mm filter paper, all of which was soaked in transfer buffer [25 mM Tris, 190 mM glycine, 20% (v/v) methanol], before being secured in the Mini Trans-Blot. Proteins were transferred at 100 V for 1 hour or overnight, depending on the size of the protein. The blot was removed and incubated in blocking buffer [20 mM Tris, 500 mM NaCl, 0.1% (v/v) Tween-20, 5% skimmed milk] for 1 hour at room temperature followed by incubation with the primary antibody diluted in blocking solution overnight at 4°C. The membrane was washed three times, for 5 minutes in TBS-Tween solution [20 mM Tris, 500 mM NaCl, 0.1% Tween-20], before incubation with appropriate secondary antibody conjugated to HRP. Bands were visualised using Hyperfilm ECL^{TM} (Amersham), by enhanced chemiluminescence (ECL), using the EZ-ECL kit (Geneflow). Films were developed in a SRX-101A developer (Konica).

2.2.3.5. Coomassie stain analysis

Proteins were visualised by incubating SDS-PAGE gel (Section 2.2.5.3) in coomassie stain [0.1% (w/v) Coomassie Blue R-250, 50% (v/v) methanol, 10% (v/v) acetic acid] for 1 hours at room temperature, followed by incubation with coomassie de-stain [25% (v/v) methanol, 10% (v/v) acetic acid] for 30 minutes. Used de-stain was then replaced with fresh de-stain and incubated for a further 30 minutes at room temperature.

2.2.4. Analysis of protein-protein interactions

2.2.4.1. Glutathione S-transferase (GST) pull down assay

To study the protein-protein interaction of ST with other target proteins, plasmids containing GST and GST tagged MCPyV ST were overexpressed in bacterial expression system. Initially, the appropriate concentration of plasmid was transformed into chemically competent BL21 cells (Stratagene) using heat shock method as described in Section 2.2.1.8. A single colony of transformant was picked and used to inoculate 10 mL of LB media for an overnight culture under antibiotic selection, which was left shaking at 37°C. The next day, the 10 mL overnight culture was added into 100 mL LB containing 50 µg/mL selection antibiotics and the incubation was continued for another 2 hours with shaking at 37°C. Following this, Isopropyl-β-D-thio-galactoside (IPTG) was added to a final concentration of 0.4 µM. For a time course study, 1 mL of culture were harvested every hour after the induction and labelled as $T_{(1\text{-}4)}$ and before induction (T_0).

The time course lysate samples were subjected to SDS-PAGE and stained with coomassie blue to see the overexpression of the proteins. The remaining culture was harvested after 4 hours incubation and was pelleted by centrifugation for 10 minutes at 5,000 × g, 4°C. The pellets were then gently resuspended in 5 mL lysis buffer [PBS, 1% Triton X-100, Complete® Protease Inhibitor EDTA free (Roche)]. To lyse the cells completely, the cells were sonicated for 10 times for 10 seconds on followed by 10 seconds off, using a Soniprep150 (MSE). The lysate was incubated for approximately 20 minutes on ice and 50 µL of the lysate was kept as whole cell lysate. After incubation, the lysate was cleared by centrifugation for 30 minutes at 5,000 × g, 4°C. Supernatant was added to 25 µL prepared GST beads. The mixture was incubated for 2 hours with continuous rotation. The GST beads were then pelleted at 500 × g, for 5 minutes and washed 3 times with 5 mL ice-cold PBS and subsequent centrifugation. The cell lysate, 293T or induced and uninduced iST-293, was added to the GST beads and incubated for 2 hours at 4°C with continuous rotation. After the

incubation, the GST beads were pelleted at 500 × g for 5 minutes, gently washed with ice cold PBS for 3 times. 100 µL of 2 × protein solubilising buffer [50 mM Tris-HCl (pH 6.8), 2% (w/v) SDS, 20% (v/v) glycerol, 50 µg/mL bromophenol blue, 10 mM DTT] was added to resuspend the GST beads, which was subsequently boiled for 10 minutes to elute bound proteins and then used for SDS-PAGE analysis and western blotting.

2.2.4.2. Immunoprecipitation of GFP-fusion proteins

HEK 293T cells were transfected with GFP or GFP-ST plasmids (Section 2.2.2.5.1). The cells were subjected to lysis 24 hours post-transfection. Lysis and immunoprecipitation of GFP-fusion proteins was performed using GFP-trap beads (Chromotek) that consist of a single-domain anti-GFP antibody conjugated to an agarose bead matrix. Cell pellets were incubated for 30 min on ice with 200 µL lysis buffer [10 mM Tris-HCl, pH 7.5, 150 mM NaCl, 0.5 mM EDTA, 0.5% NP-40, and EDTA-free protease inhibitor]. The lysate was cleared by centrifugation at 12,000 x *g* for 10 mins and diluted 5-fold with dilution buffer [10 mM Tris-HCl, pH 7.5, 150 mM NaCl, 0.5 mM EDTA, and EDTA-free protease inhibitor]. The GFP-trap beads were equilibrated with ice-cold dilution buffer and then incubated with diluted cell lysate for 2 hours at 4°C on a rotary mixer, followed by centrifugation at 2,700 × *g* for 2 min. The bead pellet was washed once with dilution buffer, followed by a single wash in buffer [10 mM Tris-HCl, pH 7.5, 300 mM NaCl, 0.5 mM EDTA, and EDTA-free protease inhibitor]. After centrifugation of the GFP-trap beads as described above and removal of the wash buffer, the beads were resuspended in 2 × protein solubilising buffer and boiled for 10 minutes to elute bound proteins. The precipitated proteins were subjected to western blotting analysis (section 2.2.4.2).

2.2.5. Immunofluorescence microscopy

Initially, the coverslips were immersed in 100% ethanol to sterilise the surface, before placing in sterile 6 well tissue culture dish. The coverslip were allowed to air dry to get rid of ethanol residues before the surfaces were treated with 0.01% poly-L-lysine solution for 15 minutes at room temperature followed by a brief wash 3 times in PBS. Approximately 1×10^5 of MCC13 cells were seeded onto the treated coverslips and incubated overnight to allow the cells to adhere to the surface. The next day, cells were transfected with appropriate constructs (as describ. After transfection and subsequent protein expression , cell monolayers were washed gently for 3 times with PBS followed by fixation with 4% (v/v) paraformaldehyde in PBS for 15 min at room temperature. The cells were again washed 3 times in 2 ml PBS and permeabilised in 1% (v/v) Triton X-100 in PBS for 10 minutes at room temperature, before 3 further washes in 2 ml PBS.

Coverslips were then covered with blocking solution [PBS, 1% (w/v) bovine serum albumin (BSA)] followed by incubation at 37°C for 1 hour. The appropriate primary antibody was applied to the cells in the blocking solutuion and incubation was continued overnight at 4°C. The cell monolayer was carefully washed 5 times in blocking solution, before an appropriate AlexaFluor conjugated secondary antibody was applied to the cells. After 1 hour incubation at 37 °C, the secondary antibody was removed and the cells were carefully washed 5 times with PBS. Coverslips were mounted onto microscope slides using VECTORSHIELD® with DAPI mounting media (Vector Laboratories) and visualised on an LSM510 META laser scanning inverted confocal microscope, using the LSM5 image browser.

2.2.6. Fractionation and proteomic analysis

2.2.6.1. Nuclear and cytoplasmic fractionation

SILAC analysis of i293-tLT cells required the protein fractionation to reduce the complexity of the sample. Approximately 1 × 10^7 cells per flask were induced with 2 µg/mL doxycycline hyclate in a volume of 30 mL R_6K_4 DMEM, while the control, left uninduced were grown in 30 mL R_0K_0 DMEM. Both i293-tLT cells grown as monolayers were washed in ice-cold phosphate buffered saline (PBS). The cells were pelleted at 1200 rpm for 3 min at room temperature and cell pellets resuspended in ice-cold 0.1% NP40 (Calbiochem, CA, USA) in PBS. The lysate was labelled "cytosolic fraction". The pellet was then resuspended in 1 ml of ice-cold 0.1% NP40 in PBS, and centrifuged as above. The pellet was resuspended with Laemmli sample buffer [65.8 mM Tris-HCl, pH 6.8, 2.1% SDS, 26.3% (w/v) glycerol, 0.01% bromophenol blue] and this sample designated as "nuclear fraction". Prior to the samples being sent for Liquid chromatography–mass spectrometry/mass spectrometry (LC-MS/MS) analysis, the proteins were quantitated by Bradford assay and samples were mixed in 1:1 ratio (uninduced : induced) for both cytoplasmic and nuclear fraction samples.

2.2.6.2. Mass spectrometry and proteomic analysis

Both mixed cytoplasmic and nuclear fractions samples were outsourced to University of Bristol Proteomics Facility to identify and quantify the precipitated proteins. Peptides were quantified and identified using Proteome Discoverer™ Software. For analysis and quantification of proteins levels, a 2.0 fold cut-off was chosen and a 2 peptide cut-off. Proteomic analysis was performed using The Database for Annotation, Visualization and Integrated Discovery (DAVID) (Huang da et al., 2009a, b) and Ingenuity Pathway Analysis (IPA) web-based softwares.

2.2.7. Analysis of protein functions

2.2.7.1. Standard cell proliferation assay

i293-GFP, i293-GFPST, HEK293 and i293-tLT cells were seeded into 6-well plates in triplicate. Protein expression was induced with doxycycline hyclate at 2 µg/mL. At the chosen time points (24, 48, 72 hours post induction), cells were detached from the tissue culture plate surface via trypsinisation [0.25% (v/v) trypsin, in PBS], washed in 1 mL PBS and centrifuged at 1,200 × *g* for 3 minutes at room temperature. The cell pellet was then resuspended in 1 mL PBS. 0.2 mL cell suspension was added to 0.3 mL PBS and 0.5 mL Trypan Blue solution 0.4% (w/v) (Sigma) and mixed thoroughly. Cells were then counted using a haemocytometer (Neubauer Improved).

2.2.7.2. Cell cycle analysis

HEK293 and i293-tLT cells were seeded into 6-well plates in triplicate and left to grow overnight. Protein expression was induced with doxycycline hyclate at 2 µg/mL. After 24 hours post induction, cells were detached from the tissue culture plate surface, washed in 1 mL PBS and centrifuged at 1,200 × *g* for 3 minutes at room temperature. The cells were resuspended in 1 mL PBS, counted and pelleted again. The supernatant was removed and the tubes flicked to disturb the pellet of cells. Ice-cold 70% ethanol was added dropwise to the pellet whilst vortexing, in order to resuspend the cells. A sufficient amount of cold ethanol was then added to obtain a cell concentration of 10^6 cells per mL. Immediately, samples were stored at −20°C for at least 24 hours to fix the cells. For analysis, the cells were pelleted at 1,200 × *g* for 3 minutes at room temperature. All ethanol residue was removed and the pellets were washed twice in ice-cold PBS. Pellets were resuspended in PBS with 0.5 mg RNAse A and 10 ug/mL Propidium Iodide. The cells were then incubated at 37°C for 3 hours, followed by centrifugation at 1,200 × *g* for 3 minutes at room temperature. The pellets

were resuspended in PBS. Samples were run on a LSR Fortessa flow cytometer (BD Biosciences). At a low flow rate and analysed with ModFit software. For experiments involving other LT plasmid constructs, HEK293 cells were seeded into 6-well plates and transfected with the appropriate constructs (section 2.2.2.5.1).

2.2.7.3. Apoptosis assay

HEK293 and i293-tLT cells were seeded into 6-well plates in triplicate and left to grow overnight. Protein expression was induced with doxycycline hyclate at 2 µg/mL. After 24 hours post-induction, staurosporine (Sigma-Aldrich) was added at a final concentration of 10 µM. The cells were incubated for at least 5 hours before being harvested. The morphology of the treated cells was observed through an inverted microscope and images were captured at different time points within the incubation time. Afterwards, the treated cells were washed in 1 mL PBS and centrifuged at 1,200 × g for 3 minutes at room temperature. The cell pellet was then resuspend in 1 mL PBS and the number of cells counted prior to labelling. Approximately 1×10^5 cells were used per sample. The cells were pelleted and washed for 2 to 3 times with ice-cold 1× Annexin V labelling buffer [10× (0.1 M Hepes pH 7.4, 1.4 M NaCl, 25 mM $CaCl_2$)]. This step is important to ensure the cell culture medium is removed completely, especially if EDTA was used to harvest the cells. 50 mL of the labelling buffer and 5 µL of Annexin-V-FITC (Abcam) were added to each pellet and resuspended thoroughly. The samples were then were incubated on ice for 15 minutes before 5 µL of Propidium Iodide (50 mg/mL) were added to each sample. After mixing, they were immediately run on the flow cytometer.

2.2.7.4. Scratch wound-healing assay

The appropriate 6-well plates were coated in poly-L-lysine prior to incubation with the cells. The next day, the monolayer of cells was scraped

in a straight line using P200 pipette tips. Excessive debris from the scratch was removed by washing the cells once and replacing the growth medium. The cells were visualized and imaged in the same area and location between 0 to 40 hours after scratching. Scratches and subsequent cell growth was visualised using the inverted microscopy.

2.2.8. Gene expression analysis by qRT-PCR

2.2.8.1. RNA extraction

i293-ST or i293-tLT cells were seeded at a density of 4 × 10^5 cells in triplicate per condition and induced for 48 hours at 37°C with 2 µg/mL doxycycline hyclate. For the i293-tLT experiment, HEK 293 cells were used as a control. For the i293-ST experiment, i293-ST cells were left uninduced and used as a control. Following incubation, cells were directly lysed by addition of 1 mL TRIzol reagent (Life Technologies™) per well according to the manufacturer's instruction. Briefly, after incubation at room temperature for 5 minutes, 200 µL chloroform were added to each sample followed by vigorous mixing for 15 seconds and incubation at room temperature for 3 minutes. Samples were then centrifuged at 12,000 × g for 15 minutes at 4°C and the upper, RNA containing, aqueous colourless phase was transferred to a fresh RNase-free tube. RNA was then precipitated by addition of 500 µL isopropanol and incubation at room temperature for 10 minutes before being centrifuged at 12,0000 × g at 4°C for 10 minutes. The supernatant was carefully aspirated and the pellet washed in 1 mL 75% ethanol and briefly vortexed, followed by centrifugation at 7,500 × *g* for 5 minutes at 4°C. The supernatant was once again aspirated and the pellet air-dried for 5 minutes. The pellet was resuspended in 49 µL DEPC-treated water with 1 µL RNaseOUT™ (Life Technologies) and incubated at 57°C for 10 minutes. The RNA was immediately DNase I treated (Section 2.2.8.2) and reverse transcribed (2.2.8.3). Any remaining RNA was stored at -80°C until further use.

2.2.8.2. DNase I treatment

A DNase I kit supplied by Ambion™ was used to remove any potential contaminating DNA from RNA samples (Section 2.2.8.1) as per the manufacturers protocol. 0.1 volume of DNase reaction buffer and 0.5 µL Amplification Grade DNase I were added to each sample, gently mixed and incubated for 30 minutes at 37°C. This was followed by addition of 0.1 volume Stop solution, thorough mixing and incubation at 70°C for 10 minutes. Samples were then briefly chilled on ice and then transferred for long term storage at -80°C. RNA concentration was measured using a NanoDrop (Eppendorf) and all samples were diluted in RNase-free water to a final concentration of 50 ng/µL prior proceed to qRT-PCR.

2.2.8.3. Reverse transcription

cDNA was synthesized from the total cellular RNA by using ProtoScript® II Reverse Transcriptase (New England Biolabs), according to the manufacturer's protocol. The initial sample mixture contained 1 µg DNase I treated RNA, 1 µL dNTP mix (2.5 mM per dNTP), 1 µL Oligo$(dT)_{12\text{-}18}$ primer and water to a total volume of 12 µL. Samples were mixed and incubated at 65°C for 5 minutes and then quick-chilled on ice. Following this, 4 µL 5 × First-Strand buffer, 2 µL 0.1 M DTT, 1 µL RNaseOUT™ and 1 µL ProtoScript® II Reverse Transcriptase were added to each sample. Samples were mixed gently and incubated at 42°C for 50 minutes, followed by enzyme inactivation at 70°C for 15 minutes. This was then followed by ethanol precipitation to remove unused dNTPs, salts and enzymes.

2.2.8.4. Ethanol precipitation

2 µL of 3 M sodium acetate, pH 5.6, and 60 µL ice cold 100% ethanol was added into each cDNA sample (Section 2.2.8.3) and mixed gently, followed by incubation at 4°C for 10 minutes. Samples were then centrifuged at 12,000 × g for 10 minutes at 4°C and the supernatant discarded. The pellet

was then washed in 1 mL ice-cold 100% ethanol and further centrifuged at 12,000 × g for 10 minutes at 4°C. The supernatant was removed and the pellet air-dried briefly, followed by resuspension of the cDNA pellet in 20 µL nuclease-free water (Sigma). The cDNA concentration was determined by NanoDrop and subsequently diluted to a final concentration of 2 ng/mL in nuclease-free water.

2.2.8.5. qRT-PCR reaction

Each reaction PCR reaction was performed in duplicate using two different primer pairs (GAPDH as a reference and a pair of test primers). The PCR master mix contained the following for each reaction: 12.5 µL SensiMix SYBR® No-ROX kit (Bioline), 2 µL primer mix (5 µM of both forward and reverse primers), 5.5 µL nuclease-free water and 5 µL cDNA (10 ng final amount). The PCR reactions were performed using a Rotor-Gene™ Q 5plex MRM Platform (Qiagen) using the Rotor-Gene 6000 series software version. A PCR program (pre-programmed 3 Step with Melt) consisted of 95°C for 10 minutes and then 40 cycles of: 95°C for 15 seconds, 60°C for 30 seconds and 72°C for 20 seconds were used in setting the qRT-PCR reaction. Quantitative analysis was then performed using the comparative C_T method (Boyne and Whitehouse, 2006). Each tested primer set was normalised to GAPDH.

Chapter 3

Analysis of potential differentially expressed cellular proteins upon MCPyV ST expression identified by a previous SILAC-based quantitative proteomic assay.

3.0. Analysis of potential differentially expressed cellular proteins upon MCPyV ST expression identified by a previous SILAC-based quantitative proteomic assay.

3.1. Introduction

The Merkel cell polyomavirus (MCPyV) genome has been found to be clonally integrated in the majority of Merkel cell carcinoma (MCC). This leads to the hypothesis that aberrant expression of MCPyV T antigens may contribute to MCC pathogenesis. Interestingly, expression of the MCPyV ST and LT antigens varies in patient samples; ST expression is detected in 92% of samples, whereas only 75% are positive for LT expression. This indicates that MCPyV ST has important roles in cell transformation and tumour maintenance in MCC.

To further investigate what effect MCPyV ST expression has upon the host cell proteome, a SILAC-based quantitative proteomic approach was performed utilizing a HEK 293 Flp-In cell line capable of inducible MCPyV ST expression, termed i293-ST. This analysis aimed to identify differentially expressed cellular proteins, which may help to determine how MCPyV ST contributes to MCC pathogenesis. Amongst the most highly upregulated proteins upon MCPyV ST expression were proteins associated with enhancing cell motility, invasion and migration. For example, previous work has confirmed that the microtubule-associated protein, stathmin is upregulated upon MCPyV ST expression and has been implicated in MCPyV ST-mediated microtubule destabilization and cell motility (Knight et al., 2015). However, from this large dataset there are several other differentially expressed protein candidates which may also be involved in MCPyV ST-induced pathogenesis. This chapter therefore describes an initial screen of three additional proteins of particular interest, which were highly upregulated upon MCPyV ST expression. These proteins were kinesin family protein (Kif14), Vitronectin (Vn) and periplakin (PPL), each have interesting and potential properties for cancer development which

may be related to MCPyV ST functioning and thus merited further investigation.

Kif14 is a member of the motor protein kinesin superfamily of proteins (KIFs), which are known to be involved in cancer progression. Specifically, depletion of KIF14 is thought to delay the metaphase-to-anaphase transition, resulting in a binucleated status, which enhances tumour progression. However, the exact correlation between KIF14 and cancer progression remains ambiguous (Xu et al., 2014), but may function through integrin activation, regulating cell spreading, cell-matrix adhesiveness and cell migration (Ahmed et al., 2012). Periplakin (PPL) is a member of the plakin family which have various functions in connecting cytoskeleton elements to form intercellular junction complexes and has been implicated in cell motility. In addition, PPL also plays a role as a localization signal for oncogenic serine/threonine protein kinase Akt/protein kinase B (PKB)-mediated signaling in human cancer cell lines. Vitronectin is a abundant glycoprotein found in serum and is also associated with the extracellular matrix. It has a defined activity in cell adhesion, promoting cell attachment, spreading, proliferation and differentiation of many normal and neoplastic types of cells.

The aim of this chapter was therefore first to confirm that these three proteins of interest were differentially expressed upon MCPyV ST expression and to determine whether they interacted with the MCPyV ST protein. If so, it would lead to a better understanding how MCPyV ST functions. Moreover, importantly this chapter would provide valuable experience in the molecular techniques required for downstream analysis of MCPyV truncated LT proteomic analysis described in later chapters and is the main focus of this thesis.

3.2. Differential expression of target cellular proteins upon expression of MCPyV ST.

The first step in elucidating whether the three highlighted proteins of interest identified by the SILAC-based quantitative proteomic screen have a role in MCPyV ST-mediated tumourigenesis, was to confirm that their expression was induced upon ST expression. Quantitative proteomic analysis suggested that Kif14, Vitronectin and periplakin were upregulated by 3.7, 2.5 and 5.2 fold, respectively (personal communication Professor Whitehouse). To this end, the expression levels of the three cellular proteins were assessed in the i293-ST cell line. This is a 293 Flp-In cell line capable of inducible MCPyV ST expression upon the addition of doxycycline hyclate. Therefore, i293-ST cells remained uninduced or were induced for 24 or 48 hours and cell lysates analysed by immunoblotting. To confirm induction of MCPyV ST expression, western blotting was performed using a FLAG-specific antibody, whereas expression of the cellular proteins were detected using commercially available monoclonal antibodies specific for Kif14-, Vitronectin- and periplakin-proteins, respectively. To ensure similar loading for each sample, GAPDH was used as a control, in addition to protein concentration determination using a Bradford assay prior to immunoblot analysis.

From the SILAC-based quantitative proteomics profiles, all three target proteins showed increased expression upon MCPyV ST induction. However, although immunoblot results showed increased levels of MCPyV ST expression at 24 and 48 hours respectively upon induction (Figure 3.1). Immunoblotting experiments demonstrate contradictory results for the three cellular proteins when comparing immunoblot analysis with the quantitative proteomic dataset. The expression levels of Periplakin were increased at 48 hours, similar to the quantitative proteomic dataset. However, both vitronectin and Kif14 protein levels were unchanged upon expression of MCPyV ST at both time points.

(i)

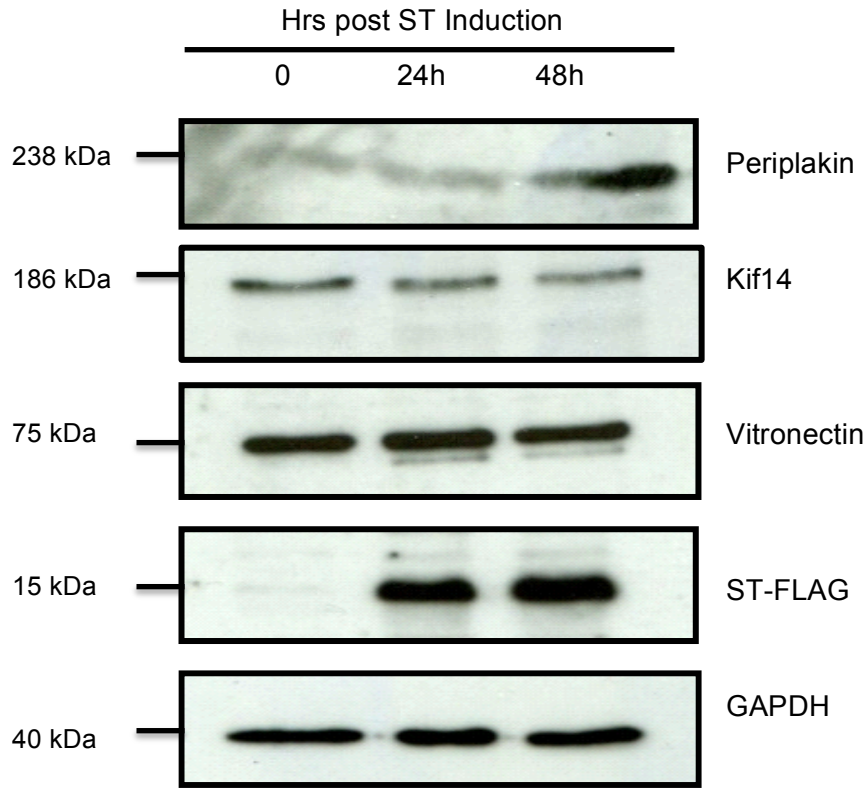

(ii)

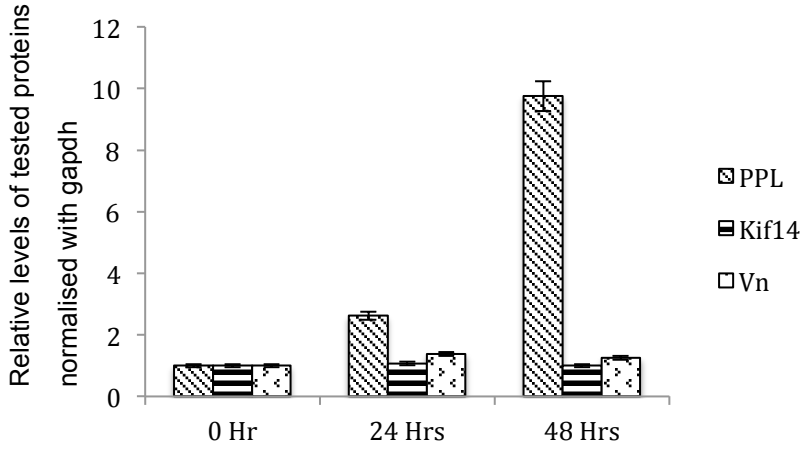

Figure 3.1: Analysis of differential cellular protein expression upon MCPyV ST induction.

(i) i293-ST cells were induced with doxycyclin hyclate and cell lysates were harvested at 0, 24 and 48 hours time point. Each sample was loaded equally to visualise the effects of respective cellular protein expression. Immunoblotting was then performed using periplakin (1:500), KIF14 (1:1000) and vitronectin (1:1000)-specific antibodies at the respective dilution shown. ST protein was tagged with FLAG and detected using polyclonal FLAG antibody (1:2500) and anti-GAPDH (1:5000) antibody was used as the loading control (n=3). (ii) Densitometry relative levels of each tested proteins expressed at 0 Hr, 24 Hrs and 48 Hrs normalised with GAPDH loading control.

3.3. Levels of mRNA transcripts in the cells expressing MCPyV ST does not reflect the levels of protein observed in immunoblot analysis.

To further investigate the discrepancy between the immunoblot results and previous quantitative proteomic analysis, qRT-PCR was performed to determine the transcript levels of each cellular protein of interest using exon specific primers for Kif14, vitronectin and periplakin. i293-ST cells remained uninduced or were induced for 24 hours and total RNA was then extracted and qRT-PCR performed (Figure 3.2). The results demonstrated that transcript levels for both periplakin and vitronectin are increased by approximately 2.5 fold upon MCPyV ST expression compared to uninduced cells, whereas mRNA levels of Kif14 varied between 0.5 to 1.5 in each of the samples evaluated. Again these results were inconsistent, showing that the transcript levels did not represent the protein expression levels observed in the above immunoblot analysis. The only cellular protein which has consistent findings between the quantitative proteomic dataset, transcript levels and immunoblot analysis is periplakin.

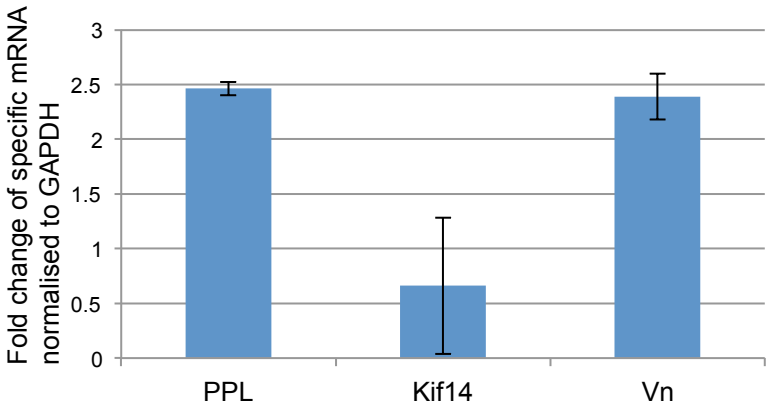

Figure 3.2: Quantification of mRNA levels of periplakin (PPL), Kinesin-like protein (Kif14) and Vitronectin (Vn) by qRT-PCR.

i293-ST cells were either left untreated or induced with doxycycline for 24 hours. RNA extractions were performed in triplicate for each condition and cDNA was generated by reverse transcription. qPCR reactions were carried out using SensiMix™ SYBR Kit No-ROX Kit with periplakin, Kif14, Vitronectin and GAPDH specific primers. The fold change in mRNA transcript were calculated based on threshold values (Ct) difference between each individual samples (with and without ST expression) and normalised with the GAPDH values. The graph shows the average fold change and standard deviations from a combination of three independent experiments.

3.4. Analysing the effect of MCPyV ST expression on the subcellular localisation of the three cellular proteins.

To further analyse whether the three cellular proteins, periplakin, vitronectin and Kif14, have any role in the functioning of MCPyV ST, immunofluorescence studies were performed. This approach aimed to determine whether the subcellular localisation of the cellular proteins were altered upon MCPyV ST expression and/or the cellular protein co-localised with the ST protein. MCC13 cells were transfected with a control plasmid, pGFP, or a plasmid expressing an GFP-tagged ST construct (previously produced by Dr David Griffiths, Whitehouse laboratory). After 24 hours post transfection, the cells were fixed, permeabilised and incubated with primary antibodies specific for each target cellular protein and secondary antibodies conjugated with Alexa fluor 546. MCPyV ST expression was analysed by direct GFP fluorescence, while the nuclear DNA was stained with DAPI.

3.4.1. MCPyV ST and Periplakin.

Periplakin (PPL) is a member of the plakin family which have various functions in connecting cytoskeleton elements to form intercellular junction complexes (Sonnenberg and Liem, 2007). Most of the plakin family function as "molecular bridges" linking the intracellular cytoskeleton and cell-cell junctions. Gene mapping of the domains utilising a variety of periplakin deletion constructs (DiColandrea et al., 2000) showed that the periplakin N-terminus localizes at the plasma membrane in a punctate distribution, whereas the C-terminus associates with keratin filaments. Of particular interest in regard to MCPyV ST-induced tumourigenesis is that PPL knockdown resulted in reduced cellular movement and attachment activity of cells (Tonoike et al., 2011).

Several studies have investigated the subcellular localization of Periplakin. It has been shown to localize to desmosomes, the interdesmosomal plasma membrane and intermediate filaments between cells (DiColandrea et al., 2000). Moreover, in transient expression studies of primary human

keratinocytes, periplakin accumulated on the apical plasma membrane and at cell-cell contacts. Therefore, to examine the subcellular localisation of periplakin in control or GFP-ST expressing cells, the MCPyV negative MCC cell line, MCC13 was transfected with GFP or GFP-ST expression constructs and after 24 hours, cells were fixed, permeabilised and periplakin staining was analysed using a periplakin-specific antibody. GFP and GFP-ST localisation was visualised by direct fluorescence (Figure 3.3). GFP staining is observed diffuse throughout the cytoplasm and nucleus, where GFP-ST localises to both the nucleus and cytoplasm, with enhanced staining in the perinuclear region of the cell (Knight et al., 2015). Indirect immunofluorescence studies of periplakin in GFP-expressing control cells shows similar staining and localisation to previously described studies, where periplakin is present throughout regions of the cytoplasm. Enhanced staining was observed in the perinuclear region with some punctate staining discernibly visible which is reminiscent of vesticular staining. However, the exact localisation needs to be confirmed with colocalisation of characterised cellular marker proteins. A similar staining was observed for periplakin in GFP-ST expressing cells. A proportion of MCPyV ST appeared to colocalise with periplakin in the cytoplasm and also around the perinuclear region, where ST is evident. This may suggest a possible interaction and relocalisation of a small proportion of periplakin to this region upon ST expression, as an enhanced concentration of periplakin is observed in this region in GFP-ST expressing cells.

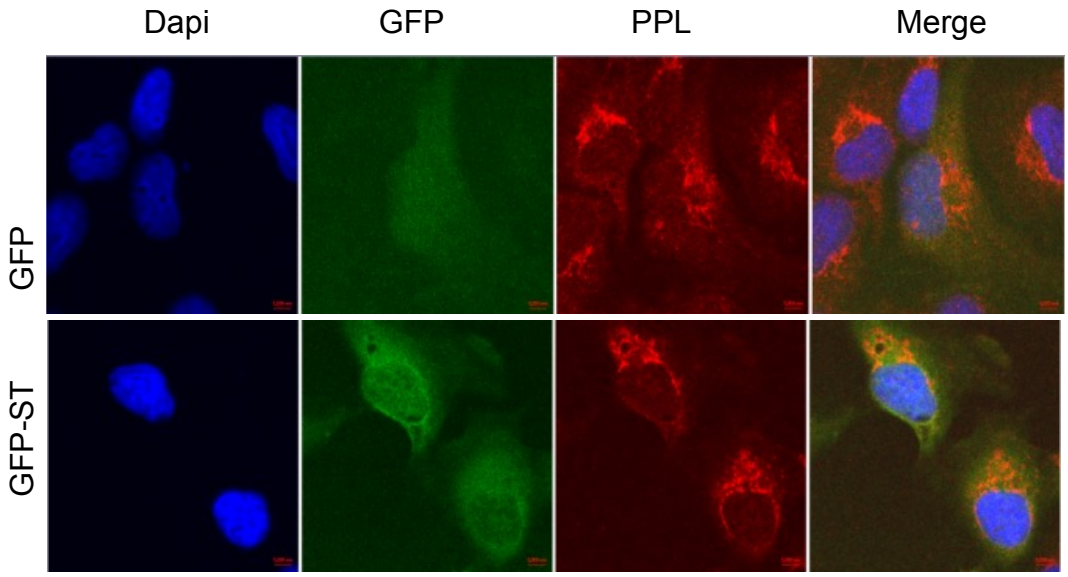

Figure 3.3: Immunofluorescence analysis of MCC13 cells transfected with GFP and GFP-ST expressing vectors.

MCC13 cells were transfected with GFP or GFP-ST expressing vectors. After 24 hours, the cells were fixed, permeabilised ,then incubated with anti-periplakin (1:100) overnight at 4°C. The secondary antibody Alexa fluor 488 goat anti rabbit used at 1:500 dilution for 1h at room temperature. Mounting medium VECTASHIELD contains 4',6-diamidino-2-phenylindole (DAPI) and used to counterstain DNA (blue).

3.4.2. MCPyV ST and the motor protein kinesin family (Kif14)

The kinesin superfamily of proteins (KIFs) generally function to transport membranous organelles and protein complexes in a microtubule- and ATP-dependent manner. KIFs have been associated with cancer progression, by disturbing the cell cycle. For example, downregulation of Kif14 expression has been shown to delay the transition of metaphase to anaphase in lung adenocarcinomas causing a binucleated status, which enhances tumour progression (Hung et al., 2013). Conversely, Kif14 overexpression inhibits anchorage-independent growth *in vitro* and also inhibits cancer cell migration, invasion and adhesion to the extracellular matrix. An adhesion molecule, cadherin 11 (CDH11), was recruited to the cellular membrane which has been implicated in the adhesive, migratory and invasive properties of the cell (Hung et al., 2013). In addition, Kif14 interacts with supervillin, a membrane protein involved in directing cellular motility (Smith et al., 2010). Considering the highly metastatic of the MCC,

the further elucidation of a possible interaction of MCPyV ST and Kif14 was also examining initially by immunofluorescence studies. KIF14 is localized to the cytoplasm during interphase, and becomes tightly localized to the midbody and central spindle during cytokinesis (Carleton et al., 2006b; Gruneberg et al., 2006a). As above, the subcellular localisation of Kif14 was examined in GFP and GFP-ST expressing MCC13 cells, using a Kif14-specific antibody (Figure 3.4). Results show that in GFP-expressing control cells, Kif14 localised to the cytoplasm, mainly diffusely but some cells contained punctate structures. Expression of MCPyV ST was observed to colocalise with a diffuse proportion of Kif14 in the cytoplasm. More noticeable nuclear puncta were also observed in GFP-ST infected cells. However, these were also observed in a non-transfected cells in this sample. Although comparison between the GFP and GFP-ST showed possible alterations of Kif14 distribution, these were not conclusive. Further optimisation of the antibody for immunofluorescence studies was performed, but failed to show any further improvement.

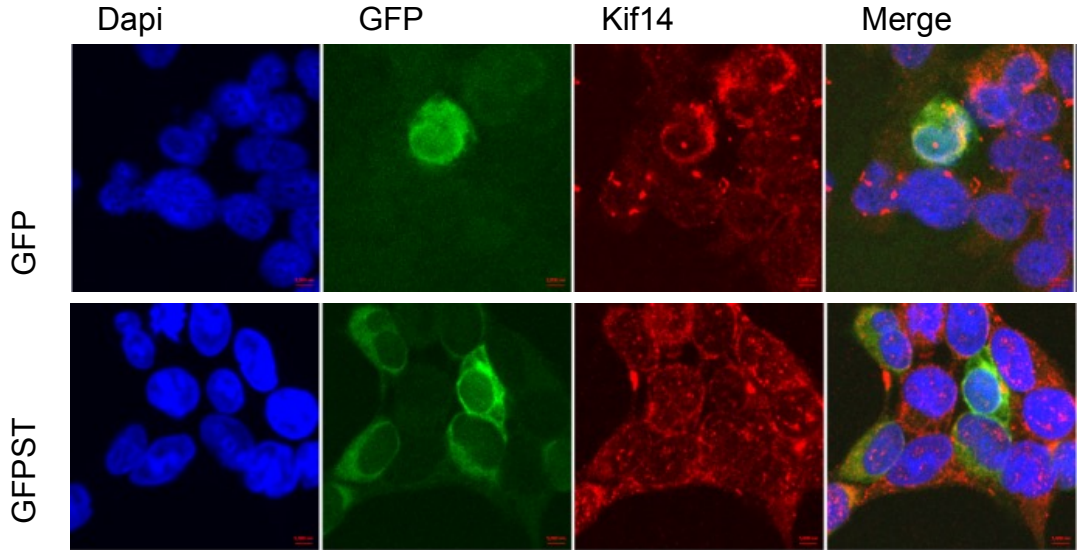

Figure 3.4: Immunofluorescence analysis of MCC13 cancer cells transfected with GFP and GFP tagged ST antigen.

MCC13 cells were transfected with GFP or GFP-ST expressing vectors. After 24 hours, the cells were fixed, permeabilised and then incubated with anti-Kif14 (1:100) overnight at 4°C. The secondary antibody Alexa fluor 488 goat anti rabbit used at 1:500 dilution for 1h at room temperature. Mounting medium VECTASHIELD contains 4',6-diamidino-2-phenylindole (DAPI) and used to counterstain DNA (blue).

3.4.3. MCPyV ST and Vitronectin.

Vitronectin is an abundant and multi-functional glycoprotein found in serum and is also associated with the extracellular matrix. It has a defined activity in cell adhesion, promoting cell attachment, spreading, proliferation and differentiation of many normal and neoplastic cell types. As such it is a key protein in regulating cell homeostasis (Preissner and Seiffert, 1998) and tumour malignancy (Felding-Habermann and Cheresh, 1993). Vitronectin also possesses binding sites for membrane-bound integrins which function to anchor cells to the cellular matrix. These interactions are thought to be associated with vitronectin's role in cell migration and signal transduction.

Immunofluorescence studies were therefore performed as above in transfected GFP and GFP-ST to determine if MCPyV ST colocalised or altered the subcellular localisation of vitronectin (Figure 3.5). Analysis of GFP-expressing cells appeared to show that vitronectin was present in the cytoplasm and the nucleus of GFP-expressing cells. This was rather surprising due to its known function as a glycoprotein. In contrast, vitronectin was observed in the cytoplasm and perhaps the extracellular matrix in MCPyV ST expressing cells. Due to the discrepancy of vitronectin staining in control cells further immunofluorescence studies are required to investigate any possible redistribution or colocalization with MCPyV ST.

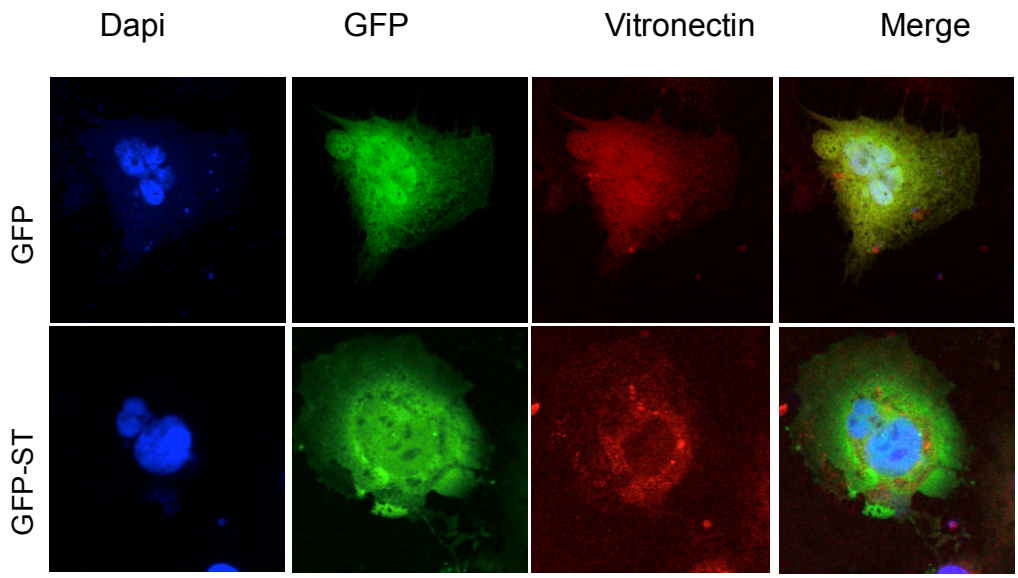

Figure 3.5: Immunofluorescence analysis of MCC13 cells transfected with GFP and GFP tagged ST antigen.

MCC13 cells were transfected with GFP or GFP-ST expressing vectors. After 24 hours, the cells were fixed, permeabilised and then incubated with anti-vitronectin (1:100) overnight at 4°C. The secondary antibody Alexa fluor 488 goat anti rabbit used at 1:500 dilution for 1h at room temperature. Mounting medium VECTASHIELD contains 4',6-diamidino-2-phenylindole (DAPI) and used to counterstain DNA (blue).

3.5. Assessing the possible interaction of prioritised cellular proteins with MCPyV ST.

The previous attempts to confirm whether the prioritised proteins identified from the SILAC-based quantitative proteomic dataset may play a role in MCPyV ST-induced cell motility proved inconsistent. In contrast to the proteomic data not all the proteins were induced upon MCPyV ST expression as assessed by immunoblotting or qRT-PCR. Moreover, immunofluorescence studies suggested little redistribution of the cellular proteins upon expression of the viral protein. However some colocalisation was observed with a proportion of MCPyV ST and the prioritised proteins, such as periplakin. Therefore, the final selection criteria to assess any relevance of the prioritise cellular proteins to MCPyV ST function was to determine whether the cellular proteins interacted with MCPyV ST using GST-pulldown assays.

3.5.1. Expression and purification of proteins to GST beads.

GST pull-down assays were performed using either recombinant expressed control GST protein or GST-ST protein incubated with HEK 293 cell lysates. Initially, an expression time course was performed to assess whether both recombinant GST and GST-ST could be expressed and purified in bacteria. Plasmids encoding GST and GST-ST (kindly provided by Dr David Griffiths) were transformed into competent *E. coli* BL21 cells for optimal expression and grown at 37ºC for 2 hours, prior to induction with IPTG. Samples were then harvested at 0, 1, 2, 3, and 4 hours post-induction and analysed by immunoblotting using a GST-specific antibody. The results demonstrated that both GST and GST-ST proteins were efficiency expressed after one hour induction (Figure 3.6).

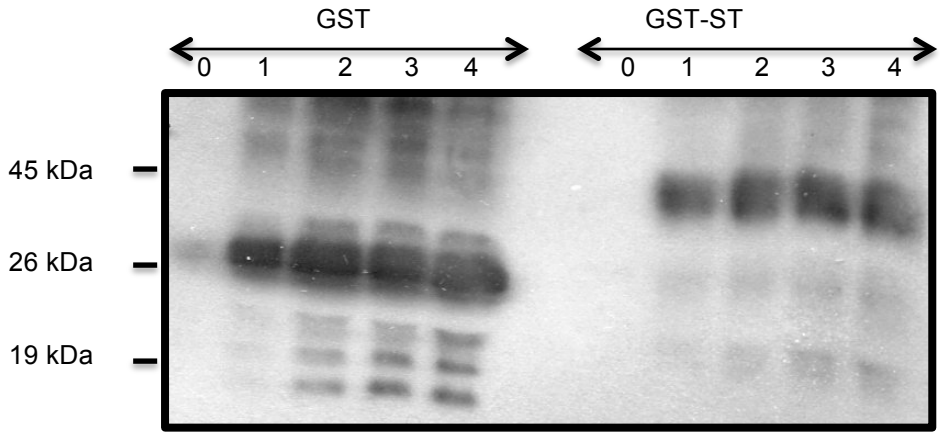

Figure 3.6: Recombinant protein expression trials of GST and GST-ST in a bacterial expression system.

Western blot analysis of the recombinant protein expression of GST and GST-ST. The recombinant expression plasmids were transformed into *E. coli* BL21. Protein samples were analysed at hourly time points post induction using a GST-specific antibody. Recombinant proteins were expressed at the correct predicted sizes, of around 45 kDa for GST-ST; while the expression of the GST control construct is shown around 26-28 kDa. The cell lysates were prepared and separated by electrophoresis on 12% polyacrylamide gels at 180V for 1 hr, protein were transferred to nitrocellulose membrane and probed against GST-monoclonal antibody; 1: 3000.

For GST-pulldown assays to be performed, it was first necessary to determine if the expressed GST and GST-ST recombinant proteins could be bound and purified using GST-affinity beads. Therefore, the 4-hour induced bacterial time points for GST and GST-ST were suspended in

protein solubilising buffer and lysed by sonication to break open the cells. The purified bacterial lysate was then incubated with GST-affinity beads to purify the protein prior to pulldown experiments. GST and GST-ST proteins were successfully shown to bind the GST-affinity beads allowing purification and pulldown assays to be performed (Figure 3.7).

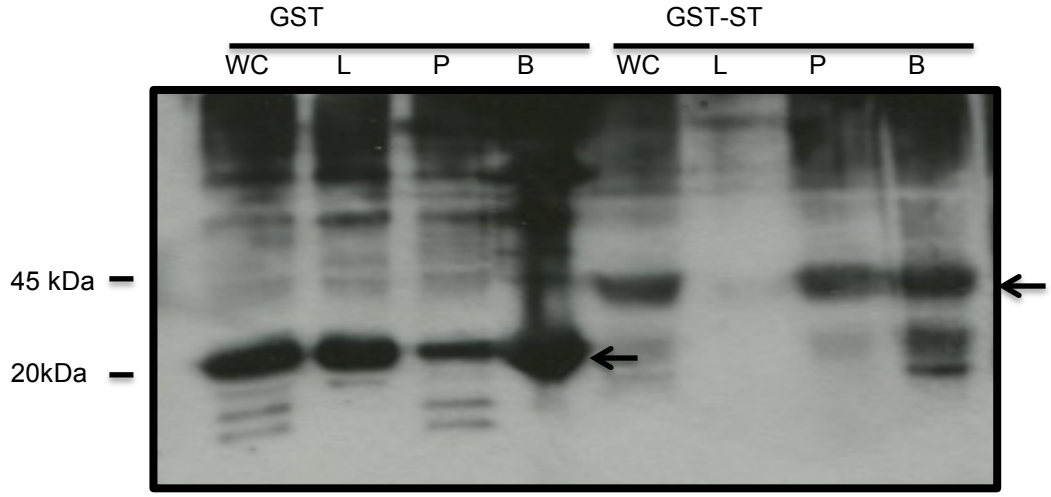

Figure 3.7: Purification of recombinant GST protein and GST-ST proteins to GST-affinity beads.

Immunoblot analysis of the expressed GST and GST-ST proteins at various stages of purification. The lanes are labelled indicating the samples that have been loaded to the gel. The labelled samples are WC (whole cell lysate); L (lysate), P (Pellet), B (Protein binds to the beads). The arrows indicate GST and GST-ST protein were successfully purified and bound to beads for GST-pulldown assays. The cell lysates were prepared and separated by electrophoresis on 12% polyacrylamide gels at 180V for 1 hr, protein were transferred to nitrocellulose membrane and probed against GST-monoclonal antibody; 1: 3000.

3.5.2. Pull-down assays to assess the interactions between GST and GST-ST with prioritised cellular proteins.

An interaction between MCPyV ST and the prioritised protein may suggest a possible role in the regulation and function of the viral protein in inducing cell motility. To assess any possible interaction between the cellular proteins and GST-ST, GST pulldown assays were performed. Bead bound GST or GST-ST proteins were incubated with a HEK293 cellular lysate for 4 hours. The precipitated proteins were then analysed by western blotting

using Kif14-, Vitronectin- and periplakin-specific antibodies. The GST-pulldown assay results showed that the MCPyV-ST did not interact with periplakin or vitronectin. However, results do show a possible interaction with Kif14 (Figure 3.8). It is also questionable why the vitronectin showed an interaction with GST but not GST-ST. To further investigate this observation the reverse pulldown experiment was performed by expressing recombinant vitronectin in bacteria and assessing whether this interacts with a cellular lysate expressing MCPyV ST protein.

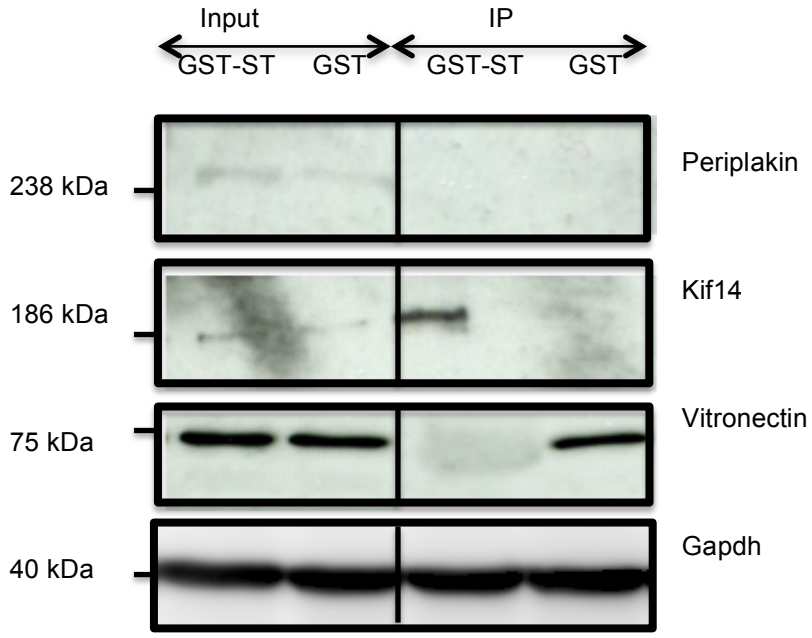

Figure 3.8: Pull down assay of GST and GST-ST with 293T cell lysates.

Immunoblot analysis of pulldown experiment of beads bound GST or GST-ST incubated with cellular lysate and immunoblotted with Kif14-, Vitronectin- and periplakin-monoclonal antibodies. Precipitated proteins were then separated by electrophoresis and transferred to nitrocellulose membrane and probed using appropriate primary antibodies against PPL (1:500), Kif14 (1:500) and Vn (1:1000) and Anti-GAPDH (1:5000) antibody was used as the loading control.

3.5.2.1. Assessing an interaction between GST-vitronectin and MCPyV ST.

Due to the interaction of vitronectin with the GST control in pulldown assays, reverse pulldown assays were attempted using recombinant GST-vitronectin. We were kindly provided with a GST-vitronectin construct from

Professor Hocking, University of Rochester Medical Centre, USA. Initial studies were therefore performed to determine whether GST-vitronectin can be expressed and purified, as in the above experiments. Samples were harvested at 0, 1, 2, 3, and 4 hours post induction and the 4 hour expression time point analysed by SDS-PAGE and coomassie staining. Results showed that significant amounts of recombinant GST-vitronectin were produced at 4 hours post induction with IPTG (Figure 3.9). The protein is expressed at the expected size of approximately 101 kDa (Vitronectin 75 kDa and GST 26 kDa).

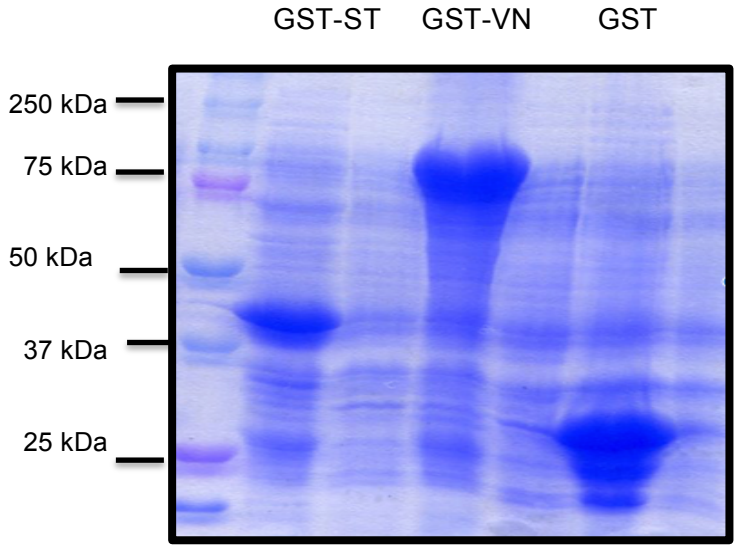

Figure 3.9: Overexpression of GST-ST, GST-VN and GST in bacterial BL21 cells.

Recombinant GST, GST-ST and GST-VN plasmids were transformed in bacteria cells, *E. coli* BL21. Samples were harvested at four hours post IPTG induction and analysed by SDS-PAGE and coomassie staining. The expected sizes of protein bands detected at approximately 50 kDa, 101 kDa and 26 kDa respectively.

Upon confirmation that vitronectin could be expressed as a recombinant GST fusion protein, GST pulldown assays where performed to assess if it interacted with MCPyV ST. GST-vitronectin was bound to GST affinity beads as described above and then incubated with uninduced and induced MCPyV ST expressing cellular lysates for two hours. The beads were then washed three times and precipitated proteins analysed by immunoblotting using a GST- and a Flag-specific antibody recognising the MCPyV ST-Flag fusion protein (Figure 3.10).

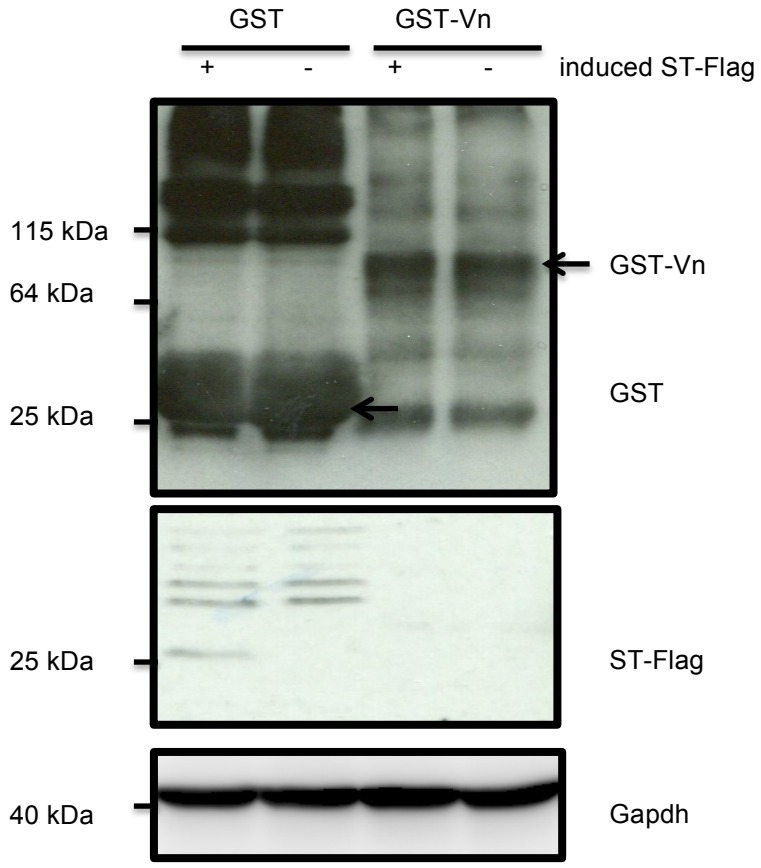

Figure 3.10: GST-pull down assay of GST and GST-VN with uninduced and induced i293-ST cell lysates.

Immunoblot analysis of pulldown experiment of GST beads bound GST or GST-Vn expressed proteins were incubated with i293-ST cellular lysate either left untreated or treated with doxycycline to study the direct interaction of MCPyV ST (Flag tagged ST) and Vitronectin. Immunoblot analysis of pull down of GST and GST-Vn incubated with untreated and treated i293-ST cell lysates.

Results demonstrate that GST and GST-Vn proteins were both successfully expressed and bound to GST-affinity beads. Unfortunately however, little can be taken from this experiment. Even though the GST-Vn was expressed and bound to the GST beads, the immunoblot using the Flag-specific antibody showed that MCPyV ST was not precipitated using uninduced or induced i293-ST cell lysates. Similar to the previous GST and GST-ST pull down assay, only GST resulted in a slight amount of precipitated ST-Flag protein. Therefore, these results suggest that vitronectin does not interact with MCPyV ST.

3.5.3. Immunoprecipitation assays to further investigate possible interactions between MCPyV ST and prioritised cellular proteins.

To further investigate any potential interaction between MCPyV ST and the prioritised cellular proteins, co-immunoprecipitations were performed using GFP-Trap®_A beads. To this end, GFP and GFP-ST expression vectors were transfected into 293 cells and after 24 hours the cell lysates were incubated with GFP-Trap beads for two hours. After subsequent washing, precipitated proteins were separated by SDS-PAGE and immunoblotted with GFP-, Vn-, Kif14- and PPL-specific antibodies.

Immunoblot results demonstrated that both GFP and GFP-ST were efficiently bound by the GFP-Trap beads. However, the results showed that no interactions were observed between MCPyV ST and all the target proteins as the IP immunoblot lanes were all blank (Figure 3.11). Although, this result was expected for periplakin and vitronectin, as no interaction was observed with the GST-pulldown analysis, an interaction between MCPyV ST and Kif14 was expected. However, the Kif14 antibody failed to identify endogenous protein even in the input lanes. This might be due to the large size of Kif14 causing low efficiency membrane transfer, even though the transfer was carried out overnight. The periplakin signals were also very weak in the input showing that very little protein had transferred or was expressed in the HEK 293 cells.

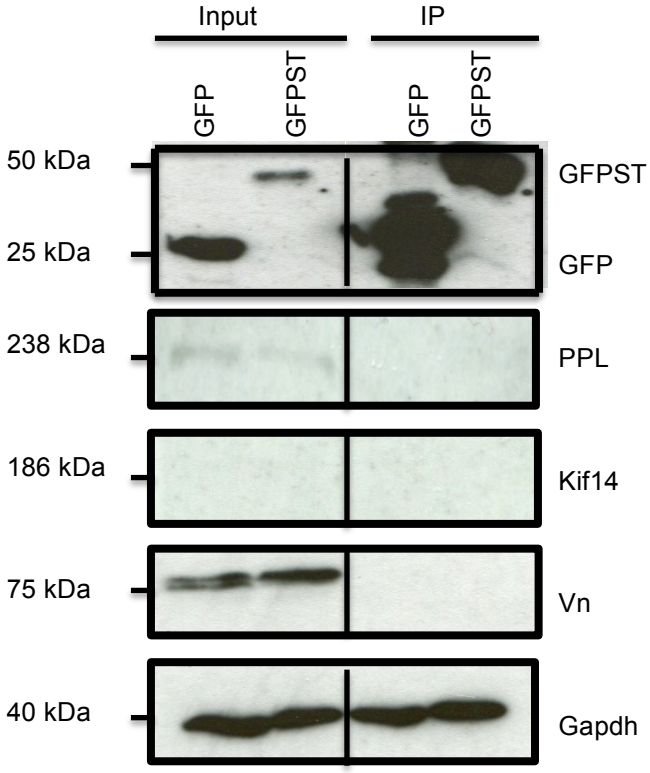

Figure 3.11: Coimmunoprecipitation assays to examine possible interactions between GFP-ST and the prioritised cellular proteins.

HEK 293 cells transfected with GFP and GFP-ST expressing vectors and after 24 hours cell lysates were bound to GFP trap beads. Precipitated proteins were then separated by electrophoresis and transferred to nitrocellulose membrane and probed using appropriate primary antibodies against PPL (1:500), Kif14 (1:500) and Vn (1:1000). ST protein was tagged with GFP (1:5000) to confirm the expression of ST in the samples and Anti-GAPDH (1:5000) antibody was used as the loading control.

3.6. Elucidation of possible function of Kif14.

The GST-pulldown assays in Figure 3.8, suggested that MCPyV ST may interact with Kif14. However, this was not confirmed using coimmunoprecipitation assays, although no Kif14 inputs were observed in this blot. To confirm a possible interaction between MCPyV ST and Kif14, immunofluorescence studies were repeated using a Kif14-His tagged expression vector (pPM-C-His). The overexpression construct may overcome the issues previously observed with the poor Kif14-specific antibody on both immunofluorescence and immunoblotting and also avoid poor western blot transfer of such a large protein (186 kDa). Immunofluorescence studies were performed in MCC13 cells transfected with GFP or GFP-ST in the presence of the Kif14-His expression vector.

After 24 hours, the cells were fixed, permeabilised and stained with either His-specific or Kif14 specific antibodies, whereas GFP and GFP-ST were identified by direct fluorescence. Results show that Kif14 overexpression results in a diffuse cytoplasmic localisation in addition to discrete nuclear puncta (Figure 3.12). This localisation was similar in both GFP and GFP-ST expressing cells. Interestingly, there was significant colocalisation between GFP-ST and Kif14 in the cytoplasm, which may suggest a possible interaction.

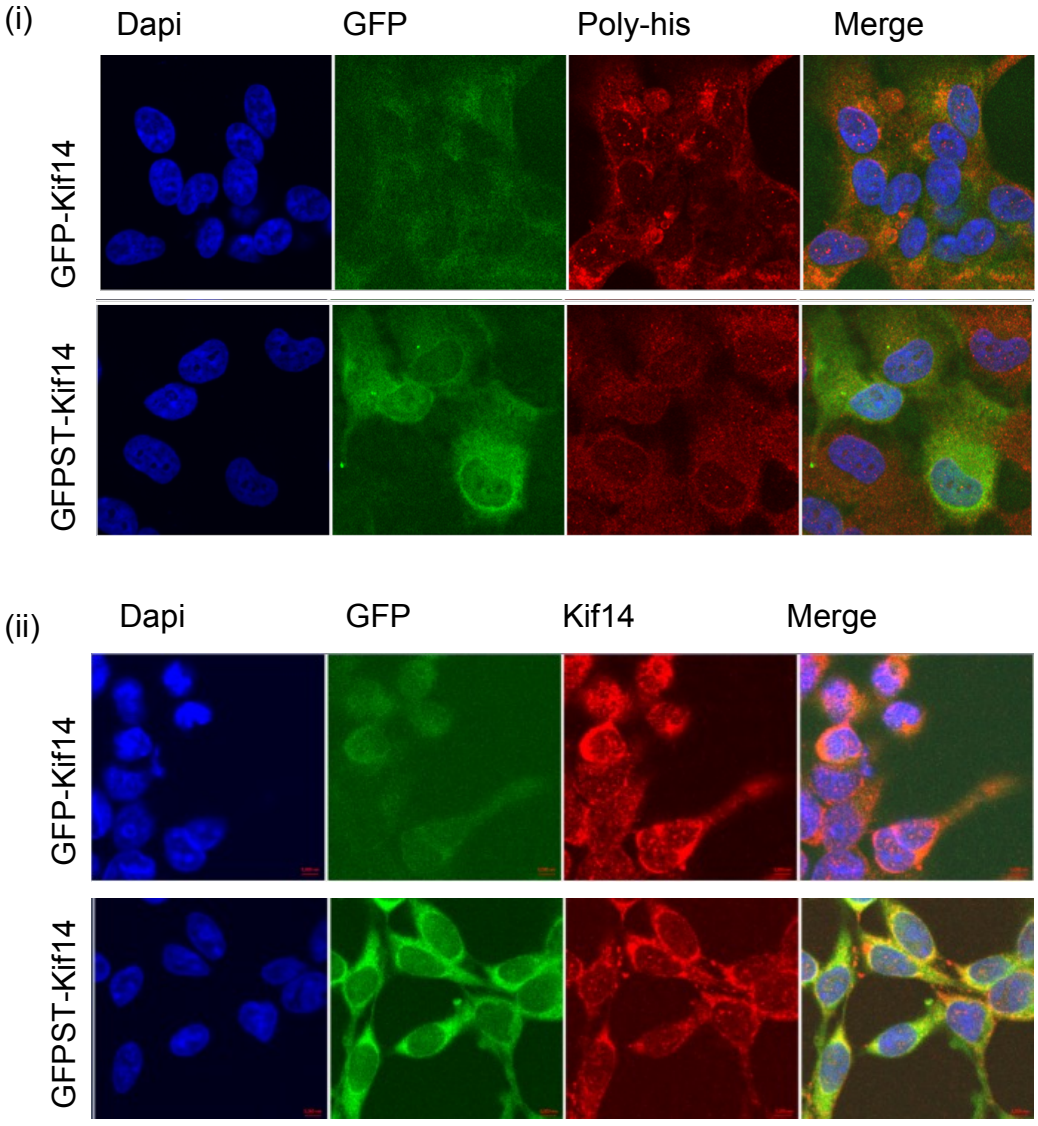

Figure 3.12: Immunofluorescence studies suggest colocalisation between GFP-ST and overexpressing Kif14-His tagged proteins.

MCC13 cells were seeded onto poly-L-lysine coated coverslips prior to transfection with either eGFP or eGFP-ST in the presence of a KiF14 overexpression construct, pPM-C-His. Cells were fixed and permeabilised prior to staining with His- or Kif14-specific antibodies (red) and mounting medium VECTASHIELD contains 4',6-diamidino-2-phenylindole (DAPI) and used to counterstain DNA (blue).

3.7. Discussion

The objective of this chapter was to screen three cellular proteins which were highlighted from a previous SILAC-based quantitative proteomic screen which were upregulated upon the expression of the MCPyV ST protein. The selected protein targets, periplakin, Kif14 and vitronectin were prioritised as their characterised role in mammalian cells could possibly be implicated in MCPyV ST-mediated roles in enhanced cell motility and cellular transformation. Therefore the aim was to perform initial screening of the interactions between these three prioritised proteins and MCPyV ST using several pulldown assays and immunofluorescence colocalisation studies. Importantly, the second purpose of these studies were also to familiarize myself with the techniques which will be used to investigate the function of cellular proteins which were differentially expressed upon MCPyV truncated large T antigen, which was the focus of the next two chapters and the main objective of my thesis.

From the initial screening of these proteins, data showed that Periplakin levels were significantly enhanced upon MCPyV ST expression which validated the previous quantitative proteomic approach. In contrast, Kif14 and vitronectin showed little increase in immunoblot analysis, in contrast to the proteomic results. Further validation was therefore performed assessing the transcript levels for each protein, but again this did not correlate with the SILAC or immunoblot result, apart from periplakin. Further experiments could now be performed to investigate how MCPyV ST upregulates periplakin protein levels, whether this is a combination of enhanced transcription and translation pathways is yet to be determined.

GST-pulldown assays suggested that MCPyV ST interacts with one of the three prioritized proteins, Kif14. Results also showed that a proportion of MCPyV ST also colocalised with overexpressed Kif14 in the cytoplasm of transfected cells. The role of Kif14 is cancer development is controversial. Results have shown that Kif14 can function either as a oncogene or a tumour suppressor in various cancer types. For example, Kif14 expression

has been found in several human malignancies, including retinoblastoma, breast cancer, ovarian cancer, lung cancer, liver cancer and laryngeal carcinoma (Ahmed et al., 2012; Basavarajappa and Corson, 2012; Corson et al., 2005; Madhavan et al., 2007; Markowski et al., 2009a; Markowski et al., 2009b; Theriault et al., 2012; Yang et al., 2014). Here, Kif14 overexpression has been demonstrated to be involved in tumour progression and also related to poor patient survival. In contrast however, high levels of Kif14 expression inhibits tumour growth and cancer metastasis in lung adenocarcinoma (Hung et al., 2013). Here, overexpression and silencing of Kif14 enhanced or reduced the recruitment of CDH11 in the membrane fraction, suggesting that Kif14 might act through recruiting adhesion molecules to the cell membrane and modulating cell adhesive, migratory and invasive properties. Therefore, at present it is unknown why MCPyV ST potentially targets Kif14. It may either utilise Kif14 for enhancing cell motility and migratory properties, or target Kif14 to rescue its inhibitory effects. Further experiments are now required to assess the role of Kif14 in MCPyV ST-induced cell motility and migration, by siRNA-mediated depletion studies to determine what effect this has upon cell motility in MCPyV ST-expressing cells.

Chapter 4

Quantitative proteomic analysis of the host cell proteome upon expression of truncated MCPyV LT

4.0. Quantitative proteomic analysis of the host cell proteome upon expression of truncated MCPyV LT

4.1. Introduction.

The large tumour (LT) antigen appears to be an important cell transforming factor in many polyomaviruses. The most extensively studied polyomavirus, simian virus 40, LT antigen has been shown to be an essential oncogene able to modulate many viral and cellular processes (Pipas, 2009). In general, polyomavirus LT antigens are believed to play roles in virus replication, transcription and virus-induced transformation, targeting multiple cellular pathways which regulate cell proliferation, cell death and the inflammatory response (An et al., 2012). In SV40 LT-induced transformation, at least three conserved domains are believed to be involved; the J domain and LxCxE motif which bind to Hsc70 and tumour suppressor retinoblastoma (Rb) proteins, respectively and a p53 binding domain. The N-terminus which includes the J domain and the LxCxE motif are sufficient for cell transformation *in vitro* (Sullivan and Pipas, 2002). Other than SV40, the LT antigen encoded by other polyomaviruses such as JC and BK also have been shown to induce transformation *in vitro* even though the transformation efficiencies are reduced compared to SV40 LT (Bollag et al., 1989; Bollag et al., 2000). This might be due to the reduced binding affinity of these proteins to the Rb family of proteins (Dyson et al., 1990). Similar to SV40, these viruses require LT to interfere with cell cycle control checkpoints forcing the host cell into entering the DNA replication stage which may eventually lead to cell transformation and tumourigenesis.

Similarly, the MCPyV LT is thought to play a role in MCC tumourigenesis as well as tumour cell maintenance. Importantly, siRNA-mediated knockdown of MCPyV LT in MCPyV positive MCC cells results in abandonment of cell growth and eventually cell death (Arora et al., 2012a), suggesting LT is essential for the development of MCC. However, there are

unique features of the MCPyV LT protein compared to other polyomaviruses. Genetic analysis has demonstrated that MCPyV LT undergoes truncated mutagenesis in MCC, which has not been shown in other polyomaviruses. These truncated mutations result in the virus becoming replicative defective, due to the truncated LT losing its DNA binding and helicase domains but retaining the retinoblastoma (Rb) binding domain (Shuda et al., 2008).

At present, a number of cellular proteins have been shown to be associated with MCPyV LT functioning. It specifically binds to Rb and VPS39, vacuolar protein sorting 39 homolog or novel cellular target protein, hVam6p (Liu et al., 2011; Shuda et al., 2008). Interestingly, LT binding results in hVam6p relocalisation from the cytoplasm to the nucleus (Chang et al., 2011; Liu et al., 2011). hVam6p is believed to function as an antiviral host factor due to its ability to reduce the number of MCPyV virions (Feng et al., 2011). The MCPyV LT also targets survivin, a member of the inhibitor of apoptosis protein family which is upregulated in lymphoma and metastatic melanoma (Ambrosini et al., 1997). Survivin mRNA transcripts and protein levels were found to be decreased upon knockdown of MCPyV LT in MCPyV-positive infected cells, whilst survivin protein expression increased in cells expressing MCPyV LT antigen (Arora et al., 2012).

Although a few LT-host cell protein interactions have been identified to date, the exact functions and transforming activities of MCPyV truncated LT antigen are still to be fully elucidated. The importance of the truncated version of LT antigen has recently been shown to be more effective in promoting growth of human and mouse fibroblasts compared to full length LT and the 57 kT proteins (Cheng et al., 2013). This is due to mutations which produce truncations in the MCPyV LT antigen found in MCC, resulting in the deletion of C-terminal residues which possess inhibitory effects on cell growth in several cell types (Liu et al., 2013). In many samples of MCC, truncated LT proteins vary in size depending on the site of their mutations (Kassem et al., 2008). This shows the strong selective pressures within the tumours to eliminate the viral replication capabilities.

Importantly, MCC containing replication defective virus retain essential LT motifs which potentially contributes to uncontrolled cell growth and cell survival.

Besides the truncating mutations within the LT antigen, several groups have also reported mutations in the origin of replication and VP1 gene in MCC-derived MCPyV genomic sequences that also prevent efficient replication and progeny virion production, respectively (Feng et al., 2011; Kassem et al., 2008; Kwun et al., 2009; Neumann et al., 2011). A replication defective feature is common in tumour viruses, as this is also observed in some papillomavirus-induced cancers. The selection of truncated mutations in MCPyV LT is probably driven to reduce active viral replication in these cells, thus preventing uncontrolled viral replication that may cause cell lysis and death (Moore and Chang, 2010).

To further explore the host cell interactions implicated in MCPyV truncated LT (tLT) functioning, an unbiased quantitative proteomic approach was used. This study provides a global perspective on cellular protein regulation upon expression of MCPyV tLT antigen in cancer cells. Initially, in order to further investigate the effects of the MCPyV tLT antigen on the cellular proteome, a stable cell line capable of inducibly expressing the truncated version of LT antigen upon treatment with doxycycline hyclate was produced. SILAC-based labelling coupled with mass spectrometry analysis was then performed comparing cells with and without expression of MCPyV tLT antigen. From the quantitative proteomic analysis, several possible pathways have been identified and selected for further analysis to elucidate the possible function of the tLT antigen in MCPyV-induced tumourigenesis.

4.2. Amplification of MCPyV tLT gene.

A truncated form of the MCPyV LT antigen is found in MCC. This mutation renders the virus replication defective and is also believed to be essential for transformation and pathogenesis. In order to further characterize the

function and possible effects of tLT protein expression on the cellular proteome, a cDNA clone comprising the tLT gene was first generated. This is required to prevent expression of the MCPyV ST, which is also contained in the genomic region encompassing LT. The Whitehouse laboratory has previously isolated the MCPyV genomic region containing ST and tLT genes from a MCC tumour sample, which was cloned into the eukaryotic expression vector, pEGFP-C1, termed pST/LT-GFP. To isolate the truncated LT cDNA, total RNA was extracted from pST/LT-GFP transfected cells. Reverse transcription was then performed using an oligo dT primer to generate cDNA. PCR was then performed using tLT specific primers to amplify the truncated form of LT cDNA. The MCPyV tLT cDNA was PCR amplified with specifically designed primers incorporating restriction enzymes *Kpn*I and *Not*I with a C-terminal FLAG tag. The MCPyV tLT was successfully amplified at the expected size (Figure 4.1).

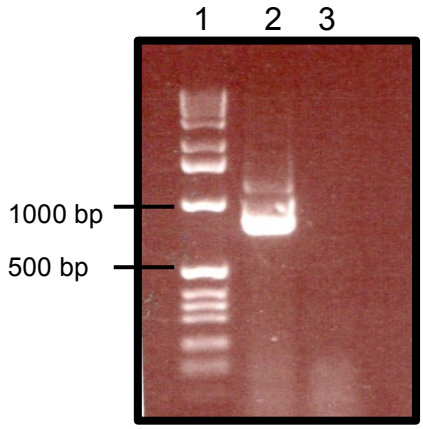

Figure 4.1: PCR amplification of MCPyV tLT cDNA.

cDNA was generated from pST/LT-GFP transfected cells and used as template for PCR amplification of MCPyV truncated LT. The PCR product was analysed by agarose gel electrophoresis, indicating that MCPyV LT cDNA was amplified successfully at expected size (approximately 825bp with FLAG-tagged at the C-terminus, lane 2). Lane 3 is a negative control PCR reaction without addition of cDNA template.

4.3. Production of a recombinant clone of FLAG-tagged MCPyV truncated LT in pcDNA5/FRT.

The first step in producing a stable cell line capable of inducibly expressing MCPyV truncated LT was to produce a eukaryotic expression vector

expressing the MCPyV truncated LT antigen. To clone the amplified truncated LT cDNA into appropriate expression vectors, the amplified PCR product was initially excised from an agarose gel, purified and ligated into a pCR product transfer vector, pCRblunt, for sequencing purposes. Upon transformation, positive colonies were selected; miniprepped and purified DNA digested using *Kpn*I and *Not*I restriction enzymes. Results are shown in Figure 4.2, which shows that all clones contained the approximately 800 bp length truncated LT cDNA PCR product. The positive clones were then confirmed by sequencing and proceeded for the subcloning into mammalian expression vectors.

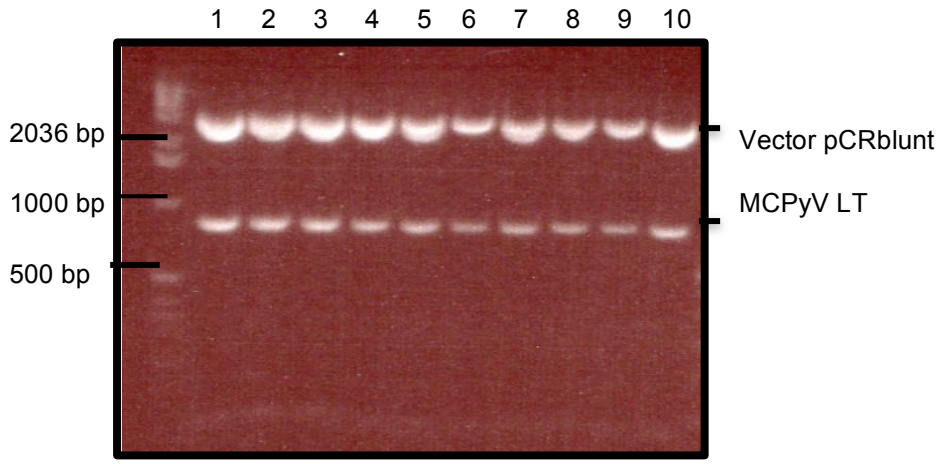

Figure 4.2: Restriction digest analysis of 10 putative cloned pCRblunt constructs containing truncated MCPyV LT.

Clones 1-10 were digested with restriction enzymes *Kpn*I and *Not*I to screen for positive recombinant clones. Digests were analysed by agarose gel electrophoresis, which indicated that MCPyV truncated LT had been cloned into pCRblunt successfully. The positive clones were sent for sequencing. The correct sequences of LT obtained from the sequencing data with Flag-tagged sequence at the C-terminus of each clone.

The truncated LT cDNA was then subcloned into the eukaryotic expression vector, pcDNA5/FRT in order to produce a inducible cell line containing the truncated LT gene. pcDNA5/FRT is a mammalian expression vector containing a FLP recombinant target (FRT) site for Flp recombinase-mediated integration of the vector into the genome of the 293 FlpIn cell line. To produce this construct, the previously selected positive pCRblunt clones were double digested with *Kpn*I and *Not*I restriction enzymes to excise the truncated MCPyV LT. This purified fragment was then ligated

with pCDNA5/FRT previously digested with the same restriction enzymes. Ligation reactions were carried out with different ratios of vector and insert to ensure that cloning was successfully performed. Upon transformation, 7 colonies were picked and grown in LB media for DNA extraction. Purified plasmid DNA was then analysed using double digestion and PCR using LT specific primers (Figure 4.3).

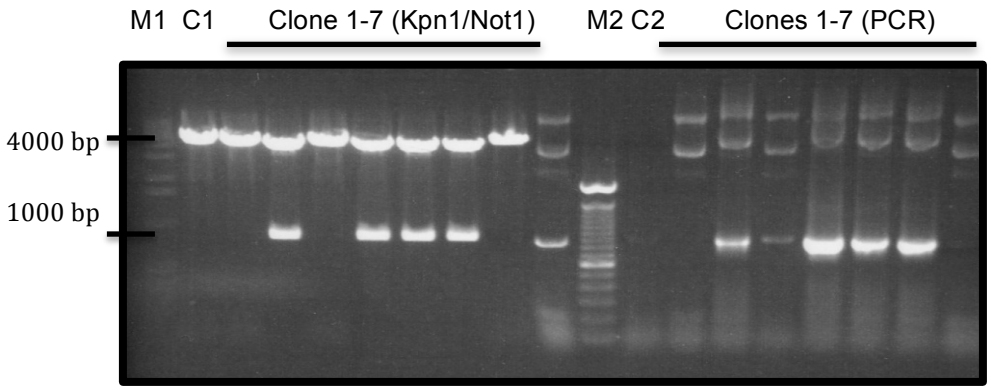

Figure 4.3: Screening of putative clones containing MCPyV tLT in pCDNA5/FRT.

Putative clones were analysed by double digestion of restriction enzyme and PCR. From the 7 clones, 4 were positive, containing the MCPyV tLT cDNA. These were sent for sequencing to ensure the correct sequence. Control for restriction enzymes analysis, C1 is an empty vector of pCDNA5/FRT and PCR without DNA template, C2 were run alongside with the test samples. DNA ladder M1, 1KB plus and M2, 100bp were also run to ensure the correct size of desired gene.

The results indicated that out of 7 clones analysed, 4 were positive for truncated LT cDNA insertion. These results were subsequently verified by DNA sequencing using the primers T7 for forward reaction and BGH reverse primers as reverse reaction to sequence the MCV LT recombinant clones. Sequences were aligned with the public database Genbank and found to be identical with MCPyV LT gene sequence. Moreover, sequencing confirmed that the Flag tag was in the correct reading frame. This construct is now referred to as pcDNAFlag-tLT.

4.4. Expression of MCPyV truncated LT in mammalian HEK 293 cells.

To confirm that recombinant clones of pcDNAFlag-tLT were able to express the MCPyV tLT protein, the plasmid construct was transfected into HEK 293 cells. After 24 hours post transfection, cell lysates were harvested and analysed by immunoblotting using a FLAG-specific antibody. Results showed that pcDNAFlag-LT was able to express a truncated form of LT, at the correct predicted size of approximately 40 kDa, with clear distinct bands detected with anti-FLAG antibody (Figure 4.4).

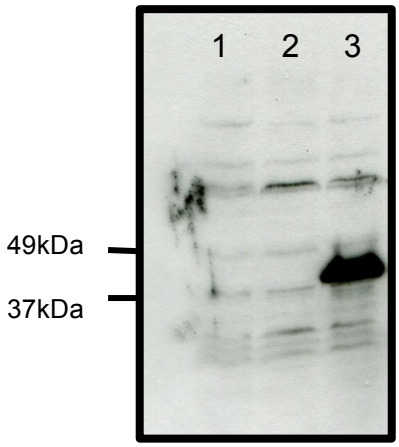

Figure 4.4: Expression of FLAG-truncated LT in HEK 293 cells.

Immunoblot analysis of lane (1) Untransfected cell lysate (2) lysate from 293 cells transfected with empty pCDNA5/FRT and (3) lysate from 293 cells transfected pcDNAFlag-LT. Immunoblot analysis was performed using a polyclonal anti-FLAG antibody (1:2500) and anti-Rabbit (1:5000) conjugated HRP antibody. The FLAG-LT is expressed at the correct expected size, approximately 40 kDa. No band is detected in both control conditions.

4.5. Using the FlpIn^{TM} system for generation of a cell line capable of inducibly expressing truncated MCPyV LT.

The generation of the pcDNAFlag-LT expression construct was essential to further investigate the effect of MCPyV truncated LT expression on the cellular proteome, as well as elucidating novel potential interaction partners for MCPyV truncated LT. The longer term aim was to perform Stable-isotope labelling by amino acids in cell culture (SILAC)-based high

throughput quantitative proteomics technique to obtain a list of differentiated cellular proteins upon expression of MCPyV truncated LT. However, to perform this type of analysis it is first necessary to generate a stable cell line which could inducibly express the MCPyV truncated LT proteins in a homogenous population of cells. Therefore, to produce this inducible cell line, 293 FlpIn cells were co-transfected with pcDNAFLAG-LT and pPGK/Flip/ObpA. This co-transfection resulted in integration of MCPyV tLT at specific site of recombination into the HEK 293 FlpIn genome. The schematic diagram of the integration and expression of a gene of interest in the HEK 293 Flp In^{TM} System is presented in Figure 4.5.

Transfected cells were then selected and maintained under Hygromycin B selection. Multiple putative MCPyV tLT cell lines were then screened and tested for induction and expression of the truncated LT protein. To this end, the expression of MCPyV truncated LT was tested by incubating each putative cell line clone with 2 µg/mL Doxycycline hyclate (Dox) for 24 and 48 hours. Each clone was then analysed for the ability to stably express the truncated LT protein at desired levels and without extensive “leaky” expression, namely background of truncated LT expression in the absence of the induced agent. This is a crucial point as the control should show no or leaky induction of truncated LT for reliable stable cell lines to be established for SILAC-based experiments. Therefore, the selection criteria for stable cell line is for the consistent expression of the protein of interest in high levels and also to ensure that tested cells are expressing the protein of choice in homogenous populations. This is important as in downstream SILAC-based quantitative proteomic analysis, the evaluation of fold changes of protein levels require 100% of populations expressing the truncated LT antigen.

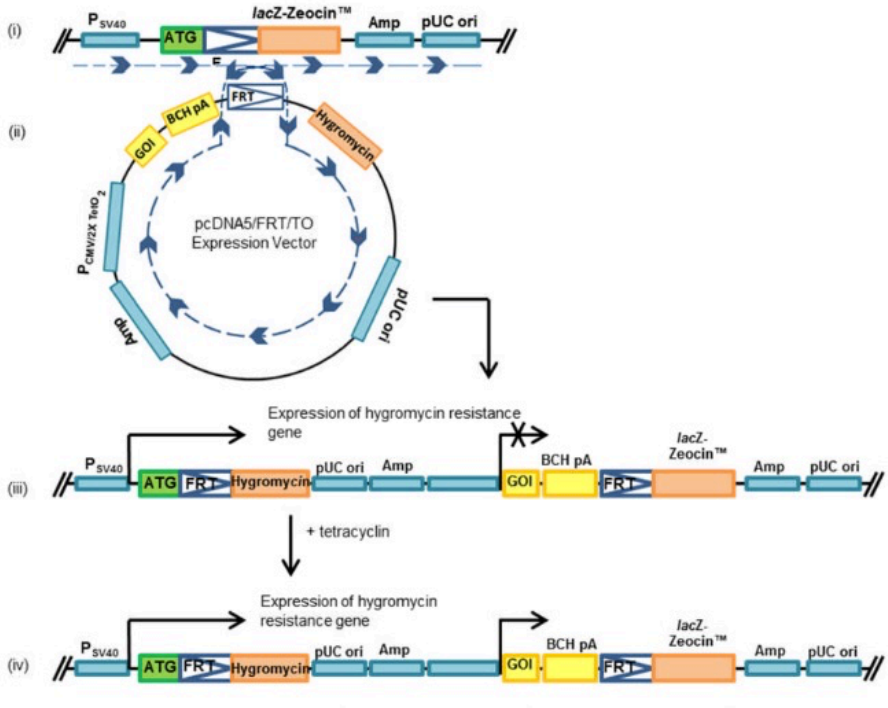

Figure 4.5. Schematic diagram of 293 Flp In system for the generation of stable cell line.

(i) and (ii) The pcDNA5/FRT/TO™ mammalian expression vector containing gene of interest (GOI), in this case is MCPyV truncated large T antigen, and co transfected with pPGK/Flip/ObpA into the HEK 293 Flp In™ parent cells. The Flp recombinase expressed from the pPGK/Flip/ObpA vector facilitates a homologous recombinant event between the FRT site in the pcDNA5/FRT/TO™ expression vector and the FRT site in the HEK 293 Flip Ins™ cells. (iii) Integration of the pCDNA5/FRT/TO™ expression vector expressing the hygromycin resistance gene. The Tet repressor (TetR) represses expression of the GOI (MCPyV truncated LT). (iv) The addition of tetracyclin (Doxycycline hyclate at 2 µg/mL) induced the MCPyV truncated LT expression. Adapted from Craig, 1988; Sauer, (1994).

Figure 4.6 presents a selection of the clones isolated and characterised for inducible expression of truncated LT antigen. Results show the high degree of variability of expression levels of FLAG-tagged MCPyV truncated LT upon doxycycline hyclate treatment of each clone. Clone four was selected for further analysis as it provided acceptable levels of induction and the least 'leaky' expression levels in untreated cells. This clone was therefore utilised in downstream SILAC-based quantitative proteomic studies and termed i293-tLT .

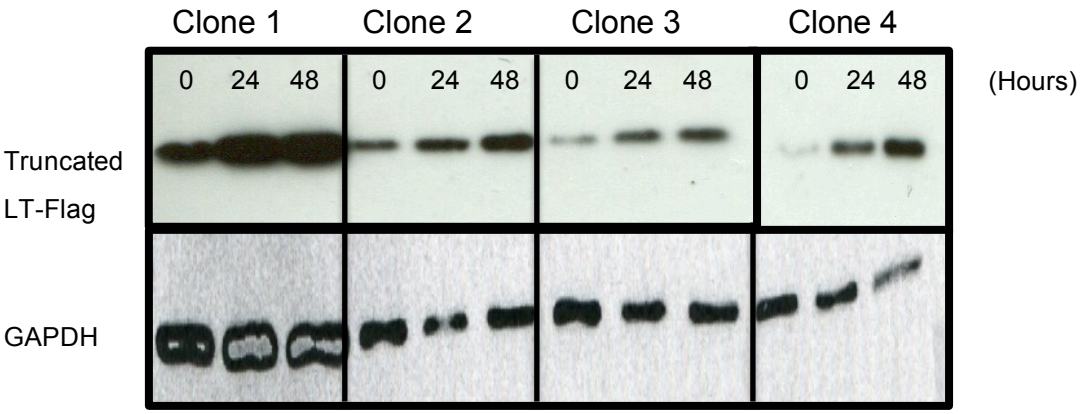

Figure 4.6: Evaluation of each inducible monoclonal clone of MCPyV tLT-Flag cell line.

Monoclonal populations of i293-tLT cells were left untreated or treated with doxycyline for 24 or 48 hours. Cells were then harvested and lysed prior to analysed by immunoblotting with FLAG-and GAPDH-specific antibodies. Clone 4 showed good inducible expression levels of MCPyV truncated LT protein after 24 hours and 48 hours of induction with the least 'leaky' expression of untreated samples. The clone 4 was therefore used in the SILAC-based quantitiaitve proteomic assay.

4.6. SILAC–based quantitative proteomics.

In order to determine the effects of MCPyV tLT expression on the host cellular proteome, SILAC-based quantitative proteomics was performed utilising the MCPyV tLT stable inducible cell line (i293-tLT). This method enables the identification of differentially expressed proteins in two different conditions, namely uninduced and induced samples, which express MCPyV tLT. Moreover the analysis can also be extended to specific sub-cellular compartments, in this case, nuclear and cytoplasmic fractions. In this experiment, two cell populations, uninduced and induced treated cells with doxycyclin are grown in cell culture media that are identical except that one condition is labelled with a 'light' and the other a 'heavy' form of amino acid media (^{12}C and ^{13}C labelled L-arginine and L-lysine, respectively). Through at least 8 passages, the labelled analogue of an amino acid supplied in the cell culture medium was incorporated into all newly synthesized proteins, which results in a mass shift of the corresponding peptides. This mass shift can then be detected by mass spectrometry. When both samples are combined, the ratio of peak intensities in the mass spectrum reflects the relative protein abundance.

Schematic representative of the methodology behind SILAC-based mass spectrometry quantitative proteomic analysis is highlighted below (Figure 4.7).

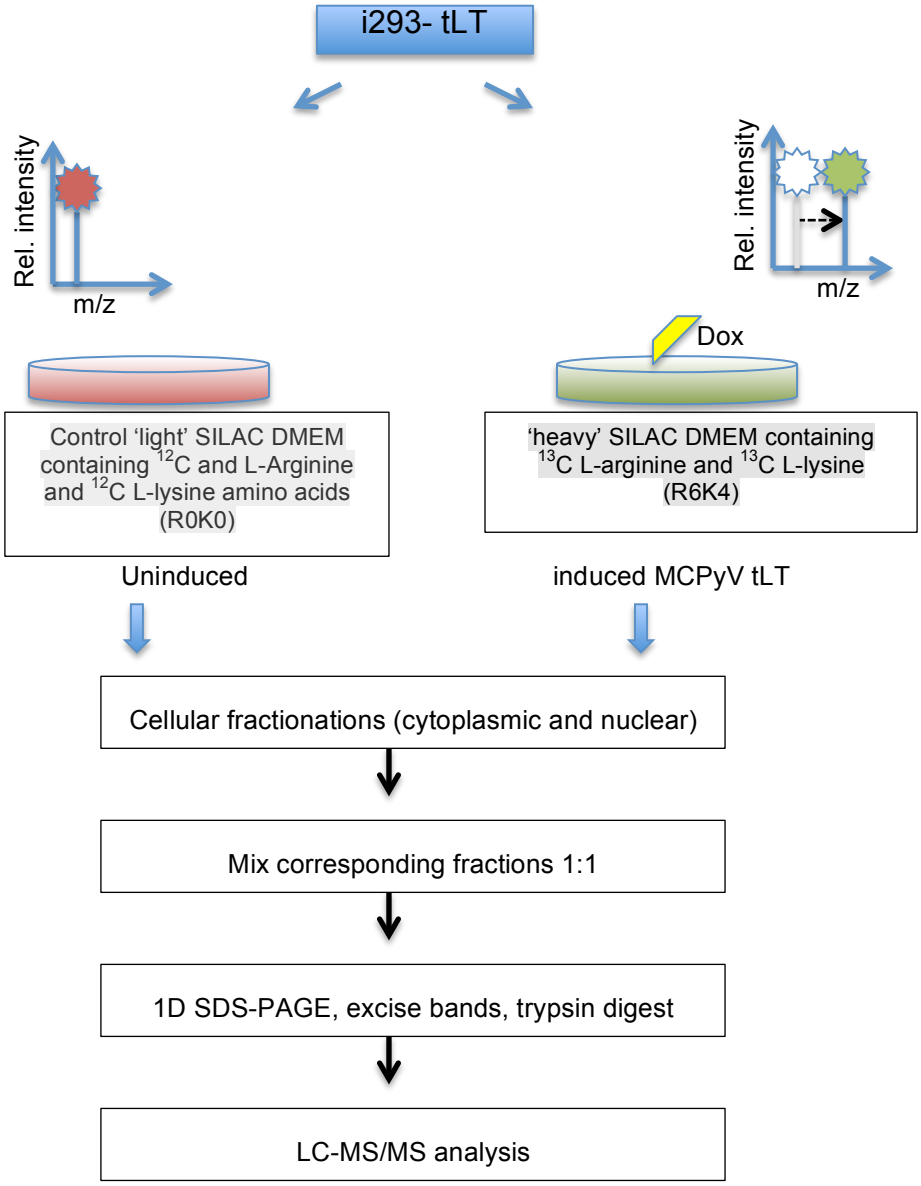

Figure 4.7: The schematic work flow on SILAC-based quantitative proteomic analysis.

i293-tLT cells are differentially labelled by growing them in 'light' medium or 'heavy' medium. Cells were then left untreated or treated with doxycycline hyclate, then subjected to cellular fractionation to reduce the complexity and increase the purity of the samples. Corresponding samples were mixed in 1:1 ratios before being separated in SDS-PAGE. 10 gel slices per lane were excised and trypsin digest prior to analysed by LC-MS/MS to determine the relative abundance of proteins in heavy labelled cells compared to light labelled cells.

4.6.1. Cell Fractionation to reduce the complexity of the samples.

Prior to LC-MS/MS analysis, cellular fractionation was carried out to semi-purify samples and reduce their complexity. To this end, the samples were fractionated into nuclear and cytoplasmic fractions (Figure 4.8). Flag-tagged truncated LT antigen was expressed in induced samples for both cytoplasmic and nuclear fractions. In addition, the Lamin B was detected in the nuclear sample with very faint bands detected in cytoplasmic fractions, and GAPDH was only found in cytoplasmic fractions, confirming that the nuclear and cytoplasmic fractions were relatively pure.

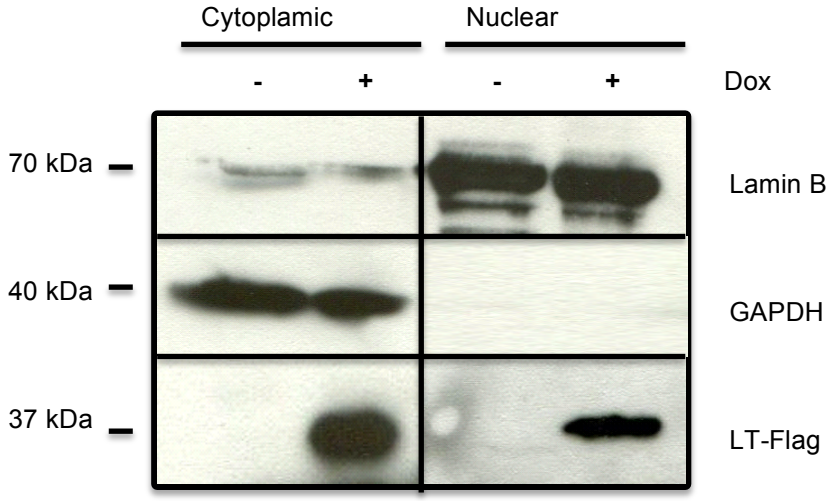

Figure 4.8: Cell fractionation of inducible cell lines uninduced (grown in light SILAC media) and induced (grown in heavy SILAC media).

(A) Cytoplasmic and nuclear fractions of light and heavy medium labelled SILAC samples. Cell lysates were prepared and equal masses of protein were separated by electrophoresis on 12% polyacrylamide gels, protein transferred to nitrocellulose membrane and probed against FLAG-, Lamin B- and GAPDH-specific antibodies. Bound antibodies were detected with HRP-conjugated secondary antibodies against the primary antibodies and the blot was developed using ECL solution and exposed to film. The FLAG-tagged large T truncated proteins were only detected in the induced samples, being absent in uninduced sample for both cytoplasmic and nuclear. Lamin B was used as the protein marker for nuclear fractions and GAPDH used as protein marker for the cytoplasmic fractions.

Both cytoplasmic and nuclear fractions were assessed for protein quantification, then mixed in equal quantities (Figure 4.9). The respective samples were then sent to the University of Bristol Proteomics Facility for LC-MS/MS analysis using a LTQ-Orbitrap Velos mass spectrometer and subsequent bioinformatic analysis.

In addition, protein samples were also visualised by SDS-PAGE to ensure the both cytoplasmic and nuclear fractions were separated and relative pure by analysing the presence of histones, which can be clearly seen in the nuclear samples and absent in cytoplasmic fractions (Figure 4.9). The figure also provides initial determination of concentrations, but precise determinations were performed by quantitation of total proteins using a Bradford assay prior to being mixed.

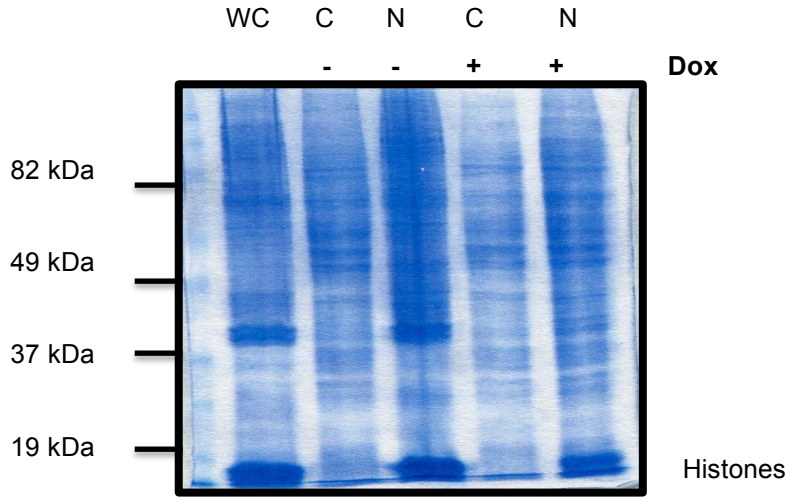

Figure 4.9: Normalisation of protein amounts to be mixed in induced and uninduced samples.

Cytoplasmic and nuclear fractions were produced for each protein sample, to reduce the complexity of the samples before both cytoplasmic and nuclear samples mixed in 1:1 ratios. Analysis to confirm the ratios were performed using SDS-PAGE and coomassie staining. Histones proteins can be clearly seen in the nuclear fractions and whole cells samples, showing show fractionation was successful.

4.6.2. Summary of SILAC data analysis.

Mass spectrometry analysis provides a list of peptides present in both cytoplasmic and nuclear fractions. Peptide identification and quantification was performed using Proteome discoverer^{TM} software. The peak list was subsequently searched with the Mascot search engine (version 2.1.04, Matrix science, London) against the International protein Index human protein database (version 3.6, forward and reverse database) of 80,412 proteins. For analysis and quantification of proteins, a two-fold cut off was chosen and a two peptide cut off. Annotation of molecular functions and affected pathway analysis was performed either by using the Database for Annotation, Visualization and Integrated Discovery (DAVID) v6.7 (Huang da et al., 2009b) or by using Ingenuity Pathway Analysis (IPA).

Interestingly, the data received identified only a small subset of proteins to be upregulated at least two-fold in samples expressing the truncated large T antigen; a total of 282 proteins in nuclear samples and 181 proteins in cytoplasmic fractions. Rather surprisingly however, a much larger number of downregulated proteins were identified in both nuclear and cytoplasmic samples, 1684 proteins and 731 proteins, respectively (Table 4.1). The changes in protein expression were more significant in nuclear samples compared in cytoplasmic samples. However, there were only a small number of proteins changes that are common in both fractions. As important controls, abundant expression of truncated LT protein was identified only in induced samples and multiple house-keeping genes were relatively unchanged in this analysis.

A

Fractions	Nuclear	Cytoplasmic
Proteins Identified	5704	4310
Upregulated (>2 fold increases)	282	181
Common increases in nuclear and cytoplasmic	3	
Downregulated (>2 fold decreases)	1684	731
Common decreases in nuclear and cytoplasmic	130	

B

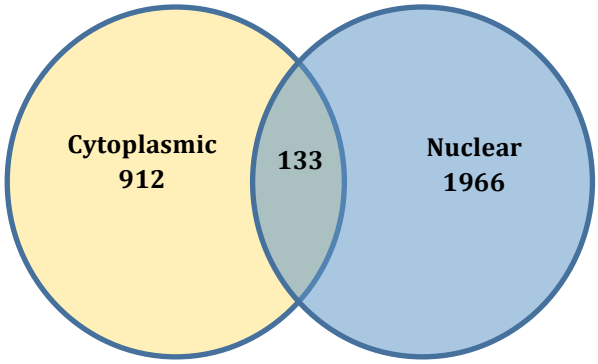

Table 4.1. Summary of SILAC data from i293-truncated LT nuclear and cytoplasmic fractions.

(A) Proteins identified in the SILAC profiles comparing induced and uninduced LT proteins in both nuclear and cytoplasmic fractions. List of proteins identified were further categorized by at least 2 fold increases and decreases in induced samples. (B) Analysis of the numbers of overall proteins that were identified and showing changes upon expression of truncated LT antigen in both cytoplasmic and nuclear fractions. Generally, most are downregulated proteins in the induced samples compared to the number of upregulated proteins. Abundant LT protein expression was observed only in induced samples and house-keeping genes were relatively unchanged.

4.7. Bioinformatic analysis of possible molecular and cellular functions affected by truncated LT antigen expression.

The list of proteins identified in both nuclear and cytoplasmic samples by LC/MS-MS were analysed using DAVID v6.7 to identify possible molecular and cellular functional significance. Table 4.2 showed a list of possible functional pathways which may be affected by MCPyV tLT highlighted from

the SILAC data. This analysis takes into account only proteins which showed changes of at least two-fold compared to the control samples. The list of identified proteins detected in the SILAC were submitted to the DAVID proteomics analysis to perform the analysis by using functional annotation tools. The analysis combined both upregulated and downregulated lists to determine the most affected molecular functions by MCPyV tLT antigen. From the results, cell death and survival function was highlighted in both nuclear and cytoplasmic fractions, specifically 246 associated proteins were identified in cytoplasmic fractions, whereas total of 764 associated proteins were in the nuclear fraction. These numbers were significantly higher than in other possible molecular functions in both fractions and were deemed to be a priority area in future work to determine if MCPyV tLT antigen played any role in causing or inhibiting cell death and survival.

Sample Fractions	Molecular and cellular functions	p-value	# molecules
Cytoplasmic fractions	Cellular assembly and organization	8.45E-07-9.87E-03	158
	Cellular Function and maintenance	8.45E-07-9.87E-03	209
	Cell death and survival	1.32E-06-9.87E-03	246
	Cell morphology	4.09E-06-9.87E-03	155
	Cellular movement	7.63E-06-9.87E-03	143
Nuclear fractions	Post-translational modification	9.70E-20-6.30E-05	130
	Nucleic acid metabolism	8.77E-19-5.26E-04	219
	Protein folding	9.88E-19-9.88E-19	43
	Small Molecule Biochemistry	4.83E-18-1.26E-03	470
	Cell death and survival	5.39E-18-1.26E-03	764

Table 4.2: List of the top five molecular and cellular functions identified with the number of proteins differentially changed upon truncated LT antigen expression, either upregulated or downregulated by at least two-fold different.

Identified protein profiles from SILAC MCPyV truncated LT data were submitted to the DAVID software and analysed in functional annotation tools. The listed possible molecular and cellular functions determined based on the number of molecules identified to be differentiated between uninduced and induced MCPyV truncated LT expression. Comparing both cytoplasmic and nuclear fractions, the common molecular and cellular functions annotation identified is cell death and survival, which both showed highest number of molecules affected in the pathway.

A similar functional pathway analysis was also performed using Ingenuity Pathway Analysis, utilising the IPA core analysis; which considers and identifies genes that are significantly changed in particular molecular and function groups. Analysis was performed separately on the list of proteins identified from the nuclear or cytoplasmic fractions. Figure 4.10 highlights the comparison of identified proteins in both cytoplasmic and nuclear fractions based on its possible functional annotations.

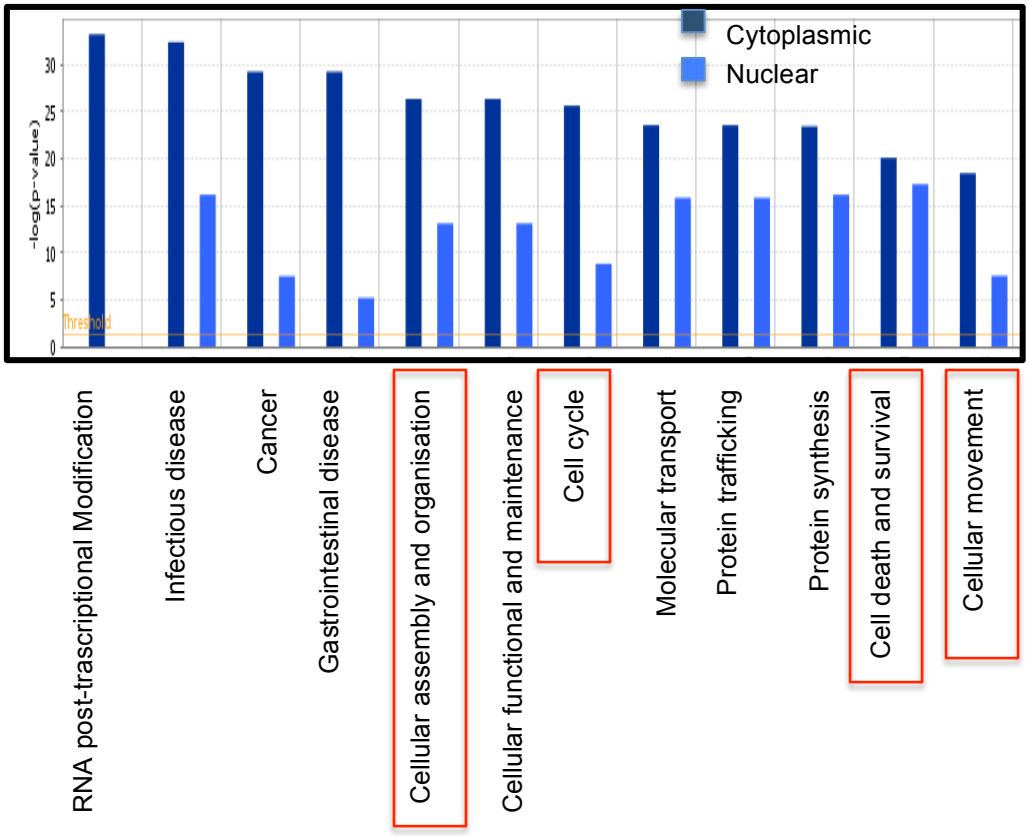

Figure 4.10: Comparison of nuclear and cytoplasmic functions on annotations of molecular and cellular functions of identified SILAC protein molecules using IPA bioinformatics software analysis.

The identified SILAC protein profiles were blasted to the IPA software and compared the annotations of possible protein function. Both cytoplasmic and nuclear differentiated proteins were analysed separately. From the 12 top molecular and cellular function identified, cell death and survival showed high identified molecules in both cytoplasmic and nuclear fraction. Beside that, other interesting possible function also being highlighted in red box to pursue their effects upon expression of MCPyV truncated LT antigen.

Among the identified pathway, again cell death and survival was highlighted in both fractions, however there were several additional functions identified by the IPA software compared to the DAVID analysis, that could possibly be affected in both cytoplasmic and nuclear fractions.

These may be of interest to pursue in further downstream assays, including cellular assembly and organization, cell cycle, as well as cellular movement. Further work on these possible functions will be the focus of investigation in Chapter five of this thesis. Further analysis of the quantitative proteomic data was also performed using the same lists of both upregulated and downregulated proteins but this time focusing on the possible top canonical pathways that were affected by MCPyV tLT antigen expression. Table 4.3 highlights the top five canonical pathways which were possibly affected by the expression of tLT antigen. The annotations of pathways were identified by submitting the lists of both cytoplasmic and nuclear SILAC datasets separately to the IPA bioinformatics software and analysing by selecting the pathway analysis to visualise the most significant affected pathways. The lists were again filtering by only considering at least two-fold changes in both upregulated and downregulated lists. The ratio stated in Table 4.3 is the ratio of the identified proteins in the SILAC datasets to known proteins involved in the stated pathways.

Samples	Top Canonical Pathways	Ratio
Cytoplasmic fraction	Virus Entry via endocytic pathways	19/101 (0.188)
	Renin-angiotensin signaling	19/126 (0.151)
	ErbB Signaling	15/90 (0.167)
	Germ Cell -Sertoli Cell junction signaling	21/169 (0.124)
	p70S6K Signaling	18/132 (0.136)
Nuclear fraction	Protein ubiquitin pathway	92/270 (0.341)
	tRNA charging	29/81 (0.358)
	Regulation of eIF4 and p70S6K Signaling	61/175 (0.349)
	mTOR Signaling	64/213 (0.3)
	Mitocondrial Dysfunction	54/201 (0.269)

Table 4.3: Top five canonical pathways affected by the expression of MCPyV truncated LT protein in nuclear and cytoplasmic fractions.

The canonical pathway, generalised pathways that represent common properties of signalling pathways effected upon expression of MCPyV truncated LT antigen in both cytoplasmic and nuclear fraction. The ratio represents the number of molecules identified in the SILAC protein profiles compared to the number molecules that involved in the particular pathway. In bracket is the percentage of the molecules.

Comparing the cytoplasmic and nuclear datasets, the common related pathways identified were related to cellular stress responses and apoptosis, such as virus entry via endocytic pathways, protein ubiquitin pathway, ErbB signaling, tRNA charging and regulation of eIF4 and p70S6K signaling. The protein ubiquitination pathway is particularly interesting to highlight here as it plays a major role in the degradation of short-lived or regulatory proteins involved in a variety of cellular processes, including the cell cycle, cell proliferation, apoptosis, DNA repair, transcription regulation, cell surface receptors, ion channels regulation and antigen presentation. The surprising observation that many differentially altered proteins appeared to be downregulated upon expression of MCPyV tLT antigen, may be linked to tLT modulation of the ubiquitin degradation pathway. This may lead to the upregulation of protein degradation pathways leading to the observed reduction in many protein levels.

The eIF4 and p70S6K signalling pathways play critical roles in translational regulation; which has key roles in the regulation of cell growth. Overexpression of eIF4E leads to cellular transformation and cell proliferation; while the translational inhibitor 4EBPI also controls the p70S6K pathway, important for cell cycle progression (Flynn and Proud, 1996; Shahbazian et al., 2010). It is interesting to note that alterations in proliferation and cell cycle pathways are high on the list of differentially altered pathways, suggesting that MCPyV tLT might target these pathways to modulate cell growth and cell cycle changes. Furthermore, P13K/AKT signalling and the mammalian target rapamycin (mTOR) pathways which regulate multiple biological processes, including cell survival, proliferation, growth, and cell and glycogen metabolism (Laplante and Sabatini, 2009) were also differentially expressed. The mTOR pathway is known to be activated during various cellular processes, such as tumour formation and angiogenesis and is deregulated in human disease. Analysis was also carried out to determine if changes seen in each fraction were due to directional movement between compartments and not protein degradation or accumulation, for example protein trafficking from the nucleus to cytoplasm or viva versa. Table 4.4 highlights the pathways affected due to

proteins upregulated in the nuclear fractions based on reduced counts of that protein from the cytoplasmic fraction. Distinct to the previous table, this analysed the upregulated protein datasets in the nucleus compared to the downregulated cytoplasmic protein datasets. However, the results identified limited pathways that were affected. These pathways included ubiquitin mediated proteolysis, cell cycle and spliceosome, although a low number count of proteins were detected in each pathway, with 5, 4 and 4 counts identified, respectively. This suggests that altered nucleocytoplasmic shuttling may not be responsible for the differential changes observed in the nuclear and cytoplasmic datasets and the dramatic reduction in many cellular proteins may be due to the upregulation of ubiquitin-mediated degradation pathways.

Pathways	**Count**	**P-value**
Ubiquitin mediated proteolysis	5	1.4E-3
Progesterone-mediated oocyte maturation	4	3.7E-3
Oocyte meiosis	4	7.4E-3
Cell cycle	4	1.1E-2
Spliceosome	4	1.1E-2
Chromatin structure and dynamics	2	9.4E-2

Table 4.4: Effected pathways in which identified SILAC proteins showed to be upregulated in nuclear fraction.

The identified peptides accession number in the SILAC protein profile were submitted to the bioinformatics tools and analysed for the possible effected pathways identified several pathway to be upregulated upon expression of MCPyV truncated LT antigen. Presented in the table is the count hit in the pathway with the P-value showing the significant of the hit.

Aligned to this rationale was the interesting correlation between ubiquitin mediated proteolysis and cell cycle regulation, as both pathways appear to be upregulated in the analysis. This could explain why many other cellular proteins are downregulated in cells expressing truncated LT antigen. The regulation of cell cycle is particularly important in cancer development. An interesting observation related to this hypothesis is that the SILAC dataset highlights that the anaphase-promoting complex (APC) is found to be

upregulated upon truncated LT expression, illustrated in Figure 4.11. APC is an E3 ubiquitin ligase required for ubiquitination and subsequent proteasome degradation of multiple cell cycle regulator and effector proteins (Fehr and Yu, 2013).

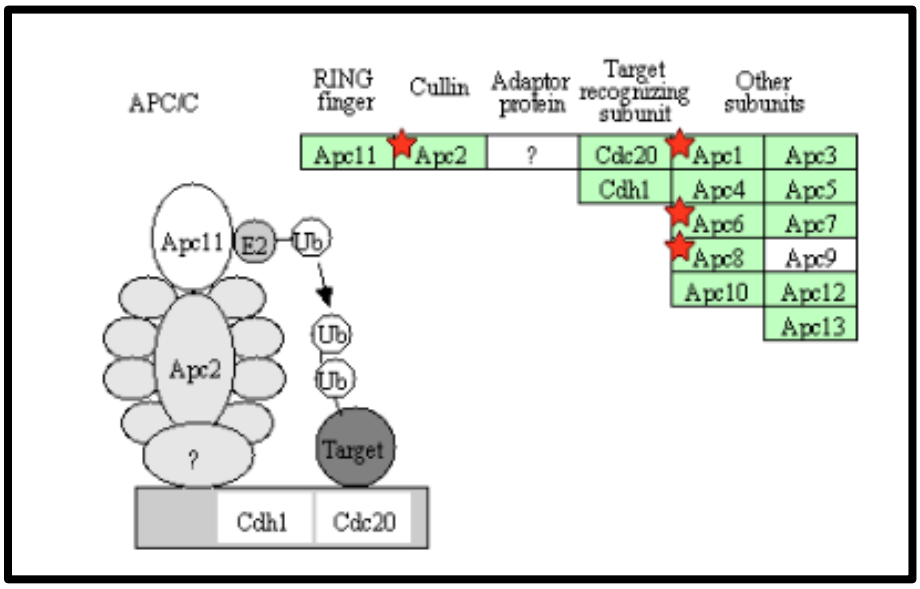

Figure 4.11: KEGG pathway shows several of APC/C molecule components are targeted in cells expressing MCPyV truncated LT antigen.

The targeted molecules identified in MCPyV truncated LT SILAC datasets are labelled with star. From the targeted molecules, Anaphase-promoting complexs APC/C was identified; Apc 2, the cullin component as well as other APC/C subunit (Apc1, Apc6 and Apc8).

Further analysis examined the downregulated datasets for identified proteins in nuclear fractions which were increased in the cytoplasmic dataset. Using the same analysis bioinformatics software, Table 4.5 shows the list of affected pathways to be downregulated in the nuclear fractions samples. As stated previously, the lists of affected pathways downregulated in the MCPyV tLT SILAC identified sample for nuclear fraction appeared to be more dramatic than the cytoplasmic dataset. Interestingly, the pathways that were highly downregulated by MCPyV tLT were pathways related to cellular cell-cell connection and movement.

Pathways	Count	%	P-value
Regulation of actin cytoskeleton	27	2.6	5.30E-02
Tight junction	26	2.5	5.3S-2
Oxidative phosphorylation	23	2.2	1.70E-03
Glycolysis/gluconeogenesis	21	2	6.80E-08
Axon guidance	17	1.6	9.50E-02
Aminoacyl-tRNA biosynthesis	16	1.5	7.80E-07
Valine,leucine and isoleucine degradation	15	1.4	1.20E-05
Gap junction	15	1.4	2.10E-02
VEGF signaling pathway	13	1.2	2.80E-02
Adherens junction	13	1.2	3.30E-02
Integrin signaling pathway	8	0.8	4.20E-02
Synaptic proteins at the synaptic junction	7	0.7	5.50E-03
uCalpain and friends in cell spread	6	0.6	5.70E-03

Table 4.5: Pathways that showed to be downregulated at least two-fold changes in cells expressing MCPyV truncated large T antigen in nuclear fraction.

The pathways presented related to cellular junctions and cell connections showed to be altered in SILAC profiles of MCPyV truncated LT antigen expression suggesting the possible effects of truncated LT in cell movement and cell migration. The count of hit, percentage and p-value of each pathway were shown in the table.

As shown in Table 4.5, pathways related to cellular junctions, such as remodelling of tight junction, epithelial adheren junctions, actin cytoskeleton signalling and integrin signalling were also showed to be altered in the differential profiles upon MCPyV tLT antigen, adding to the possibility that truncated LT, as well as MCPyV ST, may contribute to cell movement and migration. We have previously shown that MCPyV ST can enhance cell motility and migration by affected pathways controlling microtubule destabilisation (Knight et al., 2014) and the actin cytoskeleton (Stakaityte et al., manuscript in preparation). Specifically, MCPyV ST enhances expression of the microtubule control protein, Stathmin and also upregulates Rho-GTPase activity inducing filopodia formation. However, in contrast to MCPyV ST SILAC-based quantitative proteomic data, our

SILAC data suggests that expression of the truncated LT antigen may lead to a downregulation of specific pathways associated with cell movement and migration. This might suggest that truncated LT antigen does not enhance cell motility but may contribute to the initial stages of metastatic properties of the infected cells, by enhancing the downregulation of proteins involved in cell-cell connections. This may lead to the ability of cells to 'breakaway' from the main primary tumour and work in conjunction with MCPyV ST which then increases motility and migration of these cells.

In support of this hypothesis, Figure 4.12 illustrates that cellular tight junction pathways are affected upon expression of MCPyV tLT antigen. KEGG pathway analysis demonstrated that a significant number of proteins in these pathways are altered in the SILAC-based quantitative proteomic dataset, as highlighted by the red star, that shows identified cellular proteins in the SILAC dataset that been targeted. Further work related to the tight junctions has been carried out in the next chapter of the thesis. To study the effects of the MCPyV tLT on the tight junction, we selected the zona occuldens proteins, ZO-1, a family of tight junction associated proteins that function as cross-linkers, anchoring the tight junction strand proteins to the actin-based cytoskeleton (Itoh et al., 1997) as a target protein in this study (circle with yellow in the figure). From the Figure 4.11, it is apparent that the most of the proteins identified in the SILAC dataset are downstream pathways of proteins of ZO-1. Therefore, the changes in the ZO-1 might be interesting to elucidate in detail. This will be described further in the next chapter.

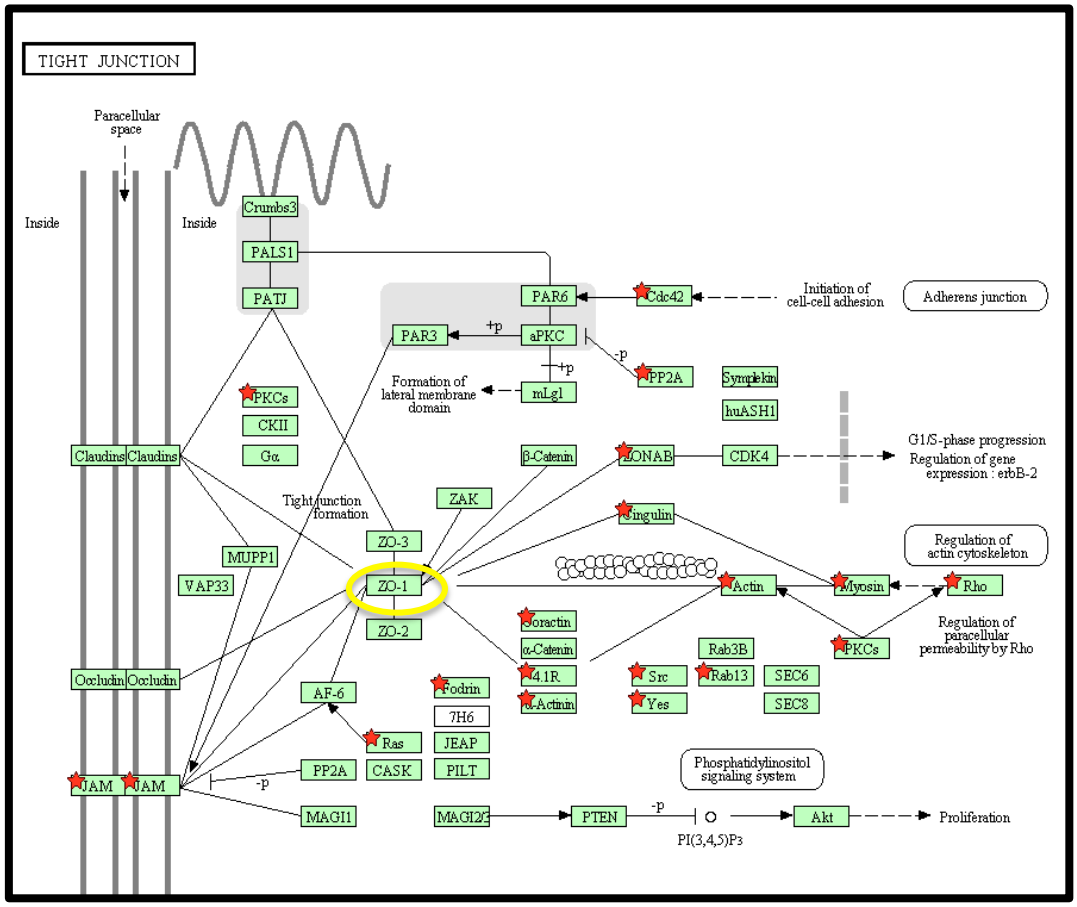

Figure 4.12: SILAC identified tight junction components.

Diagram illustrating the KEGG tight junction pathway, protein identified in SILAC cytoplasmic data set were highlighted with red star. The many proteins identified in the SILAC dataset are downstream pathway of zona occuldens protein 1 (circled in yellow) and this protein was chosen further analysis on effects of truncated LT antigen in tight junction pathway.

In addition, metabolism-related pathways were also found to be highly affected upon induction of MCPyV tLT antigen. These pathways included oxidative phosphorylation, glycolysis/gluconeogenesis, amonoacyl-tRNA biosynthesis, valine, leucine and isoleucine degradation, phosphoinositides and inositol phosphate metabolism. The targeted proteins were labelled with a star in Figure 4.13. These findings may suggest that MCPyV truncated LT leads to tumourigenesis by potentially altering the metabolic status of MCPyV-induced cancer cells. Cancer cells fundamentally possess altered metabolism pathways, which is an emerging hallmark feature for tumour development. This includes switching to aerobic glycolysis in order to provide precursors for massive biomass synthesis. Inositol phosphate metabolism components, such as inositol polyphosphate phosphatase 1

(INPP1), is highly expressed in aggressive human cancer cells (Benjamin et al., 2014). The findings showed glycolytic control in cancer cells promotes key oncogenic lipid signalling pathways essential for cancer cell motility, invasiveness and tumourigenicity. A similar mechanism might be targeted by MCPyV truncated LT to enhance transformation of Merkel carcinoma cells.

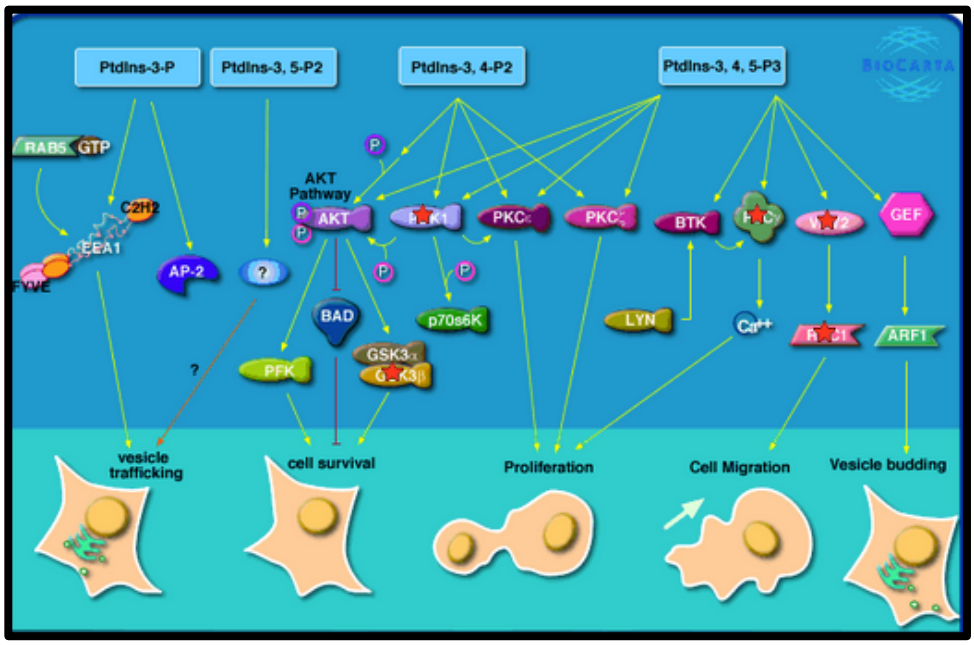

Figure 4.13: Phosphoinositides and their downstream targets pathway.

The targeted molecules involving with cell survival, proliferation and migration function (labelled with star). The targeted molecules identified were directly towards the cell survival, cell migration and proliferation downstream pathway.

Axon guidance is another pathway that was highlighted in the SILAC-based quantitative proteomic dataset (Figure 4.14). The axon guidance pathway is also particularly interesting, as this pathway has been suggested to be involved in tumour suppression (Chedotal et al., 2005). Specifically, a variety of genetic mutations have been identified within proteins associated with this pathway in human cancers. Frequent loss of heterozygosity is observed in tumours and cancer cell lines and significant hypermethylation in gene-associated promoters (Li et al., 2009; Normanno et al., 2015; Zhang et al., 2015). The number of mutated axon guidance molecules and the heterogeneity of cancer cells are significantly important as the numbers

of axon guidance molecules levels reduced were associated with mismatch repair deficiency or mutations in Kirsten Rat Sarcoma Viral Oncogene Homolog (KRAS), or serine/threonine-protein kinase B-Raf (BRAF) in the case of colorectal cancer.

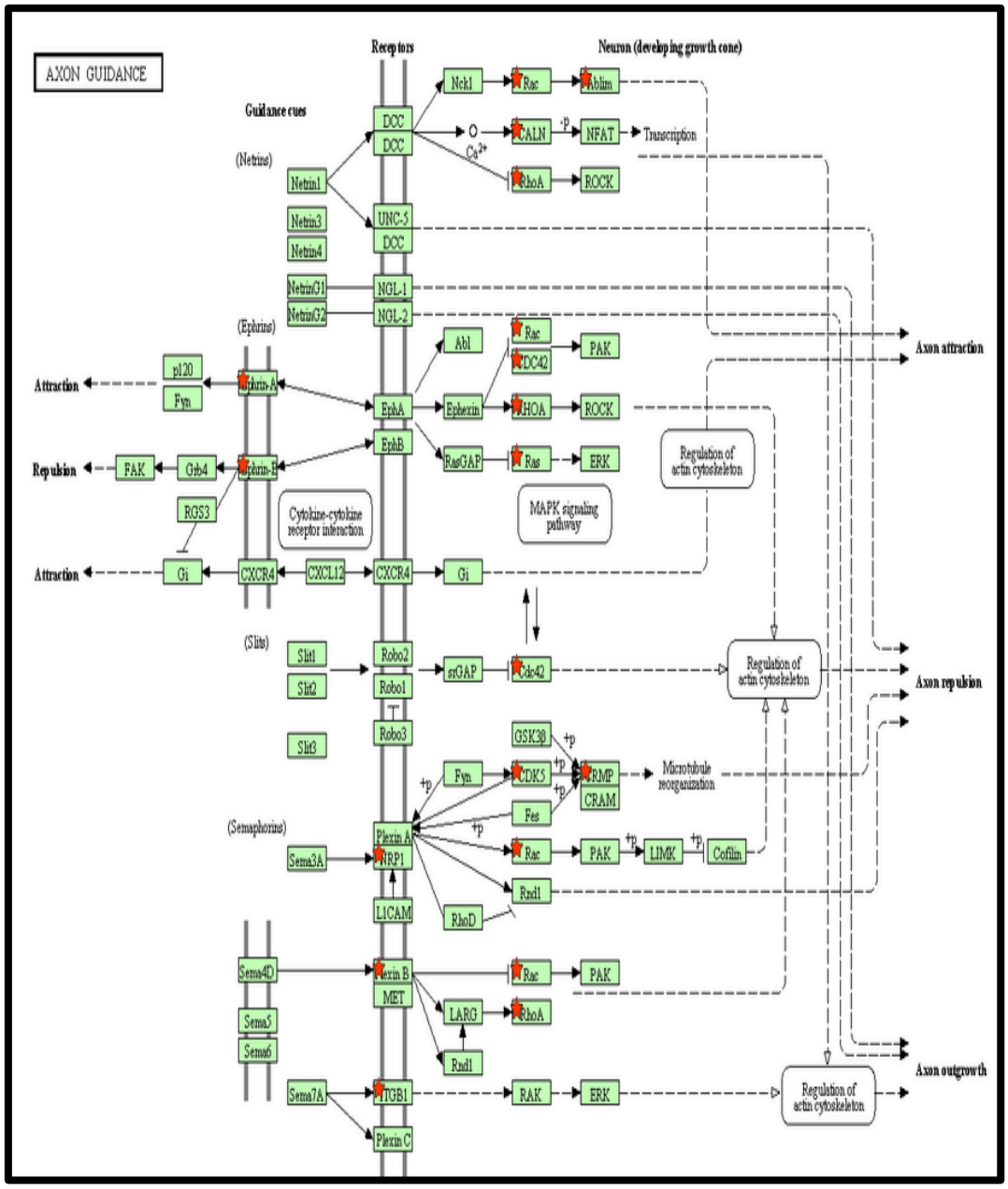

Figure 4.14: SILAC identified axon guidance pathway components.

Diagram illustrating the KEGG axon guidance pathway, protein identified in SILAC nuclear downregulated data set were highlighted with red star.

In addition, proteins associated with axon guidance have also been shown to suppress cell proliferation, cell migration and invasion, as well as increase apoptosis in both normal and cancer cells, as a response to DNA-damaging agents. As such, axon guidance molecules are found to be frequently downregulated during tumourigenesis and tumour progression in breast and colorectal cancer; suggesting they play a crucial role as tumour suppressors (Chedotal et al., 2005; Harburg and Hinck, 2011; Li et al., 2009).

In the cytoplasmic fraction, the possible affected pathways that showed to be changed either increased or decreased also related to cell-cell contacts such as focal adhesion, tight junction, and adherens junction pathways. As discussed in the nuclear fraction section earlier, therefore the same possibility exists that truncated LT antigen may contribute to the initial stages of metastatic properties of the infected cells, by enhancing the downregulation of proteins involved in cell-cell connections. In cytoplasmic fraction pathway annotation also showed related pathways such as focal adhesion, tight junction, and adherens junctions. This data suggests that this possible function of MCPyV truncated LT merits further investigation.

Pathways	Count	Up	Down	P-value
Focal adhesion	13	3	10	8.90E-01
MAPK signaling pathway	13	10	3	6.30E-02
Tight junction	9	2	7	3.10E-01
Fc epsilon RI signaling pathway	6	1	5	6.30E-02
Phosphoinositides and their downstream targets	5	0	5	2.20E-03
Inositol phosphate metabolism	5	0	5	6.00E-02
Glycolysis/gluconeogenesis	5	0	5	8.20E-02
BCR signaling pathway	4	1	3	5.20E-02
Adherens junction	5	0	5	7.00E-02
VEGF, hypoxia and angiogenesis	3	3	0	6.30E-02

Table 4.6: Pathways that showed at least two-fold changes in cells expressing MCPyV truncated LT antigen.

The annotated pathways were compared either the changes cellular proteins involved were upregulated or downregulated. The count value is the number of identified molecules for both upregulated and downregulated proteins in the annotated pathways are statistically significant based on the calculated P-value. The likelihood of the association between a set of SILAC identified genes and the pathway is measured using the right-tailed Fisher Exact Test.

4.8. Discussion

The aim of this chapter was to investigate the effects of MCPyV truncated LT protein expression on the host cell proteome, required in cell signalling and tumourigenesis on a unbiased global scale. For this, SILAC-based quantitative proteomics was utilised to determine the differential protein abundance upon expression of MCPyV truncated LT antigen. In order to delineate the effects of LT antigen on the cellular proteome, it was first necessary to produce a stable cell line capable of regulated expression of the MCPyV truncated LT antigen. This would ensure a homologous population to assess fold changes and possible functional target proteins upon induction.

Upon starting the project, this stable cell line expressing inducible truncated LT protein was not available in our laboratory. Therefore, the first objective of this chapter was to produce the MCPyV truncated LT stable cell line. To this end, truncated LT-cDNA was successfully amplified and cloned into pcDNA5FRT, mammalian expression vector plasmid enabling production of a number of monoclonal inducible cell lines. Upon production of these cell lines, it was essential to test several clones of these stable cell lines to obtain a cell line which showed high induction levels of the truncated LT protein, but also with a high degree of regulated ‘non-leaky’ expression. This selection process is highly important to ensure the homologous population of cells for validation of proteomics SILAC data later. After selection and testing of an appropriate cell line, the chosen stable cell line was grown in differentially isotope labelled DMEM medium, then left untreated or treated with the doxycylin hyclate. Simple cell fractionation was carried out to obtain extended coverage of the proteome changes in both cytoplasmic and nuclear compartments as well as to reduce complexity of the samples for the mass spectrometry experiments. Both treated and non-treated samples were mixed and analysed by mass spectrometry for both nuclear and cytoplasmic samples.

SILAC-based quantitative proteomic analysis was performed in an attempt to determine possible molecular functions of identified cellular proteins which showed differential expression upon MCPyV truncated LT expression. Bioinformatic analysis highlighted specific pathways the viral oncogene may be targetting, which could be implicated in MCPyV-induced tumourigenesis. The listed SILAC dataset identified proteins used for the bioinformatic analysis were either upregulated or downregulated by at least two-fold. The bioinformatic analysis was formed using both IPA and DAVID softwares.

Surprisingly, the SILAC datasets for each fractions showed many proteins appeared to be downregulated in the cells expressing MCPyV truncated LT antigen. However, a possible correlation for the reduction in the cellular proteome might be due to the targeting of the ubiquitin proteasomal degradation pathway. The upregulation of the ubiquitin proteasomal degradation pathway and several proteins associated with the APC complex upon expression of truncated LT suggests the regulation of cell cycle might be one of the major functions of MCPyV LT. The APC complex is essential for enabling cell progressing through anaphase, exit from mitosis and preventing premature entry into S-phase (Thornton et al., 2006). The APC complex is an important regulator in cell cycle pathway as it targets more than 30 proteins for ubiquitin-dependent proteasome degradation (Peters, 2006). Among the long list of target molecules and substrates recognized by APC are cyclin A and cyclin B. The degradation of the cyclins during mitosis reduces CDK activity, and leads to disassembly of the mitotic spindle, chromosome decondensation, reformation of the nuclear envelope and formation of cytokinetic growth (King et al., 1995; Murray et al., 1989; Sudakin et al., 1995). To determine how MCPyV truncated LT plays a role in targeting the APC and affects cyclin levels in cells, different cyclins could be compared in the cells expressing MCPyV truncated LT antigen and compared with the control. This will be further analysed and discussed in the following chapter of this thesis. For the next chapter cell cycle analysis and cell growth was also

examined to observe possible effects of truncated LT antigen on cell proliferation.

From the preliminary SILAC-based quantitiative proteomic data, the most likely pathways affected by MCPyV truncated LT antigen expression are predicted to be associated with cell death and survival, as both cytoplasmic and nuclear fractions highlighted these pathways with top hits in functional and pathways annotations. Programmed cell death or apoptosis is important for cellular destruction for variable cellular processes including the development or prevention of oncogenic transformation (Galluzzi et al., 2010; Hanahan and Weinberg, 2000; Zhivotovsky and Orrenius, 2010). This apoptosis process must be tightly controlled as dysregulated cell death relates to a large number of pathologies. Different strategies are utilised by cells to prevent cell death including regulation of apoptosis, anti-apoptotic and pro-survival pathway and identification of anti-apoptotic sequences, autophagy and necrosis (Portt et al., 2011). Further analysis of the cell death and survival pathway will be discussed further in the following chapter to delineate the effects of the MCPyV truncated LT on cell death and survival.

Other possible functions of truncated LT include cellular assembly and organisation of cell movement. The pathways associated with the cellular movement specifically identified in this dataset includes cell-cell junctions, such as tight junctions, gap junctions, adheren junctions, integrin signalling pathway, synaptic proteins at the synaptic junction and cell spreading. This finding leads to the intriguing possibility that there may be a synergistic effect on enhancing cell motility and migration upon MCPyV ST and truncated LT expression. Previous data suggests that MCPyV ST enhances cell motility and it may be the case that LT downregulates expression of junction proteins allowing the migratory cell to break away from the primary tumour enhancing metastatic spread of merkel cell carcinoma cells.

In addition, other possible targeted pathways of interest to be further analysed in the future are alterations in metabolic pathways such as oxidative phosphorylation, glycolysis/glucogenesis and inositol phosphate metabolism (Benjamin et al., 2014). This altered metabolism and link to tumourigenesis would enhance the biosynthesis of uncontrolled cell mass, as metabolic alterations are required for tumour cells to be able to respond to the proliferative signals that are delivered by oncogenic signalling pathways (Cairns et al., 2011).

Axon guidance pathways may also be of interest, as many recent studies have highlighted the importance of dysregulation of these pathways, specifically relating to tumour suppression or oncogenesis in breast cancers (Harburg and Hinck, 2011). Axon guidance-associated molecules also have important effects on vascular endothelial growth factor (VEGF), hypoxia and angiogenesis. Several molecules in this pathway such as netrins, slit proteins, semaphorins, ephrins and their cognate receptors UNC5, Robo1-4, neuropilin and EphB have been studied as potential targets for new antiangiogenic therapies (Pircher et al., 2014). Further study regarding these target molecules might give a better understanding to how MCPyV truncated LT targets these molecules and enhances cancer progression and angiogenesis.

In conclusion, this chapter has described the process of generating a stable cell line that is able to regulate expression of MCPyV truncated LT upon induction required for SILAC-based quantitative proteomics. Bioinformatic analysis discussed in this chapter highlights several potential proteins and pathways effected upon expression of MCPyV truncated LT expression. The next chapter will discuss further the effects of truncated LT in selected pathways including cell death and survival, cell cycle and cell-cell connection associated pathways in order to delineate possible functions of MCPyV truncated LT antigen in MCPyV-induced tumourigenesis.

Chapter 5

Evaluating Possible Functions of Merkel Cell Polyomavirus Truncated Large T Antigen.

5.0. Evaluating Possible Functions of Merkel Cell Polyomavirus Truncated Large T Antigen.

5.1. Introduction

The full length MCPyV large T (LT) antigen comprises 816 amino acids in length, however, LT is frequently truncated in MCC rendering the virus replication deficient. Polyomavirus LT antigens possess numerous functions in infection, including the initiation of viral replication and manipulation of the host cell cycle. MCPyV LT antigen is composed of two exons and contains several conserved domains found in many other polyomaviruses; including the retinoblastoma protein (pRb) binding domain sequence (LXCXE), a nuclear localisation signal (NLS) and the origin binding domain (OBD) (Kierstead and Tevethia, 1993; Nakamura et al., 2010; Peden et al., 1989; Topalis et al., 2013). However, some binding sites or domains within MCPyV LT appear to be distinct from other polyomaviruses. For example, MCPyV LT shares only 34% sequence identity with SV40 LT antigen (Topalis et al., 2013). MCPyV LT also contains the MCPyV unique region (MUR), an additional 200 residue domain located between the first exon and OBD; which binds to the host cytoplasmic cellular factor, vacuolar sorting protein Vam6p (Liu et al., 2011b). hVam6p is relocalised from the cytoplasm to the nucleus upon expression of MCPyV LT. Although the mechanism of relocalisation is yet to be determined, hVam6p is believed to function as an antiviral host factor due to its ability to significantly reduce the number of MCPyV virions by approximately 90% (Feng et al., 2011).

Besides hVamp6p, MCPyV LT also targets survivin, a member of the inhibitor of apoptosis protein family, which is upregulated in many forms of lymphoma and metastatic melanoma (Ambrosini et al., 1997). Survivin functions as an inhibitor of apoptosis by prolonging cell viability, and also contributes to the transformation of cells by promoting cellular resistance to

chemotherapy. Knockdown of MCPyV T antigens in MCPyV positive MCC cells leads to lower survivin mRNA and protein levels, resulting in MCC cell death (Arora et al., 2012a). Not surprisingly therefore, survivin gene expression is enhanced, as well as other S-phase proteins including E2F1 and cyclin E, in MCPyV LT expressing cells (Arora et al., 2012a). As such, it is believed survivin expression is critical to the survival of MCPyV-positive cells and this hypothesis is supported by recently experiments demonstrating that the small molecule survivin inhibitor, YM155, potently and selectively initiates irreversible and programmed cell death of MCPyV-positive MCC cells. Besides MCPyV, both SV40 and JCV infection exhibit upregulation of survivin expression (Ambrosini et al., 1997; Jiang et al., 2004; Pina-Oviedo et al., 2007; Raj et al., 2008). Identifying the survivin-controlled cellular pathways induced by LT antigens could lead to the rapid identification of additional drug candidates for treating polyomavirus infections.

MCPyV LT is also important in initiating transformation and survival of MCC tumours, as abandonment of cell growth is observed in MCPyV-LT depleted cells which eventually leads to cell death (Houben et al., 2010b). This cell death, due to the loss of LT function, surprisingly lacks any typical apoptosis features such as caspase activation, PARP cleavage and alterations in expression levels of p53 or Bcl-2 family (Houben et al., 2010b). This suggests that MCPyV LT-mediated changes in the Rb-E2F pathway, through LT-RB interactions, probably result in cell death by autophagy or necrosis-related processes.

Although it has been known for several years that the LT antigen is truncated in MCC, little research has focused on how the truncated LT contributes to tumourigenesis, in contrast to the full length LT antigen. This is rather surprising as expression of the truncated forms of LT are expressed in MCC. Therefore, the main objective of this chapter was to evaluate the role of prioritized differentially expressed cellular proteins identified in the quantitative proteomic analysis of truncated LT-expressing cells. These functions include the effects of MCPyV truncated LT antigen

on the host cell cycle, apoptosis and cell survival pathways as well as cell-cell connections.

5.2. MCPyV truncated large T antigen expression may affect cell cycle regulation.

The MCPyV truncated LT antigen SILAC-based quantitative proteomic dataset identified a number of differentially expressed cellular proteins which regulate the host cell cycle. Regulation of cell cycle checkpoints are unquestionably important in cancer development, as mutations which occur in these pathways not only affect cell proliferation, but also increase genetic instability accelerating cellular evolution (Hartwell and Kastan, 1994). The G1 checkpoint is a key step in inhibiting cancer development and genomic instability as this cell cycle arrest step allows the cell to maintain DNA integrity and to check signs of DNA damage that might cause functional problems or development of tumour growth. As such, if DNA damage is observed, G1 arrest will prevent the cells from entering S phase and further proliferation and ultimately lead to apoptosis. Therefore, it is believed that expression of MCPyV LT may enhance cell proliferation by affecting the G1 checkpoint. Supporting this theory are results which show that expression of wild type MCPyV LT antigen leads to loss of the G1 checkpoint in UISO cells without affecting DNA repair pathways. In contrast, truncated LT-expressing cells resulted in loss of DNA repair pathways as well as G1 checkpoint control (Demetriou et al., 2012). This suggests that truncated LT antigen expression generates cell cycle defects which lead to cell proliferation and also impair DNA repair pathways which may enhance genomic instability, which is observed in many MCCs.

5.2.1. Cell cycle analysis.

5.2.1.1. Cell cycle analysis of MCPyV truncated LT antigen expressing cells.

To first investigate any potential effects of MCPyV truncated LT antigen expression on cell cycle checkpoints, cell cycle analysis was performed to visualise the percentage of cells in each phase of the cell cycle. Analysis was carried out using a standard protocol of measuring the DNA content within cells by labelling DNA with propidium iodide (PI) and quantifying the amount of cell populations in every cell cycle phases using flow cytometry.

Initial experiments were performed in the control 293 cell line transfected with either a control eGFP expressing plasmid or an eGFP tagged MCPyV truncated LT (GFP-tLT). The transfected cells were harvested and sorted by fluorescence activated cell sorting (FACS), prior to being analysed by flow cytometry. The percentage of cells in each phase of the cell cycle is summarised in Figure 5.1. The cell cycle analysis of the transfected cells harbouring the respective plasmids showed there was no significant changes on G1 populations comparing control and truncated LT-expressing cells. However, expression of truncated LT showed a slight increase in the S phase population of cells, compared to control cells (6%). This may be an indication that expression of truncated LT may affect the G1 checkpoint, enhancing the transition of cells into the S phase. However, this increase in S phase cells was smaller than expected and this may have been due to inefficient transfection of cells and the resulting low number of cells which were gated to ensure only homologous cell populations were analysed in the cell cycle.

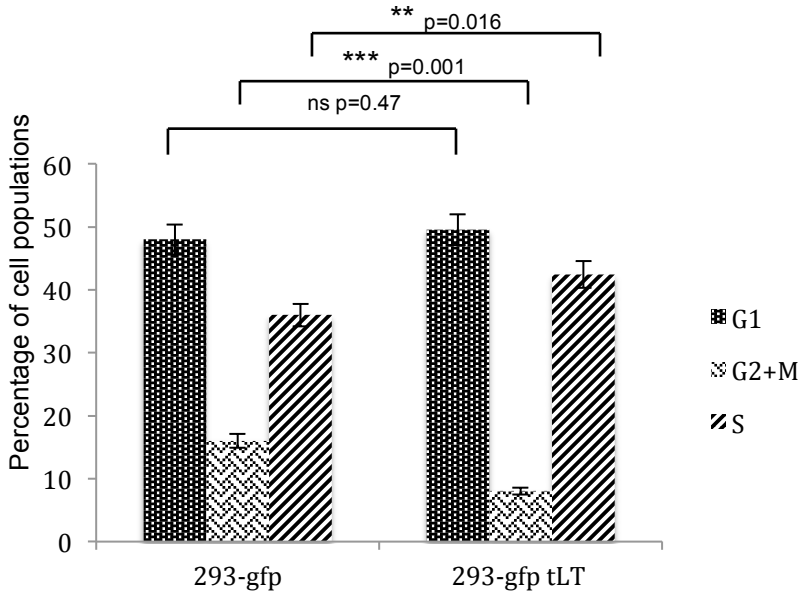

Figure 5.1: Cell cycle analysis of the HEK293-GFP and GFP-tLT expressing cells

The HEK293 cells were transfected with plasmids expressing GFP or GFP tagged MCPyV truncated LT (gfptLt) using standard lipofectamine protocols. After 24 hours, cells were harvested and sorting for GFP expression. Cells were then fixed with cold ethanol and labelled with the DNA-binding dye propidium iodide (PI). The cells were then analysed by using flow cytometry to determine the percentages of cells in each phase of the cell cycle utilising the ModFit software. P values using an unpaired test are indicated. The experiments were run in triplicate.

Therefore, to overcome the issues with the low efficiency gating of only transfected cell populations, cell cycle analysis was repeated using the stable cell line capable of inducible expression of the truncated LT, comparing the control versus induced i293-tLT cells. Results in Figure 5.2 show that expression of MCPyV truncated LT results in a small increase in the percentage of cells in S phase compared to control cells. This again suggests that truncated LT expression may bypass the G1 checkpoint and drive cells into S phase. The accumulation of cells in S phase may be related to the interactions of truncated LT antigen with the cellular Rb protein. The MCPyV truncated LT antigen still retains the ability to bind with very high affinity to Rb and can also partially relocalize Rb to the cytoplasm (Borchert et al., 2014).

During the G1 phase of the cell cycle, Rb binds and represses the cellular activator, E2F transcription factor, causing repression of G1-to-S transition.

Therefore, expression of truncated LT and its binding to Rb is thought to release E2F allowing cells to progress to S phase and overcoming the restriction checkpoint in the cell cycle. Moreover, the loss of the G1-S checkpoint can lead to genomic instability, inappropriate survival of genetically damaged cells, and further the evolution of cells to malignancy (Hartwell and Kastan, 1994). Therefore, it would also be interesting to determine whether truncated LT-expressing cells have more genomic instability than control cells. This work is continuing in the Whitehouse laboratory.

Besides the effects of the S-phase populations, drastic changes in the G2 populations were also observed in the figure 5.2. In control cells without truncated LT expression, the G2 population is approximately 12%, but no cells in G2 were observed in cell expressing truncated LT antigen. This finding is surprising and interesting as truncated LT antigen might be able to block the progression in cell cycle entering G2 phase.

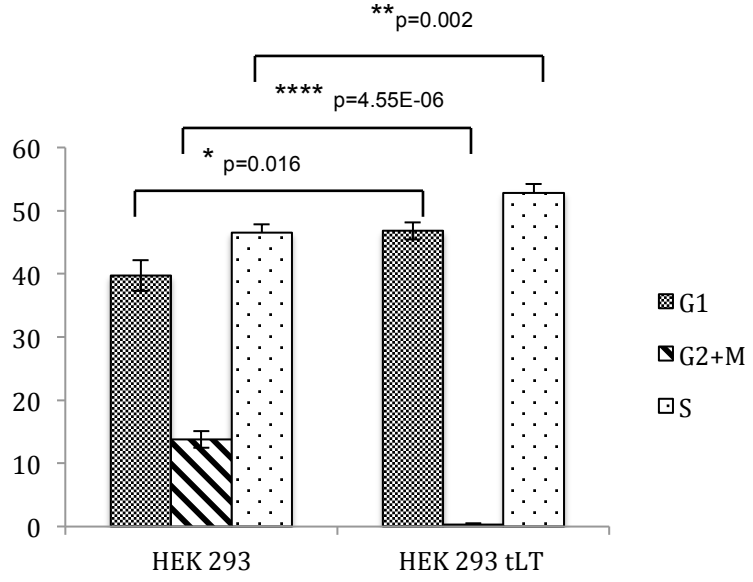

Figure 5.2: Percentage distribution of cells in each phase of the cell cycle.

The stable cell line capable of inducible expression of MCPyV truncated LT antigen remained uninduced or induced with Doxycyclin for 24 hours. Cells were then fixed with cold ethanol and labelled with the DNA-binding dye propidium iodide (PI). The cells were then analysed by using flow cytometry to determine the percentages of cells in each phase of the cell cycle utilising the ModFit software. The experiments were run in triplicate.

5.2.2. The identified proteins in SILAC that relate to the cell cycle.

An intriguing observation from the results in Figure 5.2, was the lack of cells entering the G2 phase of the cell cycle upon expression of the truncated LT. The prolonging of S-phase in cells is often caused by changes in cyclin and other cell cycle regulatory protein levels (Wataya-Kaneda et al., 2001). To further examine this phenotype, the SILAC dataset was analysed for proteins which associate with the cell cycle, cell proliferation and ubiquitin proteosomal degradation (Table 5.1).

Accession	# Peptides	Medium /Light	Description	Function
O95613	2	100.000	Pericentrin	Integral component of the centrosome that serves as a scaffold for anchoring proteins
Q9NXV6	3	100.000	CDKN2A-interacting protein	RNA binding and p53 binding; negative regulation of cell growth, positive regulation of signal transduction and regulation of protein stability
Q8TCE5	2	100.000	GBP2 protein	Interferon-induced guanylate-binding protein 2
D3DR32	7	6.321	M-phase phosphoprotein 1	Specifically phosphorylated at the G2/M transition
B4DL80	4	3.559	Cell division cycle protein 27 homolog	Component of anaphase promoting complexes/cyclosome
Q9UJX6	5	3.155	Anaphase-promoting complex subunit 2	Component of anaphase promoting complexes/cyclosome
F5GY68	3	2.942	Anaphase-promoting complex subunit 5	Component of anaphase promoting complexes/cyclosome
Q9UJX2	3	2.377	Cell division cycle protein 23 homolog	Component of the anaphase promoting complex/cyclosome

Q9H1A4	4	2.179	Anaphase-promoting complex subunit 1	Component of the anaphase promoting complex/cyclosome
Q5UIP0	5	2.163	Telomere-associated protein RIF1	Required for checkpoint mediated arrest of cell cycle progression in response to DNA damage during S-phase
Q1XBU8	3	3.573	Cell proliferation-inducing protein 23	Induce cell proliferation
B4DHK6	3	11.082	S-phase kinase associated protein 2	Skp2 is the substrate recruiting component of the SCFSkp2 complex, which targets cell cycle control elements, such as p27 and p21
E9PK91	21	4.384	Bcl-2-associated transcription factor 1	Death-promoting transcriptional repressor. May be involved in cyclin-D1/CCND1 mRNA stability
H9A532	4	3.863	BCL6 corepressor-cyclin B fusion protein	Interacting selectively with a repressing transcription factor to stop, prevent, or reduce the frequency, rate or extent of transcription
B2R9L6	6	0.449	CDC2-related kinase (CDK1 associated kinase)	To regulate important transitions in the eukaryotic cell cycle with the cyclins family.
Q59HA5	2	0.333	Cyclin G-associated kinase variant	Cyclin G is a direct transcriptional target of the p53 tumor suppressor gene product downstream of p53.

Table 5.1: The list of proteins that showed differential changes of at least two-fold upon expression of MCPyV truncated LT in quantitative proteomic datasets associated with cell cycle control.

The proteins identified in the SILAC dataset in both nuclear and cytoplasmic samples and blasts for it's functions are listed with accession ID, number of peptide identified, fold change, name and their possible functions.

In general, APC is a cell cycle-regulated E3 ubiquitin ligase that controls progression through mitosis and the G1 phase of the cell cycle. This ubiquitin ligase is required for ubiquitination and subsequent proteasome degradation of multiple cell cycle regulatory and effector proteins; where as without the APC, the cell would be unable to separate the sister chromatids during anaphase, exit mitosis, or properly enter S-phase (Thornton et al., 2006). It may also be the case that MCPyV truncated LT-mediated upregulation of APC components might also affect additional cell cycle regulatory proteins for polyubiquitination and proteasomal degradation. Well known substrates for the APC include cyclin A, cyclin B and securin (Fehr and Yu, 2013), which in turn regulate CDK activity which may affect other parts of the cell cycle. In mammalian cells, levels of cyclin-dependent kinases (CDK4, CDK2 and CDC2) in each phase correlates with expression levels of cyclins (D, E, A and B) (Sherr, 1993). The complex formation between CDK4 and several D cyclins function early and probably in response to the growth factors; CDK2 complexes with cyclin E or A or both, and is found to be essential for DNA replication; and CDC2 complexes with cyclin A and B and is essential for mitosis (Hartwell and Kastan, 1994). In the truncated LT dataset, CDK2 was found to be highly upregulated and may therefore be a target of MCPyV truncated LT. CDK2 complexes with cyclin E and A promoting the G1/S phase transition and also drives cells through S-phase (Aleem et al., 2005; Satyanarayana et al., 2008).

To determine whether expression of the truncated LT has any effect on the levels of CDKs and cyclins, 293 cells were transfected with either a control plasmid, truncated LT, wild type LT and SV40 LT expression vectors. After 24 hours, cell lysates were harvested and immunoblots were performed using a range of CDK- and cyclin-specific antibodies (Figure 5.3). Immunoblot and densitometry analysis suggest that CDK2 may be slightly increased upon truncated LT expression, although this was not as significant as the proteomic data suggests, which may be due to the transfection method utilised in contrast to the stable cell line proteomic data. A similar result was also found in cells expressing the MCPyV full

length LT. However there are no changes in CDK1 levels in any of the samples tested. Analysis of cyclin levels upon truncated LT expression also showed differential expression. Firstly, cyclin A levels appeared to be slight increased upon truncated LT expression. This result supports the flow cytometry cell cycle analysis in Figure 5.1 and 5.2, as cyclin A can activate both CDK1 and CDK2 and functions in both S-phase and mitosis (Pagano et al., 1992). Here cyclin A-CDK interactions are believed to be important for initiation and restriction of DNA replication in S-phase, whereas in mitosis it stabilises cyclin B (Yam et al., 2002). Interestingly, expression of cyclin A is found to be elevated in a variety of tumours by immunohistochemical detection, which specifically compares the cancer cells with surrounding non cancer tissue. Considering that both cyclin A and CDK2 showed slight elevation in MCPyV truncated LT transfected cells as well as CDK2 was highlighted to be upregulated in the SILAC MCPyV truncated LT dataset, suggests the possibility that MCPyV truncated LT targets CDK2-cyclin A complexes to promote the G1/S phase transition and drive cells through S-phase, which may result in cell proliferation and tumourigenesis.

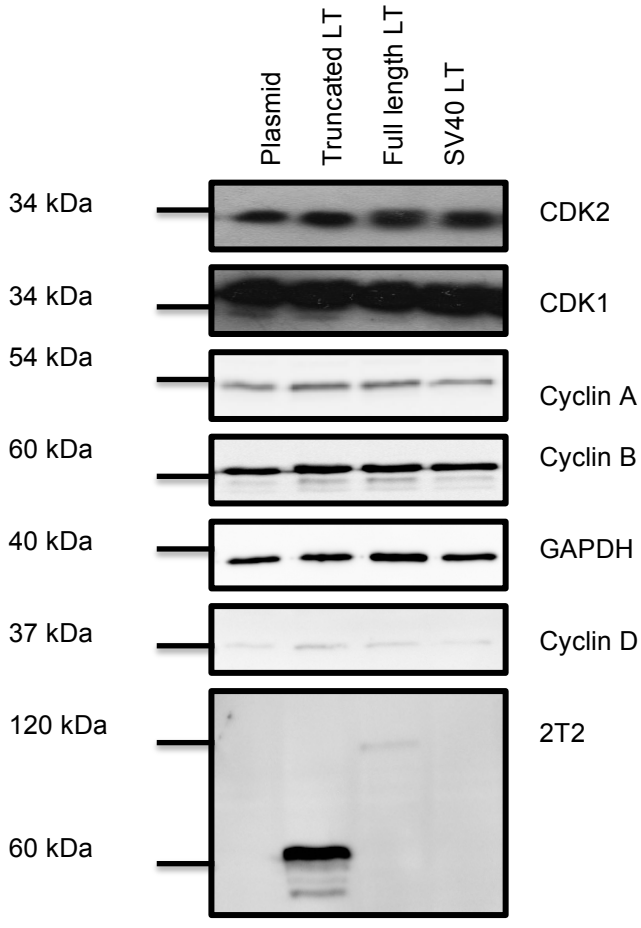

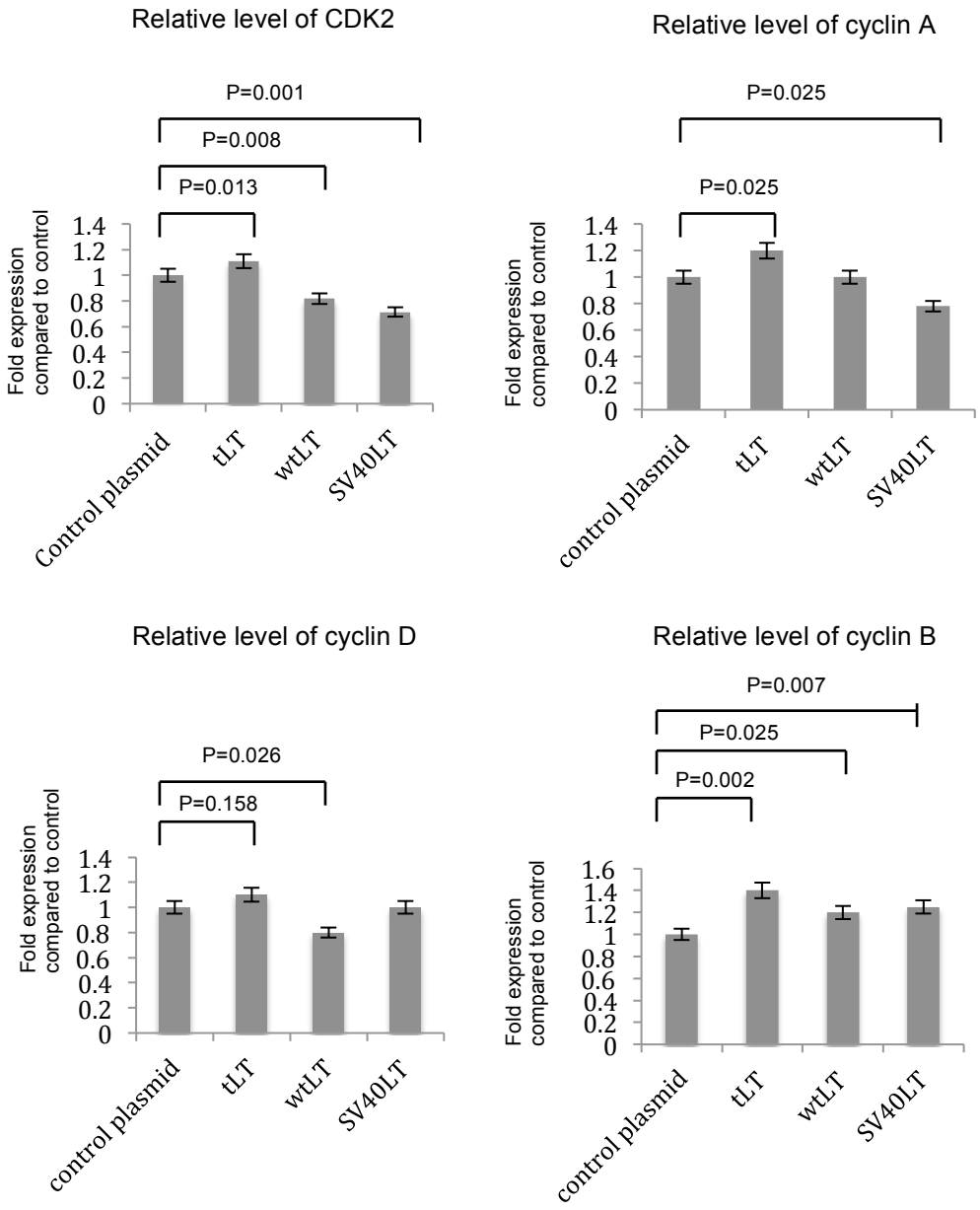

Figure 5.3: Expression of truncated LT leads to the differential expression of cyclins.

HEK293 cells were transfected with either a control plasmid, MCPyV truncated LT, wild type MCPyV LT, SV40 LT antigen. After 24 hours, cells were harvested and lysates subjected to immunoblotting using CDK- and cyclin-specific antibodies, GAPDH for used as a loading control and 2T2 monoclonal antibody was used to detect the MCPyV LT proteins. P-value for each comparison were using student t-test calculation.

Comparing expression levels of the other cyclins, cyclin B levels were also increased in MCPyV truncated LT, however this increase was not as significant upon full length MCPyV and SV40 LT expression. It may be the case that increased cyclin B levels further enhance cell proliferation in truncated LT cells, driving them through the G2/M transition. Cyclin D however remained fairly constant in MCPyV truncated LT and SV40 LT expressing cells, but slightly reduced upon MCPyV full length LT expression. Unfortunately, analysis of Cyclin E levels could not be assessed due to the reactivity of the antibody reagents available at the time of this analysis.

It is also worthy of note that the MCPyV truncated LT SILAC dataset highlights the upregulation of S-phase kinase associated protein 2 (Skp2), more than 11-fold, although this was not confirmed experimentally due to poor antibody reagents. Skp2 protein is the substrate recruiting component of the SCF Skp2 complex, targeting cell cycle control elements, such as p27 and p21. The loss of the p27 results in increased cell proliferation and p27 knockout mice show enlarged organs and pronounced tumour development (Fero et al., 1998; Kiyokawa et al., 1996; Nakayama et al., 1996). The cyclin-dependent kinase inhibitor p21 promotes cell cycle arrest and functions as both a sensor and an effector of multiple anti-proliferative signals (Abbas and Dutta, 2009). Therefore, by additionally disturbing p27 and p21 normal regulation, truncated LT expression may lead to cell transformation.

5.2.3. Cell growth and proliferation.

Alterations in the control of the cell cycle often have downstream effects on cell growth and proliferation. It is also worth noting that in the SILAC-based quantitative proteomic dataset for MCPyV truncated LT, cell proliferation-inducing protein 23 was upregulated to 3.5-fold compared to the control cells. Therefore, to determine whether the potential alteration of cell cycle regulation in MCPyV truncated LT-expressing cells also affected cell growth

and proliferation, a simple cell counting assay was carried out using cells transfected either control eGFP, eGFP-MCPyV truncated LT antigen, MCPyV full length LT, SV40 LT and SV40 genomic T antigen expression vectors. The cells were seeded at a specific density of 5000 cells and counted after 24 hrs and 48 hrs using a heamocytometer. Figure 5.4 demonstrates that expression of both MCPyV truncated LT and full length LT resulted in a increase in cell number after 24 and 48 hours compared to the control cells.

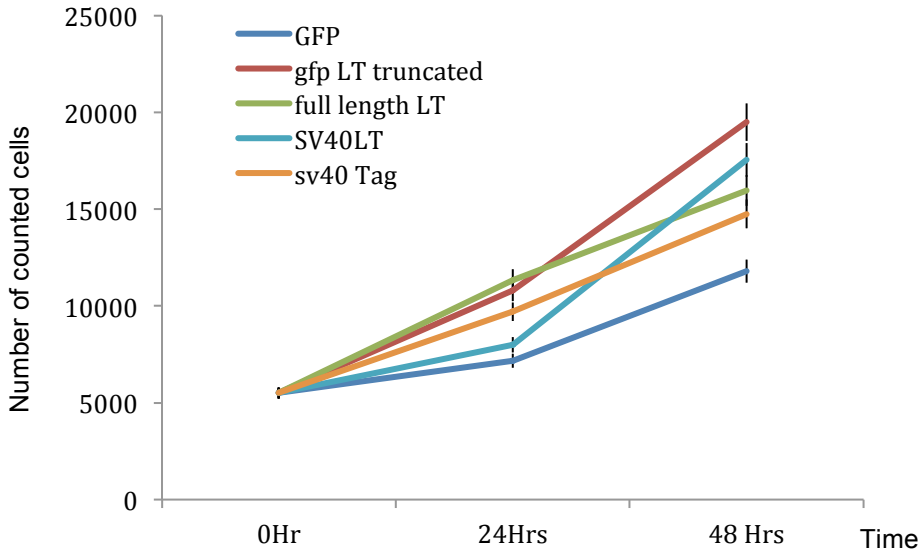

Figure 5.4: Expression of MCPyV truncated LT enhances cell proliferation.

HEK293 cells were transfected with plasmids expressing GFP, GFP-MCPyV truncated LT, MCPyV full length LT, SV40 LT and SV40 T antigen. The cells were counted and seeded with the same amount for each well (5000 cells). The cells were then counted using flow cytometry at 24 hrs and 48 hrs. The experiments were run in triplicate.

Interestingly, the truncated LT cells showed the highest rate of proliferation of all the transfected cells tested, suggesting this construct is the most potent at inducing cell proliferation. Again, this supports results in Figure 5.3 which show that expression of truncated LT showed the most significant alterations in cyclin A and B levels, compared to the other LT expression constructs. Moreover, these results support recent findings suggesting that MCPyV LT antigen expressed cells showed increased potential in supporting cellular proliferation, focus formation and

anchorage-independent cell growth compared to full length MCPyV (Li et al., 2013).

5.3. Effects of MCPyV truncated LT on apoptosis and cell survival pathways.

Quantitative proteomic analysis of the MCPyV truncated LT antigen SILAC dataset, in which both upregulated and downregulated identified proteins were combined and analysed together, highlighted that the most affected molecular function was cell death and survival. The identified molecules associated with this function were significantly higher than other possible molecular functions in both fractions suggesting that MCPyV truncated LT might play an important role in causing or inhibiting cell death and survival. Of particular interest was the observation that expression of MCPyV truncated LT resulted in the reduced expression of proapoptotic proteins, specifically the BCL-2 family member, BAD. Therefore, experiments were performed to determine if MCPyV truncated LT expression affected Bad protein levels and apoptosis induction.

5.3.1. The pro-apoptotic BAD protein is downregulated in the MCPyV truncated LT SILAC proteomic dataset.

MCPyV LT is known to target survivin, a member of the inhibitor of apoptosis protein family that is upregulated in a variety of lymphomas and metastatic melanomas (Ambrosini et al., 1997). Survivin functions as an inhibitor of apoptosis by prolonging cell viability, and later contributes to cell transformation by facilitating the insurgence of mutations and promoting cellular resistance to chemotherapy. Knockdown of MCPyV LT antigens in MCPyV positive MCC cells showed that survivin mRNA and protein levels fell resulting in MCC cell death (Arora et al., 2012a). Surprisingly, we could not detect survivin in our MCPyV truncated LT antigen SILAC proteomic dataset, which may be due to lack of coverage of the complete host cell proteome. However, aligned to apoptosis regulation, the related BCL-2

family member protein (BAD), appeared to be differentially expressed in our SILAC proteomic analysis, reduced by five-fold. It may be the case that the MCPyV LT has multiple mechanisms to regulate the apoptotic response, by increasing the expression of anti-apoptotic proteins, such as survivin, and also reducing expression of pro-apoptotic proteins, such as BAD. The BAD protein is a pro-apoptotic member of the BCL-2 gene family involved in initiating apoptosis. BAD functions by forming heterodimers with anti-apoptotic proteins, such as BCL-2, to prevent them from stopping apoptosis (Trecherel et al., 2012). Moreover, Trecherel et al., showed that expression of BAD in vascular smooth muscle cells leads to apoptosis induction, suggesting BAD promotes cell death. In our SILAC analysis, the BAD protein was found to be downregulated upon expression of truncated LT protein, suggesting a possible virus-mediated apoptotic inhibition mechanism. This is supported by experiments in which reduction of BAD expression by RNA interference (RNAi) has been shown to prevent apoptosis in response to P13K/Akt kinase pathway inhibition in PTEN-deficient tumour cells (She et al., 2005). As such, truncated LT-mediated repression of BAD function may play an important role in inhibiting apoptosis allowing the initiation of tumourigenesis. The proteomic analysis of SILAC MCPyV tLT dataset identified downregulation of protein BAD (Figure 5.5).

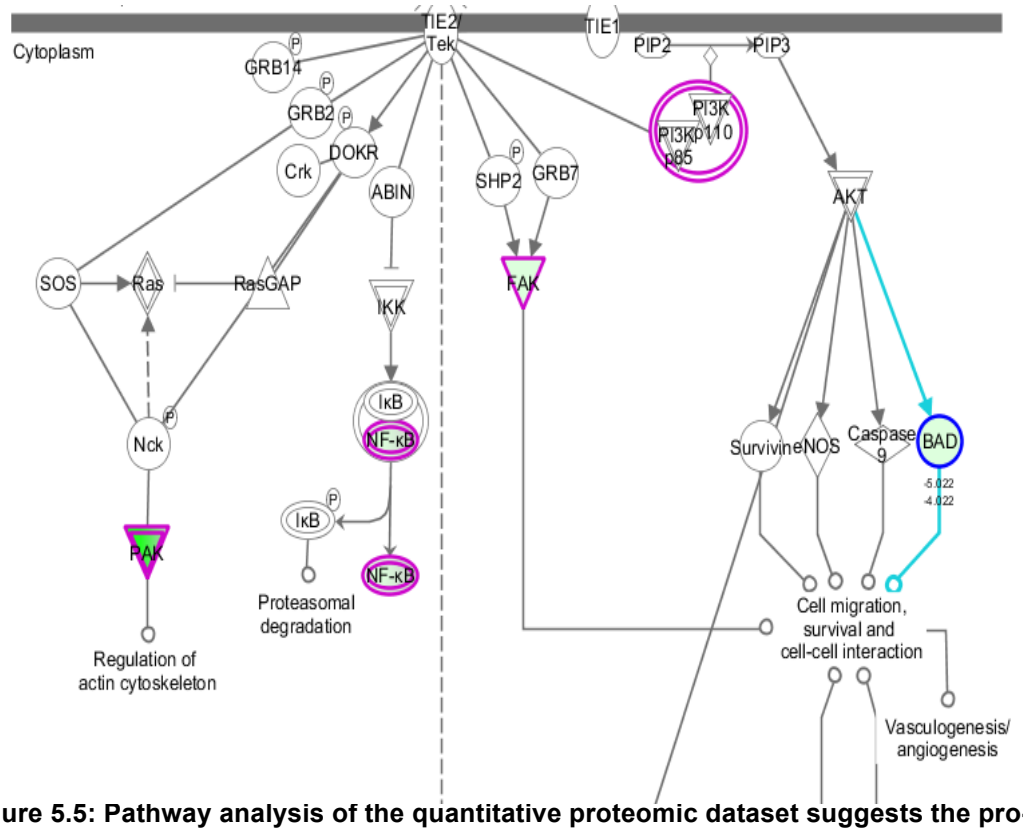

Figure 5.5: Pathway analysis of the quantitative proteomic dataset suggests the pro-apoptotic protein, BAD is downregulated upon MCPyV truncated LT expression.

The BAD protein was identified to be downregulated in the bioinformatics analysis. Besides BAD other molecules such as PAK, NF-kB and FAK were upregulated in the SILAC truncated LT. The other identified molecules in the SILAC are shown in purple.

To validate the quantitative proteomic data, immunoblot analysis was performed on cell lysates harvested from uninduced versus induced HEK293-tLT expressing cells. Results showed that levels of BAD protein were decreased in truncated LT-expressing cells compared to its uninduced non-expressing counterpart (Figure 5.6). This confirmed the results identified by the MCPyV truncated LT SILAC proteomics analysis.

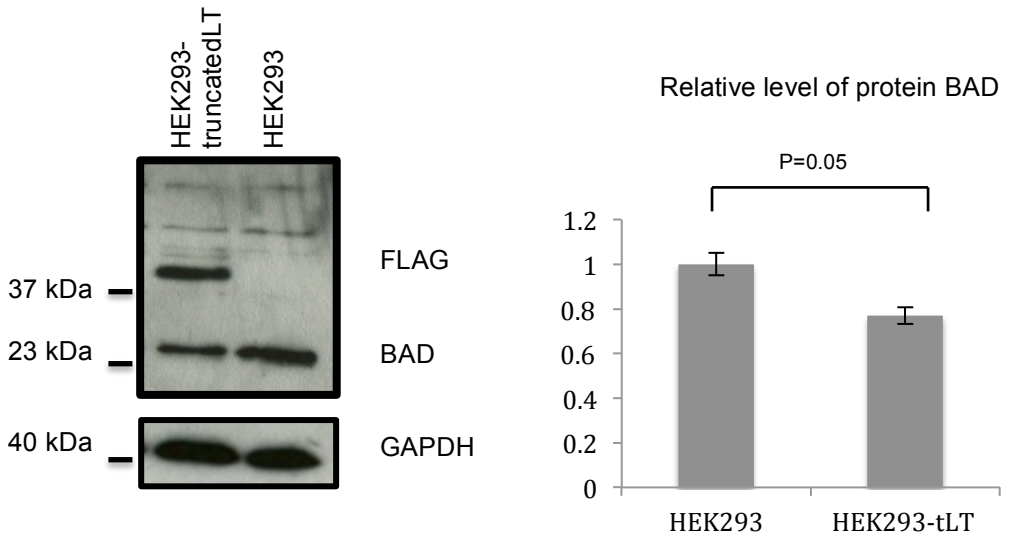

Figure 5.6: Expression of truncated LT leads to a reduction in the level of the pro-apoptotic protein, BAD.

i293-tLT cells remained uninduced or were induced by 24 hours using doxycycline. Cell lysates were then harvested and equal amounts of protein were separated by electrophoresis on 12% polyacrylamide gels, transferred to nitrocellulose membrane and probed using FLAG-, BAD- and GAPDH-specific antibodies. GAPDH was used a loading control. Densitometry quantification of the western blots was carried out using the Image J software and is shown a percentage of relative densitometry to the loading control, GAPDH.

5.3.2. Induction of apoptosis and DNA damage.

As MCPyV truncated LT expression leads to reduced protein BAD levels, experiments were next performed to determine whether truncated LT expression was sufficient to prevent apoptosis. To this end, the rates of apoptosis and cell death were examined upon the treatment of apoptosis-inducing chemicals, namely staurosporine and etoposide. Staurosporine, a protein kinase inhibitor, which has been characterized as a strong inducer of apoptosis in many different cell types. The mechanism(s) by which staurosporine induces apoptosis, however, remains controversial. It is generally believed that the mitochondrial apoptotic pathway plays a critical role in staurosporine-induced apoptosis, whereas other studies only showed a requirement for caspase activation in staurosporine-induced apoptosis. Alternatively caspase-independent mechanism(s) have also

been suggested. As such, multiple mechanisms may therefore be involved in staurosporine-induced apoptosis and these may vary between different cell types (Belmokhtar et al., 2001). Etoposide is a major anti-tumour agent that is used to treat a variety of cancers. It exerts its anti-neoplastic activity by inhibiting topoisomerase II, which leads to DNA strand breaks, inhibition of DNA replication, and apoptotic cell death (Lezcano et al., 2014).

5.3.2.1. Treatment with staurosporine.

To determine whether expression of truncated LT protects or enhances the survival time of cells after treatment with the apoptotic inducing agent, staurosporine, an apoptosis assay was carried out. This assay is based on the observation that soon after initiating apoptosis, cells translocate phosphatidylserine from the inner face of the plasma membrane to the cell surface. Once on the cell surface, phosphatidylserine can be detected with a fluorescent conjugate of Annexin V and quantified by flow cytometry. This analysis can then be represented as a percentage of apoptotic to living cells in the tested populations (Figure 5.7). Results from this analysis demonstrated that untreated uninduced and truncated LT cells had a similar high percentage of living cells. In contrast, the addition of staurosporine resulted in a higher percentage of apoptotic, annexin V positive cells, in fact approximately doubling the amount in both cases. This suggests that although truncated LT expression may affect BAD expression, it is unable to prevent the apopotic-inducing potential of staurosporine. This may be due to the multiple mechanisms involved in staurosporine-induced apoptosis described above.

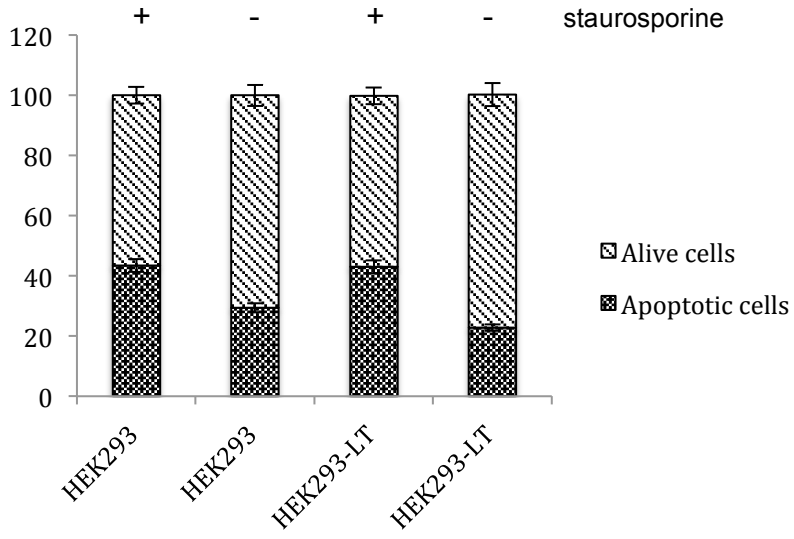

Figure 5.7: Expression of truncated LT is not sufficient to inhibit staurosporine-induced apoptosis.

The i293-tLT cell remained uninduced or were induced with doxycycline to allow MCPyV truncated LT expression for 24 hours. The cells were then left untreated or treated with 1 µM staurosporine. After 12 hours, the cells were harvested and labelled with annexin-V-FITC and propidium iodide (50µg/mL) prior to be analysed by flow cytometry. The experiments were run in triplicate (n=3).

Although the results shown in Figure 5.7 do not show any significant difference in the potential of truncated LT to inhibit apoptosis initiation as measured by the annexin V assay, this did not address the potential of truncated LT to delay the process of apoptosis upon the addition of staurosporine. To address this question, staurosporine was again added to control and truncated LT-expressing cells and the cells were visualised for cell number density and significant signs of cell death over a 24 hour period. Results are shown in Figure 5.8. Here an equal number of cells were seeded into 6 well plates, and cells remained uninduced or induced for truncated LT expression. After 24 hours, cells were then either treated with DMSO or staurosporine. In DMSO cells, both control and truncated LT-expressing cells have proliferated and started to become confluent in the dish. This is more pronounced for truncated LT expressing cells, due to their increased proliferation as previously described in Figure 5.4.

In contrast, the addition of staurosporine to control cells results in their cell death by 24 hours. The images show cells clumped together floating in media. However, truncated LT-expressing cells, although not proliferating to the same level as untreated cells, are still alive at 24 hours suggesting that truncated LT expression may delay the apoptotic-inducing properties of staurosporine. However, eventually (24 hours later) these cells are also dead. This suggests that MCPyV truncated LT might play role in the increased survival rate of infected cells, which in the longer term may contribute to cell transformation.

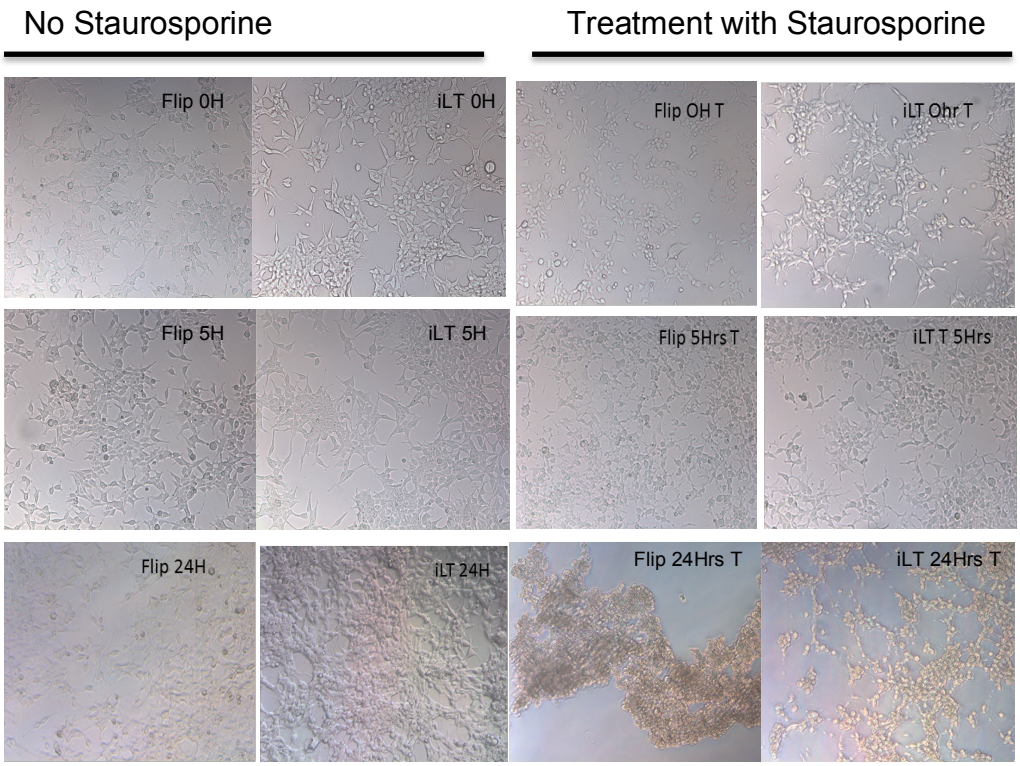

Figure 5.8: Expression of truncated MCPyV LT may delay the apoptotic-inducing properties of staurosporine.

The i293-tLT cell remained uninduced or were induced with doxycycline to allow MCPyV truncated LT expression for 24 hours. The cells were them left untreated or treated with 1 μM staurosporine. Cells were then observed at 0 Hr, 5 Hrs and 24 Hrs using an inverted microscope for the sign of apoptosis or cell death (40× magnification).

5.3.2.2. Treatment with etoposide.

Staurosporine can induce apoptosis by multiple mechanisms, therefore to further investigate any potential of truncated LT to inhibit or delay apoptosis, a more specific apoptotic inducer was utilised. Etoposide inhibits topoisomerase II, which leads to DNA strand breaks, inhibition of DNA replication, and apoptotic cell death (Pommier et al., 2010). This mechanism is particularly relevant for MCPyV as recent studies have shown that components of the ataxia telangiectasia mutated (ATM)- and ataxia telangiectasia and Rad3 related (ATR)-mediated DNA damage response pathways accumulate in MCPyV LT-positive nuclear foci (Tsang et al., 2014).

As the live cell imaging was more informative that the annexin V-based assay in previous studies with straurosporine, the effect of etoposide was initially investigated using this method. An equal number of cells were seeded into 6 well plates, and cells remained uninduced or induced for truncated LT expression. After 24 hours, cells were then either treated with DMSO or etoposide. Cells were then compared at 0 and 24 hour time points. Figure 5.9 shows images of cell sheets at 24 hours post treatment. Results clearly show that in control cells treated with etoposide large amounts of cell membrane blebbing was observed, which is a clear indication of apoptotic cells. In contrast, although a small amount of blebbing was observed in truncated LT-expressing cells, this was much less pronounced than in controls cells. Again, this may indicate that truncated LT may delay the onset of the apoptotic response upon treatment of etoposide.

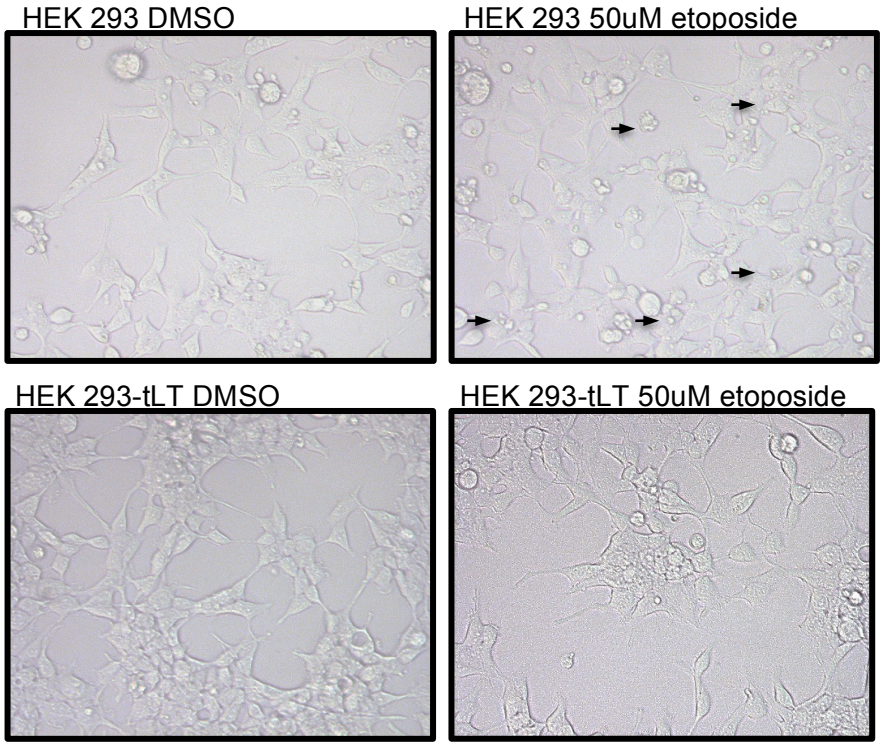

Figure 5.9: Expression of truncated LT may reduce the amount of the apoptotic blebbing induced by etoposide.

The i293-tLT cell remained uninduced or were induced with doxycycline to allow MCPyV truncated LT expression for 24 hours. The cells were them left untreated or treated with 50 μM etoposide. Cells were then observed at 24 Hrs using an inverted microscope for the sign of apoptotic blebbing.

To further investigate whether truncated LT antigen has any inhibitory effect on the apoptotic inducing properties of etoposide, immunoblotting was performed to assess proteins levels of key proteins associated with the apoptotic pathway. To this end, HEK 293 cells were transfected with a control eGFP plasmid, MCPyV truncated LT antigen (tLT), or MCPyV wild type full length LT (WTLT), after 24 hours cells were treated with either DMSO or etoposide and then immunoblotting performed using PARP-, phosphorylated p53-, BAD- and caspase 3-specific antibodies. Results show truncated LT reduced the expression of cleaved PARP, phosphorylated p53 and BAD compared to the control plasmid (Figure 5.10). A similar trend was also observed with MCPyV full length LT. However, full length LT experiments was much lower than the truncated form, as indicated by the 2T2 antibody which recognises both forms. This might due to the stability of the LT antigen in the transfected cells, where

the truncated version maybe more favourable to the cells. The difference in the levels of expression between the full length LT and truncated LT has been previous observed in the literature (Borchert et al., 2014).

The tumour suppressor protein p53 is an important regulator of the apoptotic cascade in response to DNA damage. Genomic instability and tumour development are associated with its inactivation or loss of function (Levine, 1997). Post translational modifications, such as phosphorylation of p53, play important roles in activating p53 responses to various cellular and genotoxic stresses. Specifically, phosphorylation of p53 has been proposed to stabilize p53, enhancing its apoptotic function. Therefore, if truncated LT-expressing cells do have a delayed or reduced apoptotic levels, it is not therefore surprising that a reduced level of phosphorylated p53 is observed.

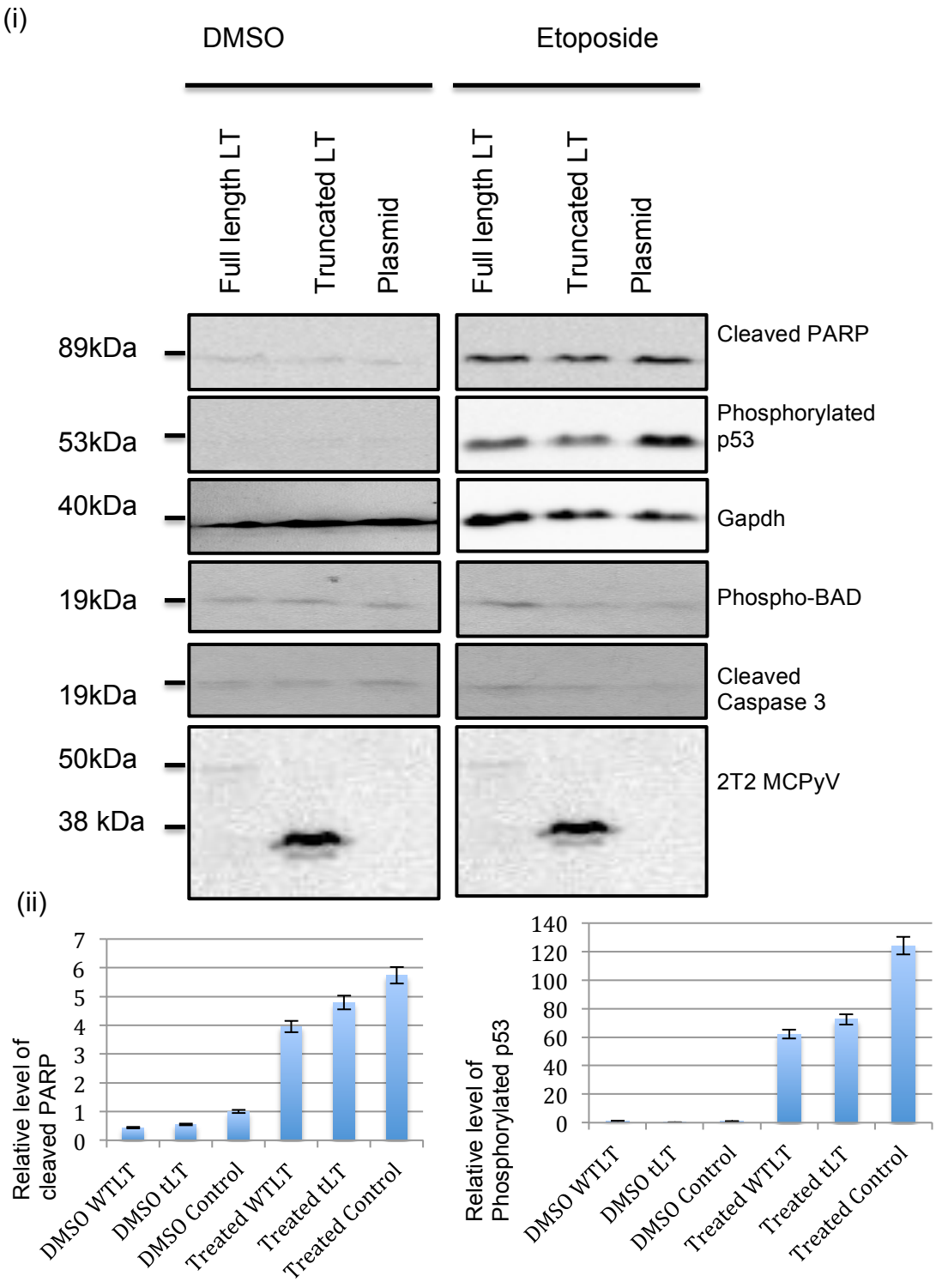

Figure 5.10: MCPyV truncated LT leads to the reduction in host cell proteins involved in cell death.

(i) HEK293 cells were transfected with either a control plasmid, MCPyV truncated LT (tLT), and MCPyV full length LT (WTLT). After 24 hours, cells were treated with DMSO or 50 μM etoposide for one hour. The cells were then harvested and lysates were detected with specific antibodies related to DNA damage and apoptosis-associated proteins. (ii) Densitometry quantification of the immunoblot was carried out using the Image J software and is shown a percentage of relative densitometry to the loading control, GAPDH.

Importantly however, to demonstrate that expression of MCPyV truncated LT reduced only the levels of phosphorylated p53, in contrast to the total levels of p53, immunoblotting was performed to assess p53 total levels in H1299 null cells, which expressed MCPyV ST and truncated LT antigen, and also a range of other viral antigens known to regulate p53 levels. The H1299 cells were chosen in this experiment as these cells have a homozygous partial deletion of the TP53 gene, therefore the tumour suppressor p53 protein were not expressed in this cell type. Thus, the amount of p53 protein in this blot was only expressed by p53 overexpression constructs that been transfected with the viral antigen. This determined whether the p53 protein levels were only affected by the viral antigen and not due to variability of p53 protein produced by the host cells.

Figure 5.11 demonstrates that total p53 levels in H1299 cells without and with cotransfection of the p53 overexpression construct and the tested viral antigen constructs. In the control sample, the cells without p53 expression, p53 bands were clearly undetected. Whereas, in cells which were cotransfected with the p53 overexpression construct, the expression of p53 varied in the range of different viral antigens. Both MCPyV ST and truncated LT antigen showed increased amounts of p53 level compared to the GFP control by 1.7-fold. This was confirmed using densitometry analysis which shows that p53 total levels are similar in MCPyV ST and truncated LT-expressing cells. Notably, the HPV16 E7 showed the highest expression of the p53. This result was expected as the expression of E7 has previously been shown to stabilize p53 in the absence of the E6 antigen (Seavey et al., 1999).

(i)

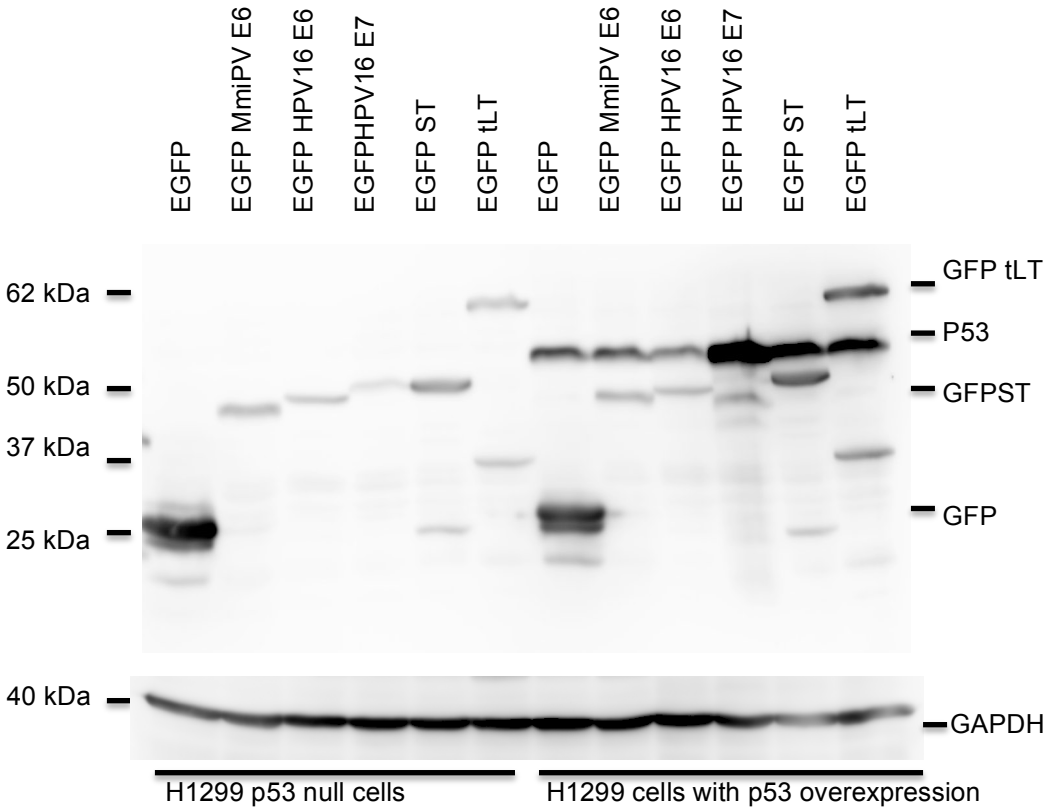

(ii)

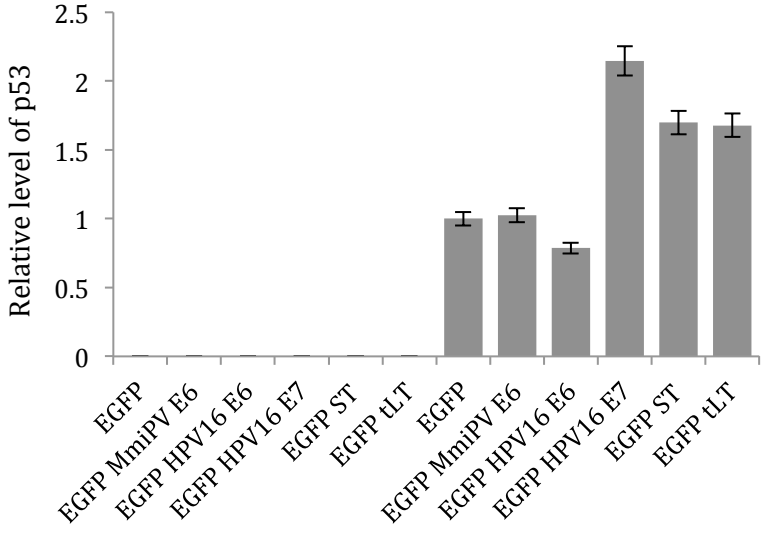

Figure 5.11: Analysis of expression levels of p53 in the MCPyV T antigen expressing cells.

(i) H1299 p53 null or wild type cells were transfected either with a range of viral oncogene expression constructed and immunoblot analysis was performed using a total p53 and GAPDH specific antibodies. GAPDH was used as a loading control. (ii) Densitometry quantification of the western blots was carried out using the Image J software and is shown a percentage of relative densitometry to the loading control, GAPDH.

5.4. Effects of MCPyV truncated LT on cell movement and cell junctions

In chapter 4, bioinformatics analysis highlighted that MCPyV truncated LT expression may affect cell-cell connections. Specifically, analysis showed that key components of cellular pathways involving tight junctions, regulation of actin cytoskeleton, gap junctions, adherens junction, integrin signaling pathways, synaptic proteins at the synaptic junction and uCalpain and friends in cell spread proteins were differentially expressed upon MCPyV truncated LT expression. This observation may be important in MCC development as tight junction proteins has been shown to be involved in the control of cellular proliferation and differentiation (Martin and Jiang, 2009). Importantly, tight junction proteins, in addition to their structural functions also regulate both signal transduction emanating from the plasma membrane and gene expression in the nucleus. In addition, studies of human tumours reveal a direct correlation between the loss of functional tight junctions and associated proteins in cancer progression and metastasis.

5.4.1. Effects of MCPyV truncated LT antigen expression on levels of tight junction protein, zona occuldens proteins

To initially study any possible effects that MCPyV truncated large T expression had upon host cell tight junctions, immunoblotting was performed to assess differential expression of the zona occuludens protein, ZO-1. This is a family member of tight junction associated proteins that function as cross-linkers, anchoring the tight junction strand proteins to the actin-based cytoskeleton (Itoh et al., 1997). ZO-1 was chosen as Kyoto Encyclopedia of Genes and Genomes (KEGG) pathway analysis in the previous chapter showed that most of the proteins targeted in the SILAC dataset were downstream of ZO-1, as such changes in ZO-1 will highlight if the pathway is affected by truncated LT expression. Immunoblot analysis of ZO-1 protein levels showed a slight increase in truncated LT-expressing cells (Figure 5.12), this was rather surprising as they result contradicted the

quantitative proteomic results. Considering the large size of ZO-1, approximately 194 kDa, and the poor quality of the western blot, the efficiency of transfer proteins onto the membrane during blotting and the antibody used may be the reason for this surprising result.

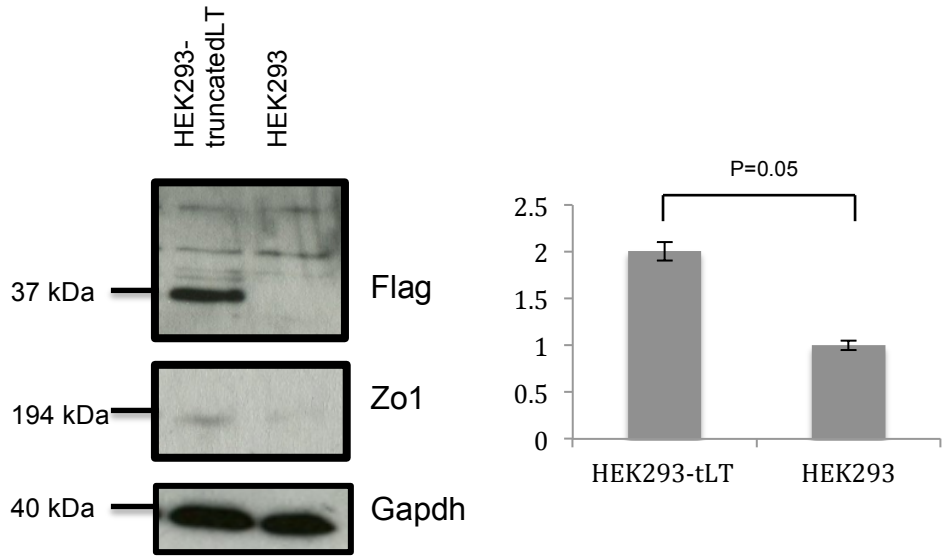

Figure 5.12: Expression levels of tight junction protein ZO-1, increase in cells expressing truncated MCPyV LT.

HEK293 cells were transfected with either a control plasmid or MCPyV truncated LT (tLT). After 24 hours, cell lysates were probed using Flag-, ZO-1- and GAPDH-specific antibodies. GAPDH was used as a loading control. P

To further investigate any possible effect of truncated LT expression on ZO-1, immunofluorescence studies were performed assessing endogenous ZO-1 subcellular localisation and also the subcellular localisation of ZO-1 myc-tagged constructs; which comprises of N-terminus and C-terminus truncation mutants. It is believed that the ZO-1 N-terminus is required for tight junction assembly, whereas the C-terminus may elicit specific properties of the tight junction, which are yet to be fully understood. Initial immunofluorescence studies attempted to assess the subcellular localisation of ZO-1 using ZO-1-specific antibodies, however, results shown in Figure 5.13 (top 2 panels), show an unexpected localisation in both control eGFP- and LT-expressing cells. Here ZO-1 was mainly present in the nucleus with weaker diffuse staining throughout the cytoplasm. No localisation was observed at tight junctions. Therefore immunofluorescence was also performed in cell expressing the ZO-1 truncation myc-tagged mutants, with ZO-1- specific antibodies (Figure 5.13, bottom 3 panels).

The subcellular localisation of these tagged constructs was surprising, with all 3 constructs concentrating around the perinuclear region and diffusely staining in the cytoplasm, which is reminiscent of microtubule staining. Therefore, taken into consideration the aberrant sub-cellular staining observed, experiments using the ZO-1 antibody and truncation mutants were not taken any further.

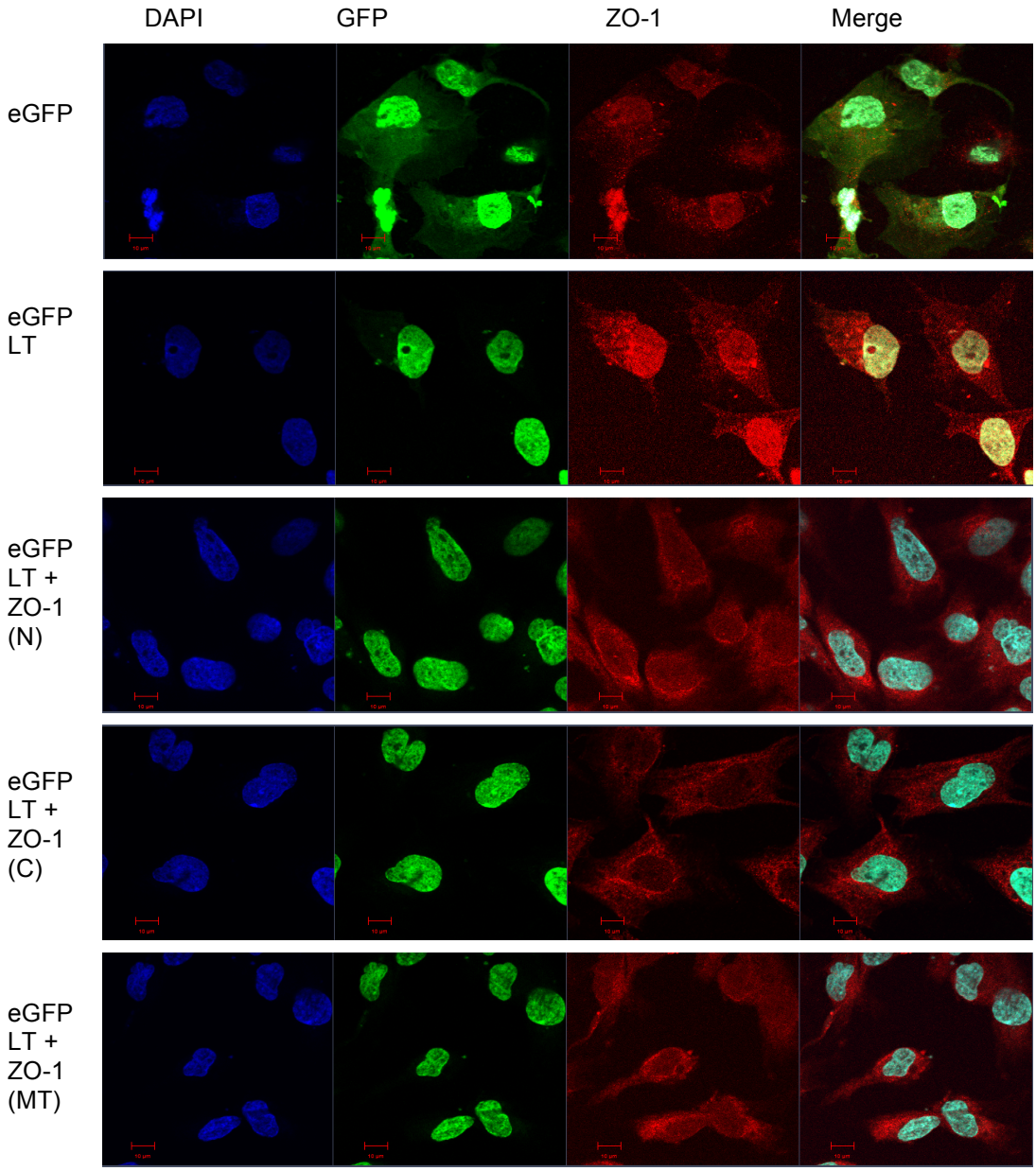

Figure 5.13: Localisation of ZO-1 proteins in control and GFP-tLT-expressing cells.

HEK293 cells were transfected with either a eGFP or eGFP-tLT expressing plasmid, in the absence or presence of ZO-1 truncation mutants (ZO-1 (N), ZO-1 (C), and ZO-1 (MT)) for 24 hours. The cells were fixed, permeabilised and stained with ZO-1 specific antibodies, whereas eGFP was directly visualised.

The previous experiments using the ZO-1-specific antibody were unable to show distinct cell-cell connection staining between neighbouring cells. Therefore, other cell-cell adhesion proteins, namely β-catenin, were used to investigate the effects of truncated LT on cell-cell connections. Figure 5.14 demonstrates the immunofluorescence staining in eGFP versus eGFP tLT-expressing cells using the β-catenin-specific antibody. Results show that significant changes in distribution and intensity of β-catenin protein staining in cells expressing MCPyV truncated LT antigen. The protein β-catenin seems to be accumulated more on the cytoplasmic membrane between the neighbouring cells. This may suggest possible breakdown or re-organisation of the cell-cell connections upon interactions of the MCPyV truncated LT antigen. This finding is preliminary and more future research is now required to elucidate further the effects of MCPyV truncated LT on downstream tight junction protein components that had been detected in the SILAC datasets.

Interestingly, a large group of tight junction-associated proteins consist of members from the diverse family of PDZ domain-containing proteins, including the ZO-family of proteins. Consistent with having multiple protein-binding domains, PDZ proteins typically function as scaffolds to assemble transmembrane and cytosolic proteins into supramolecular signaling complexes, as well as to tether such complexes to the actin cytoskeleton and to localize them at specialized membrane sites of cell-cell contacts, such as tight junctions (Martin and Jiang, 2009). It will be interesting to now determine if truncated LT affects these signalling complexes.

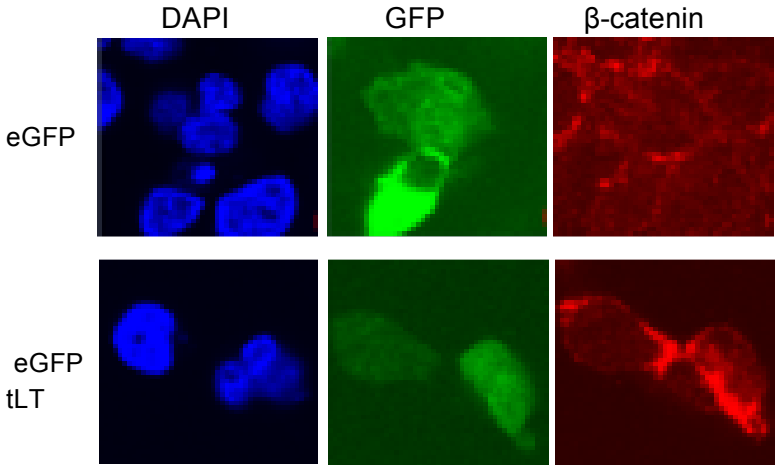

Figure 5.14: Immunofluorescence studies suggest that tight junction components may be reorganised upon coexpression with MCPyV truncated LT.

HEK293 cells were transfected with eGFP or eGFP-tLT for 24 hours, then fixed permeabilised and stained with a β-catenin-specific antibody. GFP fluorescence was directly visualised.

5.4.2. MCPyV truncated LT does not affect cell motility

MCC cells are highly metastatic and the Whitehouse group have recently demonstrated that expression of MCPyV ST enhances cell motility and the metastatic potential of MCC cells (Knight et al., 2015). To also determine if truncated LT has any additional effects on cell motility, scratch assays were performed using the truncated LT inducible cell line (Figure 5.15). A confluent cell sheet of i293-tLT and i293-ST cells remained uninduced or were induced with doxycline. Cells were then subjected to a scratch using a p200 pipette tip in a continuous straight line through the well. After 24 hours, cellular growth back into the wound was recorded for 24 hours (Figure 15). Results indicate that, in contrast to uninduced cells, expression of MCPyV ST enhanced the motility and migration of cells into the wound, confirming previous results. In contrast no enhancement in migration and cellular growth back into the wound was observed upon expression of truncated LT, suggesting that it did not play a role in cell migration.

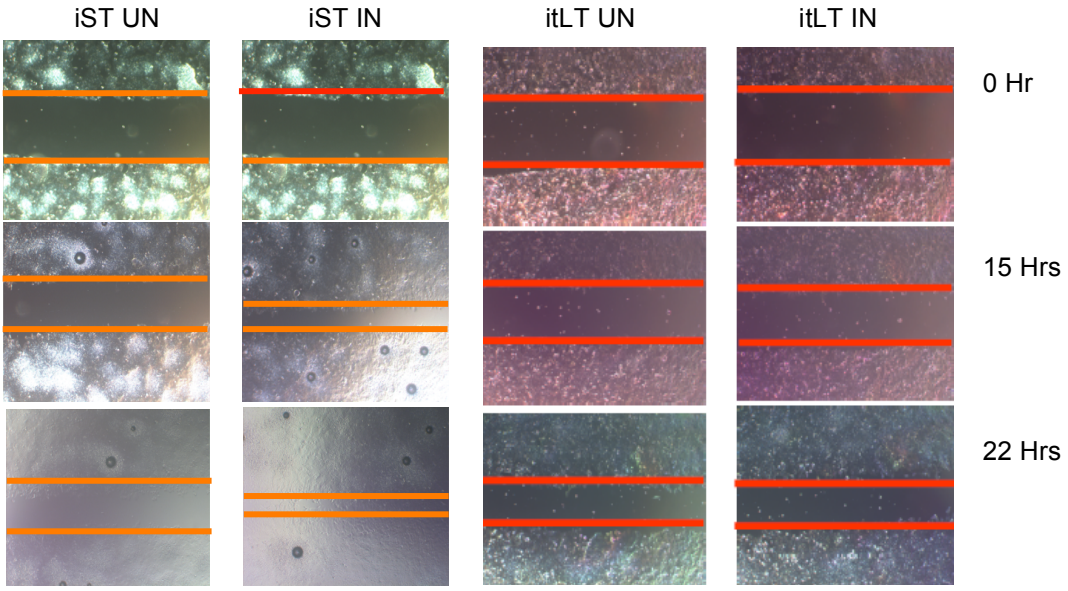

Figure 5.15: Scratch assay shows MCPyV truncated LT expression does not enhance cell migration.

i293-ST and i293-tLT cells were seeded onto poly-L-lysine coated 6 well plates and remained uninduced or were incubated in the presence of Doxycycline hyclate. After 24 hours, a scratch was created by scraping the monolayer using a P200 pipette tip. Migration of cells toward the scratch was observed over a 24 hour period and images taken under a Zeiss light microscope at 40× magnification.

5.5. Discussion

The main aim of this chapter was to evaluate the potential role of differentially expressed proteins upon truncated LT expression, highlighted by the quantitative proteomic approach in the previous chapter. The evaluations were carried out using several approaches and assays in order to investigate the possible functions that the MCPyV truncated LT has upon regulating the cellular proteome and which may relate to MCPyV pathogenesis.

Firstly, the quantitative proteomics analysis highlighted many stress-related and apoptosis pathways were affected upon truncated LT expression. For example, increases in stress response of tumour, cell death, apoptosis and movement disorders-related pathways were observed. Interestingly, pathways involved in the immortalization of fibroblast cell lines also increased, suggesting that while infected cells were suffering stress,

MCPyV truncated LT might utilise mechanisms to enhance transformation and immortalization of these cells. This feature is similar to SV40 LT antigen where episomal viral DNA can lead to stable transformation and immortalization of fibroblast cell lines (Morelli et al., 2004). This aligns with the role of many persistently infected viruses with oncogenic potential which can influence tumour sustainment and progression and induce escape pathways from apoptosis and immune surveillance (Carbone et al., 2004).

A major pathway that was highly upregulated upon truncated LT expression was involved in regulating the cell cycle. The cell cycle analysis carried out using the inducible cell line expressing MCPyV truncated LT showed significant changes in the cell population distributions across cell cycle phases, namely affecting the G1 checkpoint, enhancing the transition of cells from G1 into the S phase. These changes can be explained by the ability of MCPyV truncated LT to bind the retinoblastoma tumour suppressor protein (pRB). pRb is known as negative regulator of cell proliferation and cell cycle control. pRb prevents entry to the S phase by forming an inhibitory complex with transcription factors of the E2F family (Chau and Wang, 2003). MCPyV truncated LT antigen possesses a Rb binding motif (LXCXE) which is highly conserved across polyomaviruses allowing binding to the pocket domain of pRB with high affinity (Borchert et al., 2014). Binding of the LT with pRb results in dysregulation of E2F-mediated transcription driving cells into the S-phase, whereby the viral genome can be replicated (Becker et al., 2009). Furthermore, this LT antigen/pRb interaction is thought to be important for the growth-promoting properties of MCPyV-infected MCC cells (Houben et al., 2012). The loss of the G1-S checkpoint could also contribute to genomic instability and transformation of the cells. A recent study has demonstrated that truncated LT expression alone is sufficient to cause repair and cell cycle arrest defects in MCPyV-negative MCC cells (Demetriou et al., 2012).

Results also highlighted several protein targets associated with cell proliferation, ubiquitin proteasomal degradation and anaphase promoting

complexes (APC) that were shown to be upregulated upon expression of MCPyV truncated LT antigen. The latter two pathways may provide an explanation as to why so many cellular proteins seem to be downregulated in the quantitative proteomic truncated LT dataset. Cells often use ubiquitin as a covalent modifier of other proteins both to activate their function and to target them for degradation (Hochstrasser, 2009). Several components of APC complexes were upregulated in the SILAC dataset which may play a role in cell cycle control, poly-ubiquitination and proteasomal degradation. APC is essential for separation of sister chromatids during anaphase and regulates cells to exit mitosis or enter the S-phase (Thornton et al., 2006). Among the known substrates for the APC is cyclin A (Fehr and Yu, 2013). Interestingly, cyclin A and CDK2 were found to be slightly elevated in MCPyV truncated LT expressing cells. CDK2 binding to cyclin A is essential for DNA replication (Hartwell and Kastan, 1994) as well as promoting the G1/S phase transition and driving cells through S-phase (Aleem et al., 2005). This regulation of the cell cycle may therefore be related to the increased proliferative capacity of truncated LT-expressing cells. The cell growth counting analysis showed MCPyV truncated LT-expressing cells exhibit rapid growth activity compared to the controls suggesting that MCPyV truncated LT possesses a proliferative activity. Interestingly, the rate of growth in truncated LT cells was noticeably higher than the full length version of the LT antigen, suggesting that MCPyV LT C-terminal helicase domain contains growth inhibitory properties, as recently suggested (Li et al., 2015).

Proteomic analysis also highlighted cell death and cell survival pathways were highly affected by truncated LT expression. To validate this hypothesis we chose to focus on the pro-apoptotic protein, BAD, which is known to interact with BCL2-associated agonist of cell death (Trecherel et al., 2012). Trecherel et al., showed vascular smooth muscle cells undergo apoptosis upon induction of BAD, suggesting BAD promotes cell death. Our SILAC analysis suggested that the BAD protein is downregulated upon expression of MCPyV truncated LT. Interestingly, reduction of BAD expression by RNA interference prevents apoptosis in response to

P13K/Akt kinase pathway inhibition in PTEN-deficient tumour cells (She et al., 2005). Therefore, expression of truncated LT downregulating BAD function, may enhance cells to inhibit apoptosis and initiate tumourigenesis, as well as increasing the survival rate of the cancer cells. Further analysis on the induction of apoptosis and DNA damage were carried out to evaluate the effect of truncated LT to inhibit cell death pathways. Results suggest that truncated LT expression may delay the apoptosis-inducing properties of staurosporine and etoposide, suggesting that MCPyV truncated LT might play role in the increased survival rate of infected cells, which in the longer term may contribute to cell transformation. This may be due to truncated LT expression reducing the pro-apoptotic forms of phosphorylated p53, however how this is achieved is currently unknown. In SV40-infected cells, LT binding to p53 results in p53 stabilization leading to abundant amounts of p53 that is functionally inactive (Oren and Levine, 1981; Oren et al., 1981). However, in contrast to SV40, MCPyV truncated LT does not contain the direct binding site for p53. Thus a different mechanism is used by MCPyV truncated LT antigen to stabilise p53. Interestingly, the MCPyV full length LT antigen has also been shown not to directly bind p53, but is able to target the p53 pathway and reduce p53 dependent transcription (Borchert et al., 2014). How this is achieved is currently under investigation.

In addition to apoptosis and cell survival pathway, the other possible main function of truncated LT based on our SILAC proteomic data is in regulating cell-cell connection related pathways. The SILAC data suggests that truncated LT expression leads to the downregulation of various proteins associated with these pathways. This is particularly interesting as truncated LT might have a function in regulating the connective proteins between cells that enable cells to break apart leading to migration and metastasis. At present our preliminary analysis using cell-cell connections associated proteins could not address this question and this area of research requires further investigation.

Chapter 6
Final discussion and future perspectives

6.0. Final discussion and future perspectives

MCC is a rare but highly aggressive neuroendocrine skin cancer which is able to spread effectively through the dermal lympathic system. As such it exhibits a high mortality rate (Poulsen, 2004a; Tadmor et al., 2011a). Merkel cell polyomavirus (MCPyV) has been detected in the majority of MCC tumour samples and is monoclonally integrated in primary and metastatic tumour cells (Feng et al., 2008). Thus, infection and integration occur before the clonal expansion of the tumour cells, indicating the importance of MCPyV in the initiation of tumourigenesis. Moreover, truncation mutations of the LT antigen are commonly observed in the integrated genome of the MCPyV positive samples of MCC (Shuda et al., 2008). These LT mutations render the virus replication defective leading to aberrant expression of MCPyV tumour antigens which is implicated in cellular transformation.

To date, several studies have demonstrated the importance of the MCPyV T antigens in viral replication and host cell transformation. MCPyV ST expression is detected in 92% of MCC tumour samples, indicating a significant role of ST in tumourigenesis (Shuda et al., 2011b). Notably, expression of MCPyV ST alone is sufficient to promote anchorage independent growth of rodent cells, loss of contact inhibition and facilitates cellular transformation (Shuda et al., 2011b). Recently, MCPyV ST has also been shown to promote the destabilization of the host cell microtubule network which enhances cell motility and migration (Knight et al., 2015). This is a particularly interesting finding as it may suggest why MCC possess such highly metastatic properties. Aligned with this observation, quantitative SILAC-based proteomic analysis, which compared control and MCPyV ST expressing cells, has highlighted numerous other cellular proteins that are differentially expressed upon MCPyV ST expression which affect the host cell cytoskeleton and may also been involved in enhancing cell motility and metastasis.

The aim of chapter 3 was to further characterise three proteins of potential interest, namely kinesin protein family 14 (Kif14), vitronectin (Vn) and periplakin (PPL), in relation to MCPyV ST-induced cell motility. These proteins were prioritised as they were identified to be differentially expressed in a previous SILAC-based quantitative proteomic study and have been previously shown to be dysregulated in other types of human cancer.

From the results presented in chapter 3, it was surprisingly however that only one of the prioritised proteins, periplakin, showed a similar increase in expression levels as suggested by the quantitative proteomic data, whereas Kif14 and vitronectin levels showed only a slight, if any, increase. At present, why there is a discrepancy in the quantitative proteomic data to the western blot data is unknown. Previous work has shown consistency in the correlation between western blot and proteomic values in this dataset, namely Stathmin (Knight et al., 2015), and also a range of cytoskeletal regulatory proteins, such as cortactin, cofilin-1 and Actin-related protein 2/3 complex subunits (Personal communication Prof. A Whitehouse). Although, a caveat of the western blot data was the poor quantity of some of the antibody reagents used. Alternative experiments could be performed to further analyse whether the 3 prioritised proteins are differentially expressed upon MCPyV ST expression or in MCCs. For example, multicolour immunohistochemistry analysis could be performed on formalin-fixed, paraffin-embedded (FFPE) sections of primary MCC tumours. Here sections would be incubated with cytokeratin 20 (CK20), a marker widely used to distinguish MCC as well as the prioritised protein-specific antibodies. Importantly, an isotyped-matched control would also be needed to be included as a negative control. This methodology has been successfully used in the Whitehouse laboratory previously to show higher levels of stathmin expression coincident with CK20 staining in regions of the tumour, suggesting that MCC tumour cells express increased levels of stathmin (Knight et al., 2015).

PPL is a member of the plakin family proteins that serve as epidermal cytolinkers and are components of cell-cell and cell-matrix adhesion complexes. Proteins in this family connect the microfilament, microtubule (MT) and intermediate filament (IF) systems with each other and also connect cell junction complexes to organelle and plasma membranes (Bouameur et al., 2014). They also act as scaffolds and adaptors for signalling proteins that modulate cytoskeletal dynamics. As such, there is an emerging interest in this versatile protein family regarding their functions. Importantly, elucidating a link between periplakin and MCPyV ST-induced changes in cell motility and cytoskeletal proteins may highlight a potential role for periplakin in carcinogenesis, tumour progression, cellular movement or attachment activity.

One set of experiments which should be a priority in the future is to assess the effect of siRNA-mediated depletion of PPL in MCPyV ST-expressing cells. Interestingly, PPL knockdown in pharyngeal squamous cancer cell lines appeared to decrease tumour growth and resulted in accumulation of cells in G2/M phase (Tonoike et al., 2011). Moreover, the PPL knockdown also suppressed cellular movement and attachment suggesting that PPL potentially engages in cellular movement (Tonoike et al., 2011). Therefore, key experiments, upon effective PPL depletion, could be to examine MCPyV ST-induced cell motility by live cell imaging using an Incucyte kinetic live cell imaging system. Cells could be imaged every 30 minutes over a 24 hour period and cell motility tracked using Image J software. Additional motility assays such as a scratch assay and matrigel-based migration and invasion assays could also be performed. Moreover, a cell scatter assay could be performed which measures the dispersion of compact colonies of epithelial cells. Previous results in the Whitehouse laboratory have shown that MCPyV ST-expressing cells have enhanced dispersal rates, which may lead to a more motile and metastatic phenotype. Therefore, due to the potential link between PPL and cell junction complexes, these experiments could be performed in control and MCPyV ST-expressing cells in the presence or absence of PPL. Furthermore, the phenotype of control and MCPyV ST-expressing cells

could be examined using confocal microscopy, comparing PPL expressing and PPL-depleted cells, of particular interest would be to examine the destabilisation of the microtubule network and the potential formation of filopodia, which are both prompted by MCPyV ST expression. In addition, although the initial screening of protein-protein interactions failed to show a direct interaction between MCPyV ST and PPL, this needs to be confirmed due to the low detection level in the input samples of PPL. Considering the extremely large size of the PPL proteins and the efficiency of the immunoblotting transfer, the detection systems might be optimised to reconfirm the possible interactions of MCPyV ST and PPL. If no interaction is observed further investigations might focus on the mechanism by which MCPyV ST enhances PPL expression. One possible mechanism is that PPL upregulation is a result of MCPyV ST dysregulation of cap-dependent translation, through maintenance of the hyperphosphorylated state of the translation initiation factor 4E-BP1.

A similar set of depletion-based experiments could also be performed to assess any possible role of Kif14 in MCPyV ST-expressing cells. Kif14 was shown to directly interact with MCPyV ST using GST-pulldown assays and colocalised with overexpressed Kif14 in the cytoplasm. To date, the role of Kif14 in tumour development is still yet to be fully elucidated. Confusingly overexpression studies of Kif14 either suggest that it may have a role in progression or inhibition of various tumours (Ahmed et al., 2012; Basavarajappa and Corson, 2012; Corson et al., 2005; Hung et al., 2013; Singel et al., 2014; Yang et al., 2014; Yang et al., 2013), whereas knockdown of the Kif14 leads to the progression of tumour development by formation of binucleated cells resulting from cytokinesis failure (Carleton et al., 2006a; Gruneberg et al., 2006b; Zhu et al., 2005). As such, examining the link between Kif14 and MCPyV ST may help to resolve these questions.

In other hand, unfortunately, results examining a possible link with MCPyV ST and vitronectin failed to showed any differential expression levels or

possible interactions through our initial screening. Therefore, work on vitronectin would not be a priority in the future.

Chapters 4 and 5 focussed on examining the possible effects of MCPyV truncated LT (tLT) expression of the cellular proteome. Polyomavirus LT antigens are large, multifunctional proteins involved in viral genome replication and are also capable of manipulating multiple host cell pathways through numerous protein-protein interactions. For example, the widely studied SV40 LT protein coordinates viral DNA replication during a productive life cycle by instigating dynamic interactions with cellular DNA replication factors (Topalis et al., 2013). Moreover, the multifunctionality of SV40 LT is demonstrated through interactions with various cellular targets including pRb, p53 and Hsc70 (Saenz-Robles et al., 2001). For instance, cellular proliferation induced by SV40 involves binding and inhibition of pRb function, thus triggering E2F-dependent expression (Rathi et al., 2009). Similar to SV40, MCPyV LT also possess several conserved domains; such as the pRb binding, DNA binding and helicase domains, however MCPyV also possess an unique region (MUR). This unique LT region is responsible for interacting with the host cellular factor Vam6p and also encodes a viral miRNA (Liu et al., 2011b; Seo et al., 2009).

The widely characterised signature feature of MCPyV-positive MCC is the presence of mutations in LT. These mutations prematurely truncate the LT protein at the C-terminus, rendering the integrated viral genome replication defective (Shuda et al., 2008). There are proposed reasons for the generation of these mutations; firstly to prevent unlicensed viral gene replication or secondly the mutations are caused by selective pressure by the host upon cell transformation. Specifically, the MCPyV LT C-terminus has recently been shown to have an inhibitory effect upon growth and also to activate the cellular DNA damage response (Cheng et al., 2013). Therefore, the aim of chapters 4 and 5 were to assess what effect truncated LT protein expression had upon the host cell proteome. Moreover, this research may highlight novel avenues for future therapeutic intervention of MCC.

Therefore to explore the effects on the cellular proteome upon MCPyV tLT expression, high throughput unbiased quantitative SILAC-based proteomic analysis was conducted to identify differentially expressed host cell proteins and pathways regulated by MCPyV tLT expression. SILAC-based analysis coupled with LC-MS/MS and subsequent downstream bioinformatic analysis has been established as a highly informative tool to study virus-host interactions (Munday et al., 2012). Through this approach, my results identified that a large number of cellular differentially expressed proteins were downregulated at least two-fold. This was a rather surprising result but consistent downregulation of cellular proteins was observed in both cytoplasmic and nuclear fractions. The reason why so many cellular proteins were downregulated upon expression of MCPyV tLT is yet to be determined. Interestingly however, among the tLT-effected pathways, the ubiquitin-proteosomal degradation pathway is upregulated and thus may provide a logical explanation for the large number of downregulated cellular proteins upon tLT expression. Notably, other DNA viruses like human papillomavirus (HPV) encode oncoproteins, such as E6 and E7, can induce proteolysis of host cell tumour suppressor proteins p53 and pRb through the ubiquitin-proteosome pathway (Boyer et al., 1996; Scheffner et al., 1990). In addition, a number of herpesviruses can induce proteasome-dependent degradation of complete nuclear organelles, such as promyelocytic leukemia (PML) nuclear bodies (Chelbi-Alix and de The, 1999), which is thought to prevent PML inducing an antiviral and anti-proliferation; interferon (IFN)-mediated response (Chelbi-Alix et al., 1998). Conversely, MCPyV ST is found to inhibit MCPyV LT degradation by inhibiting the function of the cellular SCF(Fbw7) E3 ligase (Kwun et al., 2013).

We believe this is the first observation that MCPyV tLT may affect ubiquitin-proteasome degradation pathways. Considering this surprising result and the numerous cellular proteins that were downregulated in MCPyV tLT expressing cells, further work must be performed to confirm the link

between MCPyV tLT and ubiquitin-mediated degradation. A first key experiment would be to determine whether tLT-mediated degradation could occur in the presence of the proteasome inhibitor, MG132. Here, HEK 293 cells could be transfected with GFP or GFP-tLT expression constructs in the absence and presence of MG132, added to the cell media 12 hours post-transfection. The cell lysates could then be subjected to SDS-PAGE and subsequent immunoblotting with a range of antibodies to cellular proteins which were suggested to be downregulated upon tLT expression. It would also be of interest to determine where this downregulation is specific to the tLT construct compared to the full length LT. In addition, to confirm that the observed proteasomal degradation of host cell proteins in the presence of tLT is directly related to ubiquitin-mediated degradation pathways, immunoblotting could also be performed using ubiquitin-specific antibodies to determine the presence of a ladder of ubiquitinated target-protein species upon MCPyV truncated LT expression.

Bioinformatic analysis also showed dysregulation of other cellular pathways upon MCPyV truncated LT (tLT) expression, namely cell cycle alteration and cell proliferation, apoptosis and cell survival and cell-cell contacts. Following identification of these pathways, the focus of chapter 5 was to confirm the proteomic dataset using a range of assays including cell cycle analysis, cell growth and proliferation and apoptosis assays. Results demonstrated that MCPyV tLT expression altered cell cycle progression. Taking into consideration previous work on other polyomavirus LT proteins, such as SV40, it is likely that this cell cycle control is due to the interaction of LT with the tumour suppressor protein, pRb. pRb is responsible for a major G1 checkpoint to block early S-phase entry and cell growth (Weinberg, 1995). This correlates with our analysis, whereby expression of MCPyV tLT results in a slight accumulation of the cell population in S-phase. In addition, we also discovered that CDK2 and cyclin A were slightly elevated. Binding and interaction of CDK2 and cyclin A is essential for DNA replication and promotes host cell G1/S transition (Hartwell and Kastan, 1994); which may related to the cell proliferative activity of MCPyV tLT.

Interestingly, several other proteins which regulate the cell cycle where identified in the MCPyV tLT-proteomic dataset which merit further investigation, in particular components of anaphase-promoting complex/cyclosome (APC/C) and S-phase kinase associated protein 2 (Skp2). Skp2 can form a complex with the cyclin A-CDK2 complex and specifically target cell cycle control elements, such as p27 for ubiquitin degradation (Carrano et al., 1999). Skp2 is also suggested to act as proto-oncogene, as overexpression of Skp2 is frequently detected in various human cancers (Chan et al., 2010). Elevation of Skp2 by 11-fold in MCPyV tLT expressing cells indicates that Skp2 might play an important role in MCC tumourigenesis. Notably, inactivation of Skp2 restricts cancer development by triggering a cellular senescence and/or apoptosis response *in vivo* (Lin et al., 2010). Interestingly, recent studies have identified a specific Skp2 inhibitor, SZL-P1-41, using high-throughput in silico screening of large and diverse chemical libraries (Chan et al., 2013). This Skp2 inhibitor, which binds to Skp2 and suppresses Skp2 E3 ligase activity, exhibits potent antitumour activities in multiple animal models and cooperates with chemotherapeutic agents to reduce cancer cell survival. Therefore, it would be of major interest to determine whether SZL-P1-41 is a promising therapeutic compound for MCPyV-induced MCC. Similarly, components of the anaphase promoting complex/cyclosome (APC/C) were also elevated in the MCPyV tLT-proteomic dataset. The APC/C is a 13-subunit ubiquitin ligase protein complex that controls the cell cycle. Small molecule inhibitors of the APC/C called proTAME and apcin, have recently been discovered. ProTAME is a cell permeable prodrug that is converted to TAME (Tosyl-L-Arginine Methyl Ester) by intracellular esterases. TAME structurally mimics the IR-tail of the co-activators and therefore binds to APC/C, blocking the interaction of cell civision cycle 20 (Cdc20) or Cadherin-1(Cdh1) proteins with the APC/C (Zeng et al., 2010). Apcin is a small molecule that prevents substrate recognition by binding to Cdc20 (Sackton et al., 2014). Again, it would be of interest to determine if these small molecules have therapeutic potential against MCC.

The apoptosis inducing experiments showed that upon treatment with staurosporine or etoposide, MCPyV tLT may possess a specific capability to delay the apoptotic cascade, but results suggest that it was not fully capable to inhibit apoptosis. However, the true potential of tLT as a pro-survival factor in these experiments may not have been highlighted, due to the high potency of these apoptotic-inducing compounds. Therefore, to fully address the pro-survival properties of MCPyV tLT, these experiments could be repeated with a greater concentration range of staurosporine or etoposide or using alternative apoptotic-inducing stimuli, such as bleomycin or cisplatin. Interestingly, it may be the case that MCPyV tLT can target multiple stages/proteins in the apoptotic cascade. Firstly, it has previous been shown that tLT targets survivin, an inhibitor for apoptosis and found to be upregulated in various lymphoma and metastatic melanomas (Ambrosini et al., 1997). It is believed that survivin functions to inhibit apoptosis by prolonging cell viability, which eventually leads to cellular transformation. Secondly, results from the MCPyV tLT-proteomic dataset, generated in Chapter 4, suggest that MCPyV tLT also targets the pro-apoptotic protein, BCL-2-associated death promoter (BAD). BAD was found to be downregulated upon expression of MCPyV tLT in the SILAC dataset which was confirmed by immunoblot analysis. The reduction of BAD by RNA interference (RNAi) has also been shown to prevent apoptosis in PTEN-deficient tumour cells (She et al., 2005). In regards of this evidence, further work on the mechanism of how tLT downregulates BAD merits investigation.

BAD induces apoptosis by inhibiting anti-apoptotic BCL-2-family members, namely BCL-x and BCL-2; thereby allowing other pro-apoptotic proteins, such as BAK and BAX, to aggregate and induce release of cytochrome c, followed by caspase activation and apoptosis. The pro-apoptotic activity of BAD is regulated through its phosphorylation. Only the non-phosphorylated form of BAD heterodimerizes with BCL-xl or BCL-2, whereas phosphorylated BAD is sequestered and inactivated/degraded in the cytosol by binding to 14-3-3. Therefore, possible mechanisms by which tLT may downregulate bad activity could be investigated. For example, does

tLT bind BAD, preventing its heterodimerisation potential with BCL-xl or BCL-2. Alternatively does expression of tLT affect its phosphorylation status by enhancing the activity of kinases which are known to phosphorylate BAD, such as Pim-2 kinase, protein kinase A and PI 3-kinase.

Finally, bioinformatic data presented also highlighted cell-cell connection related pathways such as cell junctions, integrin signalling, and regulation of actin cytoskeleton. In contrast with MCPyV ST analysis discussed earlier, many of the proteins within these associated pathways were detected to be downregulated upon expression of MCPyV tLT. This indicates that the tLT may play a different role to ST in relation to cell motility and migration. Moreover, expression of tLT failed to enhance cell motility as observed in the scratch wound assay, in contrast with cells expressing MCPyV ST. To further investigate the link between MCPyV tLT function and cell-cell connections, we first chose to examine the zona occuldens protein, ZO-1; a tight junction-related protein. Tight junctions have been shown to be involved in the control of cellular proliferation and differentiation, whereby loss of the tight junction can lead to invasion and metastasis of cancer cells (Martin and Jiang, 2009). Here, tight junctions function as the barrier in adhesive to prevent cell dissociation (Hollande et al., 2001). Overcoming the tight junction barrier is an important step for a cancer cell to metastasize. Our downstream analysis on ZO-1 showed contradictory results compared to the proteomic dataset, although immunofluorescences studies were inconclusive due to poor antibody staining. The overexpression of ZO-1 also failed to show any cell-cell connection staining as expected. Therefore, other cell-cell connections component, namely β-catenin were selected and results showed that MCPyV tLT expression was capable of downregulating the cell-cell barrier. Initial work using immunofluorescence studies showed significant changes in the distribution and intensity of β-catenin staining upon tLT expression, suggesting the possible break-down and re-organisation of cell junctions. Further work on this protein and other cell junction components is now required to fully elucidate whether MCPyV tLT functions in cell junction

break-down and which signalling complexes are involved. Moreover, it would also be of interest to determine whether tLT acts in synergy with the MCPyV ST in this function.

In summary, results presented herein expand our current understanding on the effects of MCPyV ST and tLT antigens on the host cell proteome. These results may help to identify possible functions and binding partners of the MCPyV T antigens. Moreover, this information, in the longer term, may highlight potential therapeutic targets for the treatment of MCPyV-induced MCC.

List of References

Abbas, T., and Dutta, A. (2009). p21 in cancer: intricate networks and multiple activities. Nat Rev Cancer *9*, 400-414.

Afanasiev, O.K., Yelistratova, L., Miller, N., Nagase, K., Paulson, K., Iyer, J.G., Ibrani, D., Koelle, D.M., and Nghiem, P. (2013). Merkel polyomavirus-specific T cells fluctuate with merkel cell carcinoma burden and express therapeutically targetable PD-1 and Tim-3 exhaustion markers. Clin Cancer Res *19*, 5351-5360.

Agelli, M., and Clegg, L.X. (2003). Epidemiology of primary Merkel cell carcinoma in the United States. J Am Acad Dermatol *49*, 832-841.

Agelli, M., Clegg, L.X., Becker, J.C., and Rollison, D.E. (2010). The etiology and epidemiology of merkel cell carcinoma. Curr Probl Cancer *34*, 14-37.

Ahmed, S.M., Theriault, B.L., Uppalapati, M., Chiu, C.W., Gallie, B.L., Sidhu, S.S., and Angers, S. (2012). KIF14 negatively regulates Rap1a-Radil signaling during breast cancer progression. J Cell Biol *199*, 951-967.

Ahuja, D., Saenz-Robles, M.T., and Pipas, J.M. (2005). SV40 large T antigen targets multiple cellular pathways to elicit cellular transformation. Oncogene *24*, 7729-7745.

Aijaz, S., Balda, M.S., and Matter, K. (2006). Tight junctions: molecular architecture and function. Int Rev Cytol *248*, 261-298.

Albores-Saavedra, J., Batich, K., Chable-Montero, F., Sagy, N., Schwartz, A.M., and Henson, D.E. (2010). Merkel cell carcinoma demographics, morphology, and survival based on 3870 cases: a population based study. J Cutan Pathol *37*, 20-27.

Aleem, E., Kiyokawa, H., and Kaldis, P. (2005). Cdc2-cyclin E complexes regulate the G1/S phase transition. Nat Cell Biol *7*, 831-836.

Ali, S.H., Kasper, J.S., Arai, T., and DeCaprio, J.A. (2004). Cul7/p185/p193 binding to simian virus 40 large T antigen has a role in cellular transformation. J Virol *78*, 2749-2757.

Allander, T., Andreasson, K., Gupta, S., Bjerkner, A., Bogdanovic, G., Persson, M.A., Dalianis, T., Ramqvist, T., and Andersson, B. (2007). Identification of a third human polyomavirus. Journal of virology *81*, 4130-4136.

Ambrosini, G., Adida, C., and Altieri, D.C. (1997). A novel anti-apoptosis gene, survivin, expressed in cancer and lymphoma. Nat Med *3*, 917-921.

An, P., Saenz Robles, M.T., and Pipas, J.M. (2012). Large T antigens of polyomaviruses: amazing molecular machines. Annu Rev Microbiol *66*, 213-236.

Andres, C., Ihrler, S., Puchta, U., and Flaig, M.J. (2009). Merkel cell polyomavirus is prevalent in a subset of small cell lung cancer: a study of 31 patients. Thorax *64*, 1007-1008.

Arora, R., Shuda, M., Guastafierro, A., Feng, H., Toptan, T., Tolstov, Y., Normolle, D., Vollmer, L.L., Vogt, A., Domling, A.*, et al.* (2012a). Survivin is a therapeutic target in Merkel cell carcinoma. Sci Transl Med *4*, 133ra156.

Arora, R., Shuda, M., Guastafierro, A., Feng, H., Toptan, T., Tolstov, Y., Normolle, D., Vollmer, L.L., Vogt, A., Domling, A.*, et al.* (2012b). Survivin is a therapeutic target in Merkel cell carcinoma. Science translational medicine *4*, 133ra156.

Bagga, S., and Bouchard, M.J. (2014). Cell cycle regulation during viral infection. Methods Mol Biol *1170*, 165-227.

Basavarajappa, H.D., and Corson, T.W. (2012). KIF14 as an oncogene in retinoblastoma: a target for novel therapeutics? Future Med Chem *4*, 2149-2152.

Bates, S., Phillips, A.C., Clark, P.A., Stott, F., Peters, G., Ludwig, R.L., and Vousden, K.H. (1998). p14ARF links the tumour suppressors RB and p53. Nature *395*, 124-125.

Beavon, I.R. (2000). The E-cadherin-catenin complex in tumour metastasis: structure, function and regulation. Eur J Cancer *36*, 1607-1620.

Becker, J.C. (2010). Merkel cell carcinoma. Ann Oncol *21 Suppl 7*, vii81-85.

Becker, J.C., Schrama, D., and Houben, R. (2009). Merkel cell carcinoma. Cell Mol Life Sci *66*, 1-8.

Belmokhtar, C.A., Hillion, J., and Segal-Bendirdjian, E. (2001). Staurosporine induces apoptosis through both caspase-dependent and caspase-independent mechanisms. Oncogene *20*, 3354-3362.

Benjamin, D.I., Louie, S.M., Mulvihill, M.M., Kohnz, R.A., Li, D.S., Chan, L.G., Sorrentino, A., Bandyopadhyay, S., Cozzo, A., Ohiri, A.*, et al.* (2014). Inositol phosphate recycling regulates glycolytic and lipid metabolism that drives cancer aggressiveness. ACS Chem Biol *9*, 1340-1350.

Bichakjian, C.K., Lowe, L., Lao, C.D., Sandler, H.M., Bradford, C.R., Johnson, T.M., and Wong, S.L. (2007). Merkel cell carcinoma: critical review with guidelines for multidisciplinary management. Cancer *110*, 1-12.

Bikel, I., and Loeken, M.R. (1992). Involvement of simian virus 40 (SV40) small t antigen in trans activation of SV40 early and late promoters. Journal of virology *66*, 1489-1494.

Bikel, I., Montano, X., Agha, M.E., Brown, M., McCormack, M., Boltax, J., and Livingston, D.M. (1987). SV40 small t antigen enhances the transformation activity of limiting concentrations of SV40 large T antigen. Cell *48*, 321-330.

Bollag, B., Chuke, W.F., and Frisque, R.J. (1989). Hybrid genomes of the polyomaviruses JC virus, BK virus, and simian virus 40: identification of sequences important for efficient transformation. J Virol *63*, 863-872.

Bollag, B., Prins, C., Snyder, E.L., and Frisque, R.J. (2000). Purified JC virus T and T' proteins differentially interact with the retinoblastoma family of tumor suppressor proteins. Virology *274*, 165-178.

Borchert, S., Czech-Sioli, M., Neumann, F., Schmidt, C., Wimmer, P., Dobner, T., Grundhoff, A., and Fischer, N. (2014). High-affinity Rb binding, p53 inhibition, subcellular localization, and transformation by wild-type or tumor-derived shortened Merkel cell polyomavirus large T antigens. J Virol *88*, 3144-3160.

Bouameur, J.E., Favre, B., and Borradori, L. (2014). Plakins, a versatile family of cytolinkers: roles in skin integrity and in human diseases. J Invest Dermatol *134*, 885-894.

Boyer, S.N., Wazer, D.E., and Band, V. (1996). E7 protein of human papilloma virus-16 induces degradation of retinoblastoma protein through the ubiquitin-proteasome pathway. Cancer research *56*, 4620-4624.

Boyne, J.R., and Whitehouse, A. (2006). Nucleolar trafficking is essential for nuclear export of intronless herpesvirus mRNA. Proc Natl Acad Sci U S A *103*, 15190-15195.

Buck, C.B., Phan, G.Q., Raiji, M.T., Murphy, P.M., McDermott, D.H., and McBride, A.A. (2012). Complete genome sequence of a tenth human polyomavirus. J Virol *86*, 10887.

Cairns, R.A., Harris, I.S., and Mak, T.W. (2011). Regulation of cancer cell metabolism. Nat Rev Cancer *11*, 85-95.

Campanero-Rhodes, M.A., Smith, A., Chai, W., Sonnino, S., Mauri, L., Childs, R.A., Zhang, Y., Ewers, H., Helenius, A., Imberty, A.*, et al.* (2007). N-glycolyl GM1 ganglioside as a receptor for simian virus 40. J Virol *81*, 12846-12858.

Carleton, M., Mao, M., Biery, M., Warrener, P., Kim, S., Buser, C., Marshall, C.G., Fernandes, C., Annis, J., and Linsley, P.S. (2006a). RNA interference-mediated silencing of mitotic kinesin KIF14 disrupts cell cycle progression and induces cytokinesis failure. Mol Cell Biol *26*, 3853-3863.

Carleton, M., Mao, M., Biery, M., Warrener, P., Kim, S., Buser, C., Marshall, C.G., Fernandes, C., Annis, J., and Linsley, P.S. (2006b). RNA interference-mediated silencing of mitotic kinesin KIF14 disrupts cell cycle progression and induces cytokinesis failure. Mol Cell Biol *26*, 3853-3863.

Carrano, A.C., Eytan, E., Hershko, A., and Pagano, M. (1999). SKP2 is required for ubiquitin-mediated degradation of the CDK inhibitor p27. Nat Cell Biol *1*, 193-199.

Carter, J.J., Daugherty, M.D., Qi, X., Bheda-Malge, A., Wipf, G.C., Robinson, K., Roman, A., Malik, H.S., and Galloway, D.A. (2013). Identification of an overprinting gene in Merkel cell polyomavirus provides evolutionary insight into the birth of viral genes. Proc Natl Acad Sci U S A *110*, 12744-12749.

Cavallaro, U., and Christofori, G. (2004). Cell adhesion and signalling by cadherins and Ig-CAMs in cancer. Nat Rev Cancer *4*, 118-132.

Chan, C.H., Lee, S.W., Wang, J., and Lin, H.K. (2010). Regulation of Skp2 expression and activity and its role in cancer progression. ScientificWorldJournal *10*, 1001-1015.

Chan, C.H., Morrow, J.K., Li, C.F., Gao, Y., Jin, G., Moten, A., Stagg, L.J., Ladbury, J.E., Cai, Z., Xu, D.*, et al.* (2013). Pharmacological inactivation of Skp2 SCF ubiquitin ligase restricts cancer stem cell traits and cancer progression. Cell *154*, 556-568.

Chau, B.N., and Wang, J.Y. (2003). Coordinated regulation of life and death by RB. Nat Rev Cancer *3*, 130-138.

Chedotal, A., Kerjan, G., and Moreau-Fauvarque, C. (2005). The brain within the tumor: new roles for axon guidance molecules in cancers. Cell Death Differ *12*, 1044-1056.

Chelbi-Alix, M.K., and de The, H. (1999). Herpes virus induced proteasome-dependent degradation of the nuclear bodies-associated PML and Sp100 proteins. Oncogene *18*, 935-941.

Chelbi-Alix, M.K., Quignon, F., Pelicano, L., Koken, M.H., and de The, H. (1998). Resistance to virus infection conferred by the interferon-induced promyelocytic leukemia protein. J Virol *72*, 1043-1051.

Chen, S., and Paucha, E. (1990). Identification of a region of simian virus 40 large T antigen required for cell transformation. J Virol *64*, 3350-3357.

Chenciner, N., Meneguzzi, G., Corallini, A., Grossi, M.P., Grassi, P., Barbanti-Brodano, G., and Milanesi, G. (1980). Integrated and free viral DNA in hamster tumors induced by BK virus. Proc Natl Acad Sci U S A *77*, 975-979.

Cheng, E.H., Nicholas, J., Bellows, D.S., Hayward, G.S., Guo, H.G., Reitz, M.S., and Hardwick, J.M. (1997). A Bcl-2 homolog encoded by Kaposi sarcoma-associated virus, human herpesvirus 8, inhibits apoptosis but does not heterodimerize with Bax or Bak. Proc Natl Acad Sci U S A *94*, 690-694.

Cheng, J., Rozenblatt-Rosen, O., Paulson, K.G., Nghiem, P., and DeCaprio, J.A. (2013). Merkel cell polyomavirus large T antigen has growth-promoting and inhibitory activities. J Virol *87*, 6118-6126.

Chesters, P.M., Heritage, J., and McCance, D.J. (1983). Persistence of DNA sequences of BK virus and JC virus in normal human tissues and in diseased tissues. J Infect Dis *147*, 676-684.

Comerford, S.A., Schultz, N., Hinnant, E.A., Klapproth, S., and Hammer, R.E. (2012). Comparative analysis of SV40 17kT and LT function in vivo demonstrates that LT's C-terminus re-programs hepatic gene expression and is necessary for tumorigenesis in the liver. Oncogenesis *1*, e28.

Conkright, M.D., and Montminy, M. (2005). CREB: the unindicted cancer co-conspirator. Trends Cell Biol *15*, 457-459.

Corson, T.W., Huang, A., Tsao, M.S., and Gallie, B.L. (2005). KIF14 is a candidate oncogene in the 1q minimal region of genomic gain in multiple cancers. Oncogene *24*, 4741-4753.

Cox, J., and Mann, M. (2008). MaxQuant enables high peptide identification rates, individualized p.p.b.-range mass accuracies and proteome-wide protein quantification. Nat Biotechnol *26*, 1367-1372.

Craig, N.L. (1988). The mechanism of conservative site-specific recombination. Annu Rev Genet *22*, 77-105.

D'Souza, B., Rowe, M., and Walls, D. (2000). The bfl-1 gene is transcriptionally upregulated by the Epstein-Barr virus LMP1, and its expression promotes the survival of a Burkitt's lymphoma cell line. J Virol *74*, 6652-6658.

Daniels, R., Sadowicz, D., and Hebert, D.N. (2007). A very late viral protein triggers the lytic release of SV40. PLoS Pathog *3*, e98.

Dean, F.B., Bullock, P., Murakami, Y., Wobbe, C.R., Weissbach, L., and Hurwitz, J. (1987). Simian virus 40 (SV40) DNA replication: SV40 large T antigen unwinds DNA containing the SV40 origin of replication. Proc Natl Acad Sci U S A *84*, 16-20.

DeCaprio, J.A. (2009). How the Rb tumor suppressor structure and function was revealed by the study of Adenovirus and SV40. Virology *384*, 274-284.

DeCaprio, J.A., and Garcea, R.L. (2013). A cornucopia of human polyomaviruses. Nat Rev Microbiol *11*, 264-276.

DeCaprio, J.A., Ludlow, J.W., Figge, J., Shew, J.Y., Huang, C.M., Lee, W.H., Marsilio, E., Paucha, E., and Livingston, D.M. (1988). SV40 large tumor antigen forms a specific complex with the product of the retinoblastoma susceptibility gene. Cell *54*, 275-283.

Demetriou, S.K., Ona-Vu, K., Sullivan, E.M., Dong, T.K., Hsu, S.W., and Oh, D.H. (2012). Defective DNA repair and cell cycle arrest in cells expressing Merkel cell polyomavirus T antigen. Int J Cancer *131*, 1818-1827.

Dias, D.C., Dolios, G., Wang, R., and Pan, Z.Q. (2002). CUL7: A DOC domain-containing cullin selectively binds Skp1.Fbx29 to form an SCF-like complex. Proc Natl Acad Sci U S A *99*, 16601-16606.

DiColandrea, T., Karashima, T., Maatta, A., and Watt, F.M. (2000). Subcellular distribution of envoplakin and periplakin: insights into their role as precursors of the epidermal cornified envelope. J Cell Biol *151*, 573-586.

Dornreiter, I., Hoss, A., Arthur, A.K., and Fanning, E. (1990). SV40 T antigen binds directly to the large subunit of purified DNA polymerase alpha. Embo J *9*, 3329-3336.

Dusek, R.L., and Attardi, L.D. (2011). Desmosomes: new perpetrators in tumour suppression. Nat Rev Cancer *11*, 317-323.

Dyson, N., Bernards, R., Friend, S.H., Gooding, L.R., Hassell, J.A., Major, E.O., Pipas, J.M., Vandyke, T., and Harlow, E. (1990). Large T antigens of many polyomaviruses are able to form complexes with the retinoblastoma protein. J Virol *64*, 1353-1356.

Egli, A., Infanti, L., Dumoulin, A., Buser, A., Samaridis, J., Stebler, C., Gosert, R., and Hirsch, H.H. (2009). Prevalence of polyomavirus BK and JC infection and replication in 400 healthy blood donors. J Infect Dis *199*, 837-846.

Elgui de Oliveira, D. (2007). DNA viruses in human cancer: an integrated overview on fundamental mechanisms of viral carcinogenesis. Cancer Lett *247*, 182-196.

Enam, S., Del Valle, L., Lara, C., Gan, D.D., Ortiz-Hidalgo, C., Palazzo, J.P., and Khalili, K. (2002). Association of human polyomavirus JCV with colon cancer: evidence for interaction of viral T-antigen and beta-catenin. Cancer Res *62*, 7093-7101.

Evans, T., Rosenthal, E.T., Youngblom, J., Distel, D., and Hunt, T. (1983). Cyclin: a protein specified by maternal mRNA in sea urchin eggs that is destroyed at each cleavage division. Cell *33*, 389-396.

Farquhar, M.G., and Palade, G.E. (1963). Junctional complexes in various epithelia. J Cell Biol *17*, 375-412.

Fehr, A.R., Gualberto, N.C., Savaryn, J.P., Terhune, S.S., and Yu, D. (2012). Proteasome-dependent disruption of the E3 ubiquitin ligase anaphase-promoting complex by HCMV protein pUL21a. PLoS Pathog *8*, e1002789.

Fehr, A.R., and Yu, D. (2013). Control the host cell cycle: viral regulation of the anaphase-promoting complex. J Virol *87*, 8818-8825.

Felding-Habermann, B., and Cheresh, D.A. (1993). Vitronectin and its receptors. Curr Opin Cell Biol *5*, 864-868.

Feng, H., Kwun, H.J., Liu, X., Gjoerup, O., Stolz, D.B., Chang, Y., and Moore, P.S. (2011). Cellular and viral factors regulating Merkel cell polyomavirus replication. PLoS One *6*, e22468.

Feng, H., Shuda, M., Chang, Y., and Moore, P.S. (2008). Clonal integration of a polyomavirus in human Merkel cell carcinoma. Science *319*, 1096-1100.

Fero, M.L., Randel, E., Gurley, K.E., Roberts, J.M., and Kemp, C.J. (1998). The murine gene p27Kip1 is haplo-insufficient for tumour suppression. Nature *396*, 177-180.

Fliss, P.M., Jowers, T.P., Brinkmann, M.M., Holstermann, B., Mack, C., Dickinson, P., Hohenberg, H., Ghazal, P., and Brune, W. (2012). Viral mediated redirection of NEMO/IKKgamma to autophagosomes curtails the inflammatory cascade. PLoS Pathog *8*, e1002517.

Fluck, M.M., and Schaffhausen, B.S. (2009). Lessons in signaling and tumorigenesis from polyomavirus middle T antigen. Microbiol Mol Biol Rev *73*, 542-563, Table of Contents.

Flynn, A., and Proud, C.G. (1996). The role of eIF4 in cell proliferation. Cancer Surv *27*, 293-310.

Fries, K.L., Miller, W.E., and Raab-Traub, N. (1996). Epstein-Barr virus latent membrane protein 1 blocks p53-mediated apoptosis through the induction of the A20 gene. J Virol *70*, 8653-8659.

Fulda, S. (2010). Cell death and survival signaling in oncogenesis. Klin Padiatr *222*, 340-344.

Galluzzi, L., Morselli, E., Kepp, O., Vitale, I., Rigoni, A., Vacchelli, E., Michaud, M., Zischka, H., Castedo, M., and Kroemer, G. (2010). Mitochondrial gateways to cancer. Mol Aspects Med *31*, 1-20.

Gan, D.D., Reiss, K., Carrill, T., Del Valle, L., Croul, S., Giordano, A., Fishman, P., and Khalili, K. (2001). Involvement of Wnt signaling pathway in murine medulloblastoma induced by human neurotropic JC virus. Oncogene *20*, 4864-4870.

Gardner, S.D., Field, A.M., Coleman, D.V., and Hulme, B. (1971). New human papovavirus (B.K.) isolated from urine after renal transplantation. Lancet *1*, 1253-1257.

Gaynor, A.M., Nissen, M.D., Whiley, D.M., Mackay, I.M., Lambert, S.B., Wu, G., Brennan, D.C., Storch, G.A., Sloots, T.P., and Wang, D. (2007). Identification of a novel polyomavirus from patients with acute respiratory tract infections. PLoS pathogens *3*, e64.

Gillespie, K.A., Mehta, K.P., Laimins, L.A., and Moody, C.A. (2012). Human papillomaviruses recruit cellular DNA repair and homologous recombination factors to viral replication centers. J Virol *86*, 9520-9526.

Griffiths, D.A., Abdul-Sada, H., Knight, L.M., Jackson, B.R., Richards, K., Prescott, E.L., Peach, A.H., Blair, G.E., Macdonald, A., and Whitehouse, A. (2013). Merkel cell polyomavirus small T antigen targets the NEMO adaptor protein to disrupt inflammatory signaling. J Virol *87*, 13853-13867.

Gruneberg, U., Neef, R., Li, X., Chan, E.H., Chalamalasetty, R.B., Nigg, E.A., and Barr, F.A. (2006a). KIF14 and citron kinase act together to promote efficient cytokinesis. J Cell Biol *172*, 363-372.

Gruneberg, U., Neef, R., Li, X., Chan, E.H., Chalamalasetty, R.B., Nigg, E.A., and Barr, F.A. (2006b). KIF14 and citron kinase act together to promote efficient cytokinesis. J Cell Biol *172*, 363-372.

Gupta, S.G., Wang, L.C., Penas, P.F., Gellenthin, M., Lee, S.J., and Nghiem, P. (2006). Sentinel lymph node biopsy for evaluation and treatment of patients with Merkel cell carcinoma: The Dana-Farber experience and meta-analysis of the literature. Arch Dermatol *142*, 685-690.

Hahn, W.C., Dessain, S.K., Brooks, M.W., King, J.E., Elenbaas, B., Sabatini, D.M., DeCaprio, J.A., and Weinberg, R.A. (2002). Enumeration of the simian virus 40 early region elements necessary for human cell transformation. Mol Cell Biol *22*, 2111-2123.

Han, A.C., Soler, A.P., Tang, C.K., Knudsen, K.A., and Salazar, H. (2000). Nuclear localization of E-cadherin expression in Merkel cell carcinoma. Arch Pathol Lab Med *124*, 1147-1151.

Hanahan, D., and Weinberg, R.A. (2000). The hallmarks of cancer. Cell *100*, 57-70.

Hanahan, D., and Weinberg, R.A. (2011). Hallmarks of cancer: the next generation. Cell *144*, 646-674.

Hara, H., and Kaji, H. (1987). Random integration of SV40 in SV40-transformed, immortalized human fibroblasts. Exp Cell Res *168*, 531-538.

Harburg, G.C., and Hinck, L. (2011). Navigating breast cancer: axon guidance molecules as breast cancer tumor suppressors and oncogenes. J Mammary Gland Biol Neoplasia *16*, 257-270.

Harris, K.F., Christensen, J.B., Radany, E.H., and Imperiale, M.J. (1998). Novel mechanisms of E2F induction by BK virus large-T antigen: requirement of both the pRb-binding and the J domains. Mol Cell Biol *18*, 1746-1756.

Harrison, C.J., Meinke, G., Kwun, H.J., Rogalin, H., Phelan, P.J., Bullock, P.A., Chang, Y., Moore, P.S., and Bohm, A. (2011). Asymmetric assembly of Merkel cell polyomavirus large T-antigen origin binding domains at the viral origin. J Mol Biol *409*, 529-542.

Hartsock, A., and Nelson, W.J. (2008). Adherens and tight junctions: structure, function and connections to the actin cytoskeleton. Biochim Biophys Acta *1778*, 660-669.

Hartwell, L.H., and Kastan, M.B. (1994). Cell cycle control and cancer. Science *266*, 1821-1828.

Hartwell, L.H., and Weinert, T.A. (1989). Checkpoints: controls that ensure the order of cell cycle events. Science *246*, 629-634.

He, Y., Xu, K., Keiner, B., Zhou, J., Czudai, V., Li, T., Chen, Z., Liu, J., Klenk, H.D., Shu, Y.L.*, et al.* (2010). Influenza A virus replication induces cell cycle arrest in G0/G1 phase. J Virol *84*, 12832-12840.

Henderson, S., Huen, D., Rowe, M., Dawson, C., Johnson, G., and Rickinson, A. (1993). Epstein-Barr virus-coded BHRF1 protein, a viral homologue of Bcl-2, protects human B cells from programmed cell death. Proc Natl Acad Sci U S A *90*, 8479-8483.

Henderson, S., Rowe, M., Gregory, C., Croom-Carter, D., Wang, F., Longnecker, R., Kieff, E., and Rickinson, A. (1991). Induction of bcl-2 expression by Epstein-Barr virus latent membrane protein 1 protects infected B cells from programmed cell death. Cell *65*, 1107-1115.

Hirai, K., Lehman, J., and Defendi, V. (1971). Integration of simian virus 40 deoxyribonucleic acid into the deoxyribonucleic acid of primary infected Chinese hamster cells. J Virol *8*, 708-715.

Hochstrasser, M. (2009). Origin and function of ubiquitin-like proteins. Nature *458*, 422-429.

Hollande, F., Blanc, E.M., Bali, J.P., Whitehead, R.H., Pelegrin, A., Baldwin, G.S., and Choquet, A. (2001). HGF regulates tight junctions in new nontumorigenic gastric epithelial cell line. Am J Physiol Gastrointest Liver Physiol *280*, G910-921.

Houben, R., Adam, C., Baeurle, A., Hesbacher, S., Grimm, J., Angermeyer, S., Henzel, K., Hauser, S., Elling, R., Brocker, E.B.*, et al.* (2012). An intact retinoblastoma protein-binding site in Merkel cell polyomavirus large T antigen is required for promoting growth of Merkel cell carcinoma cells. Int J Cancer *130*, 847-856.

Houben, R., Shuda, M., Weinkam, R., Schrama, D., Feng, H., Chang, Y., Moore, P.S., and Becker, J.C. (2010a). Merkel cell polyomavirus-infected Merkel cell carcinoma cells require expression of viral T antigens. J Virol *84*, 7064-7072.

Houben, R., Shuda, M., Weinkam, R., Schrama, D., Feng, H., Chang, Y., Moore, P.S., and Becker, J.C. (2010b). Merkel cell polyomavirus-infected Merkel cell carcinoma cells require expression of viral T antigens. Journal of virology *84*, 7064-7072.

Huang da, W., Sherman, B.T., and Lempicki, R.A. (2009a). Bioinformatics enrichment tools: paths toward the comprehensive functional analysis of large gene lists. Nucleic Acids Res *37*, 1-13.

Huang da, W., Sherman, B.T., and Lempicki, R.A. (2009b). Systematic and integrative analysis of large gene lists using DAVID bioinformatics resources. Nat Protoc *4*, 44-57.

Hung, P.F., Hong, T.M., Hsu, Y.C., Chen, H.Y., Chang, Y.L., Wu, C.T., Chang, G.C., Jou, Y.S., Pan, S.H., and Yang, P.C. (2013). The motor protein KIF14 inhibits tumor growth and cancer metastasis in lung adenocarcinoma. PLoS One *8*, e61664.

Hwang, L.H., Lau, L.F., Smith, D.L., Mistrot, C.A., Hardwick, K.G., Hwang, E.S., Amon, A., and Murray, A.W. (1998). Budding yeast Cdc20: a target of the spindle checkpoint. Science *279*, 1041-1044.

Imperiale, M.J. (2001). Oncogenic transformation by the human polyomaviruses. Oncogene *20*, 7917-7923.

Ito, Y., Brocklehurst, J.R., and Dulbecco, R. (1977). Virus-specific proteins in the plasma membrane of cells lytically infected or transformed by pol-oma virus. Proc Natl Acad Sci U S A *74*, 4666-4670.

Itoh, M., Nagafuchi, A., Moroi, S., and Tsukita, S. (1997). Involvement of ZO-1 in cadherin-based cell adhesion through its direct binding to alpha catenin and actin filaments. J Cell Biol *138*, 181-192.

Janssens, V., and Goris, J. (2001). Protein phosphatase 2A: a highly regulated family of serine/threonine phosphatases implicated in cell growth and signalling. Biochem J *353*, 417-439.

Javier, R.T., and Butel, J.S. (2008). The history of tumor virology. Cancer Res *68*, 7693-7706.

Jiang, D., Srinivasan, A., Lozano, G., and Robbins, P.D. (1993). SV40 T antigen abrogates p53-mediated transcriptional activity. Oncogene *8*, 2805-2812.

Jiang, Y., Saavedra, H.I., Holloway, M.P., Leone, G., and Altura, R.A. (2004). Aberrant regulation of survivin by the RB/E2F family of proteins. The Journal of biological chemistry *279*, 40511-40520.

Joo, M., Hahn, Y.S., Kwon, M., Sadikot, R.T., Blackwell, T.S., and Christman, J.W. (2005). Hepatitis C virus core protein suppresses NF-kappaB activation and cyclooxygenase-2 expression by direct interaction with IkappaB kinase beta. J Virol *79*, 7648-7657.

Kang, S.S., Kwon, T., Kwon, D.Y., and Do, S.I. (1999). Akt protein kinase enhances human telomerase activity through phosphorylation of telomerase reverse transcriptase subunit. J Biol Chem *274*, 13085-13090.

Kantola, K., Sadeghi, M., Lahtinen, A., Koskenvuo, M., Aaltonen, L.M., Mottonen, M., Rahiala, J., Saarinen-Pihkala, U., Riikonen, P., Jartti, T.*, et al.* (2009). Merkel cell polyomavirus DNA in tumor-free tonsillar tissues and upper respiratory tract samples: implications for respiratory transmission and latency. J Clin Virol *45*, 292-295.

Kassem, A., Schopflin, A., Diaz, C., Weyers, W., Stickeler, E., Werner, M., and Zur Hausen, A. (2008). Frequent detection of Merkel cell polyomavirus in human Merkel cell carcinomas and identification of a unique deletion in the VP1 gene. Cancer research *68*, 5009-5013.

Kassem, A., Technau, K., Kurz, A.K., Pantulu, D., Loning, M., Kayser, G., Stickeler, E., Weyers, W., Diaz, C., Werner, M.*, et al.* (2009). Merkel cell polyomavirus sequences are frequently detected in nonmelanoma skin cancer of immunosuppressed patients. International journal of cancer Journal international du cancer *125*, 356-361.

Katano, H., Ito, H., Suzuki, Y., Nakamura, T., Sato, Y., Tsuji, T., Matsuo, K., Nakagawa, H., and Sata, T. (2009). Detection of Merkel cell polyomavirus in Merkel cell carcinoma and Kaposi's sarcoma. J Med Virol *81*, 1951-1958.

Kean, J.M., Rao, S., Wang, M., and Garcea, R.L. (2009). Seroepidemiology of human polyomaviruses. PLoS Pathog *5*, e1000363.

Kerr, J.F., Wyllie, A.H., and Currie, A.R. (1972). Apoptosis: a basic biological phenomenon with wide-ranging implications in tissue kinetics. Br J Cancer *26*, 239-257.

Khalili, K., Sariyer, I.K., and Safak, M. (2008a). Small tumor antigen of polyomaviruses: role in viral life cycle and cell transformation. J Cell Physiol *215*, 309-319.

Khalili, K., Sariyer, I.K., and Safak, M. (2008b). Small tumor antigen of polyomaviruses: role in viral life cycle and cell transformation. J Cell Physiol *215*, 309-319.

Khalili, K., White, M.K., Sawa, H., Nagashima, K., and Safak, M. (2005). The agnoprotein of polyomaviruses: a multifunctional auxiliary protein. J Cell Physiol *204*, 1-7.

Kierstead, T.D., and Tevethia, M.J. (1993). Association of p53 binding and immortalization of primary C57BL/6 mouse embryo fibroblasts by using simian virus 40 T-antigen mutants bearing internal overlapping deletion mutations. J Virol *67*, 1817-1829.

King, R.W., Peters, J.M., Tugendreich, S., Rolfe, M., Hieter, P., and Kirschner, M.W. (1995). A 20S complex containing CDC27 and CDC16 catalyzes the mitosis-specific conjugation of ubiquitin to cyclin B. Cell *81*, 279-288.

Kiyokawa, H., Kineman, R.D., Manova-Todorova, K.O., Soares, V.C., Hoffman, E.S., Ono, M., Khanam, D., Hayday, A.C., Frohman, L.A., and Koff, A. (1996). Enhanced growth of mice lacking the cyclin-dependent kinase inhibitor function of p27(Kip1). Cell *85*, 721-732.

Knight, L.M., Stakaityte, G., Wood, J.J., Abdul-Sada, H., Griffiths, D.A., Howell, G.J., Wheat, R., Blair, G.E., Steven, N.M., Macdonald, A.*, et al.* (2015). Merkel cell polyomavirus small T antigen mediates microtubule destabilization to promote cell motility and migration. J Virol *89*, 35-47.

Kolzau, T., Hansen, R.S., Zahra, D., Reddel, R.R., and Braithwaite, A.W. (1999). Inhibition of SV40 large T antigen induced apoptosis by small T antigen. Oncogene *18*, 5598-5603.

Komagome, R., Sawa, H., Suzuki, T., Suzuki, Y., Tanaka, S., Atwood, W.J., and Nagashima, K. (2002). Oligosaccharides as receptors for JC virus. J Virol *76*, 12992-13000.

Korup, S., Rietscher, J., Calvignac-Spencer, S., Trusch, F., Hofmann, J., Moens, U., Sauer, I., Voigt, S., Schmuck, R., and Ehlers, B. (2013). Identification of a novel human polyomavirus in organs of the gastrointestinal tract. PLoS One *8*, e58021.

Kundu, S.T., Gosavi, P., Khapare, N., Patel, R., Hosing, A.S., Maru, G.B., Ingle, A., Decaprio, J.A., and Dalal, S.N. (2008). Plakophilin3 downregulation leads to a decrease in cell adhesion and promotes metastasis. Int J Cancer *123*, 2303-2314.

Kurrey, N.K., K, A., and Bapat, S.A. (2005). Snail and Slug are major determinants of ovarian cancer invasiveness at the transcription level. Gynecol Oncol *97*, 155-165.

Kwun, H.J., Guastafierro, A., Shuda, M., Meinke, G., Bohm, A., Moore, P.S., and Chang, Y. (2009). The minimum replication origin of merkel cell polyomavirus has a unique large T-antigen loading architecture and requires small T-antigen expression for optimal replication. J Virol *83*, 12118-12128.

Kwun, H.J., Shuda, M., Feng, H., Camacho, C.J., Moore, P.S., and Chang, Y. (2013). Merkel cell polyomavirus small T antigen controls viral replication and oncoprotein expression by targeting the cellular ubiquitin ligase SCFFbw7. Cell Host Microbe *14*, 125-135.

Lane, D.P., and Crawford, L.V. (1979). T antigen is bound to a host protein in SV40-transformed cells. Nature *278*, 261-263.

Lassak, A., Del Valle, L., Peruzzi, F., Wang, J.Y., Enam, S., Croul, S., Khalili, K., and Reiss, K. (2002). Insulin receptor substrate 1 translocation to the nucleus by the human JC virus T-antigen. J Biol Chem *277*, 17231-17238.

Le Negrate, G. (2012). Viral interference with innate immunity by preventing NF-kappaB activity. Cell Microbiol *14*, 168-181.

Lee, S., Paulson, K.G., Murchison, E.P., Afanasiev, O.K., Alkan, C., Leonard, J.H., Byrd, D.R., Hannon, G.J., and Nghiem, P. (2011). Identification and validation of a novel mature microRNA encoded by the Merkel cell polyomavirus in human Merkel cell carcinomas. J Clin Virol *52*, 272-275.

Levine, A.J. (1997). p53, the cellular gatekeeper for growth and division. Cell *88*, 323-331.

Lezcano, C., Kleffel, S., Lee, N., Larson, A.R., Zhan, Q., DoRosario, A., Wang, L.C., Schatton, T., and Murphy, G.F. (2014). Merkel cell carcinoma expresses vasculogenic mimicry: demonstration in patients and experimental manipulation in xenografts. Lab Invest *94*, 1092-1102.

Li, J., Diaz, J., Wang, X., Tsang, S.H., and You, J. (2015). Phosphorylation of Merkel cell polyomavirus large tumor antigen at serine 816 by ATM kinase induces apoptosis in host cells. J Biol Chem *290*, 1874-1884.

Li, J., Wang, X., Diaz, J., Tsang, S.H., Buck, C.B., and You, J. (2013). Merkel cell polyomavirus large T antigen disrupts host genomic integrity and inhibits cellular proliferation. J Virol *87*, 9173-9188.

Li, V.S., Yuen, S.T., Chan, T.L., Yan, H.H., Law, W.L., Yeung, B.H., Chan, A.S., Tsui, W.Y., So, S., Chen, X.*, et al.* (2009). Frequent inactivation of axon guidance molecule RGMA in human colon cancer through genetic and epigenetic mechanisms. Gastroenterology *137*, 176-187.

Lim, E.S., Reyes, A., Antonio, M., Saha, D., Ikumapayi, U.N., Adeyemi, M., Stine, O.C., Skelton, R., Brennan, D.C., Mkakosya, R.S.*, et al.* (2013).

Discovery of STL polyomavirus, a polyomavirus of ancestral recombinant origin that encodes a unique T antigen by alternative splicing. Virology *436*, 295-303.

Lin, H.K., Chen, Z., Wang, G., Nardella, C., Lee, S.W., Chan, C.H., Yang, W.L., Wang, J., Egia, A., Nakayama, K.I.*, et al.* (2010). Skp2 targeting suppresses tumorigenesis by Arf-p53-independent cellular senescence. Nature *464*, 374-379.

Liu, X., Hein, J., Richardson, S.C., Basse, P.H., Toptan, T., Moore, P.S., Gjoerup, O.V., and Chang, Y. (2011a). Merkel cell polyomavirus large T antigen disrupts lysosome clustering by translocating human Vam6p from the cytoplasm to the nucleus. The Journal of biological chemistry *286*, 17079-17090.

Liu, X., Hein, J., Richardson, S.C., Basse, P.H., Toptan, T., Moore, P.S., Gjoerup, O.V., and Chang, Y. (2011b). Merkel cell polyomavirus large T antigen disrupts lysosome clustering by translocating human Vam6p from the cytoplasm to the nucleus. J Biol Chem *286*, 17079-17090.

Low, J.A., Magnuson, B., Tsai, B., and Imperiale, M.J. (2006). Identification of gangliosides GD1b and GT1b as receptors for BK virus. J Virol *80*, 1361-1366.

Lunder, E.J., and Stern, R.S. (1998). Merkel-cell carcinomas in patients treated with methoxsalen and ultraviolet A radiation. N Engl J Med *339*, 1247-1248.

Madhavan, J., Coral, K., Mallikarjuna, K., Corson, T.W., Amit, N., Khetan, V., George, R., Biswas, J., Gallie, B.L., and Kumaramanickavel, G. (2007). High expression of KIF14 in retinoblastoma: association with older age at diagnosis. Invest Ophthalmol Vis Sci *48*, 4901-4906.

Mandl, C.W., and Frisque, R.J. (1986). Characterization of cells transformed by the human polyomavirus JC virus. J Gen Virol *67 (Pt 8)*, 1733-1739.

Mao, J.H., Perez-Losada, J., Wu, D., Delrosario, R., Tsunematsu, R., Nakayama, K.I., Brown, K., Bryson, S., and Balmain, A. (2004). Fbxw7/Cdc4 is a p53-dependent, haploinsufficient tumour suppressor gene. Nature *432*, 775-779.

Maricich, S.M., Wellnitz, S.A., Nelson, A.M., Lesniak, D.R., Gerling, G.J., Lumpkin, E.A., and Zoghbi, H.Y. (2009). Merkel cells are essential for light-touch responses. Science *324*, 1580-1582.

Markowski, J., Oczko-Wojciechowska, M., Gierek, T., Jarzab, M., Paluch, J., Kowalska, M., Wygoda, Z., Pfeifer, A., Tyszkiewicz, T., Jarzab, B.*, et al.* (2009a). Gene expression profile analysis in laryngeal cancer by high-density oligonucleotide microarrays. J Physiol Pharmacol *60 Suppl 1*, 57-63.

Markowski, J., Tyszkiewicz, T., Jarzab, M., Oczko-Wojciechowska, M., Gierek, T., Witkowska, M., Paluch, J., Kowalska, M., Wygoda, Z., Lange, D.*, et al.* (2009b). Metal-proteinase ADAM12, kinesin 14 and checkpoint suppressor 1 as new molecular markers of laryngeal carcinoma. Eur Arch Otorhinolaryngol *266*, 1501-1507.

Martel-Jantin, C., Filippone, C., Cassar, O., Peter, M., Tomasic, G., Vielh, P., Briere, J., Petrella, T., Aubriot-Lorton, M.H., Mortier, L.*, et al.* (2012). Genetic variability and integration of Merkel cell polyomavirus in Merkel cell carcinoma. Virology *426*, 134-142.

Martin, T.A., and Jiang, W.G. (2009). Loss of tight junction barrier function and its role in cancer metastasis. Biochim Biophys Acta *1788*, 872-891.

Martinato, F., Cesaroni, M., Amati, B., and Guccione, E. (2008). Analysis of Myc-induced histone modifications on target chromatin. PLoS One *3*, e3650.

Maser, R.S., Choudhury, B., Campbell, P.J., Feng, B., Wong, K.K., Protopopov, A., O'Neil, J., Gutierrez, A., Ivanova, E., Perna, I.*, et al.* (2007). Chromosomally unstable mouse tumours have genomic alterations similar to diverse human cancers. Nature *447*, 966-971.

Mateo, M., Generous, A., Sinn, P.L., and Cattaneo, R. (2015). Connections matter--how viruses use cell-cell adhesion components. J Cell Sci *128*, 431-439.

Matter, K., Aijaz, S., Tsapara, A., and Balda, M.S. (2005). Mammalian tight junctions in the regulation of epithelial differentiation and proliferation. Curr Opin Cell Biol *17*, 453-458.

McDonald, E.R., 3rd, and El-Deiry, W.S. (2000). Cell cycle control as a basis for cancer drug development (Review). Int J Oncol *16*, 871-886.

McLean, J.E., Ruck, A., Shirazian, A., Pooyaei-Mehr, F., and Zakeri, Z.F. (2008). Viral manipulation of cell death. Curr Pharm Des *14*, 198-220.

Mietz, J.A., Unger, T., Huibregtse, J.M., and Howley, P.M. (1992). The transcriptional transactivation function of wild-type p53 is inhibited by SV40 large T-antigen and by HPV-16 E6 oncoprotein. Embo J *11*, 5013-5020.

Moens, U., Van Ghelue, M., and Johannessen, M. (2007). Oncogenic potentials of the human polyomavirus regulatory proteins. Cell Mol Life Sci *64*, 1656-1678.

Moore, P.S., and Chang, Y. (2010a). Why do viruses cause cancer? Highlights of the first century of human tumour virology. Nature Reviews Cancer, 12.

Moore, P.S., and Chang, Y. (2010b). Why do viruses cause cancer? Highlights of the first century of human tumour virology. Nat Rev Cancer *10*, 878-889.

Moreno, C.S., Ramachandran, S., Ashby, D.G., Laycock, N., Plattner, C.A., Chen, W., Hahn, W.C., and Pallas, D.C. (2004a). Signaling and transcriptional changes critical for transformation of human cells by simian virus 40 small tumor antigen or protein phosphatase 2A B56gamma knockdown. Cancer Res *64*, 6978-6988.

Moreno, C.S., Ramachandran, S., Ashby, D.G., Laycock, N., Plattner, C.A., Chen, W., Hahn, W.C., and Pallas, D.C. (2004b). Signaling and transcriptional changes critical for transformation of human cells by simian virus 40 small tumor antigen or protein phosphatase 2A B56gamma knockdown. Cancer research *64*, 6978-6988.

Morin, P.J. (1999). beta-catenin signaling and cancer. Bioessays *21*, 1021-1030.

Morrison, K.M., Miesegaes, G.R., Lumpkin, E.A., and Maricich, S.M. (2009). Mammalian Merkel cells are descended from the epidermal lineage. Dev Biol *336*, 76-83.

Mumby, M. (2007). PP2A: unveiling a reluctant tumor suppressor. Cell *130*, 21-24.

Munday, D.C., Surtees, R., Emmott, E., Dove, B.K., Digard, P., Barr, J.N., Whitehouse, A., Matthews, D., and Hiscox, J.A. (2012). Using SILAC and quantitative proteomics to investigate the interactions between viral and host proteomes. Proteomics *12*, 666-672.

Murray, A.W., Solomon, M.J., and Kirschner, M.W. (1989). The role of cyclin synthesis and degradation in the control of maturation promoting factor activity. Nature *339*, 280-286.

Nakamura, T., Sato, Y., Watanabe, D., Ito, H., Shimonohara, N., Tsuji, T., Nakajima, N., Suzuki, Y., Matsuo, K., Nakagawa, H.*, et al.* (2010). Nuclear localization of Merkel cell polyomavirus large T antigen in Merkel cell carcinoma. Virology *398*, 273-279.

Nakayama, K., Ishida, N., Shirane, M., Inomata, A., Inoue, T., Shishido, N., Horii, I., Loh, D.Y., and Nakayama, K. (1996). Mice lacking p27(Kip1) display increased body size, multiple organ hyperplasia, retinal dysplasia, and pituitary tumors. Cell *85*, 707-720.

Neu, U., Hengel, H., Blaum, B.S., Schowalter, R.M., Macejak, D., Gilbert, M., Wakarchuk, W.W., Imamura, A., Ando, H., Kiso, M.*, et al.* (2012). Structures of Merkel cell polyomavirus VP1 complexes define a sialic acid binding site required for infection. PLoS Pathog *8*, e1002738.

Neu, U., Woellner, K., Gauglitz, G., and Stehle, T. (2008). Structural basis of GM1 ganglioside recognition by simian virus 40. Proc Natl Acad Sci U S A *105*, 5219-5224.

Neumann, F., Borchert, S., Schmidt, C., Reimer, R., Hohenberg, H., Fischer, N., and Grundhoff, A. (2011). Replication, gene expression and particle production by a consensus Merkel Cell Polyomavirus (MCPyV) genome. PLoS One *6*, e29112.

Nicol, J.T., Robinot, R., Carpentier, A., Carandina, G., Mazzoni, E., Tognon, M., Touze, A., and Coursaget, P. (2013). Age-specific seroprevalences of merkel cell polyomavirus, human polyomaviruses 6, 7, and 9, and trichodysplasia spinulosa-associated polyomavirus. Clin Vaccine Immunol *20*, 363-368.

Noda, T., Satake, M., Yamaguchi, Y., and Ito, Y. (1987). Cooperation of middle and small T antigens of polyomavirus in transformation of established fibroblast and epithelial-like cell lines. Journal of virology *61*, 2253-2263.

Normanno, N., Rachiglio, A.M., Lambiase, M., Martinelli, E., Fenizia, F., Esposito, C., Roma, C., Troiani, T., Rizzi, D., Tatangelo, F.*, et al.* (2015). Heterogeneity of KRAS, NRAS, BRAF and PIK3CA mutations in metastatic colorectal cancer and potential effects on therapy in the CAPRI GOIM trial. Ann Oncol *26*, 1710-1714.

Nozawa, A., Kato, K., and Uchida, S. (1987). Surface antigens on hamster cells transformed by SV40, BK virus and JC virus. Jpn J Exp Med *57*, 267-275.

Nunbhakdi-Craig, V., Craig, L., Machleidt, T., and Sontag, E. (2003). Simian virus 40 small tumor antigen induces deregulation of the actin cytoskeleton and tight junctions in kidney epithelial cells. J Virol *77*, 2807-2818.

Orban, E., Szabo, E., Lotz, G., Kupcsulik, P., Paska, C., Schaff, Z., and Kiss, A. (2008). Different expression of occludin and ZO-1 in primary and metastatic liver tumors. Pathol Oncol Res *14*, 299-306.

Oren, M., and Levine, A.J. (1981). Immunoselection of simian virus 40 large T antigen messenger rnas from transformed cells. Virology *113*, 790-793.

Oren, M., Maltzman, W., and Levine, A.J. (1981). Post-translational regulation of the 54K cellular tumor antigen in normal and transformed cells. Mol Cell Biol *1*, 101-110.

Ozanne, B.W., Spence, H.J., McGarry, L.C., and Hennigan, R.F. (2007). Transcription factors control invasion: AP-1 the first among equals. Oncogene *26*, 1-10.

Padgett, B.L., and Walker, D.L. (1973). Prevalence of antibodies in human sera against JC virus, an isolate from a case of progressive multifocal leukoencephalopathy. J Infect Dis *127*, 467-470.

Padgett, B.L., Walker, D.L., ZuRhein, G.M., Eckroade, R.J., and Dessel, B.H. (1971). Cultivation of papova-like virus from human brain with progressive multifocal leucoencephalopathy. Lancet *1*, 1257-1260.

Pagano, M., Pepperkok, R., Verde, F., Ansorge, W., and Draetta, G. (1992). Cyclin A is required at two points in the human cell cycle. Embo J *11*, 961-971.

Pallas, D.C., Shahrik, L.K., Martin, B.L., Jaspers, S., Miller, T.B., Brautigan, D.L., and Roberts, T.M. (1990). Polyoma small and middle T antigens and SV40 small t antigen form stable complexes with protein phosphatase 2A. Cell *60*, 167-176.

Paris, L., Tonutti, L., Vannini, C., and Bazzoni, G. (2008). Structural organization of the tight junctions. Biochim Biophys Acta *1778*, 646-659.

Parkin, D.M. (2006). The global health burden of infection-associated cancers in the year 2002. International journal of cancer Journal international du cancer *118*, 3030-3044.

Paulson, K.G., Iyer, J.G., Byrd, D.R., and Nghiem, P. (2013). Pathologic nodal evaluation is increasingly commonly performed for patients with Merkel cell carcinoma. J Am Acad Dermatol *69*, 653-654.

Peden, K.W., Srinivasan, A., Farber, J.M., and Pipas, J.M. (1989). Mutants with changes within or near a hydrophobic region of simian virus 40 large tumor antigen are defective for binding cellular protein p53. Virology *168*, 13-21.

Peters, J.M. (2006). The anaphase promoting complex/cyclosome: a machine designed to destroy. Nat Rev Mol Cell Biol *7*, 644-656.

Piette, J., Neel, H., and Marechal, V. (1997). Mdm2: keeping p53 under control. Oncogene *15*, 1001-1010.

Pina-Oviedo, S., Urbanska, K., Radhakrishnan, S., Sweet, T., Reiss, K., Khalili, K., and Del Valle, L. (2007). Effects of JC virus infection on anti-apoptotic protein survivin in progressive multifocal leukoencephalopathy. Am J Pathol *170*, 1291-1304.

Pines, J., and Hunter, T. (1991). Cyclin-dependent kinases: a new cell cycle motif? Trends Cell Biol *1*, 117-121.

Pipas, J.M. (2009). SV40: Cell transformation and tumorigenesis. Virology *384*, 294-303.

Pircher, A., Wellbrock, J., Fiedler, W., Heidegger, I., Gunsilius, E., and Hilbe, W. (2014). New antiangiogenic strategies beyond inhibition of vascular endothelial growth factor with special focus on axon guidance molecules. Oncology *86*, 46-52.

Piva, R., Belardo, G., and Santoro, M.G. (2006). NF-kappaB: a stress-regulated switch for cell survival. Antioxid Redox Signal *8*, 478-486.

Pommier, Y., Leo, E., Zhang, H., and Marchand, C. (2010). DNA topoisomerases and their poisoning by anticancer and antibacterial drugs. Chem Biol *17*, 421-433.

Portt, L., Norman, G., Clapp, C., Greenwood, M., and Greenwood, M.T. (2011). Anti-apoptosis and cell survival: a review. Biochim Biophys Acta *1813*, 238-259.

Poulsen, M. (2004a). Merkel-cell carcinoma of the skin. Lancet Oncol *5*, 593-599.

Poulsen, M. (2004b). Merkel-cell carcinoma of the skin. Lancet Oncol *5*, 593-599.

Preissner, K.T., and Seiffert, D. (1998). Role of vitronectin and its receptors in haemostasis and vascular remodeling. Thromb Res *89*, 1-21.

Prisco, M., Santini, F., Baffa, R., Liu, M., Drakas, R., Wu, A., and Baserga, R. (2002). Nuclear translocation of insulin receptor substrate-1 by the simian virus 40 T antigen and the activated type 1 insulin-like growth factor receptor. The Journal of biological chemistry *277*, 32078-32085.

Quelle, D.E., Zindy, F., Ashmun, R.A., and Sherr, C.J. (1995). Alternative reading frames of the INK4a tumor suppressor gene encode two unrelated proteins capable of inducing cell cycle arrest. Cell *83*, 993-1000.

Radkov, S.A., Kellam, P., and Boshoff, C. (2000). The latent nuclear antigen of Kaposi sarcoma-associated herpesvirus targets the retinoblastoma-E2F pathway and with the oncogene Hras transforms primary rat cells. Nat Med *6*, 1121-1127.

Raghava, S., Giorda, K.M., Romano, F.B., Heuck, A.P., and Hebert, D.N. (2011). The SV40 late protein VP4 is a viroporin that forms pores to disrupt membranes for viral release. PLoS Pathog *7*, e1002116.

Raj, D., Liu, T., Samadashwily, G., Li, F., and Grossman, D. (2008). Survivin repression by p53, Rb and E2F2 in normal human melanocytes. Carcinogenesis *29*, 194-201.

Rajagopalan, H., Jallepalli, P.V., Rago, C., Velculescu, V.E., Kinzler, K.W., Vogelstein, B., and Lengauer, C. (2004). Inactivation of hCDC4 can cause chromosomal instability. Nature *428*, 77-81.

Randall, C.M., Jokela, J.A., and Shisler, J.L. (2012). The MC159 protein from the molluscum contagiosum poxvirus inhibits NF-kappaB activation by interacting with the IkappaB kinase complex. J Immunol *188*, 2371-2379.

Rathi, A.V., Saenz Robles, M.T., Cantalupo, P.G., Whitehead, R.H., and Pipas, J.M. (2009). Simian virus 40 T-antigen-mediated gene regulation in enterocytes is controlled primarily by the Rb-E2F pathway. J Virol *83*, 9521-9531.

Reichgelt, B.A., and Visser, O. (2011). Epidemiology and survival of Merkel cell carcinoma in the Netherlands. A population-based study of 808 cases in 1993-2007. Eur J Cancer *47*, 579-585.

Reisinger, D.M., Shiffer, J.D., Cognetta, A.B., Jr., Chang, Y., and Moore, P.S. (2010). Lack of evidence for basal or squamous cell carcinoma infection with Merkel cell polyomavirus in immunocompetent patients with Merkel cell carcinoma. J Am Acad Dermatol *63*, 400-403.

Reya, T., and Clevers, H. (2005). Wnt signalling in stem cells and cancer. Nature *434*, 843-850.

Robert, A., Miron, M.J., Champagne, C., Gingras, M.C., Branton, P.E., and Lavoie, J.N. (2002). Distinct cell death pathways triggered by the adenovirus early region 4 ORF 4 protein. J Cell Biol *158*, 519-528.

Rodriguez-Viciana, P., Collins, C., and Fried, M. (2006). Polyoma and SV40 proteins differentially regulate PP2A to activate distinct cellular signaling pathways involved in growth control. Proc Natl Acad Sci U S A *103*, 19290-19295.

Rowland, B.D., and Bernards, R. (2006). Re-evaluating cell-cycle regulation by E2Fs. Cell *127*, 871-874.

Ruediger, R., Hentz, M., Fait, J., Mumby, M., and Walter, G. (1994). Molecular model of the A subunit of protein phosphatase 2A: interaction with other subunits and tumor antigens. J Virol *68*, 123-129.

Sachsenmeier, K.F., and Pipas, J.M. (2001). Inhibition of Rb and p53 is insufficient for SV40 T-antigen transformation. Virology *283*, 40-48.

Sackton, K.L., Dimova, N., Zeng, X., Tian, W., Zhang, M., Sackton, T.B., Meaders, J., Pfaff, K.L., Sigoillot, F., Yu, H.*, et al.* (2014). Synergistic blockade of mitotic exit by two chemical inhibitors of the APC/C. Nature *514*, 646-649.

Saenz-Robles, M.T., Sullivan, C.S., and Pipas, J.M. (2001). Transforming functions of Simian Virus 40. Oncogene *20*, 7899-7907.

Safak, M., and Khalili, K. (2003). An overview: Human polyomavirus JC virus and its associated disorders. J Neurovirol *9 Suppl 1*, 3-9.

Sarid, R., Sato, T., Bohenzky, R.A., Russo, J.J., and Chang, Y. (1997). Kaposi's sarcoma-associated herpesvirus encodes a functional bcl-2 homologue. Nat Med *3*, 293-298.

Satyanarayana, A., Hilton, M.B., and Kaldis, P. (2008). p21 Inhibits Cdk1 in the absence of Cdk2 to maintain the G1/S phase DNA damage checkpoint. Mol Biol Cell *19*, 65-77.

Sauer, B. (1994). Site-specific recombination: developments and applications. Curr Opin Biotechnol *5*, 521-527.

Scheffner, M., Werness, B.A., Huibregtse, J.M., Levine, A.J., and Howley, P.M. (1990). The E6 oncoprotein encoded by human papillomavirus types 16 and 18 promotes the degradation of p53. Cell *63*, 1129-1136.

Schowalter, R.M., and Buck, C.B. (2013). The Merkel cell polyomavirus minor capsid protein. PLoS Pathog *9*, e1003558.

Schowalter, R.M., Pastrana, D.V., and Buck, C.B. (2011). Glycosaminoglycans and sialylated glycans sequentially facilitate Merkel cell polyomavirus infectious entry. PLoS Pathog *7*, e1002161.

Schowalter, R.M., Pastrana, D.V., Pumphrey, K.A., Moyer, A.L., and Buck, C.B. (2010). Merkel cell polyomavirus and two previously unknown polyomaviruses are chronically shed from human skin. Cell Host Microbe *7*, 509-515.

Scuda, N., Hofmann, J., Calvignac-Spencer, S., Ruprecht, K., Liman, P., Kuhn, J., Hengel, H., and Ehlers, B. (2011). A novel human polyomavirus closely related to the african green monkey-derived lymphotropic polyomavirus. J Virol *85*, 4586-4590.

Seavey, S.E., Holubar, M., Saucedo, L.J., and Perry, M.E. (1999). The E7 oncoprotein of human papillomavirus type 16 stabilizes p53 through a mechanism independent of p19(ARF). J Virol *73*, 7590-7598.

Segawa, K., Minowa, A., Sugasawa, K., Takano, T., and Hanaoka, F. (1993). Abrogation of p53-mediated transactivation by SV40 large T antigen. Oncogene *8*, 543-548.

Seinsoth, S., Uhlmann-Schiffler, H., and Stahl, H. (2003). Bidirectional DNA unwinding by a ternary complex of T antigen, nucleolin and topoisomerase I. EMBO Rep *4*, 263-268.

Seo, G.J., Chen, C.J., and Sullivan, C.S. (2009). Merkel cell polyomavirus encodes a microRNA with the ability to autoregulate viral gene expression. Virology *383*, 183-187.

Shackelton, L.A., Rambaut, A., Pybus, O.G., and Holmes, E.C. (2006). JC virus evolution and its association with human populations. J Virol *80*, 9928-9933.

Shahbazian, D., Parsyan, A., Petroulakis, E., Hershey, J., and Sonenberg, N. (2010). eIF4B controls survival and proliferation and is regulated by proto-oncogenic signaling pathways. Cell Cycle *9*, 4106-4109.

She, Q.B., Solit, D.B., Ye, Q., O'Reilly, K.E., Lobo, J., and Rosen, N. (2005). The BAD protein integrates survival signaling by EGFR/MAPK and PI3K/Akt kinase pathways in PTEN-deficient tumor cells. Cancer Cell *8*, 287-297.

Sherr, C.J. (1993). Mammalian G1 cyclins. Cell *73*, 1059-1065.

Sherr, C.J. (1996). Cancer cell cycles. Science *274*, 1672-1677.

Shi, Y., Dodson, G.E., Shaikh, S., Rundell, K., and Tibbetts, R.S. (2005). Ataxia-telangiectasia-mutated (ATM) is a T-antigen kinase that controls SV40 viral replication in vivo. J Biol Chem *280*, 40195-40200.

Shuda, M., Arora, R., Kwun, H.J., Feng, H., Sarid, R., Fernandez-Figueras, M.T., Tolstov, Y., Gjoerup, O., Mansukhani, M.M., Swerdlow, S.H.*, et al.* (2009). Human Merkel cell polyomavirus infection I. MCV T antigen expression in Merkel cell carcinoma, lymphoid tissues and lymphoid tumors. International journal of cancer Journal international du cancer *125*, 1243-1249.

Shuda, M., Feng, H.C., Kwun, H.J., Rosen, S.T., Gjoerup, O., Moore, P.S., and Chang, Y. (2008). T antigen mutations are a human tumor-specific signature for Merkel cell polyomavirus. Proc Natl Acad Sci U S A *105*, 16272-16277.

Shuda, M., Kwun, H.J., Feng, H., Chang, Y., and Moore, P.S. (2011a). Human Merkel cell polyomavirus small T antigen is an oncoprotein targeting the 4E-BP1 translation regulator. The Journal of clinical investigation *121*, 3623-3634.

Shuda, M., Kwun, H.J., Feng, H., Chang, Y., and Moore, P.S. (2011b). Human Merkel cell polyomavirus small T antigen is an oncoprotein targeting the 4E-BP1 translation regulator. J Clin Invest *121*, 3623-3634.

Siebrasse, E.A., Reyes, A., Lim, E.S., Zhao, G., Mkakosya, R.S., Manary, M.J., Gordon, J.I., and Wang, D. (2012a). Identification of MW polyomavirus, a novel polyomavirus in human stool. J Virol *86*, 10321-10326.

Siebrasse, E.A., Reyes, A., Lim, E.S., Zhao, G., Mkakosya, R.S., Manary, M.J., Gordon, J.I., and Wang, D. (2012b). Identification of MW polyomavirus, a novel polyomavirus in human stool. J Virol *86*, 10321-10326.

Singel, S.M., Cornelius, C., Zaganjor, E., Batten, K., Sarode, V.R., Buckley, D.L., Peng, Y., John, G.B., Li, H.C., Sadeghi, N.*, et al.* (2014). KIF14

promotes AKT phosphorylation and contributes to chemoresistance in triple-negative breast cancer. Neoplasia *16*, 247-256, 256 e242.

Smith, T.C., Fang, Z., and Luna, E.J. (2010). Novel interactors and a role for supervillin in early cytokinesis. Cytoskeleton (Hoboken) *67*, 346-364.

Soini, Y. (2012). Tight junctions in lung cancer and lung metastasis: a review. Int J Clin Exp Pathol *5*, 126-136.

Sonnenberg, A., and Liem, R.K. (2007). Plakins in development and disease. Exp Cell Res *313*, 2189-2203.

Sontag, E., Fedorov, S., Kamibayashi, C., Robbins, D., Cobb, M., and Mumby, M. (1993). The interaction of SV40 small tumor antigen with protein phosphatase 2A stimulates the map kinase pathway and induces cell proliferation. Cell *75*, 887-897.

Spitkovsky, D., Hehner, S.P., Hofmann, T.G., Moller, A., and Schmitz, M.L. (2002). The human papillomavirus oncoprotein E7 attenuates NF-kappa B activation by targeting the Ikappa B kinase complex. J Biol Chem *277*, 25576-25582.

Stahl, H., Droge, P., and Knippers, R. (1986). DNA helicase activity of SV40 large tumor antigen. Embo J *5*, 1939-1944.

Stakaityte, G., Wood, J.J., Knight, L.M., Abdul-Sada, H., Adzahar, N.S., Nwogu, N., Macdonald, A., and Whitehouse, A. (2014). Merkel cell polyomavirus: molecular insights into the most recently discovered human tumour virus. Cancers *6*, 1267-1297.

Stewart, S.E., Eddy, B.E., and Borgese, N. (1958). Neoplasms in mice inoculated with a tumor agent carried in tissue culture. J Natl Cancer Inst *20*, 1223-1243.

Sudakin, V., Ganoth, D., Dahan, A., Heller, H., Hershko, J., Luca, F.C., Ruderman, J.V., and Hershko, A. (1995). The cyclosome, a large complex containing cyclin-selective ubiquitin ligase activity, targets cyclins for destruction at the end of mitosis. Mol Biol Cell *6*, 185-197.

Sullivan, C.S., Cantalupo, P., and Pipas, J.M. (2000). The molecular chaperone activity of simian virus 40 large T antigen is required to disrupt Rb-E2F family complexes by an ATP-dependent mechanism. Mol Cell Biol *20*, 6233-6243.

Sullivan, C.S., and Pipas, J.M. (2002). T antigens of simian virus 40: molecular chaperones for viral replication and tumorigenesis. Microbiol Mol Biol Rev *66*, 179-202.

Suryadinata, R., Sadowski, M., and Sarcevic, B. (2010). Control of cell cycle progression by phosphorylation of cyclin-dependent kinase (CDK) substrates. Biosci Rep *30*, 243-255.

Suzuki, T., Orba, Y., Okada, Y., Sunden, Y., Kimura, T., Tanaka, S., Nagashima, K., Hall, W.W., and Sawa, H. (2010). The human polyoma JC virus agnoprotein acts as a viroporin. PLoS Pathog *6*, e1000801.

Swanton, C., and Jones, N. (2001). Strategies in subversion: de-regulation of the mammalian cell cycle by viral gene products. Int J Exp Pathol *82*, 3-13.

Sweet, B.H., and Hilleman, M.R. (1960). The vacuolating virus, S.V. 40. Proc Soc Exp Biol Med *105*, 420-427.

Tadmor, T., Aviv, A., and Polliack, A. (2011a). Merkel cell carcinoma, chronic lymphocytic leukemia and other lymphoproliferative disorders: an old bond with possible new viral ties. Ann Oncol *22*, 250-256.

Tadmor, T., Aviv, A., and Polliack, A. (2011b). Merkel cell carcinoma, chronic lymphocytic leukemia and other lymphoproliferative disorders: an old bond with possible new viral ties. Ann Oncol *22*, 250-256.
Talbot, L.J., Bhattacharya, S.D., and Kuo, P.C. (2012). Epithelial-mesenchymal transition, the tumor microenvironment, and metastatic behavior of epithelial malignancies. Int J Biochem Mol Biol *3*, 117-136.

Talis, A.L., Huibregtse, J.M., and Howley, P.M. (1998). The role of E6AP in the regulation of p53 protein levels in human papillomavirus (HPV)-positive and HPV-negative cells. J Biol Chem *273*, 6439-6445.

Theriault, B.L., Pajovic, S., Bernardini, M.Q., Shaw, P.A., and Gallie, B.L. (2012). Kinesin family member 14: an independent prognostic marker and potential therapeutic target for ovarian cancer. Int J Cancer *130*, 1844-1854.

Thornton, B.R., Ng, T.M., Matyskiela, M.E., Carroll, C.W., Morgan, D.O., and Toczyski, D.P. (2006). An architectural map of the anaphase-promoting complex. Genes Dev *20*, 449-460.

Tiemann, F., Zerrahn, J., and Deppert, W. (1995). Cooperation of simian virus 40 large and small T antigens in metabolic stabilization of tumor suppressor p53 during cellular transformation. J Virol *69*, 6115-6121.

Tobioka, H., Isomura, H., Kokai, Y., Tokunaga, Y., Yamaguchi, J., and Sawada, N. (2004). Occludin expression decreases with the progression of human endometrial carcinoma. Hum Pathol *35*, 159-164.

Toker, C. (1972). Trabecular carcinoma of the skin. Arch Dermatol *105*, 107-110.

Tonoike, Y., Matsushita, K., Tomonaga, T., Katada, K., Tanaka, N., Shimada, H., Nakatani, Y., Okamoto, Y., and Nomura, F. (2011). Adhesion molecule periplakin is involved in cellular movement and attachment in pharyngeal squamous cancer cells. BMC Cell Biol *12*, 41.

Topalis, D., Andrei, G., and Snoeck, R. (2013). The large tumor antigen: a "Swiss Army knife" protein possessing the functions required for the polyomavirus life cycle. Antiviral Res *97*, 122-136.

Tope, W.D., and Sangueza, O.P. (1994). Merkel cell carcinoma. Histopathology, immunohistochemistry, and cytogenetic analysis. J Dermatol Surg Oncol *20*, 648-652; quiz 653-644.

Touze, A., Gaitan, J., Arnold, F., Cazal, R., Fleury, M.J., Combelas, N., Sizaret, P.Y., Guyetant, S., Maruani, A., Baay, M.*, et al.* (2010). Generation of Merkel cell polyomavirus (MCV)-like particles and their application to detection of MCV antibodies. J Clin Microbiol *48*, 1767-1770.

Trojanek, J., Croul, S., Ho, T., Wang, J.Y., Darbinyan, A., Nowicki, M., Del Valle, L., Skorski, T., Khalili, K., and Reiss, K. (2006). T-antigen of the human polyomavirus JC attenuates faithful DNA repair by forcing nuclear interaction between IRS-1 and Rad51. J Cell Physiol *206*, 35-46.

Tsai, B., Gilbert, J.M., Stehle, T., Lencer, W., Benjamin, T.L., and Rapoport, T.A. (2003). Gangliosides are receptors for murine polyoma virus and SV40. Embo J *22*, 4346-4355.

Tsang, S.H., Wang, X., Li, J., Buck, C.B., and You, J. (2014). Host DNA damage response factors localize to merkel cell polyomavirus DNA replication sites to support efficient viral DNA replication. J Virol *88*, 3285-3297.

Usui, H., Imazu, M., Maeta, K., Tsukamoto, H., Azuma, K., and Takeda, M. (1988). Three distinct forms of type 2A protein phosphatase in human erythrocyte cytosol. J Biol Chem *263*, 3752-3761.

Van der Meijden, E., Janssens, R.W., Lauber, C., Bouwes Bavinck, J.N., Gorbalenya, A.E., and Feltkamp, M.C. (2010). Discovery of a new human polyomavirus associated with trichodysplasia spinulosa in an immunocompromized patient. PLoS Pathog *6*, e1001024.

Van Ghelue, M., Khan, M.T., Ehlers, B., and Moens, U. (2012). Genome analysis of the new human polyomaviruses. Rev Med Virol.

Vermeulen, K., Van Bockstaele, D.R., and Berneman, Z.N. (2003). The cell cycle: a review of regulation, deregulation and therapeutic targets in cancer. Cell Prolif *36*, 131-149.

Vousden, K.H., and Lane, D.P. (2007). p53 in health and disease. Nat Rev Mol Cell Biol *8*, 275-283.

Wang, X., Li, J., Schowalter, R.M., Jiao, J., Buck, C.B., and You, J. (2012). Bromodomain protein Brd4 plays a key role in Merkel cell polyomavirus DNA replication. PLoS Pathog *8*, e1003021.

Wataya-Kaneda, M., Kaneda, Y., Hino, O., Adachi, H., Hirayama, Y., Seyama, K., Satou, T., and Yoshikawa, K. (2001). Cells derived from tuberous sclerosis show a prolonged S phase of the cell cycle and increased apoptosis. Arch Dermatol Res *293*, 460-469.

Weinberg, R.A. (1995). The retinoblastoma protein and cell cycle control. Cell *81*, 323-330.

Welcker, M., and Clurman, B.E. (2008). FBW7 ubiquitin ligase: a tumour suppressor at the crossroads of cell division, growth and differentiation. Nat Rev Cancer *8*, 83-93.

Wessel, R., Schweizer, J., and Stahl, H. (1992). Simian virus 40 T-antigen DNA helicase is a hexamer which forms a binary complex during bidirectional unwinding from the viral origin of DNA replication. J Virol *66*, 804-815.

White, M.K., and Khalili, K. (2004). Polyomaviruses and human cancer: molecular mechanisms underlying patterns of tumorigenesis. Virology *324*, 1-16.

Wong, H.H., and Wang, J. (2010). Merkel cell carcinoma. Arch Pathol Lab Med *134*, 1711-1716.

Wood, L.D., Parsons, D.W., Jones, S., Lin, J., Sjoblom, T., Leary, R.J., Shen, D., Boca, S.M., Barber, T., Ptak, J.*, et al.* (2007). The genomic landscapes of human breast and colorectal cancers. Science *318*, 1108-1113.

Xu, H., Choe, C., Shin, S.H., Park, S.W., Kim, H.S., Jung, S.H., Yim, S.H., Kim, T.M., and Chung, Y.J. (2014). Silencing of KIF14 interferes with cell cycle progression and cytokinesis by blocking the p27(Kip1) ubiquitination pathway in hepatocellular carcinoma. Exp Mol Med *46*, e97.

Yam, C.H., Fung, T.K., and Poon, R.Y. (2002). Cyclin A in cell cycle control and cancer. Cell Mol Life Sci *59*, 1317-1326.

Yanai, N., and Obinata, M. (1994). Apoptosis is induced at nonpermissive temperature by a transient increase in p53 in cell lines immortalized with temperature-sensitive SV40 large T-antigen gene. Exp Cell Res *211*, 296-300.

Yang, C.S., Vitto, M.J., Busby, S.A., Garcia, B.A., Kesler, C.T., Gioeli, D., Shabanowitz, J., Hunt, D.F., Rundell, K., Brautigan, D.L.*, et al.* (2005). Simian virus 40 small t antigen mediates conformation-dependent transfer of protein phosphatase 2A onto the androgen receptor. Mol Cell Biol *25*, 1298-1308.

Yang, S.I., Lickteig, R.L., Estes, R., Rundell, K., Walter, G., and Mumby, M.C. (1991). Control of protein phosphatase 2A by simian virus 40 small-t antigen. Mol Cell Biol *11*, 1988-1995.

Yang, T., Li, X.N., Li, L., Wu, Q.M., Gao, P.Z., Wang, H.L., and Zhao, W. (2014). Sox17 inhibits hepatocellular carcinoma progression by downregulation of KIF14 expression. Tumour Biol *35*, 11199-11207.

Yang, T., Zhang, X.B., and Zheng, Z.M. (2013). Suppression of KIF14 expression inhibits hepatocellular carcinoma progression and predicts favorable outcome. Cancer Sci *104*, 552-557.

Yeh, E., Cunningham, M., Arnold, H., Chasse, D., Monteith, T., Ivaldi, G., Hahn, W.C., Stukenberg, P.T., Shenolikar, S., Uchida, T.*, et al.* (2004). A signalling pathway controlling c-Myc degradation that impacts oncogenic transformation of human cells. Nat Cell Biol *6*, 308-318.

Yu, G., Greninger, A.L., Isa, P., Phan, T.G., Martinez, M.A., de la Luz Sanchez, M., Contreras, J.F., Santos-Preciado, J.I., Parsonnet, J., Miller, S.*, et al.* (2012). Discovery of a novel polyomavirus in acute diarrheal samples from children. PLoS One *7*, e49449.

Yu, J., Boyapati, A., and Rundell, K. (2001). Critical role for SV40 small-t antigen in human cell transformation. Virology *290*, 192-198.

Yuan, T.L., and Cantley, L.C. (2008). PI3K pathway alterations in cancer: variations on a theme. Oncogene *27*, 5497-5510.

Zeng, X., Sigoillot, F., Gaur, S., Choi, S., Pfaff, K.L., Oh, D.C., Hathaway, N., Dimova, N., Cuny, G.D., and King, R.W. (2010). Pharmacologic inhibition of the anaphase-promoting complex induces a spindle checkpoint-dependent mitotic arrest in the absence of spindle damage. Cancer Cell *18*, 382-395.

Zerrahn, J., Knippschild, U., Winkler, T., and Deppert, W. (1993). Independent expression of the transforming amino-terminal domain of SV40 large I antigen from an alternatively spliced third SV40 early mRNA. Embo J *12*, 4739-4746.

Zhang, C., Liu, F., He, Z., Deng, Q., Pan, Y., Liu, Y., Zhang, C., Ning, T., Guo, C., Liang, Y.*, et al.* (2014). Seroprevalence of Merkel cell polyomavirus in the general rural population of Anyang, China. PloS one *9*, e106430.

Zhang, K., Xu, J., Yan, L., Liu, X., Xu, F., and Liu, Y. (2015). [Detection of KRAS,NRAS and BRAF gene mutations in colorectal carcinoma]. Zhonghua Bing Li Xue Za Zhi *44*, 254-257.

Zhao, J.J., Gjoerup, O.V., Subramanian, R.R., Cheng, Y., Chen, W., Roberts, T.M., and Hahn, W.C. (2003). Human mammary epithelial cell transformation through the activation of phosphatidylinositol 3-kinase. Cancer Cell *3*, 483-495.

Zhivotovsky, B., and Orrenius, S. (2010). Cell death mechanisms: cross-talk and role in disease. Exp Cell Res *316*, 1374-1383.

Zhou, A.Y., Ichaso, N., Adamarek, A., Zila, V., Forstova, J., Dibb, N.J., and Dilworth, S.M. (2011). Polyomavirus middle T-antigen is a transmembrane protein that binds signaling proteins in discrete subcellular membrane sites. J Virol *85*, 3046-3054.

Zhou, J., Pham, H.T., Ruediger, R., and Walter, G. (2003). Characterization of the Aalpha and Abeta subunit isoforms of protein phosphatase 2A: differences in expression, subunit interaction, and evolution. Biochem J *369*, 387-398.

Zhu, C., Zhao, J., Bibikova, M., Leverson, J.D., Bossy-Wetzel, E., Fan, J.B., Abraham, R.T., and Jiang, W. (2005). Functional analysis of human microtubule-based motor proteins, the kinesins and dyneins, in mitosis/cytokinesis using RNA interference. Mol Biol Cell *16*, 3187-3199.

Appendices

DNA sequence of MCPyV LT truncated gene

ATGGATTTAGTCCTAAATAGGAAAGAAAGAGAGGCTCTCTGCAAGCTT
TTAGAGATTGCTCCTAATTGTTATGGCAACATCCCTCTGATGAAAGCT
GCTTTCAAAAGAAGCTGCTTAAAGCATCACCCTGATAAAGGGGGAAAT
CCTGTTATAATGATGGAATTGAACACCCTTTGGAGCAAATTCCAGCAA
AATATCCACAAGCTCAGAAGTGACTTCTCTATGTTTGATGAGGTTGAC
GAGGCCCCTATATATGGGACCACTAAATTCAAAGAATGGTGGAGATCA
GGAGGATTCAGCTTCGGGAAGGCATACGAATATGGGCCCAATCCACA
CGGGACCAACTCAAGATCCAGAAAGCCTTCCTCCAATGCATCCAGGG
GAGCCCCCAGTGGAAGCTCACCACCCCACAGCCAGAGCTCTTCCTCT
GGGTATGGGTCCTTCTCAGCGTCCCAGGCTTCAGACTCCCAGTCCAG
AGGACCCGATATACCTCCCGAACACCATGAGGAACCCACCTCATCCT
CTGGATCCAGTAGCAGAGAGGAGACCACCAATTCAGGAAGAGAATCC
AGCACACCCAATGGAACCAGTGTACCTAGAAATTCTTCCAGAACTGAT
GGCACCTGGGAGGATCTCTTCTGCGATGAATCACTTTCCTCCCCTGA
GCCTCCCTCGTCCTCTGAGGAGCCTGAGGAGCCCCCCTCCTCAAGAA
GCTCGCCCCGGCAGCCCCCGTCTTCCTCTGCCGAGGAGGCCTCGTC
ATCTCAGTTTACAGATGAGGAATACAGATCCTCCTCCTTCACCACCCC
GAAGACCCCTCCTCCATTCGATCATGATTACAAGGATGACGACGATAA
GTGAGCGGCCGCTCGAGTCTAGAGGGCCCGTACGCCGCC

Protein sequence of tLT

M D L V L N R K E R E A L C K L L E I A P N C Y G N I P L M K A A F K R
S C L K H H P D K G G N P V I M M E L N T L W S K F Q Q N I H K L R S
D F S M F D E V D E A P I Y G T T K F K E W W R S G G F S F G K A Y E
Y G P N P H G T N S R S R K P S S N A S R G A P S G S S P P H S Q S
S S S G Y G S F S A S Q A S D S Q S R G P D I P P E H H E E P T S S S
G S S S R E E T T N S G R E S S T P N G T S V P R N S S R T D G T W
E D L F C D E S L S S P E P P S S S E E P E E P P S S R S S P R Q P P
S S S A E E A S S S Q F T D E E Y R S S S F T T P K T P P P F D H D Y
K D D D D K **Stop**

Additional identified proteins from MCPyV truncated LT SILAC proteomic dataset

Accession	# Peptides	MW [kDa]	Score	Description
B3KUD7	25	68.5	317.50	DNA REPLICATION LICENSING FACTOR MCM7
Q59GM9	22	98.8	256.69	Phosphorylase
Q14315	11	290.8	114.20	Filamin-C
Q8IVF2	4	616.2	72.65	Protein AHNAK2
Q9NRW1	6	23.4	66.71	Ras-related protein Rab-6B
B7ZKR7	4	115.2	40.69	AP-3 complex subunit beta-2
A8MPP7	3	55.4	39.47	SRSF protein kinase 3
Full length LT	5	92.3	39.44	Full length LT
Q9UQ05	2	111.6	36.86	Potassium voltage-gated channel subfamily H member 4
B1WB49	3	293.2	34.51	BDP1 protein
Q96L93	2	151.9	32.06	Kinesin-like protein
Q9NS88	2	282.4	22.13	Alpha1A-voltage-dependent calcium channel
H7C5G4	3	10.8	19.39	Replication factor C subunit 2
Q5SGD2	2	41.0	18.97	Protein phosphatase 1L
B7Z6T2	2	77.5	14.13	Type II inositol-3,4-bisphosphate4-phosphatase
H0Y843	2	136.7	13.94	EF-hand calcium-binding domain-containing protein 5
J3QQZ1	2	208.0	10.80	Sodium channel protein type 4 subunit alpha
B4DHK6	3	44.2	9.59	S-phase kinase-associated protein 2
B4E1J7	2	70.1	15.68	Centromere/kinetochore protein
C9JBZ4	3	44.8	13.42	HAUS augmin-like complex subunit 8
B4DW39	2	67.6	10.30	Fc receptor-like protein 5
O14513	3	208.4	34.80	Nck-associated protein 5
B4DXG2	2	36.1	5.75	Son of sevenless homolog 1
Q6IEH8	2	315.9	16.30	Transcriptional regulator

Accession	# Peptides	MW [kDa]	Score	Description
Q8WUM4	29	96.0	444.04	Programmed cell death 6-interacting protein
Q14222	6	24.2	420.00	EEF1A protein
P46821	33	270.5	364.25	Microtubule-associated protein
P11216	23	96.6	301.10	Glycogen phosphorylase
Q5R370	15	21.2	243.75	Calcyclin binding protein
P27824	15	67.5	241.28	Calnexin
Q10567	20	104.6	193.50	AP-1 complex subunit beta-1
P63010	17	104.5	184.19	AP-2 complex subunit beta
P16989	8	40.1	164.83	DNA-binding protein A
G3V1R9	13	44.8	155.82	Inositol-3-phosphate synthase 1
H3BSC1	11	22.5	127.84	Ras-related protein Rab-11A
Q9BSJ8	19	122.8	127.64	Extended synaptotagmin-1
E7EVA0	7	245.3	126.67	Microtubule-associated protein
P31947	5	27.8	123.53	14-3-3 protein sigma
P60953	7	21.2	59.01	Cell division control protein
Q07157	4	195.3	24.96	Tight junction protein ZO-1
H0Y564	3	161.5	24.37	Anaphase-promoting complex subunit 1
O75843	2	87.1	21.66	AP-1 complex subunit gamma-like 2
Q00653	3	96.7	21.11	Nuclear factor NF-kappa-B p100 subunit
A0JLQ9	2	66.5	19.82	STAT2 protein
O75747	3	165.6	19.42	Phosphatidylinositol 4-phosphate 3-kinase C2
G5E9Y3	3	151.0	18.18	Arf-GAP with Rho-GAP domain, ANK repeat and PH domain-containing protein 3
A8K9T5	2	105.1	15.97	E3 ubiquitin-protein ligase
B1ALD0	2	64.5	11.77	AP-4 complex subunit beta-1
Q9BRQ8	2	40.5	11.42	Apoptosis-inducing factor 2
B7Z1I0	2	36.4	10.88	Integrin-linked protein kinase
E5RGA6	2	18.2	9.82	Focal adhesion kinase 1
Q59GT9	2	66.9	7.61	Gap junction protein
Q96BT7	2	75.2	4.65	Alkylated DNA repair protein alkB homolog 8